Charles University in Prague

Faculty of Science, Department of Inorganic Chemistry

Ph.D. Study program: Inorganic Chemistry

RNDr. Jiří Schulz

Polární ferrocenové amidofosfiny pro katalytické aplikace

Polar ferrocene amidophosphines for catalytic applications

Ph.D. Thesis

Supervisor: Prof. RNDr. Petr Štěpnička, Ph.D.

Prague, 2012

Declaration

I declare that this thesis is my own original work except as cited in the references. The thesis has not been submitted, or is being concurrently submitted, for any other degree.

Prague, 26.7.2012

Jiří Schulz

Acknowledgement

The Grant Agency of the Charles University in Prague (project no. 69309) and the Ministry of Education, Youth, and Sports of the Czech Republic (project nos. LC06070 and MSM0021620857) are gratefully acknowledged for their financial support.

Personal Acknowledgment

Here I would like to express my cordial gratitude to prof. RNDr. Petr Štěpnička, Ph.D. who has supervised me during the whole time I have spent at the Faculty of Science at Charles University in Prague. I am grateful to him for his kind and inspiring attitude as well as for immense number of invaluable advices and gained experiences.

For a friendly atmosphere and pleasant cooperation I am grateful to all the present as well as former colleagues from the "organometallic lab" at the Department of Inorganic Chemistry. Special thanks belong to my classmate and friend Dr. Jiří Tauchman.

Dr. Ivana Císařová as well as the other co-workers are gratefully acknowledged for their contributions to this Ph.D. Thesis.

I would like to express immense gratitude to my family, especially my mother for her support, but also to my girlfriend for her tolerance and patience. Last, but not least, I owe thanks to my friends who can always cheer me up.

Abstrakt

Hydroxyamid $Ph_2PfcC(O)NHCH_2CH_2OH$ **1**, publikovaný již dříve, a nově syntetizované ligandy $Ph_2PfcC(O)NHCH_{3-n}(CH_2OH)_n$ (**3**: *n* = 2; **4**: *n* = 3) poskytly reakcí s dimérními prekurzory $[(\eta^6\text{-arén})Ru(\mu\text{-Cl})Cl]_2$ (arén = C_6H_6, *p*-cymén, C_6Me_6) sérii strukturně příbuzných ruthenatých komplexů typu $[(\eta^6\text{-arén})RuCl_2(L\text{-}\kappa P)]$ **6-8** (L = **1**, **3** a **4**). Katalytické testování připravených komplexů v redoxní isomerizaci allylových alkoholů ukázalo, že komplex $[(\eta^6\text{-}p\text{-cymén})RuCl_2(\mathbf{1}\text{-}\kappa P)]$ **6b** je nejaktivnějším z celé série.

Struktura fotolytického rozkladného produktu $[(\mu\text{-Cl})_3\{Ru(\eta^6\text{-}C_6Me_6)\}_2][FeCl_4]$ **9** komplexu $[(\eta^6\text{-}C_6Me_6)RuCl_2(\mathbf{2}\text{-}\kappa P)]$ (**2** = $Ph_2PfcC(O)N(CH_2CH_2OH)_2$) byla stanovena pomocí rentgenostrukturní analýzy.

In vitro testování bis-fosfinových komplexů $[M^{II}Cl_2(\mathbf{1}\text{-}\kappa P)_2]$ (M = *trans*-Pd (**10**), *cis*-Pt (**11**) and *trans*-Pt (**12**)), volného ligandu a jeho chalkogenidů $Ph_2P(O)fcC(O)NH(CH_2)_2OH$ (**13**) a $Ph_2P(S)fcC(O)NH(CH_2)_2OH$ (**14**) ukázalo průměrnou cytotoxicitu studovaných komplexů vůči nádorovým buňkám lidského karcinomu vaječníků.

Reakcí triol-amidu $FcC(O)NHC(CH_2OH)_3$ **15** s dekavanadičnanem $(Bu_4N)_2[H_3V_{10}O_{28}]$ byl získán hybridní hexavanadičnan $(Bu_4N)_2[\{FcC(O)NHC(CH_2O)_3\}_2V_6O_{13}]$ **16** nesoucí redoxně aktivní ferrocenylové substituenty. Připravená látka byla charakterizována prostřednictvím fyzikálně-chemických metod včetně rentgenostrukturní analýzy, cyklické voltametrie a také teoretických výpočtů. Teoretické výpočty provedené na základě struktury izolovaného hexavanadičnanového aniontu v pevném stavu poskytly možné vysvětlení elektrochemického chování látky a odhalily vazebné poměry v hexavaničnanovém skeletu.

Fosfinoferrocenové amidosulfonáty $(Et_3NH)[Ph_2PfcC(O)NH(CH_2)_nSO_3]$ (**17**: *n* = 1, **18**: *n* = 2, **19**: n = 3; fc = ferrocen-1,1′-diyl) byly získány konjugací 1′-(difenylfosfino)ferrocen-1-karboxylové kyseliny (Hdpf) a *ω*-aminosulfonových kyselin $H_2N(CH_2)_nSO_3H$ (*n* = 1-3) a izolovány ve formě svých triethylamoniových solí. Palladnaté komplexy *trans*-$[PdCl_2(L\text{-}\kappa P)_2]$ (**23**: L = **17**; **24**: L = **18**; **25**: L = **19**) odvozené od těchto ligandů posloužily jako definované pre-katalyzátory pro kyanační reakce arylbromidů pomocí $K_4[Fe(CN)_6]$.

Klíčová slova: Ferrocen; Fosfinové ligandy; Vodná katalýza; Teoretické výpočty; Protirakovinné účinky; Polyoxovanadičnany; Strukturní analýza.

Abstract

The formerly reported hydroxyamide $Ph_2PfcC(O)NHCH_2CH_2OH$ **1** and its respective novel congeneric analogues $Ph_2PfcC(O)NHCH_{3-n}(CH_2OH)_n$ (**3**: n = 2; **4**: n = 3) were used to prepare a series of arene-ruthenium(II) complexes [(η^6-arene)$RuCl_2$(L-κ*P*)] **6-8** (arene = C_6H_6, *p*-cymene, C_6Me_6; L = **1**, **3** or **4**). These complexes were studied as pre-catalysts in redox isomerization of allylic alcohols to carbonyl compounds. Among the compounds prepared, complex **6b** [(η^6-*p*-cymene)$RuCl_2$(**1**-κ*P*)] showed best results.

The solid state structure of the product of photolytic decomposition of complex [(η^6-C_6Me_6)$RuCl_2$(**2**-κ*P*)] (**2** = $Ph_2PfcC(O)N(CH_2CH_2OH)_2$), *viz*, [($\mu$-Cl)$_3${Ru($\eta^6$-$C_6Me_6$)}$_2$] [$FeCl_4$] **9**, was determined by single-crystal X-ray diffraction analysis.

The bis-phosphane complexes [$M^{II}Cl_2$(**1**-κ*P*)$_2$] (M = *trans*-Pd (**10**), *cis*-Pt (**11**) and *trans*-Pt (**12**)) together with chalcogenide derivatives $Ph_2P(O)fcC(O)NH(CH_2)_2OH$ (**13**) and $Ph_2P(S)fcC(O)NH(CH_2)_2OH$ (**14**) derived from hydroxyamide **1** were tested *in vitro* for their cytotoxicity against human ovarian A2780 cancer cell line. Complexes tested showed moderate cytotoxicity.

Triol-amide $FcC(O)NHC(CH_2OH)_3$ **15** (Fc = ferrocenyl) reacted with decavanadate $(Bu_4N)_2[H_3V_{10}O_{28}]$ at elevated temperature and prolonged reaction time yielding the hybrid hexavanadate $(Bu_4N)_2$[{$FcC(O)NHC(CH_2O)_3$}$_2V_6O_{13}$] **16** capped with the redox-active ferrocenyl pendants. The novel compound was thoroughly studied by standard spectral methods, X-ray diffraction analysis, cyclic voltammetry and theoretical calculations. Single-point DFT calculations performed for the isolated hexavanadate anion gave an insight into the bonding scheme within hexavanadate cage and offered an explanation for electrochemical behavior of the compound.

Conjugation of 1′-(diphenylphosphanyl)ferrocene-1-carboxylic acid (Hdpf) with ω-aminosulfonic acids $H_2N(CH_2)_nSO_3H$ (n = 1-3) afforded amidosulfonates (Et_3NH) [$Ph_2PfcCONH(CH_2)_nSO_3$] (**17**: n = 1, **18**: n = 2, **19**: n = 3; fc = ferrocene-1,1′-diyl), isolated as the respective triethylammonium salts. These ligands were employed in the synthesis of palladium(II) complexes *trans*-[$PdCl_2$(L-κ*P*)$_2$] (**23**: L = **17**; **24**: L = **18**; **25**: L = **19**) which, in turn, were probed as defined pre-catalysts for aqueous cyanation of aryl bromides with potassium hexacyanoferrate(II).

Keywords: Ferrocene; Phosphane ligands; Aqueous catalysis; Theoretical calculations; Anticancer properties; Polyoxovanadates ; Structure elucidation.

Table of Contents

Chapter 1

Introduction

Research into transition metal-mediated catalytic processes and catalyst design represents one of the most important fields of contemporary chemical science. Increasing number of available organic transformations and a growing demand for production of fine chemicals are the major driving forces for the development of new catalytic systems carefully tailored for a specific purpose. Search for catalysts having superior catalytic performance is motivated not only by efforts to improve efficiency and selectivity of chemical transformations but also by economic and environmental issues.

Much attention has been devoted to find synthetic strategies that minimise the reaction time, temperature, catalyst loading, and simplify product purification. Among the most challenging topics still remain catalyst separation and recycling both on a laboratory and large scale synthesis. Whereas it is possible to separate heterogeneous catalyst from a reaction mixture easily by simple decantation, filtration or centrifugation, the same is not applicable for homogeneous catalysts. Separation of a homogeneous catalyst requires typically an application of advanced workup procedures, for instance, extractions or chromatographic techniques, causing the production of additional waste and making the whole process more energy demanding. Even though the use of heterogeneous catalysts is favoured in potential industrial applications, there is still a great attention paid to the development of new catalytic systems that would combine the most attractive features of both catalyst classes, *i.e.*, homogeneous and heterogeneous. Possibility to carefully design a homogeneous catalyst by means of ligand tailoring remains still unmatched in the field of heterogeneous catalysis. On the other hand, the ease of separation of heterogeneous catalyst allows for efficient catalyst recovery and reuse that offer further economical and environmental benefits.

The known synthetic strategies used to combine the attractive properties of both catalyst classes usually make use of immobilisation of the known and well-established homogeneous catalyst onto solid supports.[1] Various inorganic materials may serve a solid support, for instance mesoporous silica, hydroxyapatite, hydrotalcite and activated charcoal. [2] Alternative strategy is to immobilise the catalyst on polymeric materials, *e.g.*, cross-linked polystyrene or polyaniline. [3] Although the immobilised catalysts offer a

number of advantages, easier catalyst recovery from a reaction mixture and improved selectivity to name just few, there are however also disadvantages including transition metal leaching into a reaction mixture or lowering of catalytic activity upon repeated use.

Another perspective approach towards catalyst immobilisation is to constrain the catalytic species in an immiscible liquid phase.[4] Since the reactants and the catalyst reside in different liquid phases, this approach is called biphasic catalysis. Sufficient interaction between the catalyst and the reactants is ensured by stirring and emulsification of the reaction mixture, while separation upon the reaction completion is achieved by simple decantation. As the "liquid catalyst carrier" may be used a variety of solvents differing in their physical and chemical characteristics. Well-established is the use of ionic liquids,[5] fluorous solvents,[6] supercritical carbon dioxide[7] and, advantageously, also water.[8]

Several industrial processes already utilize concept of aqueous biphasic catalysis.[8,9] The initial application of this concept in industry is the rhodium catalysed hydroformylation of propene (Scheme 1.1) introduced by Ruhrchemie/Rhône-Poulenc in 1984. [10]

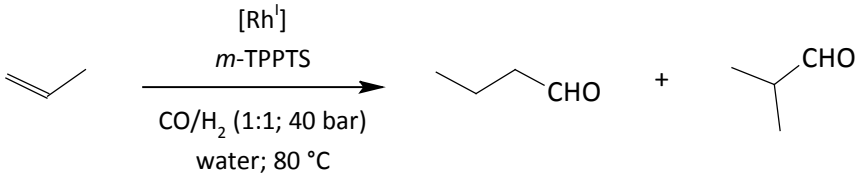

Scheme 1.1. Ruhrchemie /Rhône-Poulenc oxo-process (hydroformylation of propene).

The development of this process enabled to replace the less selective but cheaper cobalt(I) catalyst with the more expensive rhodium(I) analogue owing to possibility of catalyst recycling. The rhodium catalyst promotes the hydroformylation reaction with excellent linear/branched product ratio (24:1). The ligand triphenylphosphane-3,3′,3′′-trisulfonate trisodium salt (*m*-TPPTS, Scheme 1.2) is used to direct the catalytic species into aqueous phase.

The use of water as a "liquid catalyst carrier" enabling catalyst recovery is not the only reason for its application in organic synthesis. Water is a cheap, non-toxic and non-flammable, easily accessible solvent that provides expedient physical properties such as high polarity or specific heat capacity. Hence, it attracted much attention as a potent "green chemistry" alternative to solvents commonly used in organic synthesis, since the majority of waste produced by chemical processes is due to the used solvents.[11]

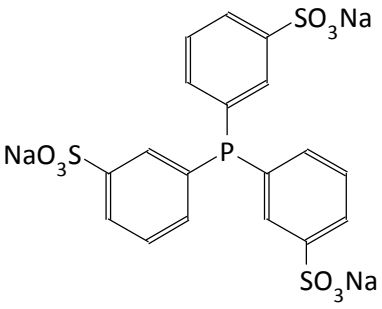

m-TPPTS

Scheme 1.2. Triphenylphosphane-3,3′,3′′-trisulfonate trisodium salt (*m*-TPPTS).

Water may also effectively affect the selectivity of organic transformations and accelerate their reaction rates.[12] Water features unique, highly ordered inner structure given by its ability to form intramolecular hydrogen bonds. Hydrophobic organic compounds tend to associate in aqueous media to minimise surface contact with water. As a result, water may accelerate reactions with negative volume of activation due to the so-called hydrophobic effect firstly postulated by Breslow.[13,14] Breslow and co-workers have studied influence of water on selectivity and reaction rates of Diels-Alder reaction. They have observed that the use of water significantly enhances reaction rates of cycloaddition of 3-buten-2-one and 1,3-cyclopentadiene as compared to organic solvents (Scheme 1.3).

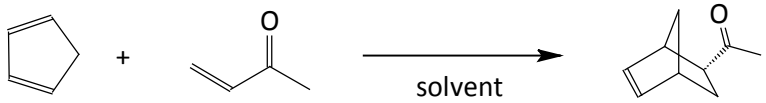

Scheme 1.3. Diels-Alder [4+2] cycloaddition of 1,3-cyclopentadiene (**3**) and 3-buten-2-one (**4**).

However, hydrophobic effect isn't the only reason for which water influences the course of organic reactions. For instance, hydrogen bonding in aqueous solvents may lower the values of reaction Gibbs activation energy ($\Delta G^{\ddagger}$). The formation of hydrogen bonds changes the relative energy of the frontier orbitals of reactants that possess acceptor group capable of forming hydrogen bonds.[15,16] Moreover, water is a highly polar solvent and thus favours reactions going through polar transitions states.[17] As a Lewis base, water can effectively moderate the reactivity of Lewis acids.[18] In the case of transition metal-catalysed reactions performed in water, the possible formation of aqua complexes must be taken into the account. Water also provides the opportunity to carefully control pH of the reaction mixture and, in addition, may serve as an acid or a base itself. The scope of

organic transformations performed in aqueous media ranges from simple two-component processes ([3+2] cycloaddition reactions, Claisen rearrangement) to transition metal-catalysed reactions (cross-coupling reactions, olefin metathesis). Several comprehensive reviews were recently published on this topic.[11,12d,19]

The application of transition metals in aqueous catalysis is obviously facilitated by the use of appropriate hydrophilic ligands. The role of the ligand is to constrain the resulting transition metal complex in aqueous phase and to tune its properties to obtain the required efficiency and selectivity.[8, 20] The most frequently used method to make a ligand hydrophilic is to functionalize its conventional hydrophobic counterpart with highly polar, typically ionic substituents. Well established are hydrophilic ligands bearing anionic substituents, typically sulfonate, sulfinate, phosphonate or carboxylate groups, but also those pined up with cationic substituents, *i.e.*, ammonium or phosphonium groups. Extensive synthetic methodology has been developed to introduce these ionic substituents into ligand molecules, including direct functionalization or less straightforward strategies allowing for synthesis of the less accessible derivatives.[20]

Solubility of a ligand molecule in aqueous media can be enhanced also by introduction of neutral hydrophilic groups, *i.e.*, carbohydrates (or other polyols) and polyether or polyamine chains.[20] Ligands bearing neutral hydrophilic substituents are of great interest. Usually, they exert good solubility in polar organic solvents as well as in water. Derivatives bearing polyether and polyhydroxyl substituents may display thermoregulated solubility in aqueous phase.[21] This behaviour is caused by the formation of hydrogen bonding interactions that are affected by heating or cooling of the reaction mixture. Hydrogen bonding is broken at higher temperatures what brings about a decreased solubility in water and, consequently, an increased solubility in non-polar solvents. Ligands exerting these properties are particularly attractive for potential use in aqueous biphasic catalysis, since catalyst may be easily separated by a simple change of temperature.

The described strategies leading to hydrophobic ligands soluble in aqueous media have been successfully applied to a variety of diverse ligand types. Phosphane ligands attracted particular attention as they are the most widely used in transition metal catalysis. However, nitrogen-based donors are also of great interest especially due to the stability of nitrogen atom towards oxidation and a large amount of readily accessible chiral diamines. The *N*-heterocyclic carbenes are growing in importance ever since they have been introduced.

Their remarkable σ-donor ability makes them highly attractive ligands for a broad scope of transition metal-catalysed organic transformations.

Nevertheless, the opportunity to finely tune electronic and steric properties of phosphane donors is unmatched and precisely explored. Coordination behaviour of phosphanes towards transition metals, such as σ-donating and π-accepting ability or steric demands, may be significantly altered by selection of substituents at the phosphorus atom. A number of empirical and computational parameters were proposed to describe electronic and steric properties of phosphane donors.

Experimentally, the electronic properties of phosphanes may be expressed in terms of the Tolman electronic parameter χ.[22,23] This empirical parameter is defined for a general phosphane ligand L as the difference between the carbonyl stretching frequencies in $[Ni(CO)_3L]$ and $[Ni(CO)_3(P\mathit{t}Bu_3)]$ complexes. The σ-donating and π-accepting ability of phosphane ligand L alters the electron density at the metal center and, hence, also the magnitude of back-donation to π-orbitals of the carbonyl ligands. The stretching frequency of CO corresponds therefore to electronic properties of L.

To describe steric properties of phosphanes, the Tolman cone angle θ is the most frequently used parameter.[22] Tolman defined this parameter for a general phosphane PR_3 (R refers to any aryl or alkyl) as the apex angle of the cone specified by van der Waals radii of the external atoms of the substituents R with the vertex at a distance of 2.28 Å from the phosphorus atom.

Furthermore, the steric and electronic features of phosphanes may be experimentally followed by means of ^{31}P NMR spectroscopy.[24,25] A correlation was found between σ-donating ability of phosphane donors and $^1J_{P,Se}$ coupling constants of the respective phoshane selenides. The stronger σ-donors exert smaller values of the $^1J_{P,Se}$ coupling constant. Likewise, ^{31}P NMR shift of complexes of the type *trans*-$[PdCl_2L_2]$ (L refers to a phosphane ligand) correlate with Tolman cone angle.[26,27] Consequently, this parameter may be used to assess steric demands of a ligand for which no structural data are available.

The introduction of hydrophilic polar groups into the molecules of phosphane ligands affects considerably their coordination properties. Especially the electron-withdrawing character of the majority of ionic substituents alters the σ-donating and π-accepting properties of phosphane donors. The resultant effect may be nicely demonstrated by the data obtained for triphenylphosphane (TPP, Scheme 1.4) based ligands *m*-TPPTS (Scheme 1.2) and triphenylphosphane-3,3′,3′′-tricarboxylate trilithium salt (*m*-TPPTC, Scheme 1.4).

The sulfonate groups in *meta*-position of the phenyl substituents decrease significantly the σ-donating properties of the phosphorus atom (Table 1.1) which may be rationalized by the value of the respective Hammett constant (σ_m = 0.30) for sulfonate group.[28] The influence of *meta*-carboxylate group on the electronic properties of phosphane ligand is lower (Table 1.1) which is in accordance with the corresponding Hammett constant (σ_m = –0.10).[28]

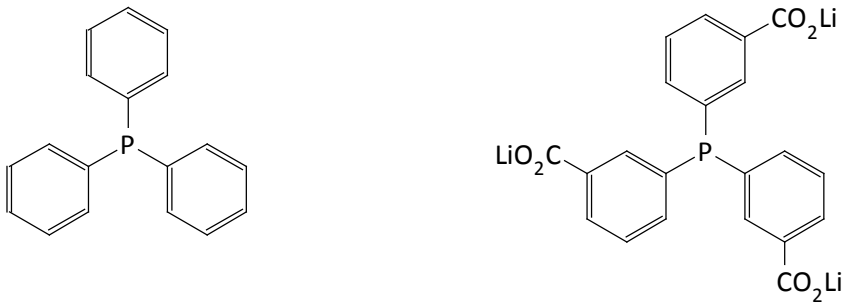

TPP *m*-TPPTC

Scheme 1.4. Triphenylphosphane (TPP) and triphenylphosphane-3,3′,3′′-tricarboxylate trilithium salt (*m*-TPPTC).

The steric demands of *m*-TPPTS and *m*-TPPTC were considerably increased by introduction of the ionic substituents into their molecules. The increase was rationalized by the values of the Tolman cone angle estimated on the basis of ^{31}P NMR spectra of the respective complexes *trans*-[$PdCl_2L_2$] (Table 1.1).

Table 1.1. Electronic and steric characteristics of triphenylphosphane (TPP) and hydrophilic ligands *m*-TPPTS and *m*-TPPTC derived thereof.

Ligand	$^1J_{P,Se}$ [a] [Hz][29,30]	ν(CO) [b] [cm^{-1}] [30,31]	χ [°][22,30]
TPP	735	2023	145
m-TPPTS	757	2025	166[c]
m-TPPTC	733	2020	166[c]

[a] Estimated for the respective phosphane-selenide. [b] Carbonyl stretching frequency found in the corresponding complexes *cis*-[$Mo(CO)_4L_2$]. [c] The Tolman cone angles based on ^{31}P NMR chemical shifts.

The introduction of hydrophilic substituents affects not only the electronic and steric properties of phosphane ligands. Further consequences arise from the secondary effects resulting from Coulombic interactions and/or hydrogen bonding interactions. The secondary interactions may significantly affect coordination behavior of ionic phosphane ligands as well as catalytic performance of their transition metal complexes.

For instance, mutual cooperation of Coulombic interligand repulsion and enhanced steric demand is believed to be responsible for lower coordination numbers achieved in Pd(0), Ni(0), Ag(+I) and Au(+I) complexes with *m*-TPPTS[32,33] as compared to those derived from TPP.[34,35,36,37] Moreover, the enhanced Coulombic repulsion between negatively charged ionic substituents may influence the modified preference for *cis/trans* isomers of $[PtX_2L_2]$ type complexes (X = halide, L = ionic phosphane ligand). For instance, the ligand triphenylphosphane-4,4′,4′′-triphosphonate hexasodium salt (*p*-TPPTP$(Na)_6$, Scheme 1.5) affords exclusively *trans*-$[PtCl_2\{p\text{-TPPTP}(Na)_6\}_2]$ isomer when reacted with $K_2[PtCl_4]$.[38] In contrast, the non-ionic form of this ligand, *i.e.*, triphenylphosphane-4,4′,4′′-triphosphonic acid (*p*-TPPTP$(H)_6$, Scheme 1.5), forms solely the *cis*-$[PtCl_2\{p\text{-TPPTP}(H)_6\}_2]$ isomer in the same reaction.[39]

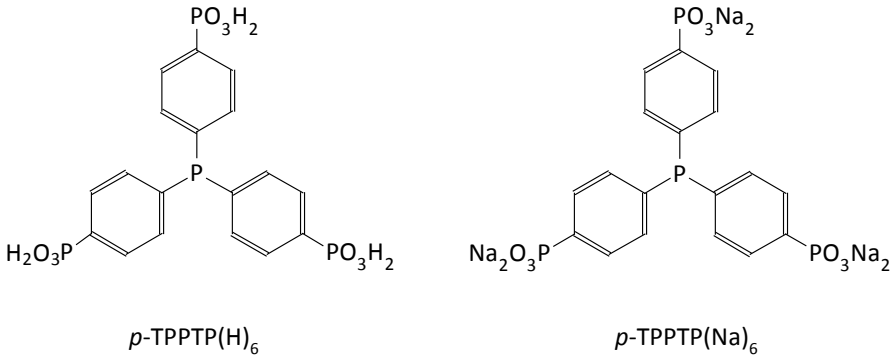

p-TPPTP$(H)_6$ *p*-TPPTP$(Na)_6$

Scheme 1.5: Triphenylphosphane-4,4′,4′′-triphosphonic acid (*p*-TPPTP$(H)_6$) and the respective hexasodium salt (*p*-TPPTP$(Na)_6$).

Formation of *cis* isomer is most likely facilitated by predisposition of *p*-TPPTP$(H)_6$ to associate through intra- and intermolecular hydrogen bonds (as evidenced by X-ray diffraction analysis of the platinum complex).

Hydrogen bonding interactions can alter catalytic behavior of transition metal complexes containing ionic ligands. A significant influence was observed in the case of *m*-TPPTS based complex $[RhH(CO)(m\text{-TPPTS})_3]$. The sulfonate groups form intramolecular hydrogen bonds in aqueous media that contribute to stabilization of the coordination compound towards ligands dissociation as compared to $[RhH(CO)(TPP)_3]$ in toluene. A higher dissociation energy is required to form the bisphosphane $[RhH(CO)(m\text{-TPPTS})_2]$ and monophosphane [RhH(CO)(*m*-TPPTS)] complexes, that are assumed to be the real catalytic species in hydroformylation of olefins.[40] As a result, the lower reaction rates but

higher regioselectivity were observed in hydroformylation reactions promoted by [RhH(CO)(*m*-TPPTS)$_3$] than for [RhH(CO)(TPP)$_3$].[41]

Nowadays, the number of the known phosphane ligands is enormous, which correlates with a broad scope of their possible coordination and catalytic applications.[42] They span from simple monodentate[43] to multidentate donors[44] and mixed-donor compounds that possess additional nitrogen,[45] sulfur[46] or oxygen[47] based donor groups. A variety of possible structure types led to the development of diverse chiral phosphane ligands that found manifold use in asymmetric catalysis. Amongst the immense number of different ligand types phosphanylferrocenes developed into specific class of donors with special electronic and steric properties.[48,49]

Ferrocene derivatives attracted great attention ever since the discovery of ferrocene in the early 1950's.[50,51] The first efforts were devoted mainly to understanding of the exceptional features of the ferrocene molecule, mainly its unexpected stability and puzzling structure,[52,53] while the later investigations were aimed at exploring its rich and remarkable reactivity.[54] The vigorous research over the last few decades set up the scope of possible applications of ferrocene derivatives that range from analytical chemistry (molecular recognition, ion sensing, electrochemical labeling)[55] and material science (luminescent systems, polymer design, magnetic materials)[56] to coordination chemistry (homogeneous catalysis, asymmetric organic synthesis), biochemistry (design of functionalized peptides)[57] and even medicinal chemistry (treatment of cancer).[58]

Ferrocene derived donors stand out as a particularly attractive class of ligands because of their unique electronic and steric properties. Ferrocene is a coordination and organometallic compound itself. It possesses the canonical sandwich structure[59] resulting in its specific spatial properties. The ferrocene backbone is relatively rigid towards tilting of its cyclopentadienyl rings from the parallel arrangement. On the other hand, it is flexible in their mutual rotation along molecular axis. Furthemore, ferrocene is endowed with a high electron density making it a useful electron-donating substituent. The cyclopentadienyl ligands retain their aromatic character and readily undergo electrophilic aromatic substitution.

Ferrocene donors are easily accessible by numerous synthetic procedures enabling relatively straightforward synthesis of mono- or disubstituted derivatives (Scheme 1.6) that represent the most frequently studied ferrocene-derived ligand types.[48,49] Nonetheless, attention attracted also other derivatives, for instance the ferrocene-derived

polyphosphanes.[60] Nowadays, the chemistry of ferrocenes comprises the broad scope of various ligand classes, amongst them monodentate[61] and bidentate donors.[62] Still, the most studied are the phosphanylferrocenes bearing at least one phosphanyl group bound directly to the ferrocene backbone.

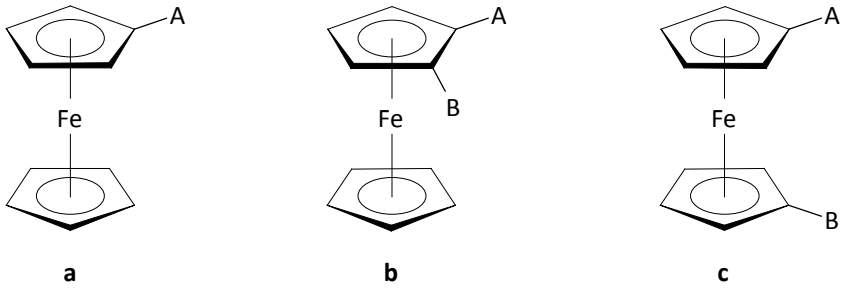

Scheme 1.6. Mono- and disubstituted unsymmetric ferrocene derivatives.

The number of monodentate phosphanylferrocene donors is rather scarce in comparison to bidentate derivatives. However, they found distinct applications in homogeneous catalysis. For instance, a series of ligands $FcPR_2$ (Fc = ferrocenyl) was utilized in Baylis-Hillman reaction of aldehydes with acrylates (Scheme 1.7).

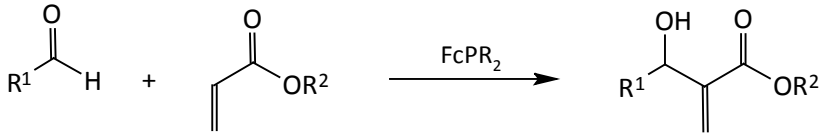

Scheme 1.7. Baylis-Hillman reaction of aldehydes and acrylates.

The ferrocene-derived ligands performed in this organocatalytic reaction remarkably better than PPh_3 and PCy_3, with $FcPEt_2$ being the most active catalyst.[63] Some of sterically demanding monodentate phosphanylferrocenes gave rise to active catalyst for palladium catalysed cross-coupling reactions of challenging substrates. For instance, the complexes derived from FcP(*t*-Bu)$_2$ (**I**) and the cognate ligand Q-phos (Scheme 1.8) performed efficiently amination of aryl halides and Suzuki-Miyaura cross-coupling of aryl chlorides and unactivated aryl bromides.[64]

The chemistry of bidentate phosphanylferrocene donors is represented predominantly by two ligand classes, namely by 1,1′-disubstituted and 1,2-disubstituted derivatives (Scheme 1.6). The chiral 1,2-disubstituted bidentate phosphanylferrocene donors became probably the most successful ferrocene ligands.[62a,b,g] They have found extensive applications in

asymmetric catalysis, even at industrial scale. Very likely the largest enantioselective catalytic process in industry makes use of chiral ferrocene ligand Xyliphos in the synthesis of herbicide (*S*)-metolachlor (Scheme 1.9) via iridium-catalysed asymmetric hydrogenation reaction.[65]

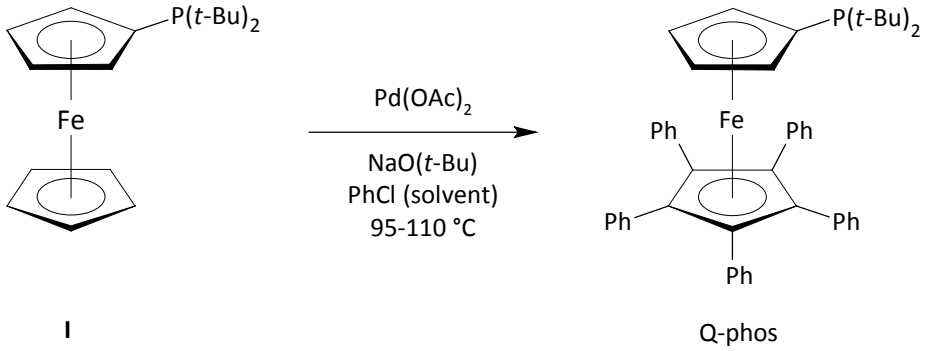

Scheme 1.8. Preparation of phosphanylferrocene ligand Q-Phos.

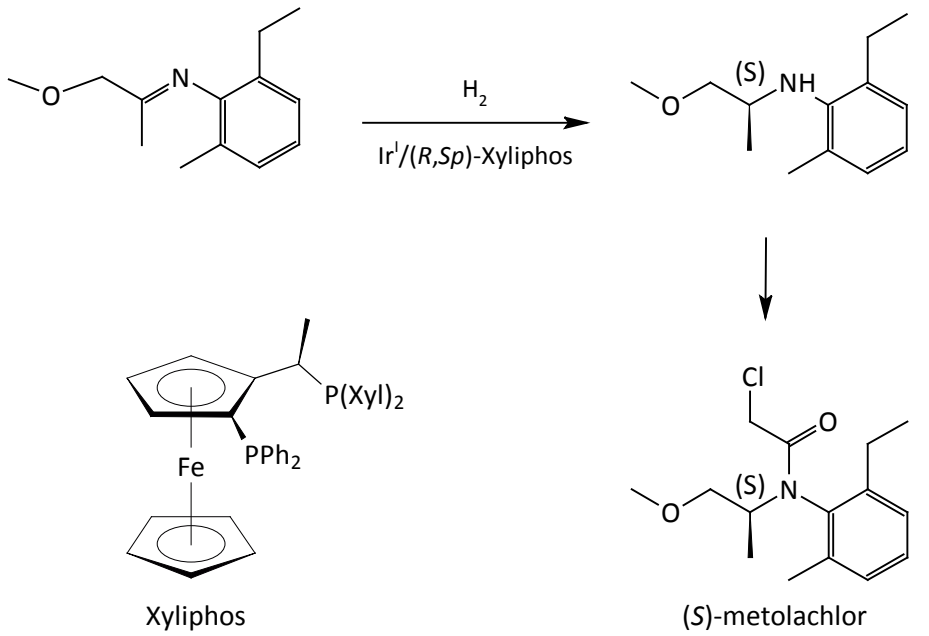

Scheme 1.9. Industrial synthesis of herbicide (*S*)-metolachlor (Xyl = 3,5-dimethylphenyl).

The initial impulse preceding the interest in the chemistry of planar-chiral phosphanylferrocene ligands was the discovery of highly diastereoselective *ortho*-lithiation of (*R*)-*N*,*N*-dimethyl-1-ferrocenylethylamine (Ugi's amine)[66] and the preparation of chiral *P*,*N*-ligand PPFA (Scheme 1.10).[67]

In the following years this strategy was supplemented by other efficient chiral *ortho*-directing groups, for instance sulfoxides, acetals or oxazolines.[68,69,70] Moreover, it was

found that dimethylamino group in PPFA-type ligands can be replaced with secondary phosphanes with retention of the configuration at the stereogenic carbon atom.[71] This discovery led to the development of the very successful Josiphos-type ligands (Scheme 1.10). Other nucleophiles can be used equally well.[62b,g;72]

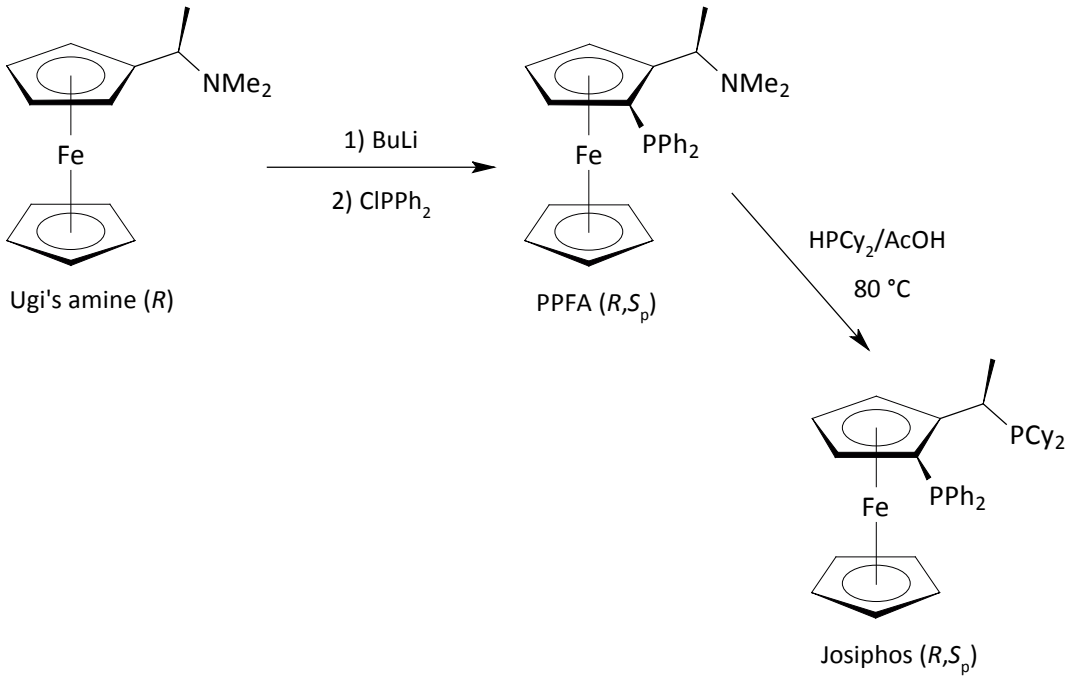

Scheme 1.10. Preparation of planar chiral phosphanylferrocene ligands PPFA and Josiphos.

The planar chiral phosphanylferrocene donors are readily accessible ligands that may be easily modified by a plenty of synthetic methods to match the requirements of a particular catalytic reaction and, accordingly, they have found wide use in asymmetric organic synthesis.[62b,g]

The archetypal representative of the non-chiral 1,1′-disubstituted bidentate phosphanylferrocene donors is definitely 1,1′-bis(diphenylphosphanyl)ferrocene (dppf, Scheme 1.11).[73] Dppf is a remarkably versatile ligand owing to its ability to change molecular conformation and thus meet the coordination and steric demands of the coordinated metal centre.[74] The ferrocen-1,1′-diyl moiety may adopt the appropriate arrangement of donor groups by rotation of the cyclopentadienyl rings or, in a lesser extent, by their tilting. The conformational flexibility of dppf may be expressed by the values of "bite angles" found in its chelated transition metal complexes.[75] The observed values of the bite angles range from 90° to 120°, affecting greatly the steric and electronic

properties of coordinated dppf.[76] This coordination versatility brought about the practical success of dppf[77] and the cognate ligands (Scheme 1.11) [78,79] in transition metal catalysis.

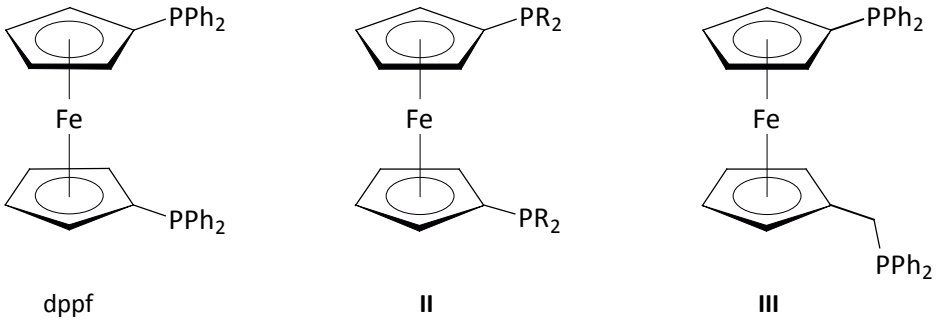

Scheme 1.11. Archetypal bidentate phosphanylferrocene ligand 1,1′-bis(diphenylphosphanyl)ferrocene (dppf) and its congeners.

The remarkable versatility of dppf and its congeners motivated search for analogous 1,1′-disubstituted mixed-donor ligands combining the phosphanyl moiety with a donor group of different type.[62b-d;80] This diversification of the two donor groups may further increase coordination versatility of the ligand, by altering their ligating preferences. The ligands containing at least two donor groups that differ in their nature according to the Pearson's theory of hard and soft acids and bases (HSAB)[81] are denoted as "hybrid ligands".[82] The hybrid ligands may coordinate to the metal centre in diverse coordination modes depending on the nature of transition metal (according to HSAB theory), *e.g.*, as monodentate or multidentate (chelating or bridging) ligands. The coordination modes of the hybrid ligands may be in principal interchangeable and dependent of other factors (competition with another donor group or replacement with an external reagent). A plenty of 1′-functionalised dppf analogues have been reported (Scheme 1.12).

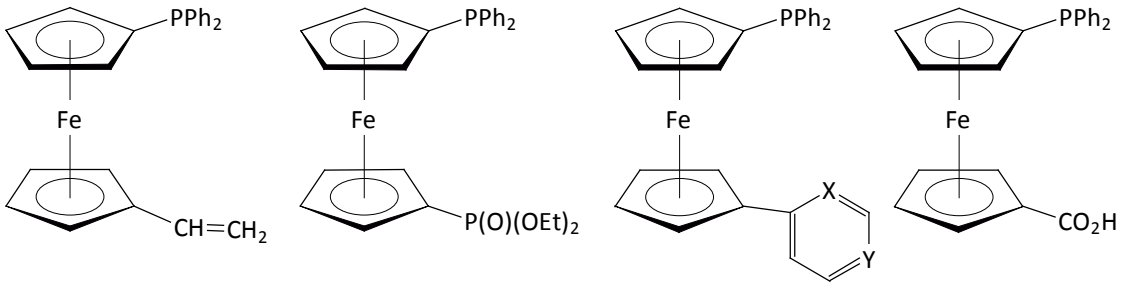

Scheme 1.12. Selected 1′-functionalised phosphanylferrocene ligands.

As representative examples can serve derivatives bearing vinyl, [83] phosphonate, [84] carboxyl[85] or pyridyl[86] substituents (Scheme 1.12) that were studied in our group. These compounds were typically utilized as ligands in transition metal complexes and for metal-catalysed C–C bond forming reactions. 1′-(Diphenylphosphanyl)ferrocene-1-carboxylic acid (Hdpf in Scheme 1.12)[85] is a typical representative of hybrid ligands and its coordination preferences towards selected metal ions were thoroughly studied. [87] Expectedly, Hdpf coordinates as a simple monodentate donor when reacted with soft metal ions. For instance, a series of square-planar complexes *trans*-[PdX_2(Hdpf-κ*P*)$_2$] (X = Cl, Br) was obtained by the reaction of two equivalents of Hdpf with palladium(II) salts $K_2[PdCl_4]$ or [PdX_2(cod)] (X = Cl, Br; cod = η^2:η^2-cycloocta-1,5-diene).[88] Analogous reactions with different platinum(II) salts allowed isolation of both *cis*-[$PtCl_2$(Hdpf-κ*P*)$_2$] and *trans*-[$PtCl_2$(Hdpf-κ*P*)$_2$] owing to kinetic inertness of platinum(II) complexes.[88] *P*-monodentate coordination of Hdpf was observed also in the case of other transition metal-ions, for instance copper(I) and mercury(II).[87,89,90]

Two different coordination modes of Hdpf, *i.e.*, *P*-monodentate and *O,P*-bidentate, were encountered in a particular series of rhodium(I) complexes. The reaction of rhodium(I) precursors [Rh(acac)(CO)(L)] (L = PPh_3, PCy_3 or $FcPPh_2$; acac = pentan-2,4-dionate(1–)) with Hdpf afforded the chelated complexes [Rh(CO)(L)(dpf-κ*O,P*)] (dpf$^-$ = 1′-(diphenylphosphanyl)ferrocene-1-carboxylate). [91] Another rhodium(I) complex, *i.e.*, [Rh(Hdpf-κ*P*)(dpf-κ*O,P*)] **VII** resulting from the reaction of [Rh(acac)$(CO)_2$] with two equivalents of Hdpf, features the protonated (*P*-monodentate) as well as the deprotonated (*O,P*-bidentate) form of the ligand (Scheme 1.13).[91]

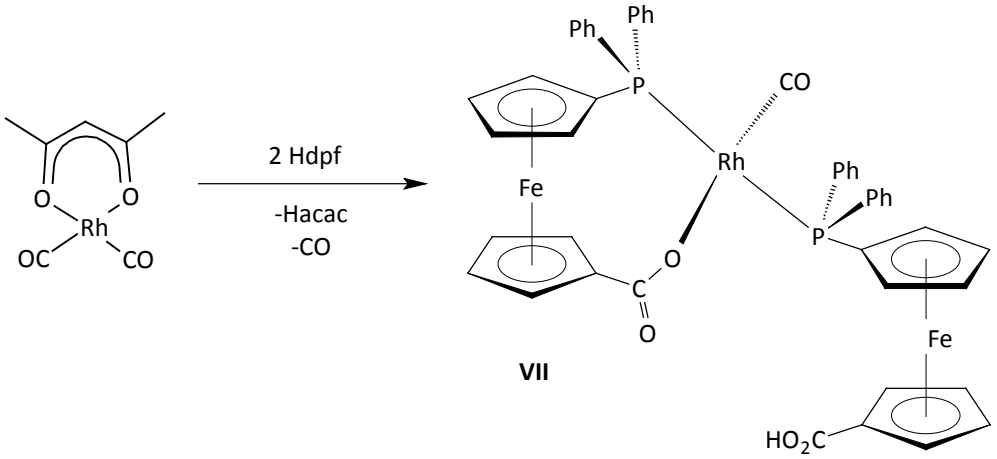

Scheme 1.13. Preparation of the chelated rhodium(I) complex **VII** bearing *O,P*-bidentate (dpf$^-$) and *P*-monodentate form of Hdpf (Hacac = pentan-2,4-dion).

The spectral characteristics of **VII** indicate hemilabile coordination of dpf^- anion resulting in rapid exchange of the carboxylic proton between the protonated and the deprotonated form. Thus, the dynamic behavior results in averaging of signals observed in ^{31}P NMR, while IR spectra display clearly both ligand forms. Complex **VII** proved to be an efficient pre-catalyst for hydroformylation of 1-hexene giving rise to a recyclable catalyst.[92]

Although Hdpf coordinates in the most cases preferentially via its phosphane group, reported was also exclusive coordination by carboxylate group. Deprotonated Hdpf was shown to act as an *O,O′*-bidentate donor towards titanocene moiety in complex **VIII** (Scheme 1.14) obtained upon reacting Hdpf with titanocene $[(\eta^5\text{-}C_5HMe_4)_2Ti(\eta^2\text{-}Me_3SiC{\equiv}CSiMe_3)]$.[93]

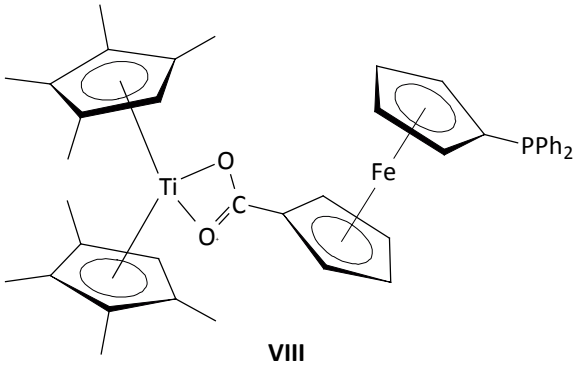

VIII

Scheme 1.14. The bis(metallocene) complex $[(\eta^5\text{-}C_5HMe_4)_2Ti(dpf\text{-}\kappa O,O')]$ **VIII** bearing dpf^- anion coordinated solely via its carboxylate group.

The carboxyl group may serve not only as a supplementary donor group, but also as a site of further functionalization and structural diversification of the molecule. Recently, Hdpf was utilized as an anchoring agent to anchor the ruthenium pre-catalysts to the solid support (MCM-41).[94] In another study, transformation of Hdpf into corresponding secondary amides $Ph_2fcCONR_2$ (fc = ferrocen-1,1′-diyl) and subsequent reaction with group 6 metal carbonylates afforded *P*-chelated Fisher-type carbenes.[95] More recently, Hdpf served as a synthetic precursor for for phosphanylferrocene heterocycles,[96] including chiral phosphanylferrocene oxazolines.[97] Nonetheless, the most frequently studied Hdpf derivatives are phosphane-amides bearing various simple and purposeful fragments in the amide part of the molecule.

Conversion of Hdpf into corresponding amides enables one to design the corresponding phosphane-amide for a specific purpose. The amide part of the molecule may serve as a

new functional periphery or a structure directing element (the overall effect is usually collaborative).[98] For instance, amidation of Hdpf was utilized to install new donor groups into the molecule and to bring them into specific positions. The group of structurally-related phosphane-amides modified with 2- (**IX**) and 4-pyridyl (**X**) substituents (Scheme 1.15) showed remarkably flexible coordination behaviour especially towards group 12 metal ions.[99] Different coordination assemblies were obtained depending on the spatial properties of the respective ligand, ranging from discrete oligonuclear structures to coordination polymers. Besides, while the phosphane-amide **IX** coordinated to palladium(II) as a *trans*-spanning *N*,*P*-donor when reacted with one equivalent of [Pd(cod)Cl_2] (cod = η^2:η^2-cycloocta-1,5-diene), its ethylene-bridged analogue **XI** behaved as a bridging ligand yielding the dinuclear complex [(μ-**XI**-*N*,*P*)$_2${$PdCl_2$}].[100]

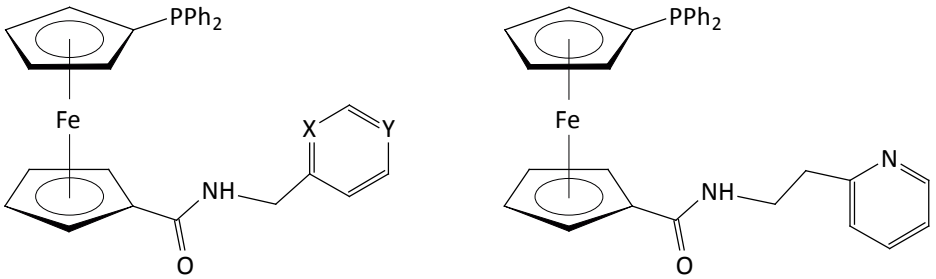

IX (X = N, Y = CH), **X** (X = CH, Y = N) **XI**

Scheme 1.15. The phosphane-amides modified with pyridyl-based donor groups.

The amide-moiety itself is a potential donor group. It may coordinate to a metal centre as either a neutral *O*- or an anionic *N*-donor. Hence, all the phosphane-amides derived from Hdpf may be classified as hybrid ligands. Their flexibility was demonstrated by the coordination study of the glycine-based phosphane-amide $Ph_2PfcCONHCH_2CO_2Me$ (**XII,** fc = ferrocene-1,1′-diyl) towards palladium(II) (Scheme 1.16).[101] The palladium(II) complex [(L^{CN})Pd(Cl)(**XII**-κ*P*)] (**XIII**) bearing 2-[(dimethylamino-κ*N*)methyl]phenyl-κC^1 (L^{CN}) auxiliary ligand afforded *O*,*P*-chelated complex [(L^{CN})Pd(**XII**-κ^2*O*,*P*)]ClO_4 (**XIV**) when reacted with silver(I) perchlorate. The *N*,*P*-chelated complex [(L^{CN})Pd(**XII**-κ^2*N*,*P*)] (**XV**) was obtained upon reacting **XI** with potassium *tert*-butoxide (Scheme 1.16).

In another study, Hdpf and its planar-chiral analogue[102] (S_p/R_p)-2-(diphenylphosphanyl)-ferrocenecarboxylic acid served together with the selected chiral amino acids as synthons for the preparation of chiral phosphane-amides suitable for use in asymmetric catalysis (Scheme 1.17). The obtained library of ligands was tested in copper-catalysed asymmetric

conjugate addition of diethylzinc to chalcones,[103] and in palladium-mediated asymmetric allylic substitution.[104] Interestingly, the phosphane-amides derived from Hdpf provided in the copper-catalysed conjugate addition better reactivity and enantioselectivity than their planar-chiral counterparts (although they combine planar and central chirality). The authors assigned the enhanced asymmetric induction obtained by 1′-functionalised derivatives to *O,P*-chelating coordination that brings the asymmetric centre into the vicinity of the catalytic site, but does not destabilise the reaction intermediate.[103]

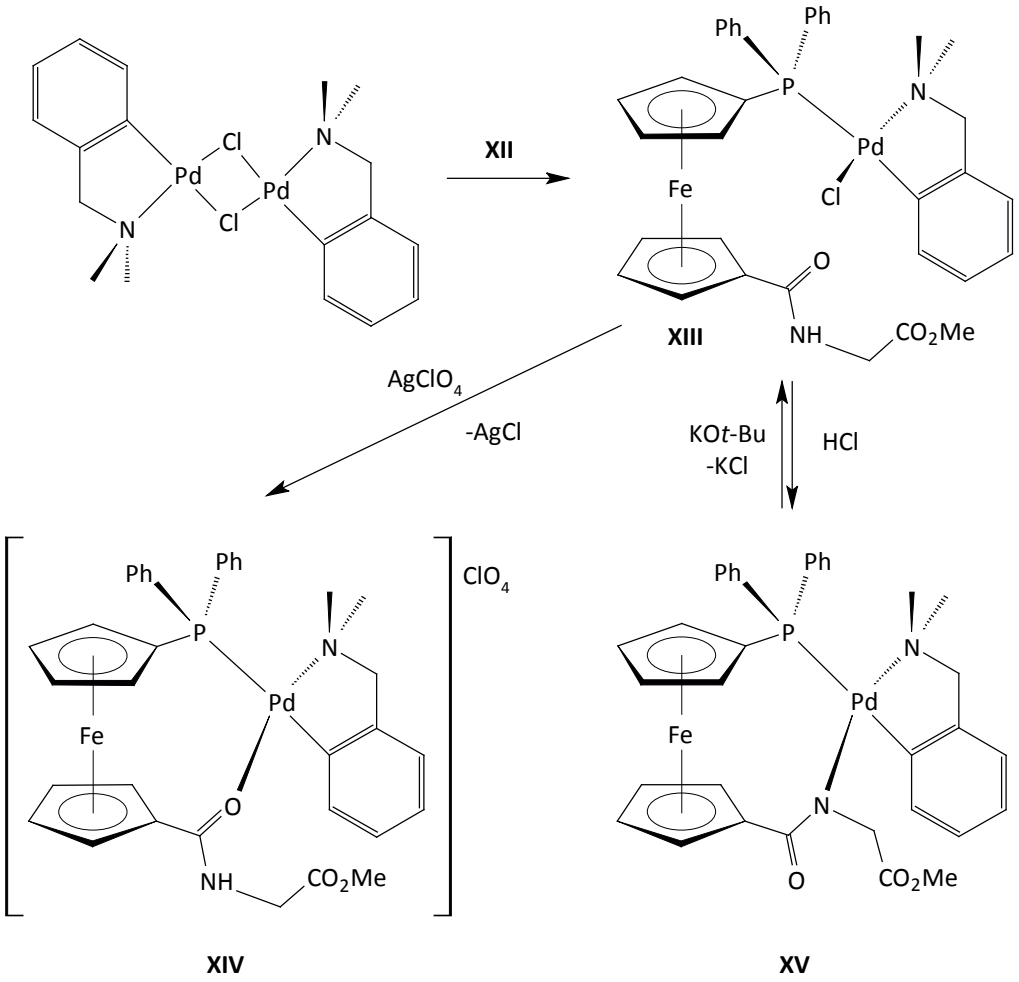

Scheme 1.16. Variable coordination modes of phosphane-amide **XII** towards palladium(II).

Conversion to amides can also be used to introduce hydrophilic substituents. This approach was used in the preparation of phosphane-amides bearing 2-hydroxyethyl pendant arms at the amide nitrogen (Scheme 1.18).[105] The 2-hydroxyethyl-amide moiety renders the molecule more hydrophilic and also participates in supramolecular interactions in the solid state (as evidenced by X-ray crystallography). The palladium(II) complexes

trans-[$PdCl_2$(L-κ*P*)$_2$] derived from **XXII** and **XXIII** were tested in Suzuki-Miyaura cross-coupling reaction of aryl bromides in aqueous media. It is noteworthy that complex *trans*-[$PdCl_2$(**XXII**-κ*P*)$_2$] gave rise to active catalyst for coupling of 4-bromotoluene and phenylboronic acid that might be reused under biphasic conditions (toluene–water, 1:1 v/v) in five consecutive reaction runs without any loss of efficiency.[105]

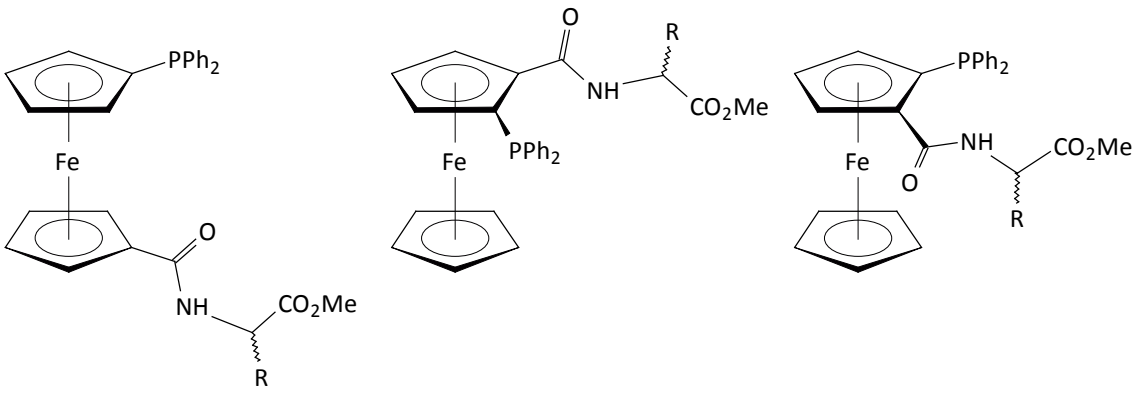

(*S*)-**XVI** [R = (*S*)-Me] (*S,Sp*)-**XIX** [R = (*S*)-Me] (*S,Rp*)-**XIX** [R = (*S*)-Me]

(*R*)-**XVI** [R = (*R*)-Me] (*R,Sp*)-**XIX** [R = (*R*)-Me]

(*S*)-**XVII** [R = (*S*)-*i*-Pr] (*S,Sp*)-**XX** [R = (*S*)-*i*-Pr]

(*R*)-**XVII** [R = (*R*)-*i*-Pr] (*R,Sp*)-**XX** [R = (*R*)-*i*-Pr]

(*S*)-**XVIII** [R = (*S*)-CH_2Ph] (*S,Sp*)-**XXI** [R = (*S*)-CH_2Ph]

(*R*)-**XVIII** [R = (*R*)-CH_2Ph] (*R,Sp*)-**XXI** [R = (*R*)-CH_2Ph]

Scheme 1.17. Amino-acid conjugates with phosphanylferrocenecarboxylic acids.

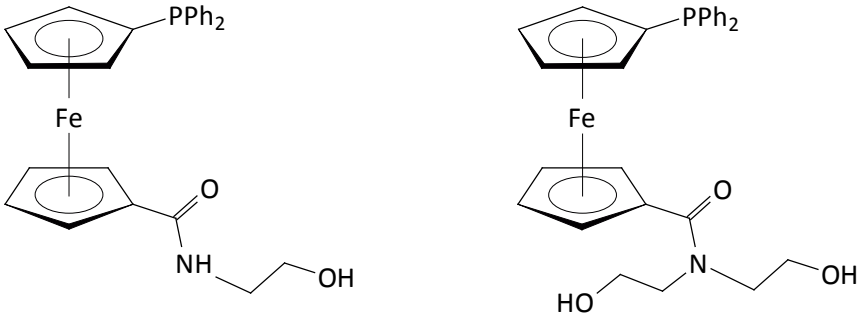

XXII **XXIII**

Scheme 1.18. Phosphane-amides bearing 2-hydroxyethyl pendant arms.[a]

[a] The phosphane-amides **XXII** and **XXIII** are denoted as **1** and **2** in Chapter 2.

Aims of the Thesis

As a continuation of the research that has been done in our group during the study of coordination behaviour and catalytic use of phosphanylferrocenecarboxylic acids, we focused our attention in the last couple of years towards their derivatives, particularly carboxamides. Basically, we made use of the phosphanylferrocenecarboxylic acids as synthons for the preparation of specifically functionalised donors. A particular attention was paid to phosphane-amides derived from 1′-(diphenylphosphanyl)ferrocene-1-carboxylic acid (Hdpf). The conjugation of Hdpf with suitable amines proved to be a convenient method to introduce functional fragments, for instance an additional donor group, an asymmetric centre or a hydrophilic pendant (see previous Chapter). The main goal of the presented Thesis was to continue in their recent research and to broaden the scope of phosphane-amides derived from Hdpf by the novel donors equipped with highly polar substituents.

The primary objective of this Thesis was to expand my previous work done on phosphane-amides bearing 2-hydroxyethyl pendant arms **1** (**XXII** in Scheme 1.18) and **2** (**XXIII** in Scheme 1.18). [b] The intention was to extend the series of such hydroxyamides by two novel, structurally related donors (**3** and **4**, Scheme 1.19). Simultaneously, a series of phosphane-amides bearing anionic sulfonate tags (**17-19**, Scheme 1.19) was designed and prepared.

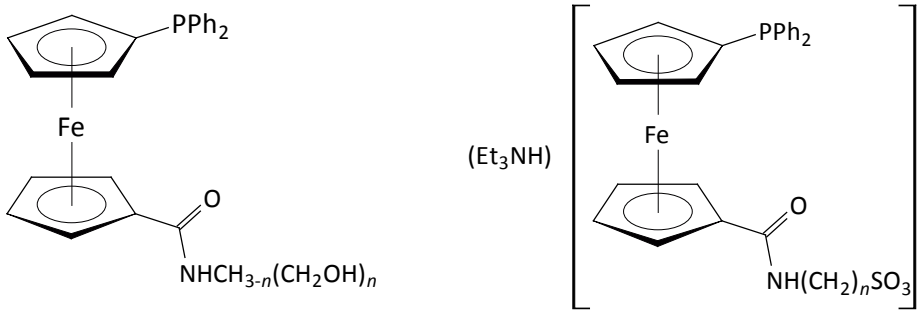

3 (*n* = 2), **4** (*n* = 3)

17 (*n* = 1), **18** (*n* = 2), **19** (*n* = 3)

Scheme 1.19. The novel hydrophilic phosphane-amides derived from Hdpf.

[b] The phosphane-amides **XXII** and **XXIII** are denoted as **1** and **2** in the following text.

The incorporation of the hydrophilic pendants was supposed to render the resulting donors more soluble in aqueous media and endow them with attractive ligating properties, since the phosphanylferrocene-carboxamides can be looked upon as typical hybrid ligands (it simultaneously possesses *O*-, *N*- and *P*-donor atoms). Besides, the hydrophilic pendant arms keep the polar substituents at the periphery of the molecule, limiting the interference with the coordination sites.

The secondary objective of this Thesis was to assess the catalytic potential of the newly prepared ligands in transition metal-mediated organic reactions in aqueous media and to study the influence of the hydrophilic pendants on their catalytic performance.

Chapter 2

Concise Summary of Results

The successful catalytic testing of phosphane-amides **1** and **2** derived from Hdpf (Scheme 1.18) in palladium(II)-catalysed Suzuki-Miyaura cross-coupling of aryl bromides and boronic acids in aqueous media[105] was the decisive impulse for the search of other promising structures. For this reason, the first part of my Ph.D. Thesis was devoted to continuation of the previous research and the family of these Hdpf-based hydroxyamide ligands was extended by two new compounds **3** and **4** resulting from bis- and tris(hydroxymethyl)methanamine (Scheme 2.1, Appendix 1). The newly synthesized derivatives complete the series of structurally related phosphane-amides of the general formula $Ph_2PfcCONHCH_{3-n}(CH_2OH)_n$ (n = 1-3; fc = ferrocene-1,1′-diyl).

The first attempt to synthesize hydroxyamide **4** was inspired by the synthetic procedure reported for the preparation of compound **2**. Thus, Hdpf pentafluorophenyl ester **5** was reacted with 2-amino-2-(hydroxymethyl)propan-1,3-diol (TRIS) in the presence of 4-(dimethylamino)pyridine (DMAP) in pure *N*,*N*-dimethylformamide (DMF) (Scheme 2.1). The subsequent isolation by column chromatography and recrystallization from ethyl acetate-hexane mixture afforded compound **4** only in a rather poor yield (27 %). Hence, an alternative amide coupling agent, *i.e.*, EEDQ (2-ethoxy-1-ethoxycabonyl-1,2-dihydroquinoline), was employed. This reagent was used earlier for a coupling of TRIS with organic carboxylic acids, avoiding a possible formation of esters.[106] Gratifyingly, the direct coupling of Hdpf with an excess of TRIS in the presence of EEDQ and 4-(dimethylamino)pyridine (DMAP) in pyridine (120 °C/1 h) afforded **4** in a good yield (56 %) after chromatographic purification and recrystallization from hot ethyl acetate-hexane (Scheme 2.1). Hydroxyamide **3** was prepared similarly from Hdpf and 2-amino-1,3-propanediol (Scheme 2.1).

Single-crystal X-ray diffraction analysis of thus prepared donors revealed extensive supramolecular association. The molecular packing of **3** and **4** is dominated by hydrogen bonding interactions that are very similar in their patterns, although they differ in their complexity. The simplified view of hydrogen bonded arrays found in crystal structures of **3** and **4** are depicted in Figure 2.1.

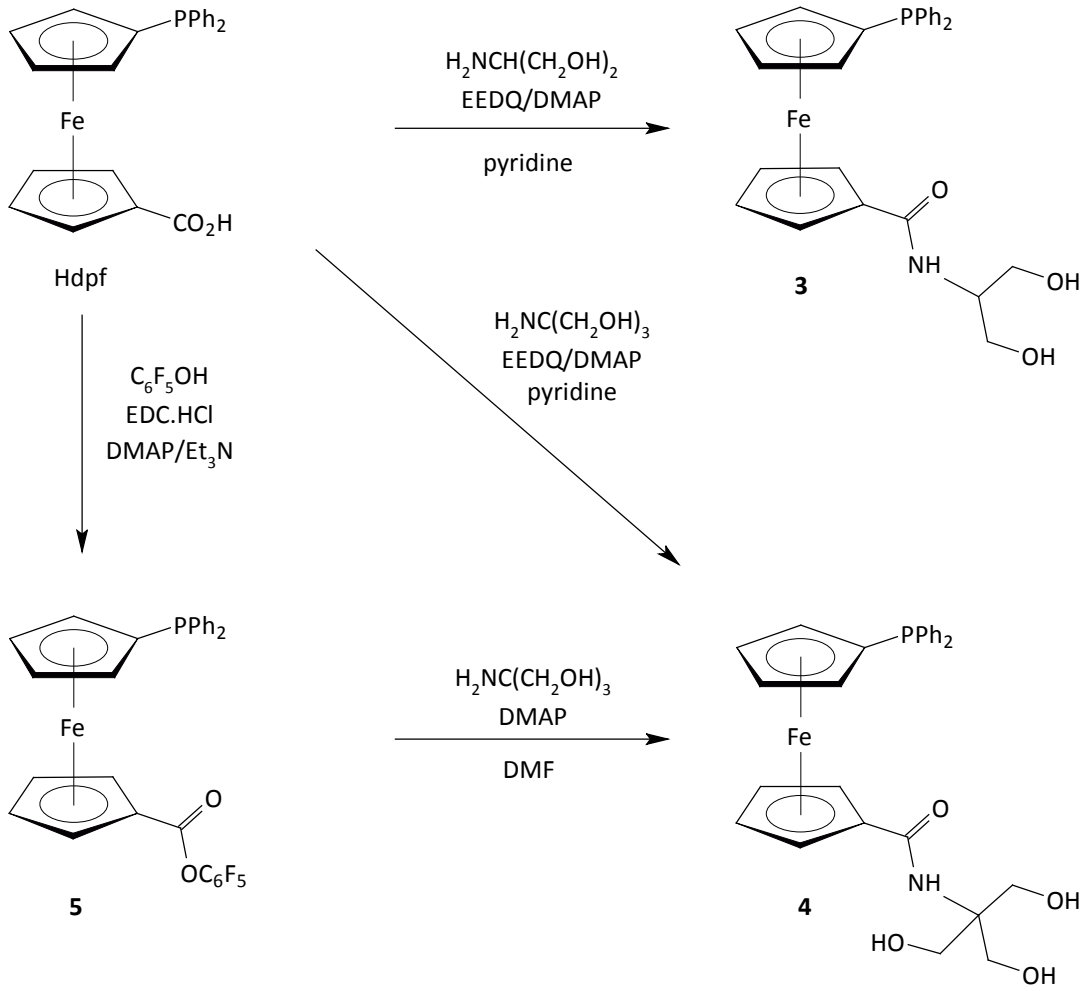

Scheme 2.1. Synthesis of hydroxyamides **3** and **4** (DMAP = 4-(dimethylamino)pyridine, DMF = *N*,*N*-dimethylformamide, EDC·HCl = *N*-ethyl-*N*'-[(3-dimethylamino)propyl]-carbodiimide hydrochloride, EEDQ = 2-ethoxy-1-ethoxycabonyl-1,2-dihydroquinoline).

In their crystals, the molecules of both compounds associate into centrosymmetric dimers that constitute the basic structural motif and that, in turn, assemble to form parallel hydrogen-bonded sheets.

The molecules of **3** associate into dimers via O2-H2O···O1 intermolecular hydrogen bonds (Figure 2.1a) that are supported by C8-H8···O3 intramolecular interactions. Thus formed dimers are connected by pivotal N-H1N···O2 contacts to four adjacent dimeric units giving rise, in combination with supporting interactions through O3-H3O···P and C2-H2···O3 contacts, to layers that are parallel to the crystallographic *bc* plane with the (diphenylphosphanyl)ferrocenyl moieties oriented above and below these layers (Figure 2.2.a).

The structural motif found in the crystal structure of **3** is practically identical with that reported previously for hydroxyamide **1**.[105] The added hydromethyl group participates in

supramolecular association by the rather unusual O3-H3O···P hydrogen bonds. This type of interactions was reported for several hydroxyphosphanes and adducts of phosphanes with alcohols.[107]

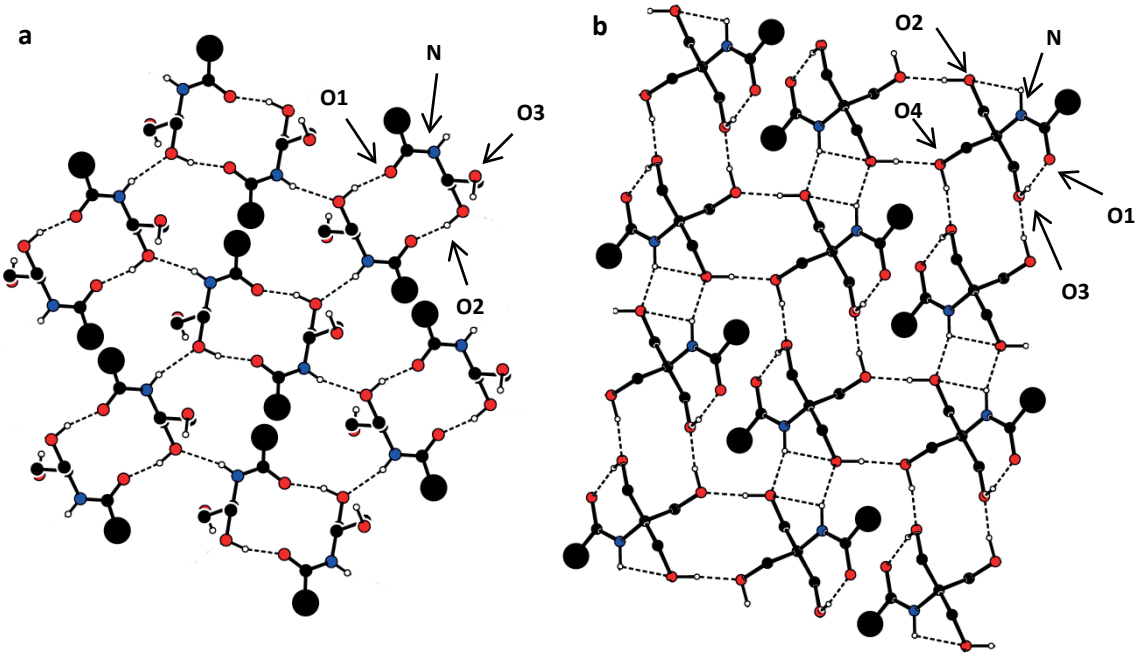

Figure 2.1. Sections of hydrogen-bonded arrays found in the crystal structures of **3** (a) and **4** (b). For clarity, only the N/O-H hydrogens are shown and the bulky (diphenylphosphanyl)ferrocenyl moieties are replaced with black circles.

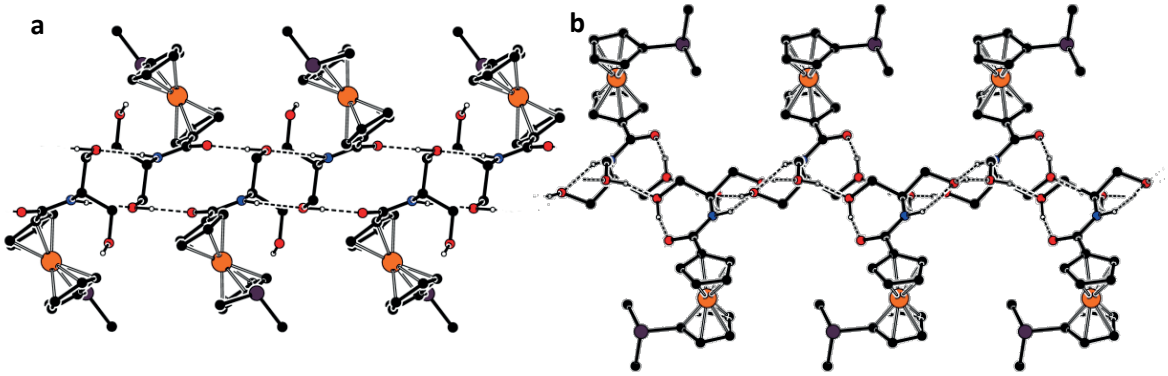

Figure 2.2. View of the crystal packing of **3** (a) and **4** (b). For clarity, only the N/O-H hydrogens and pivotal carbons from the phenyl rings are shown.

Each molecule of amide **4** associates with three inversion-related adjacent molecules into three types of centrosymmetric dimers (Figure 2.1b). Thus, the supramolecular hydrogen bonded array found in the crystal structure of **4** may be described as an assembly of three basic structural motifs. Each molecule of amide **4** acts simultaneously as threefold donor and threefold acceptor of hydrogen bonds for adjacent molecules. The combination of

N/O-H···O interaction gives rise to hydrogen-bonded layers that are parallel to crystallographic *ab* plane, with (diphenylphosphanyl)ferrocenyl moieties pointing above and below this plane (Figure 2.2b). Although the hydrogen-bonded array is stabilised by intramolecular interactions N-H1N···O2 and O3-H3O···O1, it lacks supportive soft C-H···O contacts that are observed in the crystal structure of **3**.

For an evaluation of catalytic properties of the hydroxyamide phosphanes I choose the ruthenium-promoted redox isomerization of allylic alcohols into unsaturated carbonyl compounds. This catalytic reaction represents a useful atom-economical process that has been growing in importance over the last decade.[108] Recently, arene-ruthenium(II) complexes of type [(η^6-arene)$RuCl_2$(L)], where L represents a hydrophilic ligand, were shown to be efficient pre-catalysts for redox isomerization of allylic alcohols in aqueous media, which prompted my interest.[109]

For the intended catalytic testing, a series of arene-ruthenium(II) complexes **6-8** (Scheme 2.2) was prepared from hydroxyamide ligands **1**, **3** and **4** by the standard bridge-cleavage reactions of the corresponding dimers [(η^6-arene)Ru(μ-Cl)Cl]$_2$.

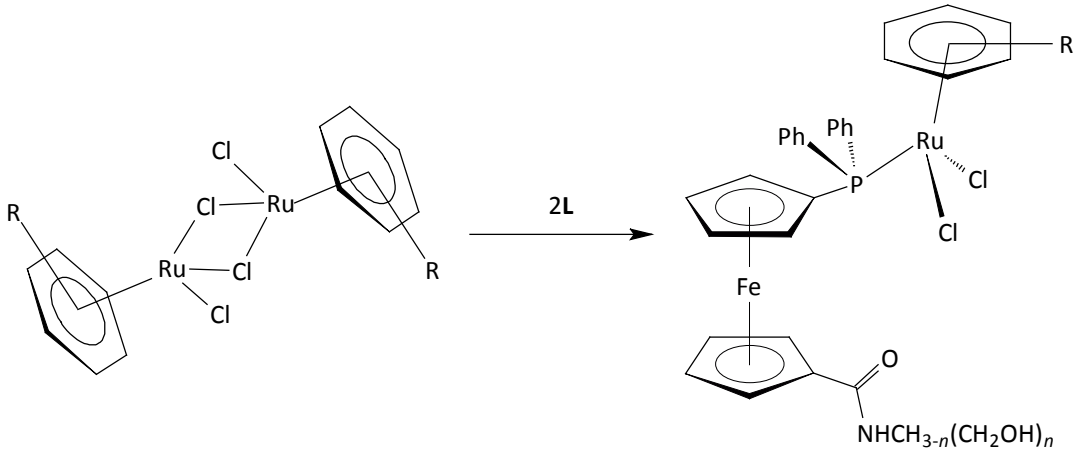

	Ligand (n)	1	3	4
	benzene	**6a**	**7a**	**8a**
arene =	p-cymene	**6b**	**7b**	**8b**
	C_6Me_6	**6c**	**7c**	**8c**

Scheme 2.2. Preparation of arene-ruthenium(II) complexes **6-8**.

The initial catalytic experiments were conducted to optimize the reaction conditions.[110] The most easily accessible ruthenium(II) complex **6b** was chosen as the representative,

being assessed in the isomerization of 1-octen-3-ol as the model substrate in various solvents (0.5 mol. % of **6b** and 2.5 mol. % of KOBu-*t*, Scheme 2.3).

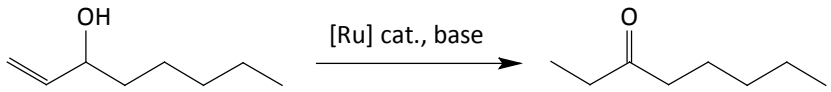

Scheme 2.3. The redox isomerization of 1-octen-3-ol into octan-3-one.

The reaction performed at 80 °C was completed within 1 h in 1,2-dichloroethane and dioxane. The same reaction performed in *N*-methylpyrrolidone afforded the carbonyl product only with 33 % conversion, while the use of *N*,*N*-dimethylformamide, *N*,*N*-dimethylacetamide, dimethylsulfoxide, propionitrile and 1-propanol gave no conversion to carbonyl compound. Interestingly, the reaction in pure water afforded octan-3-one with 55 % conversion, but no reaction was observed in dioxane-water mixture (1:1; v/v). Subsequent experiments in 1,2-dichloroethane revealed that the presence of the catalytic amount of a base is essential for the isomerization reaction, since the isomerization of 1-octen-3-ol did not proceed without base added, while addition of any common base gave complete conversion to octan-3-one within 1 h.

Next, the whole series of prepared arene-ruthenium(II) complexes was evaluated in the model isomerization reaction in order to assess the influence of the catalyst structure (0.5 mol. % Ru, 2.5 mol. % KOBu-*t*, 1,2-dichloroethane, 80 °C/1 h). The results summarized in Table 2.1 indicate that the influence of the phosphane ligand is substantial.

Table 2.1. Redox isomerization of 1-octen-3-ol into octan-3-one using **6-8**.[a]

phosphane/arene	Pre-catalyst/NMR yield[b] [%]		
	C_6H_6	*p*-cymene	C_6Me_6
1	100 **(6a)**	100 **(6b)**	98 **(6c)**
3	100 **(7a)**	98 **(7b)**	37 **(7c)**
4	29 **(8a)**	55 **(8b)**	27 **(8c)**

[a] 1-octen-3-ol (1.0 mmol), [Ru] pre-catalyst (0.5 mol. %), KOBu-*t* (2.5 mol. %), 1,2-dichloroethane (4 mL), 1 h/80 °C. [b] Yields determined by NMR spectroscopy.

Complexes derived from ligand **4** performed considerably worse than those derived from ligands **1** and **3**. On the other hand, the influence of the arene ligand was less significant. Nevertheless, the obtained results indicate that complexes possessing the most electron-rich and sterically demanding arene ligand, *i.e.*, hexamethylbenzene, afford lower conversions than their benzene and *p*-cymene counterparts.

The most active pre-catalyst **6b** chosen on the basis of the previous experiments was further evaluated in redox isomerization of various substituted allylic alcohols (Scheme 2.4). The catalytic experiments were designed to probe the catalytic properties of **6b** in isomerization reactions of allylic alcohols bearing substituents at the double bond and to compare in detail its performance in 1,2-dichloroethane and water. The obtained results are collected in Table 2.2. It is obvious, that the presence of any substituent at the double bond in both primary and secondary allylic alcohols results in relatively lower conversions regardless of the solvent used. Furthemore, the formation of unsaturated carbonyl compound as a side-product (Scheme 2.4), was noticed in some experiments performed in 1,2-dichloroethane (Table 2.2).

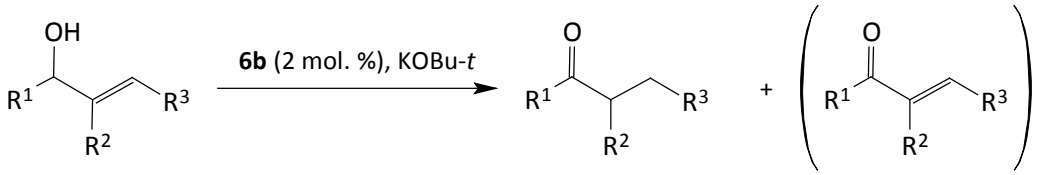

Scheme 2.4. Redox isomerization of substituted allylic alcohols.

Table 2.2. Redox isomerization of primary and secondary allylic alcohols using complex **6b** in 1,2-dichloroethane and water.[a]

Substrate				NMR yield [%][b]	
Entry	R^1	R^2	R^3	1,2-dichloethane	water
1	Me	H	H	78 (3)	17
2	H	Me	H	7 (0)	< 5
3	H	H	Me	25 (0)	< 5
4	Me	H	Me	23 (37)	< 5
5	Ph	H	H	79 (0)	29
6	H	H	Ph	30 (6)	6
7	Ph	H	Ph	40 (0)	100

[a] Allylic alcohol (1.0 mmol), **6b** (2 mol. %), KOBu-*t* (5 mol. %), solvent (4 mL), 80 °C, 20 h. [b] Yields determined by NMR analysis. The yield of α,β-unsaturated ketone is given in parentheses.

The reactions conducted in pure water afforded generally lower conversions as compared with those in 1,2-dichloroethane. Only the secondary allylic alcohols without any substituents at the double bond, *i.e.*, but-3-en-2-ol (entry 1, Table 2.2) and 1-phenylprop-2-en-1-ol (entry 5, Table 2.2), were converted to the corresponding ketones in an appreciable extent. Rather surprisingly, 1,3-diphenylprop-2-en-1-ol (Entry 7, Table 2.2) was cleanly and completely isomerized in pure water to 1,3-diphenylprop-1-one. This result was

ascribed to the highly hydrophobic nature of this allylic alcohol that resulted in acceleration of the process due to "reaction on water".[12d]

An attempted crystallization of arene-ruthenium(II) complex [(η^6-C_6Me_6)$RuCl_2$(**2**-κ*P*)] resulted in the formation of a decomposition product formulated as [(μ-Cl)$_3${Ru^{II}(η^6-C_6Me_6)}$_2$][$Fe^{III}Cl_4$] **9** (Figure 2.3, Appendix 2) based on X-ray diffraction analysis.

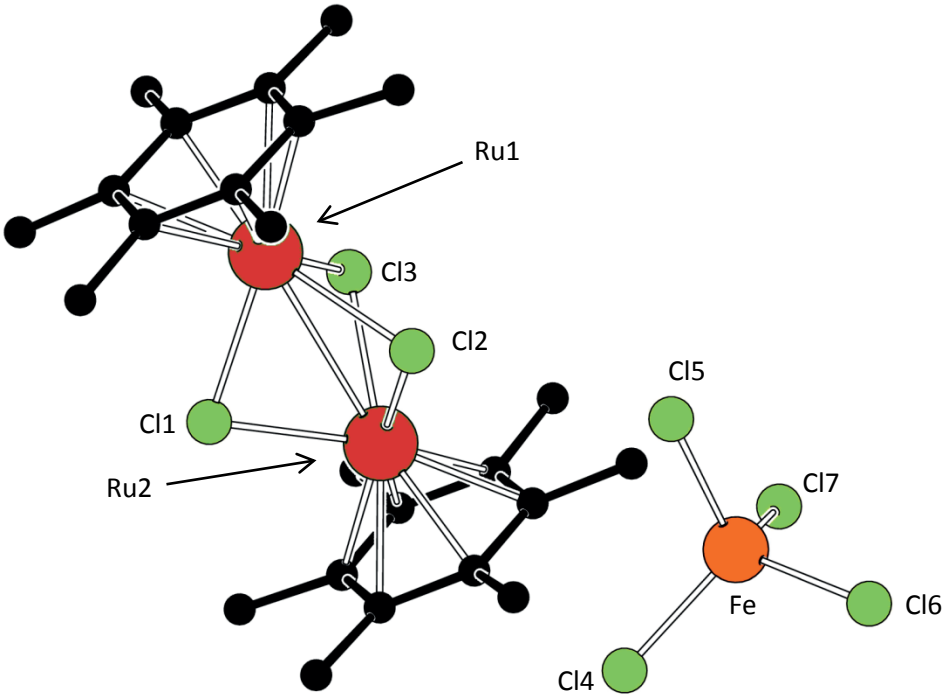

Figure 2.3. A view of the molecular structure of [(μ-Cl)$_3${Ru^{II}(η^6-C_6Me_6)}$_2$][$Fe^{III}Cl_4$] **9**. Hydrogen atoms are omitted for clarity.

Since the crystallization was attempted from chloroform-diethyl ether mixture, the decomposition occurred probably via photolytic cleavage of the ferrocene moiety in the chlorinated solvent (Appendix 2). The geometry of the complex cation in the crystal structure of **9** is very similar to that previously reported for [(μ-Cl)$_3${Ru(η^6-C_6Me_6)}$_2$][PF_6].[111] The π-coordinated arene ligands are practically coplanar (the dihedral angle of their mean planes is 2.31°) and assume an almost perfect staggered conformation. No significant hydrogen-bonding or π···π stacking interactions were detected in the structure. The packing in the crystal structure of **9** is governed predominantly by electrostatic interactions of the complex ions that form separate layers perpendicular to the crystallographic *a*-axis.

While seeking for other potential applications of phosphane-amides equipped with hydrophilic pendants, I noticed a growing interest in transition metal-based anticancer

agents containing ligands of the so-called dual character.[112] Such ligands combine highly lipophilic part that is counterbalanced by hydrophilic pendants with strong hydrogen bonding capacity. In order to probe possible applications of the studied hydroxyamides in the design of such anticancer drugs, the series of palladium(II) (**10**) and platinum(II) complexes **11** and **12** was prepared from ligand **1** (Scheme 2.5, Appendix 3).

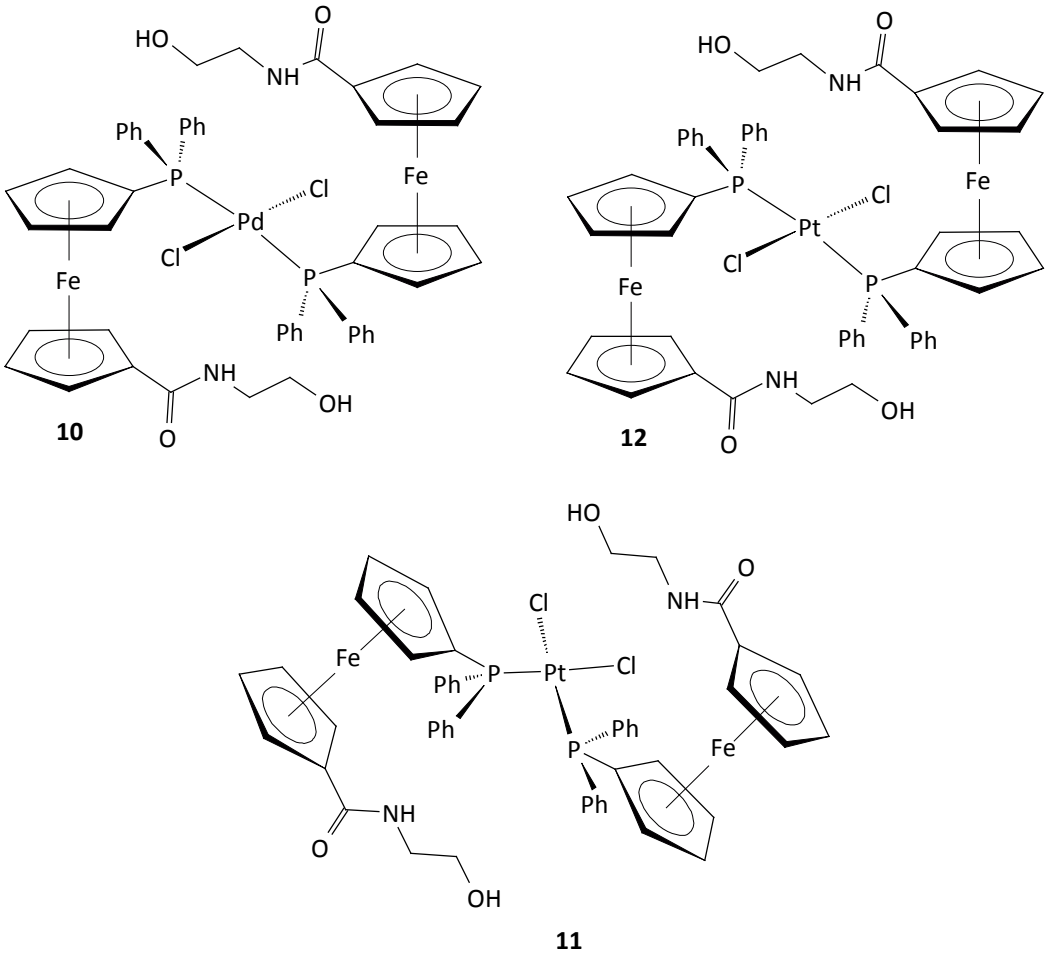

Scheme 2.5. Palladium(II) and platinum(II) complexes with ligand **1**.

Displacement of the cod ligand in $[M^{II}Cl_2(cod)]$ (M = Pd or Pt, cod = η^2:η^2-cycloocta-1,5-diene) with two equivalents of **1** afforded the complexes *trans*-$[PdCl_2(\mathbf{1}\text{-}\kappa P)_2]$ **10** and *cis*-$[PtCl_2(\mathbf{4}\text{-}\kappa P)_2]$ **11**. The platinum(II) complex *trans*-$[PtCl_2(\mathbf{1}\text{-}\kappa P)_2]$ **12** was obtained by the reaction of $K_2[PtCl_4]$ with two equivalents of hydroxyamide **1**.

The prepared transition metal complexes were studied together with free **1** and its P-chalcogenide derivatives, namely the phosphane-oxide $Ph_2P(O)fcC(O)NH(CH_2)_2OH$ **13** and phosphane-sulfide $Ph_2P(S)fcC(O)NH(CH_2)_2OH$ **14**, on their antiproliferative activity against the A2780 ovarian cancer cell line. The cytotoxicity experiments summarized in

Table 2.3 revealed that uncoordinated ferrocene derivatives, *i.e.*, **1**, **13** and **14**, do not possess any appreciable cytotoxicity (IC_{50} > 200 μM). Complexes **10-12** exhibited moderate activity with IC_{50} values ranging from 19 to 155 μM. Interestingly, the most cytotoxic compound in the series tested showed to be complexes *trans*-[$PtCl_2$(**1**-κ*P*)$_2$] **12** and *trans*-[$PdCl_2$(**1**-κ*P*)$_2$] **10** with complex *cis*-[$PdCl_2$(**1**-κ*P*)$_2$] **11** being the least active.

Table 2.3. IC_{50} values as determined for compounds **1** and **10-14** in the ovarian A2780 cancer cell line.

Compound	IC_{50} [μM]	Compound	IC_{50} [μM]
1	> 200	**10**	25 ± 2
13	> 200	**11**	19 ± 2
14	> 200	**12**	155 ± 5

The literature research aimed at the utilization of "simple" organic hydroxyamides brought about the idea to synthesize the non-phosphane analogue of ligand **4**, *i.e.*, hydroxyamide **15** (Scheme 2.6, Appendix 4). Triols of the type R–C(CH_2OH)$_3$ were previously utilized in the synthesis of functionalised hexavanadates [{R–C(CH_2O)$_3$}$_2V_6O_{13}$] that, in turn, were employed in the design of new materials for oxidation reactions [113] or polyoxometalates (POM's) of manganese-Anderson-type. [114] Covalently bound molecular hybrids of ferrocene with polyoxometalate frameworks (POM's) remain still very uncommon in literature.[115] This led us to synthesise amide **15** and use this compound for conjugation of the ferrocene moiety with the hexavanadate core (Scheme 2.6).

The necessary triol derivative FcC(O)NHC(CH_2OH)$_3$ **15** (Fc = ferrocenyl) was obtained upon reacting (fluorocarbonyl)ferrocene with tris(hydroxymethyl)methanamine in the presence of 4-(dimethylamino)pyridine and triethylamine in *N*,*N*-dimethylformamide (Scheme 2.6). A subsequent reaction of the triol-amide **15** with (Bu_4N)$_3$[$H_3V_{10}O_{28}$] in *N*,*N*-dimethylacetamide (DMA) at 90 °C/60 h afforded anionic hexavanadate (Bu_4N)$_2$[FcC(O)NHC(CH_2O)$_3V_6O_{13}$(OCH_2)$_3$CNHC(O)Fc] **16**, which was isolated by column chromatography and crystallization from DMF-MeCN-Et_2O as a solvate **16**·2DMF.

The crystal structures of **15** and **16** were determined by X-ray diffraction analysis (the view of the hexavanadate anion present in the crystal structure of **16** is presented in Figure 2.4; see also Appendix 4).

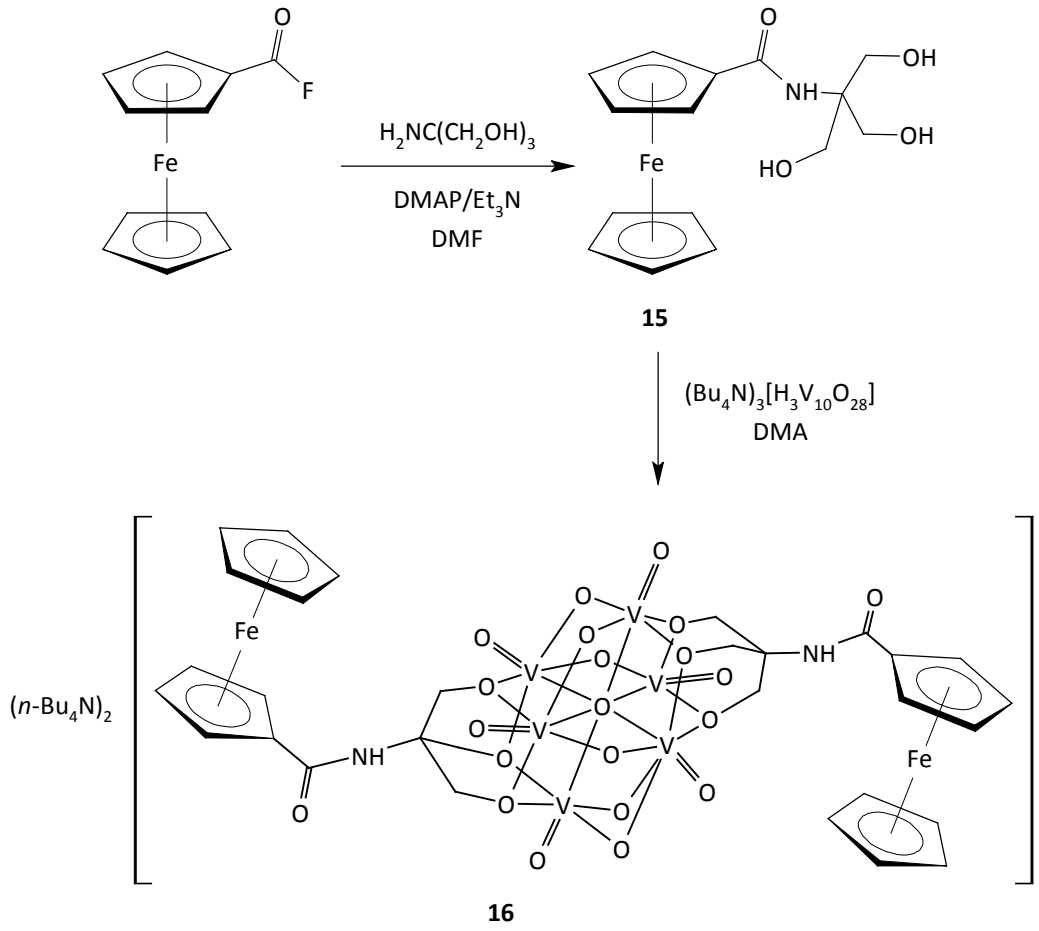

Scheme 2.6. The preparation of triol-amide **15** and doubly ferrocenylated hexavanadate **16** (DMAP = 4-(dimethylamino)pyridine, DMF = *N*,*N*-dimethylformamide, DMA = *N*,*N*-dimethylformamide).

Diffraction analysis revealed the presence of two independent hexavandate anions in the crystal structure of **16** that are almost identical in their structural parameters. Since the central oxygen atom of hexavanadate cage O1 coincides with the crystallographic inversion centre, the asymmetric unit of **16**·2DMF comprise two Bu_4N^+ cations, half of each structurally independent $[\{FcC(O)NHC(CH_2O)_3\}_2V_6O_{13}]$ anions and two hydrogen-bonded DMF molecules. The triolate pendants adopt *trans* orientation due to the imposed symmetry and the ferrocenyl moieties appear almost unchanged when compared to **15**. The geometry of hexavanadate cage is quite regular with V-O bond lengths changing in the order V-O (terminal) < V-O (oxo-bridge) < V-O (alkoxide) < V-O1.

Compounds **15** and **16** were studied by cyclic voltammetry. The triol-amide expectedly showed a single, one-electron reversible wave attributable to the ferrocene/ferrocenium redox couple. This wave was observed at more positive potentials than for ferrocene itself ($E°'$ = 0.20 V) owing to an electron-withdrawing nature of the carbamoyl unit. A single

oxidative wave was also seen in the cyclic voltammogram of hexavanadate **16** (Figure 2.5). However, this was found to be electrochemically irreversible (anodic peak potential, E_{pa} = +0.12 V; no reduction counter-peak was observed up to 10 $V \cdot s^{-1}$). The redox response of **16** contrasts with the behaviour observed for other hexavanadates $[\{R–C(CH_2O)_3\}_2V_6O_{13}]$ (R = CH_3, CH_2CH_3, CH_2Ph, NO_2 and NMe_2)[113a,116] that all displayed reversible reductions in the range of –0.67 V to –1.2 V (vs. ferrocene/ferrocenium), and suggests that some structural changes are associated with the electron-transfer process.

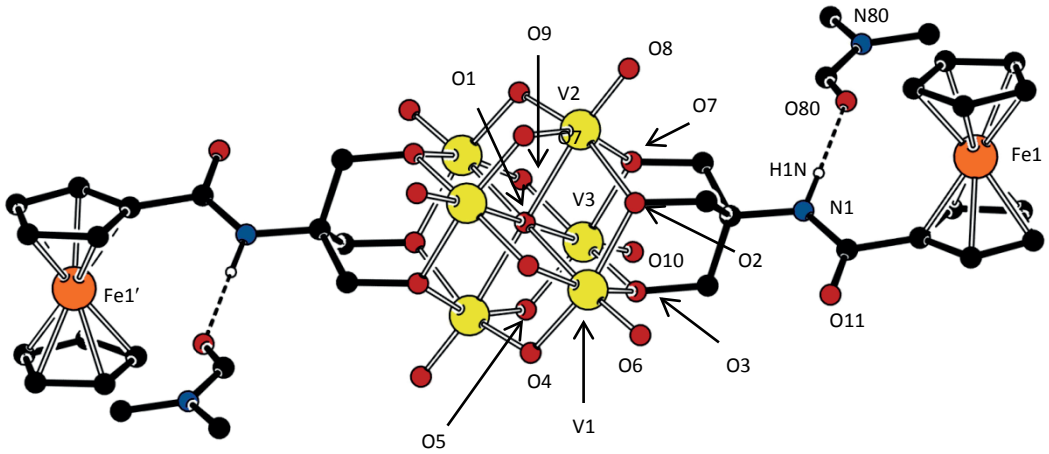

Figure 2.4. One of the structurally independent hexavanadate anions present in the crystal structure of **16**·2DMF with hydrogen-bonded molecules of solvating DMF. Only N-H hydrogens shown for clarity.

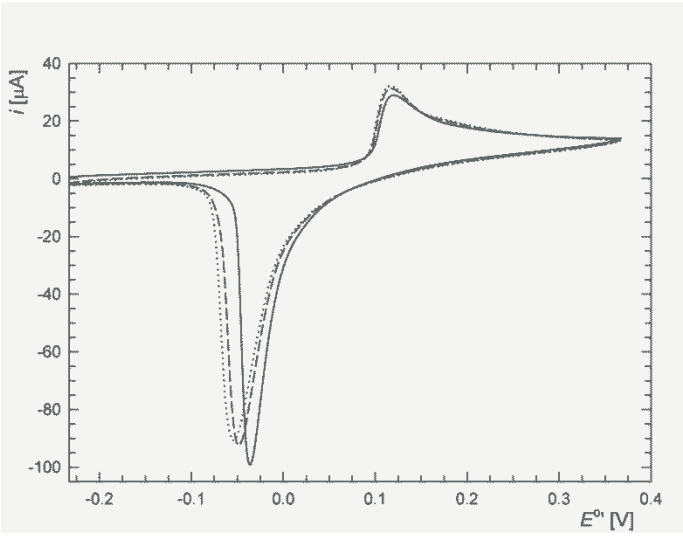

Figure 2.5. Cyclic voltammogram of **16**. The recorded scans (Pt-disc electrode, MeCN, c = 0.5 mM in 0.1 M $(Bu_4N)[PF_6]$) are distinguished by the line type (first scan in full line, second scan in dashed line, third in dotted line).

In order to explain the electrochemical behaviour of **16**, theoretical computations were performed mainly to gain an insight into the bonding situation within the hexavanadate cage. Single-point DFT calculations based on the solid-state structure performed for the isolated hexavanadate anion revealed the presence of 3-centre-4-electron (3c4e) O–V–O bonds on the hexavanadate cage, that are responsible for a high energy of the occupied frontier orbitals. The upper eleven occupied molecular orbitals including the HOMO are delocalized over the hexavanadate cage and, therefore, any electrochemical oxidation can be expected to occur preferentially at the hexavanadate anion without affecting the ferrocene moiety.

During the study of phosphane-amides bearing hydroxyalkyl pendant arms we decided to turn our attention also to donors functionalised by other highly polar anionic substituents. Thus, a series of conjugates of Hdpf with ω-aminosulfonic acids $H_2N(CH_2)_nSO_3H$ (n = 1, 2, 3), namely amidosulfonates **17-19** (Scheme 2.7, Appendix 5), was designed and prepared. These hybrid ligands combine three donor groups that differ substantially in their ligating properties, *i.e.*, phosphanyl group (*P*-donor), carboxamide moiety (anionic *N*- or neutral *O*-donor) and sulfonate group (anionic *O*-donor). Moreover, they may be viewed as so-called surface active ligands. Compounds of this type combine hydrophobic metal-binding moiety with hydrophilic peripheries separated by long aliphatic chains. Donors with the surface active structure can facilitate contacts between the catalytic centre and a hydrophobic reaction phase, *e.g.*, an interior of micelles or an immiscible liquid organic phase.[117]

Considering the highly polar nature of the starting ω-aminosulfonic acids, I decided to use the synthetic procedure employed in the synthesis of phosphane-amide **2**.[105] Amido-sulfonates **17-18** were prepared by the reaction of Hdpf pentafluorophenyl ester **5**[118] with appropriate ω-aminosulfonic acid (Scheme 2.7). The reaction was catalysed by 4-(dimethylamino)pyridine and performed in *N*,*N*-dimethylformamide in the presence of triethylamine as an auxiliary base. The initial attempts showed that in pure DMF is Hdpf coupled smoothly only with aminomethanesulfonic acid. Subsequent isolation by column-chromatography and recrystallization from hot ethyl acetate afforded the amidosulfonate **17** in good yield. In contrast, the same reaction gave no amide-products from 2-aminoethanesulfonic acid and 3-aminopropanesulfonic acid, likely due to a lower solubility of these acids in the reaction medium. Therefore, the reactions $H_2N(CH_2)_2SO_3H$ and $H_2N(CH_2)_3SO_3H$ were than conducted in aqueous DMF (1 vol. % of distilled water)

affording amidosulfonates **18** and **19** in good yields after chromatographic purification and recrystallization from hot ethyl acetate.

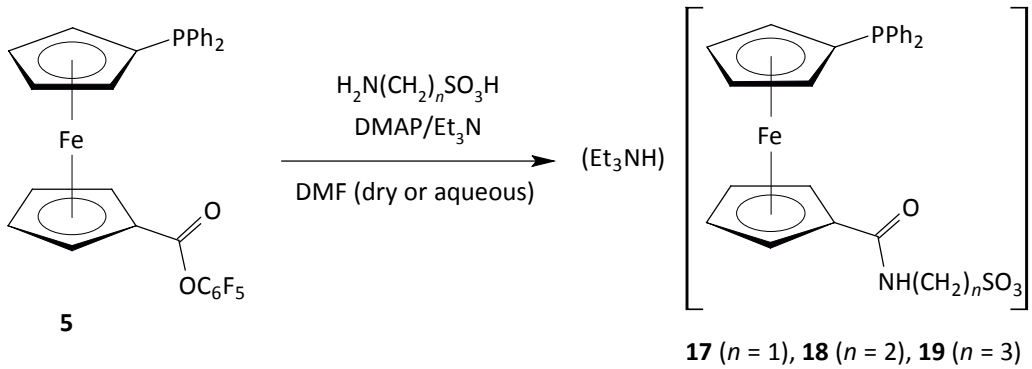

Scheme 2.7. Preparation of amidosulfonates **17-19**.

The crystal structures of amidosulfonates **17** and **19** were determined by single-crystal X-ray diffraction analysis (for the views of the molecular structures, see Appendix 5). The amidosulfonate ligands do not form supramolecular assemblies as complicated as the cognate Hdpf-based hydroxyamides **1-4**. Nevertheless, the same basic motif was found in the structures of amidosulfonates **17** and **19**. Anions of these compounds associate into similar dimers with through N-H1N···O3/O4 contacts (Figure 2.6). Triethylammonium cations are attached to these dimers by N-H···O hydrogen bonds to the amidosulfonate pendants (Figure 2.6).

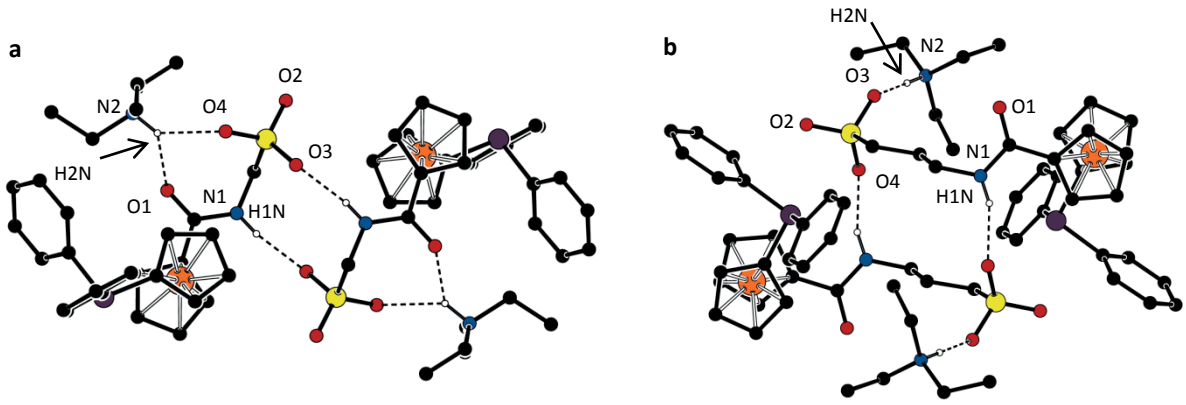

Figure 2.6. Views of the hydrogen-bonded dimers in the crystal structures of **17** (a) and **19** (b). Only N-H hydrogens are shown for clarity.

In order to investigate the coordination preferences of the amidosulfonate ligands, the reactivity of **17** as a representative was studied toward palladium(II) dimeric precursors of the type $[(L^{CN})PdX]_2$ bearing auxiliary *C*,*N*-chelated ligand 2-[(dimethylamino-κ*N*)methyl]phenyl-κC^1 (L^{CN}) (X = Cl or AcO). The reaction of $[(L^{CN})PdCl]_2$ with two

equivalents of **17** afforded exclusively complex **20** with amidosulfonate ligand coordinated in *P*-monodentate fashion (Scheme 2.8).

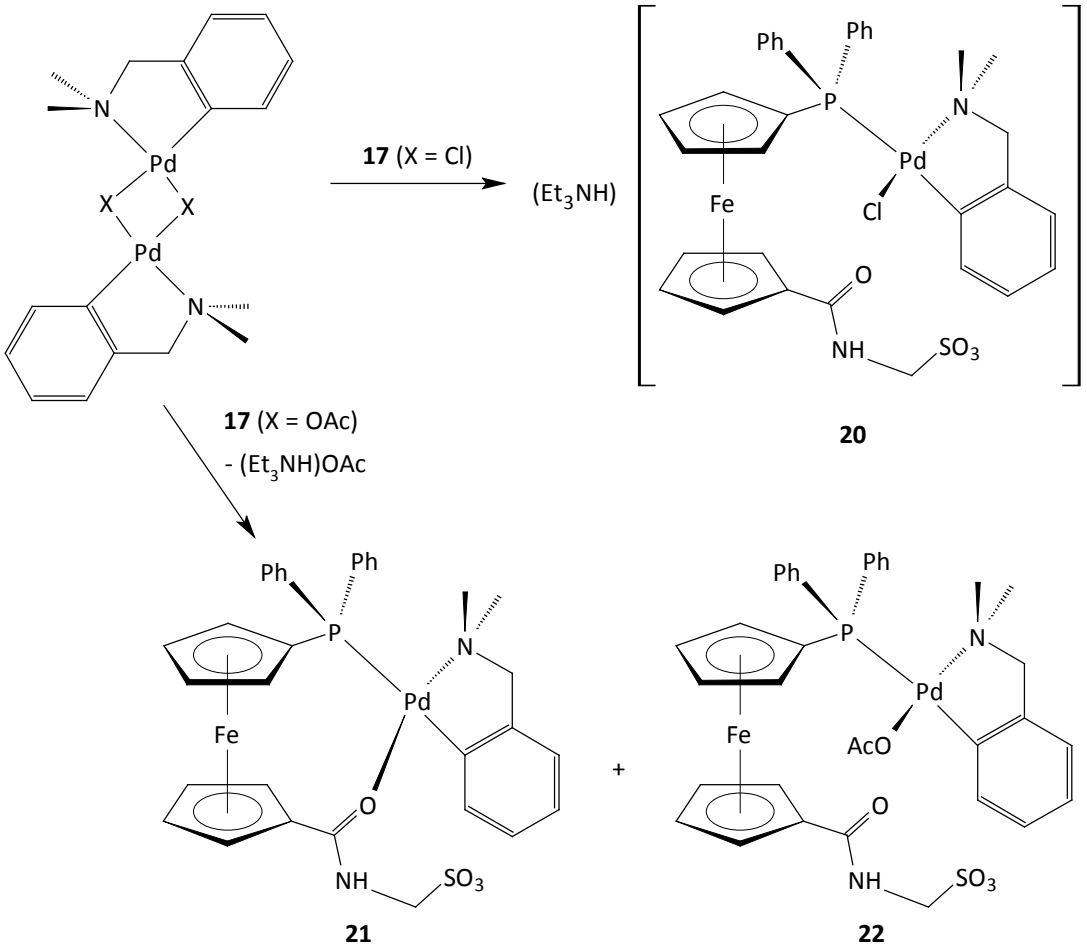

Scheme 2.8. Preparation of palladium complexes with auxiliary *C,N*-chelated ligand 2-[(dimethylamino-κ*N*)methyl]phenyl-κC^1 (L^{CN}).

On the other hand, an analogous reaction of **17** with the dimeric precursor $[(L^{CN})Pd(OAc)]_2$ led to a mixture of two new *P*-coordinated palladium(II) complexes (Scheme 2.8). The major product (yield ca. 60%) was obtained in crystalline form upon crystallisation from the reaction mixture by its layering with hexanes as a less polar solvent. This product was identified as *O,P*-coordinated zwitterionic complex $[(L^{CN})Pd(Ph_2PfcCONHCH_2SO_3$-κ*O,P*$)]$ **21** (fc = ferrocene-1,1′-diyl). The view of hydrogen-bonded motif as found in the crystal structure of chloroform solvate **21**·2$CHCl_3$ is shown in Figure 2.7. This complex is probably formed via metathesis-like elimination of the coordinated acetate ligand with **17** resulting in the formation of $(Et_3NH)OAc$. This type of *O,P*-chelating coordination was previously reported also for other Hdpf-based phosphane-amides. [101,119]

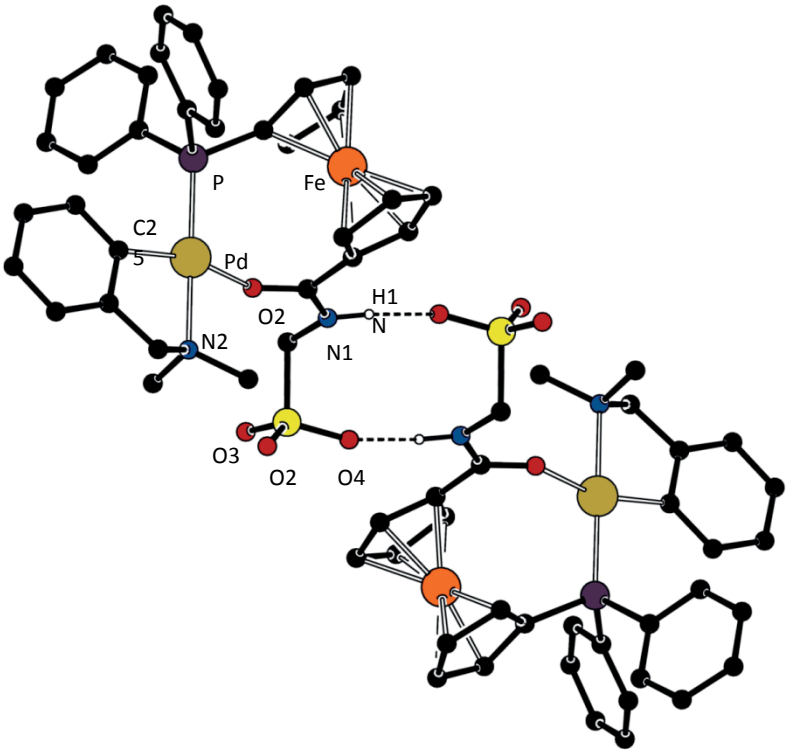

Figure 2.7. A view of the hydrogen-bonded dimer in the crystal structure of **21**·2$CHCl_3$. Only N-H hydrogen atoms are shown.

The structure of the minor product was unravelled mainly from a comparative ESI-MS study of the reaction mixture, pure **21** and the model reaction of $[(L^{CN})Pd(OAc)]_2$ with *P*-monodentate ligand $FcPPh_2$ (Fc = ferrocenyl). The model reaction afforded cleanly (L^{CN})Pd-acetato complex $[(L^{CN})Pd(OAc)(FcPPh_2$-κ*P*$)]$, as evidenced by NMR and IR spectroscopy. ESI-MS study showed ions attributable to $[(L^{CN})Pd(Ph_2PfcCONHCH_2SO_3$-κ*P*$)(X) - H]$, where X = OAc (m/z 805) and Cl (m/z 781), supporting the formulation of the minor product as $(Et_3NH)[(L^{CN})Pd(OAc)(Ph_2PfcCONHCH_2SO_3$-κ*P*$)]$ **22**. This complex results via a direct bridge-cleavage reaction of the dimeric precursor $[(L^{CN})Pd(OAc)]_2$ and seems to be a reaction intermediate of the reaction leading to **21** (Scheme 2.8).

Palladium(II)-mediated cyanation of aryl halides was selected to assess the prepared amidosulfonate donors in aqueous transition metal catalysis.[120] Recently, potassium hexacyanoferrate(II), $K_4[Fe(CN)_6]$, was shown to be a useful alternative to the traditional cyanation agents, as it is non-toxic, cheap and easy-to-handle.[121] Very recently, the scope of this reaction was extended also to aqueous systems and more challenging substrates.[122]

Considering these results, palladium(II) complexes *trans*-$[PdCl_2(L$-κ*P*$)_2]$ **23** (L = **17**), **24** (L = **18**) and **25** (L = **19**) (Scheme 2.9) were prepared and then used as defined catalyst

precursors for cyanation of various aryl bromides using $K_4[Fe(CN)_6]$ as the cyanide source in aqueous reaction media.

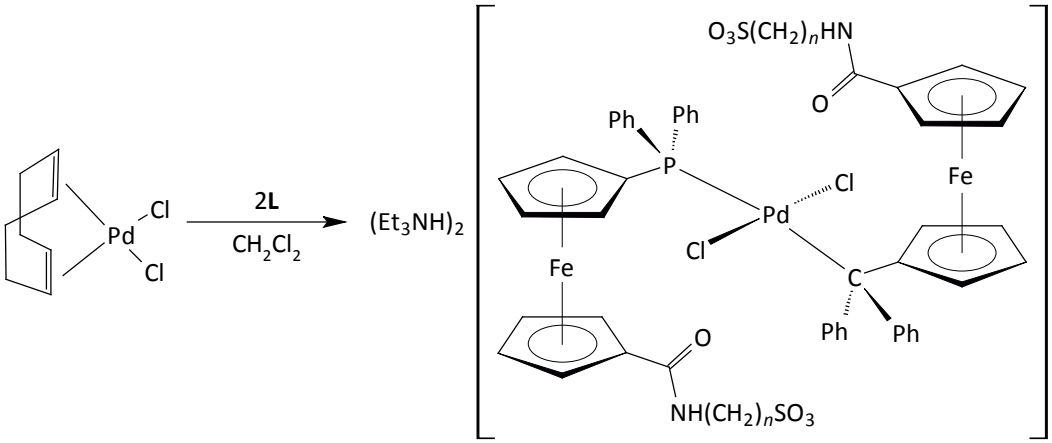

23 (*n* = 1), **24** (*n* = 2), **25** (*n* = 3)

Scheme 2.9. Preparation of palladium(II) complexes **23**-**25**.

The initial experiments were conducted to compare the catalytic performance of palladium(II) complexes **23-25** in cyanation of 4-bromoanisole (**26a**) in dioxane-water (1:1, v/v) reaction media (Scheme 2.10). Under the same reaction conditions, complex **23** gave rise to the most active catalyst (see entries 1-3 in Table 2.4), and was therefore used as a pre-catalyst for further study.

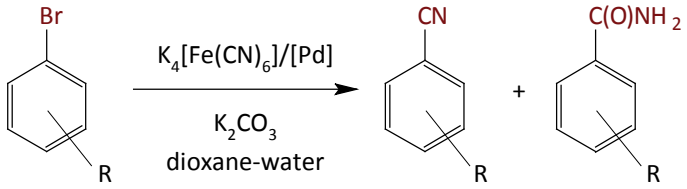

26 **27** **28** hydrolytic side-product

R = 4-OMe (a), 4-Me (b), 3-Me (c), 2-Me (d), 4-CMe_3 (e), 4-CF_3 (f), 4-C(O)Me (g), 4-Ph (h), 4-Cl (i), 4-NO_2 (j), 4-NMe_2 (k), 4-CO_2H (l), 4-CH_2CO_2H (m).

Scheme 2.10. Cyanation of aryl bromides using palladium(II) complexes **23-25**.

The following experiments were aimed at understanding the influence of the composition of the reaction medium composition on the course of the catalysed reaction. These experiments revealed that the yields and even selectivity of the cyanation reaction are

strongly altered the composition of the reaction solvent, namely by the dioxane-water ratio (Figure 2.8).

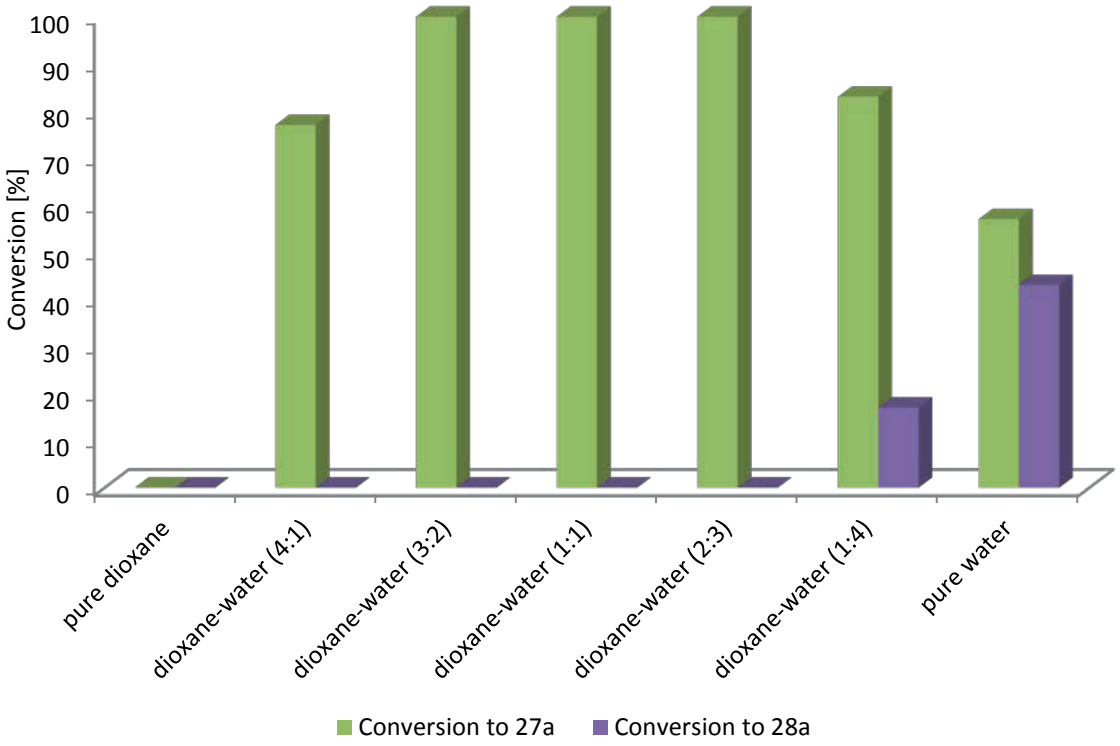

Figure 2.8. Influence of water-dioxane ratio on catalytic performance of **23**. Conditions: 4-bromoanisole (1.0 mmol), potassium carbonate (1.0 mmol), and potassium hexacyanoferrate(II)·trihydrate (0.5 mmol), palladium complex **23** (2 mol %), dioxane-water (4 mL), 100 °C/18 h.

The cyanation of 4-bromoanisole (**26a**) in the presence of 2 mol. % of catalyst **23** didn't proceed at all in pure dioxane, while complete conversion to corresponding nitrile product (**27a**) was achieved using the mixed solvents containing 40-60 % of water. The use of pure water or reaction media containing water in a large excess led to formation of the respective carboxamide **28a** as a hydrolytic side-product in considerable amounts. Based on these results, dioxane-water mixture (1:1, v/v) was selected as the optimal reaction medium for the cyanation of various aryl bromides bearing different electron-withdrawing and electron-donating substituents (Table 2.4). From the performed catalytic tests, it is obvious that complex **23** affords an active catalyst promoting smoothly cyanation of *para*-substituted aryl bromides bearing electron-donating substituents, *i.e.*, alkyl-, aryl and acetyl groups. Its efficiency was not affected by the substitution pattern in the series of tolyl bromides.

Table 2.4. Summary of obtained catalytic results in palladium(II)-mediated cyanation of aryl bromides.[a]

Entry	Aryl bromide **26**	Catalyst	Nitrile **27** ^{1}H NMR yield (isolated yield) [%]	Amide **28** ^{1}H NMR yield [%]
1	**26a** (4-MeO)	**23**[b]	58	n.d.
2	**26a** (4-MeO)	**24**[b]	20	n.d.
3	**26a** (4-MeO)	**25**[b]	27	n.d.
4	**26a** (4-MeO)	**23**	100 (95)	n.d.
5	**26a** (4-MeO)	**23**[c]	0	n.d.
6	**26a** (4-MeO)	**23**[d]	56	n.d.
7	**26b** (4-Me)	**23**	100 (90)	n.d.
8	**26c** (3-Me)	**23**	100 (76)	n.d.
9	**26d** (2-Me)	**23**	100 (86)	n.d.
10	**26e** (4-CMe_3)	**23**	100 (82)	n.d.
11	**26f** (4-CF_3)	**23**	62	38
12	**26g** (4-C(O)Me)	**23**	100 (93)	n.d.
13	**26h** (4-Ph)	**23**	100 (91)	n.d.
14	**26i** (4-Cl)	**23**	56	44
15	**26j** (4-NO_2)	**23**	<5	n.d.
16	**26k** (4-NMe_2)	**23**	17	n.d.
17	**26l** (4-CO_2H)	**23**[e]	100 (87)	n.d.
18	**26m** (4-CH_2CO_2H)	**23**[e]	100 (89)	n.d.

[a] Conditions: aryl bromide **23** (1.0 mmol), K_2CO_3 (1.0 mmol), and $K_4[Fe(CN)_6]\cdot 3H_2O$ (0.5 mmol), 2 mol % of Pd catalyst in dioxane-water (1:1 mixture, 4 mL) at 100 °C for 18 h (n.d. = product was not detected in the reaction mixture). [b] Reaction with 1 mol % of Pd complex. [c] Reaction without added K_2CO_3. [d] Reaction in the presence of 0.50 mmol of K_2CO_3. [e] Reaction in the presence of 2.0 mmol of K_2CO_3 (2 equiv with respect to the substrate). The product was isolated after acidification of the reaction mixture.

On the other hand, cyanations of aryl bromides bearing electron-withdrawing substituents *p*-CF_3 (**26f**) and *p*-Cl (**26i**), were accompanied by a partial hydration of the corresponding nitrile products (**27f** and **27i**) yielding the respective carboxamides (**28f** and **28i**). Only poor conversions to nitrile products were achieved in the case of 4-(dimethylamino)bromobenzene (**26k**) and 4-nitrobromobenzene (**26j**), while heterocyclic bromides, *i.e.*, 2-bromopyridine, 3-bromopyridine and 4-bromopyridine hydrochloride proved to be completely unreactive under the conditions applied. This may be explained by the *N*-donating character of **26k** and heterocyclic bromides (catalyst scavengers), while **26j** is the most electron-poor substrate tested.

Conclusions

The main topic of the presented Ph.D. Thesis was to continue and extend the previous research focusing on the coordination chemistry and catalytic properties of phosphane-amides derived from 1′-(diphenylphosphanyl)ferrocene-1-carboxylic acid (Hdpf). With this Thesis the scope of such domors was extended by several new ligands equipped with highly polar functional groups.

The formerly reported work focused on the coordination chemistry and catalytic use of phosphane-amides **1** and **2** bearing 2-hydroxyethyl pendant arms was extended as a part of this Thesis. The hydroxyamides **3** and **4** were designed and prepared in order to complete the series of congeneric ligands of the type $Ph_2PfcC(O)NHCH_{3-n}(CH_2OH)_n$ (fc = ferrocene-1,1′-diyl; n = 1-3). Thus prepared ligands were employed in the synthesis of a group of arene-ruthenium(II) complexes of the type $[(\eta^6\text{-arene})RuCl_2(L\text{-}\kappa P)]$ **6-8** (arene = C_6H_6, *p*-cymene or C_6Me_6; L = **1**, **3** or **4**). The subsequent catalytic study demonstrated the catalytic properties of these complexes in redox isomerization of allylic alcohols to carbonyl compounds. The performed experiments suggested a major influence of the coordinated ligands on the catalytic performance of the ruthenium(II) pre-catalysts. The catalytic experiments performed in pure water and 1,2-dichloroethane showed that the most active pre-catalyst $[(\eta^6\text{-}p\text{-cymene})RuCl_2(\mathbf{1}\text{-}\kappa P)]$ (**6b**)**,** efficiently mediates only redox isomerization of secondary allylic alcohols with unsubstituted double-bonds. The reactions carried out in water afforded considerably worse conversions to carbonyl products than those in 1,2-dichloroethane.

An attempted crystallization of complex $[(\eta^6\text{-}C_6Me_6)RuCl_2(\mathbf{2}\text{-}\kappa P)]$ resulted in the formation of a dinuclear arene-ruthenium(II) complex $[(\mu\text{-}Cl)_3\{Ru^{II}(\eta^6\text{-}C_6Me_6)\}_2][Fe^{III}Cl_4]$ **9**, which was structurally characterized. The decomposition occurred probably through photolytic cleavage of the ferrocene moiety and halogenated solvent used for crystalization.

Amidosulfonates $(Et_3NH)[Ph_2PfcC(O)NH(CH_2)_nSO_3]$ (n = 1-3) **17-19** were successfully applied as ligands in aqueous transition metal catalysis. The series of complexes *trans*-$[PdCl_2(L\text{-}\kappa P)_2]$ **23-25** (L = **17**, **18** or **19**) was tested in cyanation reaction of aryl bromides using $K_4[Fe(CN)_6]$ as a cyanation agent. A decisive influence of the reaction medium was noticed on the course of the catalytic reaction. The most active pre-catalyst complex **23**

was shown to be efficient in the cyanation of variously substituted aryl bromides. It is noteworthy that the use of aqueous conditions for this catalytic reaction remains still rather scarce. Moreover, amidosulfonate **17** proved to be a very flexible hybrid donor. It possess diverse coordination modes as was shown in the performed coordination study toward palladium(II) as a soft metal ion. Depending on the used Pd-precursor it can coordinate as a simple monodentate *P*- or bidentate *O*,*P*-donor.

Generally, the performed catalytic study towards palladium-promoted cyanation reaction of aryl bromides and ruthenium-mediated redox isomerization of allyllic alcohols showed that structural modifications at the amide part of the molecule may considerably influence the catalytic performance of phosphane-amide ligands derived from Hdpf.

Additional originally unintended research topics arose during the studies concerning the principal aims of this Thesis. Thus, complexes $[M^{II}Cl_2(\mathbf{1}\text{-}\kappa P)_2]$ **10** (M = *trans*-Pd), **11** (M = *cis*-Pt) and **12** (M = *trans*-Pt) derived from ligand **1** were synthesised with an aim of using the hydrophilic phosphane-amides as targeting auxiliaries in the design of new anticancer drugs. The *in-vitro* study towards cytotoxic activity in ovarian A2780 cancer cell line showed rather moderate cytotoxicity of these complexes. However, an interesting influence of stereochemistry of studied complexes was observed, with **11** being the least active.

Furthemore, triol **15** was utilized as a synthon for conjugation of the ferrocene moiety with the hexavanadate core. Covalently bound molecular hybrids of ferrocene with polyoxometalates (POM's) remain still rather uncommon in the literature. Hexavanadate **16** was characterised by ^{1}H, ^{13}C and ^{51}V NMR, FTIR, ESI MS and its formulation was confirmed by X-ray diffraction analysis. The electrochemical study by cyclic voltammetry revealed rather unexpected electrochemical behaviour that indicated no pronounced electronic interaction between the ferrocenyl pendants and the hexavanadate core. DFT theoretical calculations provided an insight into the bonding situation within the hexavanadate anion and offered plausible explanation for the observed electrochemical behaviour.

Abbreviations and Symbols

$\Delta G^{\ddagger}$	reaction Gibbs activation energy
θ	Tolman cone angle [°]
χ	Tolman electronic parametr
σ_m	Hammet constant for a substituent in *meta*-position
acac	pentan-2,4-dionate(1−)
cod	η^2:η^2-cycloocta-1,5-diene
Cy	cyclohexyl
dpf^-	1-(diphenylphosphanyl)ferrocene-1′-carboxylate
dppf	bis(diphenylphosphanyl)ferrocene
EDC	*N*-ethyl-*N*'-[(3-dimethylamino)propyl]carbodiimide
EEDQ	2-ethoxy-1-ethoxycabonyl-1,2-dihydroquinoline
fc	ferrocene-1,1′-diyl
Fc	ferrocenyl
Hacac	pentan-2,4-dion
Hdpf	1-(diphenylphosphanyl)ferrocene-1′-carboxylic acid
HSAB	Pearson's theory of Hard and soft acids and bases
IC_{50}	half maximal inhibitory concentration
i-Pr	isopropyl
m-TPPTC	triphenylphosphane-3,3′,3′′-tricarboxylate trilithium salt
m-TPPTS	triphenylphosphane-3,3′,3′′-trisulfonate trisodium salt
Ph	phenyl
PPFA	1-[1-(*N*,*N*-dimethylamino)ethyl]-2-(diphenylphosphanyl)ferrocene
p-TPPTP$(H)_6$	triphenylphosphane-4,4′,4′′-triphosphonic acid
p-TPPTP$(Na)_6$	triphenylphosphane-4,4′,4′′-triphosphonate hexasodium salt
t-Bu	*tert*-butyl
TPP	triphenylphosphane
TRIS	tris(hydroxymethyl)methanamine
Xyl	3,5-dimethylphenyl

References

1. For general reviews aimed at supported palladium catalysts, see: (a) L. Yin, J. Liebscher, *Chem. Rev.*, 2007, **107**, 133; (b) M. Lamblin, L. Nassar-Hardy, J.-C. Hierso, E. Fouquet, F.-X. Felpin, *Adv. Synth. Catal.*, 2010, **352**, 33; (c) Á. Molnár, *Chem. Rev.*, 2011, **111**, 2251.
2. (a) J. Huang, F. Zhu, W. He, F. Zhang, W. Wang, H. Li, *J. Am. Chem. Soc.*, 2010, **132**, 1492; (b) A. Corma, H. Garcia, *Adv. Synth. Catal.*, 2006, **348**, 1391.
3. (a) N. E. Leadbeater, M. Marco, *Chem. Rev.*, 2002, **102**, 3217; (b) C. A. McNamara, M. J. Dixon, M. Bradley, *Chem. Rev.*, 2002, **102**, 3275; (c) D. E. Bergbreiter, *Chem. Rev.*, 2002, **102**, 3345; (d) D. E. Bergbreiter, J. Tian, C. Hongfa, *Chem. Rev.*, 2009, **109**, 530.
4. (a) M. J. Muldoon, *Dalton Trans.*, 2010, 39, 337; (b) M. Lombardo, A. Quintavalla, M. Chiarucci, C. Trombini, *Synlett*, 2010, **12**, 1746.
5. V. I. Pârvulescu, C. Hardacre, *Chem. Rev.*, 2007, **107**, 2615.
6. (a) D. P. Curran, *Angew. Chem. Int. Ed.*, 1998, **37**, 1174; (b) W. Zhang, *Green Chem.*, 2009, **11**, 911.
7. W. Leitner, *Acc. Chem. Res.*, 2002, **35**, 746.
8. *Aqueous-Phase Organometallic Catalysis: Concepts and Applications*, 2nd ed. (Eds.: B. Cornils, W. A. Herrmann), Wiley-VCH, Weinheim, 2004.
9. (a) B. Cornils, *Org. Process. Res. Dev.*, 1998, **2**, 121. (b) B. Cornils, *J. Mol. Catal.A*, 1999, **143**, 1.
10. C. W. Kohlpaintner, R. W. Fischer, B. Cornils, *Appl. Catal., A*, 2001, **221**, 219.
11. M. O. Simon, C.-J. Li, *Chem. Soc. Rev.*, 2012, **41**, 1415.
12. (a) J. B. F. N. Engberts, M. J. Blandamer, *Chem. Commun.*, 2001, 1701; (b) M. C. Pirrung, *Chem. Eur. J.*, 2006, **12**, 1312; (c) Y. Hayashi, *Angew. Chem. Int. Ed.*, 2006, 45, 8103; (d) R. N. Butler, A. G. Coyne, *Chem. Rev.*, 2010, **110**, 6302.
13. (a) D. C. Rideout, R. Breslow, *J. Am. Chem. Soc.*, 1980, **102**, 7816; (b) R. Breslow, *Acc. Chem. Res.*, 1991, **24**, 159; (c) R. Breslow, *Acc. Chem. Res.*, 2004, **37**, 471.
14. S. Otto, J. B. F. N. Engberts, *Pure Appl. Chem.*, 2000, **72**, 1365.

15. (a) J. Chandrasekhar, S. Shariffskul, W. L. Jorgensen, *J. Phys. Chem. B*, 2002, **106**, 2078; (b) T. R. Furlani, J. L. Gao, *J. Org. Chem.*, 1996, **61**, 5492; (c) J. F. Blake, W. L. Jorgensen, *J. Am. Chem. Soc.*, 1991, **113**, 7430.
16. T. Rispens, J. B. F. N. Engberts, *J. Phys. Org. Chem.*, 2005, **18**, 908.
17. J. J. Gajewski, *J. Org. Chem.*, 1992, **57**, 5500.
18. S. Ribe, P. Wipf, *Chem. Commun.*, 2001, 299.
19. Recent reviews aimed at organic synthesis in aqueous media: (a) U. M. Lindstöm, *Chem. Rev.*, 2002, **102**, 2751; (b) C.-J. Li, *Chem. Rev.*, 2005, **105**, 3095; (c) S. Narayan, J. Muldoon, M. G. Finn, V. V. Fokin, H. C. Kolb, K. B. Sharpless, *Angew. Chem. Int. Ed.*, 2005, **44**, 3275; (d) A. Chanda, V. V. Fokin, *Chem. Rev.*, 2009, **109**, 725.
20. For general reviews dealing with design, synthesis and catalytic application of hydrophilic ligands, see: (a) N. Pinault, D. W. Bruce, *Coord. Chem. Rev.*, 2003, **241**, 1; (b) K. H. Shaughnessy, *Eur. J. Org. Chem.*, 2006, 1827; (c) K. H. Shaughnessy, *Chem. Rev.*, 2009, **109**, 643.
21. D. E. Bergbreiter, S. D. Sung, *Adv. Synth. Catal.*, 2006, **348**, 1352.
22. C. A. Tolman, *Chem. Rev.*, 1977, **77**, 313.
23. C. A. Tolman, *J. Am. Chem. Soc.*, 1970, **92**, 2953.
24. D. W. Allen, B. F. Taylor, *J. Chem. Soc. Dalton Trans.*, 1982, 51.
25. D. W. Allen, I. W. Nowell, B. F. Taylor, *J. Chem. Soc. Dalton Trans.*, 1985, 2505.
26. T. Bartik, T. J. Himmler, *J. Organomet. Chem.*, 1985, **293**, 343.
27. T. Bartik, B. Bartik, B. E. Hanson, I. Guo, I. Toth, *Organometallics*, 1993, **12**, 164.
28. C. Hansch, A. Leo, R. W. Taft, *Chem. Rev.*, 1991, **91**, 165.
29. R. P. Pinnell, C. A. Megerle, S. L. Manatt, P. A. Kroon, *J. Am. Chem. Soc.*, 1973, **95**, 977.
30. E. Genin, R. Amengual, V. Michelet, M. Savignac, A. Jutand, L. Neuville, J. Genet, *Adv. Synth. Catal.*, 2004, **346**, 1733.
31. P. Machnitzki, M. Tepper, K. Wenz, O. Stelzer, E. Herdtweck, *J. Organomet. Chem.*, 2000, **602**, 158.
32. W. A. Herrmann, J. A. Kulpe, J. Kellner, H. Riepl, H. Bahrmann, W. Konkol, *Angew. Chem. Int. Ed.*, 1990, **29**, 391.
33. W. A. Herrmann, J. Kellner, H. Riepl, *J. Organomet. Chem.*, 1990, **389**, 103.
34. R. Mynott, A. Mollbach, G. Wilke, *J. Organomet. Chem.*, 1980, **199**, 107.

35. C. A. Tolman, W. C. Siedel, D. H. Gerlach, *J. Am. Chem. Soc.*, 1972, 94, 2669.

36. S. M. Socol, J. G. Verkade, *Inorg. Chem.*, 1984, **23**, 3487.

37. R. V. Parish, O. Parry, C. A. McAuliffe, *J. Chem. Soc. Dalton Trans.*, 1981, 2098.

38. B. A. Harper, D. A. Knight, C. George, S. L. Brandow, W. J. Dressick, C. S. Dalcey, T. L. Schull, *Inorg. Chem.*, 2003, **42**, 516.

39. T. L. Shull, R. Butcher, W. J. Dressick, S. L. Brandow, L. K. Byington, D. A. Knight, *Polyhedron*, 2004, **23**, 1375.

40. *Rhodium-Catalyzed Hydroformylation* (Eds.: P. W. N. M. van Leeuwen, C. Claver), Kluwer Academic, Dordrecht, 2000.

41. (a) H. Ding, B. E. Hanson, *J. Chem. Soc. Chem. Commun.*, 1994, 2747; (b) H. Ding, B. E. Hanson, *J. Mol. Catal. A*, 1995, **99**, 131; (c) H. Ding, B. E. Hanson, T. E. Glass, *Inorg. Chim. Acta*, 1995, **229**, 329.

42. D. W. Allen, *Organophosphorus Chem.*, 2011, **40**, 1.

43. C. A. Fleckenstein, H. Plenio, *Chem. Soc. Rev.*, 2010, **39**, 694.

44. (a) Z. Feixa, P. W. N. M van Leeuwen, *Coord. Chem. Rev.*, 2008, 252, 1755; (b) A. Pascariu, S. Iliescu, A. Popa, G. Ilia, *J. Organomet. Chem.*, 2009, **694**, 3982; (c) J.-C. Hierso, R. Amardeil, E. Bentabet, R. Broussier, B. Gautheron, B. Meunier, P. Kalck, *Coord. Chem. Rev.*, 236, 143.

45. G. C. Hargaden, P. J. Guiry, 2009, 109, 2505.

46. (a) D. Lorcy, N. Bellec, M. Fourmigué, N. Avarvari, *Coord. Chem. Rev.*, 2009, 253, 1398; (b) J. W. Dilworth, N. Wheatley, *Coord. Chem. Rev.*, 2000, **199**, 89.

47. (a) V. V. Grushin, *Chem. Rev.*, 2004, **104**, 1629; (b) H. Fernández-Pérez, P. Etayo, A. Panossian, A. Vidal-Ferran, *Chem. Rev.*, 2011, **111**, 2119.

48. *Ferrocenes: Homogeneous catalysis, Organic synthesis, Materials science* (Eds.: A. Togni, T. Hayashi), VCH, Weinheim, Germany, 1995.

49 . *Ferrocenes: Ligands, Materials and Biomolecules* (Ed.: P. Štěpnička), Wiley, Chichester, U. K., 2008.

50. T. J. Kealy, P. L. Pauson, *Nature*, 1951, **15**, 1039.

51. S. A. Miller, J. A.Tebboth, J. F. Tremaine, *J. Chem. Soc.*, 1952, **114**, 632.

52. G. Wilkinson, M. Rosenblum, M. C. Whiting, R. B. Woodward, *J. Am. Chem. Soc.*, 1952, **74**, 2125.

53. E. O. Fischer, W. Pfab, *Z. Naturforsch.*, 1952, **7b**, 377.

54. (a) J. W. Irvine, G. Wilkinson, *Science*, 1961, *113*, 742; (b) B. Floris, G. Illuminati, P. E. Jones, G. Ortaggi, *Coord. Chem. Rev.*, 1972, **8**, 39; (c) G. Wilkinson, *J. Organomet. Chem.*, 1975, **100**, 273; (d) *Comprehansive Organometallic Chemistry II, vol 7*, (Eds.: E. W. Abel, F. G. A. Stone, G. Wilkinson), Pergamon, Oxford, U. K., 1995.

55. For review articles on analytical applications of ferrocene derivatives, see: (a) C. M. Casado, I. Cuadrado, M. Morán, B. Alonso, B. García, B. Gonzáles, J. Losada, *Coord. Chem. Rev.*, **185–186**, 53; (b) P. A. Gale, P. D. Beer, G. Z. Chen, *J. Chem. Soc. Dalton Trans.*, 1999, 1897; (c) J. Huo, L. Wang, T. Chen, L. Deng, H. Ju, Q. Tan, *Des. Monomers Polym.*, 2007, **10**, 389; (d) W. E. Geiger, *Organometallics*, 2007, **26**, 5738; (e) P. Molina, A. Tárraga, A. Caballero, *Eur. J. Inorg. Chem.*, 2008, 3401.

56. (a) S. Fery-Forgues, B. Delavaux-Nicot, *J. Photochem. Photobiol., A*, 2000, **132**, 137; (b) R. D. A. Hudson, *J. Organomet. Chem.*, 2001, **637-639**, 47; (c) Y. Gao, J. M. Shreeve, *J. Inorg. Organomet. Polym. Mater.*, 2007, **17**, 19; (d) B. Fabre, *Acc. Chem. Res.*, 2010, **43**, 1509; (e) V. Ganesh, V. S. Sudhir, T. Kundu, S. Chandrasekaran, *Chem. Asian J.*, 2011, **6**, 2670.

57. (a) D. R. van Staveren, N. Metzler-Nolte, *Chem. Rev.*, 2004, **104**, 5931; (b) H. B. Kraatz, *J. Inorg. Organomet. Polym. Mater.*, 2005, **15**, 83; (c) C. Bucher, C. H. Devillers, J.-C. Moutet, G. Royal, E. Saint-Aman, *Coord. Chem. Rev.*, 2009, **253**, 21; (d) A. Lataifeh, S. Beheshti, H. B. Kraatz, *Eur. J. Inorg. Chem.*, 2009, 3205; (e) T. Moriuchi, T. Hirao, *Acc. Chem. Res.*, 2010, **43**, 1040.

58. (a) J. C. Swarts, *Macromol. Symp.*, 2002, **186**, 123; (b) E. W. Neuse, *J. Inorg. Organomet. Polym. Mater.*, 2005, **12**, 3; (c) L. V. Snegur, V. N. Babin, A. A. Simenel, Y. S. Nekrasov, L. A. Ostrovskaya, N. S. Sergeeva, *Russ. Chem. Bull.*, 2010, **59**, 2167; (d) C. Ornelas, *New. J. Chem.*, 2011, **35**, 1973.

59. *Metallocenes: An Introduction to Sandwich Complexes* (Ed.: N. J. Long), Blackwell Science, London, U. K., 1998.

60. J.-C. Hierso, R. Smaliy, R. Amardeil, P. Meunier, *Chem. Soc. Rev.*, 2007, **36**, 1754.

61. R. C. J. Atkinson and N. J. Long, *Monodentate Ferrocene Donor Ligands*, in *Ferrocenes: Ligands, Materials and Biomolecules* (Ed.: P. Štěpnička), Wiley, Chichester, U. K., 2008, part 1, ch. 1, p. 3.

62. (a) T. J. Colacot, *Platinum Metals Rev.*, 2001, **45**, 22; (b) T. J. Colacot, *Chem. Rev.*, 2003, **103**, 3101; (c) P. Barbaro, C. Bianchini, G. Giambastiani, S. L. Parisel, *Coord. Chem. Rev.*, 2004, **248**, 2131; (d) R. C. J. Atkinson, V. Gibson, N. J. Long, *Chem. Soc. Rev.*, 2004, **33**, 313; (e) U. Siemeling, T.-C. Auch, *Chem. Soc. Rev.*, 2005, **34**, 584; (f) S. P. Flanagan, P. J. Guiry, *J. Organomet. Chem.*, 2006, **691**, 2124; (g) R.G. Arrayás, J. Adrio, J. C. Carretero, *Angew. Chem. Int. Ed.*, 2006, **45**, 7674.

63. S. I. Pereira, J. Adrio, A. M. S. Silva, J. C. Carretero, *J. Org. Chem.*, 2005, 70, 10175.

64. N. Kataoka, Q. Shelby, J. P. Stambuli, J. F. Hartwig, *J. Org. Chem.*, 2002, **67**, 5553.

65. (a) H. U. Blaser, *Adv. Synth. Catal.*, 2003, **344**, 17; (b) R. Dorta, D. Broggini, R. Stoop, H. Rüegger, F. Spindler, A. Togni, *Chem. Eur. J.*, 2004, **10**, 267.

66. D. Marquarding, H. Klusacek, G. Gokel, P. Hoffmann, I. Ugi, *J. Am. Chem. Soc.*, 1970, **92**, 5389.

67. T. Hayashi, K. Yamamoto, M. Kumada, *Tetrahedron Lett.*, 1974, 4405.

68. (a) F. Rebiére, O. Riant, L. Ricard, H. B. Kagan, *Angew. Chem. Int. Ed.*, 1993, 32, 568; (b) N. M. Lagneau, Y. Chen, P. M. Robben, H.-S. Sin, K. Tasaku, J.-S. Chen, P. D. Robinson, D. H. Hua, *Tetrahedron*, 1998, **54**, 7301.

69. (a) O. Riant, O. Samuel, H. B. Kagan, *J. Am. Chem. Soc.*, 1993, **115**, 5835; (b) O. Riant, O. Samuel, T. Flessner *et al*., *J. Org. Chem.*, 1997, **62**, 6733.

70. (a) C. J. Richards, T. Damalis, D. E. Hibbs, M. B. Hursthouse, *Synlett*, 1995, 74; (b) T. Sammakia, H. A. Latham, D. R. Schaad, *J. Org. Chem.*, 1995, **60**, 10; (c) Y. Nishibayashi, S. Uemura, *Synlett*, 1995, 79.

71. A. Togni, C. Breutel, A. Schnyder, F. Spindler, H. Landert, A. Tijani, *J. Am. Chem. Soc.*, 1994, **116**, 4062.

72. W. Chen, W. Mbafor, S. M. Roberts, J. Whittall, *J. Am. Chem. Soc.*, 2006, **128**, 3922.

73. G. P. Sollot, J. L. Snead, S. Portnoy, W. R. Peterson, Jr., H. E. Mertwoy, *Chem. Abstr.*, 1965**, 63**, 18147.

74. G. Bandoli, A. Dolmella, *Coord. Chem. Rev.*, 2000, **209**, 161.

75. P. Dierkes, P. W. N. M. van Leeuwen, *J. Chem. Soc., Dalton Trans.*, 1999, 1519.

76. Z. Freixa, P. W. N. M. van Leeuwen, *Dalton Trans.*, 2003, 1890.

77. (a) S. W. Chien, T. S. A. Hor, *The Coordination and Homogeneous Catalytic Chemistry of 1,1′-Bis(diphenylphosphino)ferrocene and its Chalcogenide Derivatives*, in *Ferrocenes: Ligands, Materials, Biomolecules* (Ed.: P. Štěpnička),

Wiley, Chichester, U. K., 2008, part 1, ch. 2, p. 33; (b) T. J. Colacot, *Platinum Met. Rev.*, 2001, **45**, 22; (c) K.-S. Gan, T. S. A. Hor, *1,1'-Bis(diphenylphosphino)-ferrocene – Coordination Chemistry, Organic Syntheses, and Catalysis*, in *Ferrocenes: Homogeneous catalysis, Organic synthesis, Materials science* (Eds.: A. Togni, T. Hayashi), VCH, Weinheim, Germany, 1995, part 1, ch. 1, p. 3.

78. A. Fihri, P. Meunier, J.-C. Hierso, *Coord. Chem. Rev.*, 2007, **251**, 2007.
79. P. Štěpnička, I. Císařová, J. Schulz, *Organometallics*, 2011, **30**, 4393.
80. P. Štěpnička, *1'-Functionalised Ferrocene Phosphines: Synthesis, Coordination Chemistry and Catalytic Applications*, in *Ferrocenes: Ligands, Materials, Biomolecules* (Ed.: P. Štěpnička), Wiley, Chichester, U. K., 2008, part 1, ch. 5, p. 177.
81. (a) R. G. Pearson, *J. Am. Chem. Soc.*, 1963, **85**, 3533; (b) R. G. Pearson, *J. Chem. Educ.*, 1987, **64**, 561.
82. (a) A. Bader, E. Lindner, Coord. Chem. Rev., 1991, **108**, 27; P. Braunstein, F. Naud, Angew. Chem. Int. Ed., 2001, 40, 680; (c) A. B. Charette, A. Côté, J.-N. Desrosiers, I. Bonnaventure, V. N. G. Lindsay, C. Lauzon, J. Tannous, A. A. Boezio, *Pure Appl. Chem.*, 2008, **80**, 881; (d) W.-H. Zhang, S. W. Chien, T. S. A. Hor, *Coord. Chem. Rev.*, 2011, **255**, 1991.
83. (a) P. Štěpnička, I. Císařová, *Collect. Czech. Chem. Commun.*, 2006, **71**, 215; (b) P. Štěpnička, *J. Organomet. Chem.*, 2008, **693**, 297.
84. (a) S. Basra, J. G. De Vries, D. J. Hyett, G. Harrison, K. M. Heslop, A. G. Orpen, P. G. Pringle, K. von der Luehe, *Dalton Trans.*, 2004, 1901; (b) P. Štěpnička, I,. Císařová, R. Gyepes, *Eur. J. Inorg. Chem.*, 2006, 926.
85. J. Podlaha, P. Štěpnička, J. Ludvík, I. Císařová, *Organometallics*, 1996, **15**, 543.
86. (a) P. Štěpnička, J. Schulz, T. Klemann, U. Siemeling, I. Císařová, *Organometallics*, 2010, **29**, 3187; (b) U. Siemeling, T. Klemann, C. Bruhn, J. Schulz, P. Štěpnička, *Dalton Trans.*, 2011, 4722; (c) U. Siemeling, T. Klemann, C. Bruhn, J. Schulz, P. Štěpnička, *Z. Anorg. Allg. Chem.*, 2011, **637**, 1824.
87. P. Štěpnička, *Eur. J. Inorg. Chem.*, 2006, 3787.
88. P. Štěpnička, J. Podlaha, R. Gyepes, M. Polášek, J. Organomet. Chem., 1998, **552**, 293.
89. P. Štěpnička, R. Gyepes, J. Podlaha, *Collect. Czech. Chem. Commun.*, 1998, **63**, 64.
90. P. Štěpnička, I. Císařová, J. Podlaha, J. Ludvík, *J. Organomet. Chem.*, 1999, **582**, 319.
91. P. Štěpnička, I. Císařová, *J. Chem. Soc., Dalton Trans.*, 1998, 2807.

92. A. M. Trzeciak, P. Štěpnička, E. Mieczyńska, J. J. Ziołkowski, *J. Organomet. Chem.*, 2005, **690**, 3260.

93. K. Mach, J. Kubišta, I. Císařová, P. Štěpnička, *Acta Cryst., Sect. C: Cryst. Struct. Commun.*, 2002, **58**, m116.

94. P. Štěpnička, J. Demel, J. Čejka, *J. Mol. Catal. A*, 2004, **224**, 161.

95. L. Meca, D. Dvořák, J. Ludvík, I. Císařová, P. Štěpnička, *Organometallics*, 2004, **23**, 2541.

96. P. Štěpnička, H. Solařová, I. Císařová, *J. Organomet. Chem.*, 2011, **696**, 3727.

97. D. Drahoňovský, I. Císařová, P. Štěpnička, H. Dvořáková, P. Maloň, D. Dvořák, *Collect. Czech Chem. Commun.*, 2001, **66**, 588.

98. Chemistry of phosphane-amides was only recently comprehensively reviewed: P. Štěpnička, *Chem. Soc. Rev.*, 2012, **41**, 4273.

99. J. Kühnert, I. Císařová, M. Lamač, P. Štěpnička, *Dalton Trans.*, 2008, 2454.

100. J. Kühnert, M. Dušek, J. Demel, H. Lang, P. Štěpnička, *Dalton Trans.*, 2007, 2802.

101. J. Tauchman, I. Císařová, P. Štěpnička, *Organometallics*, 2009, **28**, 3288.

102. (a) P. Štěpnička, *New. J. Chem.*, 2002, **26**, 567; (b) B. Breit, D. Breuninger, *Synthesis*, 2005, 2782.

103. J. Tauchman, I. Císařová, P. Štepnička, *Eur. J. Org. Chem.*, 2010, 4276.

104. J. Tauchman, I. Císařová, P. Štěpnička, *Dalton Trans.*, 2011, **40**, 11748.

105. J. Schulz, I. Císařová, P. Štěpnička, *J. Organomet. Chem.*, 2009, **694**, 2519.

106. I. Villanueva, B. Hernandez, V. Chang, M. D. Heagy, *Synthesis*, 2000, 1435.

107. For literature references, see Appendix 1.

108. For a general reviews on redox isomerization of allylic alcohols, see: (a) R. C. van der Drift, E. Bouwman and E. Drent, *J. Organomet. Chem.*, 2002, **650**, 1; (b) R. Uma, C. Crévisy and R. Grée, *Chem. Rev.*, 2003, **103**, 27; (c) V. Cadierno, P. Crochet and J. Gimeno, *Synlett*, 2008, 1105; (d) L. Mantilli and C. Mazet, *Chem. Lett.*, 2011, **40**, 341; (e) N. Ahlsten, A. Bartoszewicz and B. Martín-Matute, *Dalton Trans.*, 2012, **41**, 1660; (f) P. Lorenzo-Luis, A. Romerosa and M. Serrano-Ruiz, *ACS Catal.*, 2012, **2**, 1079.

109. (a) V. Cadierno, P. Crochet, S. E. García-Garrido and J. Gimeno, *Dalton Trans.*, 2004, 3635; (b) P. Crochet, J. Díez, M. A. Fernández-Zúmel and J. Gimeno, *Adv. Synth. Catal.*, 2006, **348**, 93; (c) A. E. Díaz-Álvarez, P. Crochet, M. Zablocka, C. Duhayon, V. Cadierno, J. Gimeno and J.-P. Majoral, *Adv. Synth. Catal.*, 2006, **348**,

1671; (d) M. Fekete and F. Joó, *Catal. Commun.*, 2006, **7**, 783; (g) B. Lastra-Barreira, J. Díez and P. Crochet, *Green Chem.*, **11**, 1681; (h) A. Azua, S. Sanz and E. Peris, *Organometallics*, 2010, **29**, 3661.

110. The preliminary catalytic study was performed by Helena Šrámková: H. Šrámková, *Diplomová práce*, Univerzita Karlova, Praha, 2011.

111. D. S. Pandey, A. N. Sahay, O. S. Sisodia, N. K. Jha, P. Sharma, H. E. Klaus, A. Cabrera, *J. Organomet. Chem.*, 1999, **592**, 278.

112. (a) W. H. Ang, P. J. Dyson, *Eur. J. Inorg. Chem.*, 2006, 4003; (b) G. Süss-Fink, *Dalton Trans.*, 2010, **39**, 1673.

113. (a) Q. Chen, J. Zubieta, *Inorg. Chem.*, 1990, 29, 1456; (b) Q. Chen, J. Zubieta, *Inorg. Chim. Acta*, 1992, 198-200, 95; (c) J. W. Han, K. I. Hardcastle, C. L. Hill, *Eur. J. Inorg. Chem.*, 2006, 2598; (d) C. L. Hill, T. M. Anderson, J. W. Han, D. A. Hillesheim, Y. V. Geletii, N. M. Okun, R. Cao, B. Botar, D. G. Musaev, K. Morokuma, *J. Mol. Catal. A: Chem.*, 2006, **251**, 234; (e) J. W. Han, C. L. Hill, *J. Am. Chem. Soc.*, 2007, **129**, 15094.

114. (a) P. R. Marcoux, B. Hasenknopf, J. Vaissermann, P. Gouzerh, *Eur. J. Inorg. Chem.*, 2003, 2406; (b) Y. F. Song, D. L. Long, L. Cronin, *Angew. Chem. Int. Ed.*, 2007, **46**, 3900.

115. (a) L. S. Joseph, G. Y. Victor Jr., E. A. Maatta, *Angew. Chem. Int. Ed.*, 1995, **34**, 2547; (b) J. H. Kang, J. A. Nelson, M. Lu, B. H. Xie, Z. H. Peng, D. R. Powell, *Inorg. Chem.*, 2004, 43, 6408; (c) Y. Yan, B. Li, Q. He, Z. He, H. Ai, H. Wang, Z. Yin, L. Wu, *Soft Matter*, 2012, **8**, 1593.

116. Q. Chen, D. P. Goshorn, C. P. Scholes, X. Tan, J. Zubieta, *J. Am. Chem. Soc.*, 1992, **114**, 4667.

117. For the example of a catalytic use of surface active donors, see: (a) T. Bartik, B. Bartik, B. E. Hanson, *J. Mol. Catal.*, 1994, **88**, 43; (b) H. Ding. B. E. Hanson, *J. Chem. Soc., Chem. Commun.*, 1994, 2747; (c) H. Ding, B. E. Hanson, T. Bartik. B. Bartik, *Organometallics*, 1994, **13**, 3761; (d) M. S. Goedheijt, B. E. Hanson, J. N. H. Reek, P. C. J. Kaver, P. W. N. M. van Leeuwen, *J. Am. Chem. Soc.*, 2000, 122, 1650; (c) H. Ding, J. Kang, B. E. Hanson, C. W. Kohlpaintner, *J. Mol. Catal. A: Chem.*: 1997, **124**, 21;

118. W. Zhang, Y. Yoneda, T. Kida, Y. Nakatsui, I. Ikeda, *Tetrahedron: Asymmetry*, 1998, **9**, 3371.

119. P. Štěpnička, H. Solařová, M. Lamač, I. Císařoví, *J. Organomet. Chem.*, 2010, **695**, 2423.

120. (a) M. Sundermeier, A. Zapf, M. Beller, *Eur. J. Inorg. Chem.*, 2003, 3513; (b) P. Anbarasan, T. Schareina, M. Beller, *Chem. Soc. Rev.*, 2011, **40**, 5049.

121. T. Schareina, A. Zapf, M. Beller, 2004, 1388.

122. (a) P. Y. Yeung, C. M. So, C. P. Lau and F. Y. Kwong, *Angew. Chem., Int. Ed.*, 2010, **49**, 8918; (b) J. L. Zhang, X. R. Chen, T. J. Hu, Y. A. Zhang, K. L. Xu, Y. P. Yu, J. Huang, *Catal. Lett.*, 2010, **139**, 56.

Appendices

List of Appendices

1) J. Schulz, I. Císařová, P. Štěpnička: "Arene-Ruthenium Complexes with Phosphanylferrocene Carboxamides Bearing Polar Hydroxyalkyl Groups: Synthesis, Molecular Structure and Catalytic Use in Redox Isomerization of Allylic Alcohols to Carbonyl Compounds." Submitted to the *European Journal of Inorganic Chemistry*.

2) P. Štěpnička, I. Císařová, J. Schulz: "Tri-μ-chlorido-bis[(η^6-hexamethylbenzene)-ruthenium(II)] tetrachloridoferrate(III)." *Acta Cryst.*, 2011, **E67**, m1363.

3) J. Schulz, A. K. Renfrew, I. Císařová, P. J. Dyson, P. Štěpnička: "Synthesis and Anticancer Activity of Chalcogenide Derivatives and Platinum(II) and Palladium(II) Complexes Derived from a Polar Ferrocene Phosphanyl-carboxamide." *Appl. Organometal. Chem.*, 2010, **24**, 392.

4) J. Schulz, R. Gyepés, I. Císařová, P. Štěpnička: "Synthesis, Structural Characterisation and Bonding in an Anionic Hexavanadate Bearing Redox-Active Ferrocenyl Groups at the Periphery." *New. J. Chem.*, 2010, **34**, 2749.

5) J. Schulz, I. Císařová, P. Štěpnička: "Phosphinoferrocene Amidosulfonates: Synthesis, Palladium Complexes, and Catalytic Use in Pd-Catalyzed Cyanation of Aryl Bromides in an Aqueous Reaction Medium." *Organometallics*, 2012, **31**, 729.

Appendix 1

J. Schulz, I. Císařová, P. Štěpnička: "Arene-Ruthenium Complexes with Phosphanylferrocene Carboxamides Bearing Polar Hydroxyalkyl Groups: Synthesis, Molecular Structure and Catalytic Use in Redox Isomerization of Allylic Alcohols to Carbonyl Compounds." Submitted to the *European Journal oh Inorganic Chemistry*.

DOI: 10.1002/ejic.2012((will be filled in by the editorial staff))

Arene-Ruthenium Complexes with Phosphanylferrocene Carboxamides Bearing Polar Hydroxyalkyl Groups: Synthesis, Molecular Structure and Catalytic Use in Redox Isomerization of Allylic Alcohols to Carbonyl Compounds

Jiří Schulz,[a] Ivana Císařová[a] and Petr Štěpnička*[a]

In memory of Professor Jaroslav Podlaha

Keywords: Phosphane ligands / Metallocenes / Ruthenium / Isomerization / Structure Elucidation

Phosphanylferrocene carboxamide $Ph_2PfcCONHCH_2CH_2OH$ (**1**, fc = ferrocene-1,1′-diyl) and its newly synthesized congeners, $Ph_2PfcCONHCH(CH_2OH)_2$ (**2**) and $Ph_2PfcCONHC(CH_2OH)_3$ (**3**) were used to prepare a series of (η^6-arene)ruthenium complexes [(η^6-arene)$RuCl_2$(L-κ*P*)], where arene = benzene, *p*-cymene and hexamethylbenzene, and L = **1**–**3**. All compounds have been characterized by multinuclear NMR and IR spectroscopy, mass spectrometry and by elemental analysis. In addition, the molecular structures have been determined for **2**, **3**, **3O** (a phosphane oxide resulting by oxidation of **3**), **5c**·CH_2Cl_2, and **6c**·Et_2O by single-crystal X-ray diffraction analysis. The (arene)ruthenium complexes were studied as catalysts for redox isomerization of allyl alcohols to carbonyl compounds. The best results were achieved with [(η^6-*p*-cymene)$RuCl_2$(**1**-κ*P*)] resulting from the readily available Ru-precursor and the simplest ligand. Substrates with unsubstituted double bonds were cleanly isomerized with this catalyst in 1,2-dichloroethane, while those bearing substituents at the double bond (particularly in position closer to the OH group) achieved lower conversions and selectivity. A similar trend was observed when pure water was used as the solvent, except that the best result (complete conversion) were seen for 1,3-diphenylallyl alcohol as the most hydrophobic substrate.

[a] Department of Inorganic Chemistry, Faculty of Science, Charles University in Prague; Hlavova 2030, 12840 Prague, Czech Republic
Fax: +420 221 951 2543
E-mail: stepnic@natur.cuni.cz

Supporting information for this article is available on the WWW under http://www.eurjic.org/ or from the author.

Introduction

Phosphanylcarboxylic amides are versatile ligands finding manifold applications in catalysis.[1] The possibility of practically unlimited combining of various molecular fragments by amide coupling makes phosphanylcarboxylic amides structurally very flexible and can be advantageously utilized in the preparation of purpose-tailored donors. In such compounds, the phosphanyl moiety typically acts as a metal binding site while the amide moiety is used to impart the desired property and/or to increase the affinity of these donors and their complexes to a particular solvent or phase. For instance, a number of ligands has been designed using this approach for the use in transition metal-catalyzed reactions performed in ionic liquids, water and mixed-solvent aqueous reaction media.[1,2]

Only a handful of such modified donors have been reported for the practically very successful phosphanylferrocene ligands.[3,4] Pugin *et al*. prepared chiral phosphanylferrocene donors (Josiphos analogues) bearing polar, solvent-directing imidazolium and polycarboxylate tags.[5] We have recently reported several polar ferrocene-based amidophosphane donors resulting by conjugation of 1′-(diphenylphosphanyl)ferrocene-1-carboxylic acid (Hdpf; Scheme 1)[6] with amino-sulfonic acids,[7] amino acids[8] or—hydroxyamines.[9] Since phosphanylamides bearing hydroxyalkyl substituents have only few precedents even among simple (organic) ligands,[10,11,12] we set out to extend our earlier study focused on ligand **1**[9,13] (Scheme 1) toward the structurally related bis- and tris(hydroxymethyl)methanamine derivatives **2** and **3**.

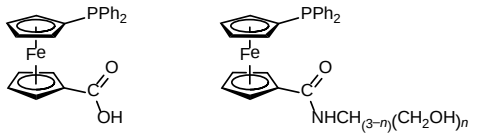

Hdpf — **1** (*n* = 1), **2** (*n* = 2), **3** (*n* = 3)

Scheme 1.

This contribution describes the preparation and structural characterization of new phosphanylferrocene hydroxyamides **2** and **3** and (η^6-arene)ruthenium complexes featuring compounds **1**–**3** as P-monodentate ligands. Also reported are the results of catalytic testing of the Ru-complexes in redox isomerization of allylic alcohols to carbonyl compounds.

Results and Discussion

Synthesis and structural characterization of the ligands

The 2-hydroxyethyl amide **1** was obtained by amide coupling of Hdpf with 2-ethanolamine upon the actions of 1-ethyl-3-[(3-dimethylamino)propyl]carbodiimide and 1-hydroxybenzotriazole as reported earlier.[9a] Amides **2** and **3** completing the series of structurally related ligands have been also prepared (Scheme 2) by direct amidation of Hdpf with an excess the respective amine

mediated by 2-ethoxy-1-ethoxycarbonyl-1,2-dihydroquinoline (EEDQ) as an amide coupling agent and 4-(dimethylamino)pyridine (DMAP) as a base in pyridine solvent. The coupling agent was chosen mainly to avoid an undesired formation of esters.[14,15] This procedure afforded amides **2** and **3** in good yields (40 and 56 %, respectively) after isolation by column chromatography and subsequent crystallization from ethyl acetate-hexane. Alternatively, compound **3** was synthesized from active pentafluorophenyl ester **4**[9a, 16] and 2-amino-2-hydroxymethyl-propane-1,3-diol (TRIS; route B in Scheme 2). However, this reaction performed in the presence of DMAP in DMF at room temperature afforded the amide with a considerably lower isolated yield (27 %).

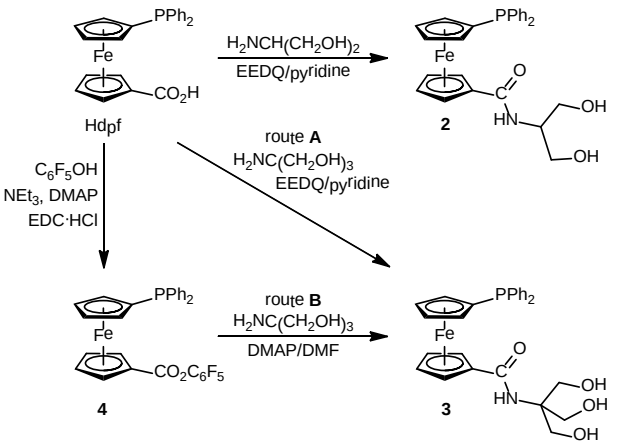

Scheme 2. Synthesis of amides **2** and **3**. Legend: EEDQ = 2-ethoxy-1-ethoxycarbonyl-1,2-dihydroquinoline, EDC = 1-[3-(dimethylamino)propyl]-3-ethylcarbodiimide, DMF = *N*,*N*-dimethylformamide, DMAP = 4-(dimethylamino)pyridine.

The formulation of amides **2** and **3** was confirmed by elemental analysis and by electrospray ionization (ESI) mass spectra that show abundant pseudomolecular ions ($[M - H]^-$). The NMR spectra of **2** and **3** comprise the signals due to the 1′-(diphenylphosphanyl)ferrocen-1-yl group and the amide pendants. It is noteworthy that the positions of the ^1H, $^{13}C\{^1H\}$ and $^{31}P\{^1H\}$ NMR signals due to the former moiety are practically identical with those found for **1**. Differences are seen for the signals of the $NHCH_{3-n}(CH_2OH)_n$ groups, which shift to lower fields in both ^1H and $^{13}C\{^1H\}$ NMR spectra upon increasing substitution at C^α (i.e., with increasing *n*). The presence of the amide moiety is clearly manifested in IR spectra through characteristic amide I (ca. 1620 cm^{-1}), amide II (ca. 1540 cm^{-1}) and ν_{NH} bands (3260–3300 cm^{-1}).

Molecular structures of compounds 2, 3 and 3O

Single crystals of **2** and **3** suitable for X-ray diffraction analysis were grown from ethyl acetate-hexane. The same procedure also afforded crystals of phosphane oxide **3O**, resulting obviously by slow oxidation of the parent phosphane with air. Intentionally, this compound was prepared by the reaction of phosphane **3** with hydrogen peroxide (see Experimental Section). Views of the molecular structures of **2**, **3** and **3O** are presented in Figures 1-3, respectively. Selected geometric data are summarized in Table 1.

The ferrocene moieties in **2**, **3** and **3O** are regular, showing marginal variations in the individual Fe-C distances and, accordingly, tilt angles of only ca. 1°. The structures differ by the orientation of the substituents attached to the ferrocene moiety. As indicated by the τ angles in Table 1, the cyclopentadienyl rings in **2** and **3** adopt a conformation close to anticlinal eclipsed (ideal value: τ = 144°) and synclinal eclipsed (ideal value: τ = 72°), respectively, while, in **3O**, they assume an intermediate orientation. In all three cases, the amide substituents are rotated from the plane of their bonding cyclopentadienyl ring Cp1. The largest deviation from a coplanar arrangement is seen for compound **3** (see φ angle in Table 1). Otherwise, the molecular structures compare well to those determined for other, uncoordinated Hdpf-based amides.[7,8a,9a,17]

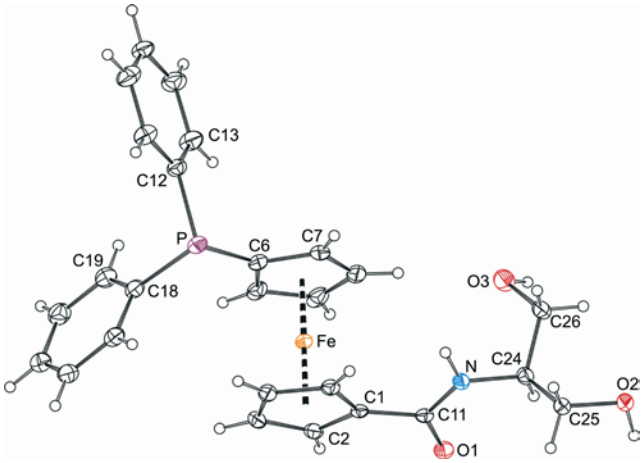

Figure 1. PLATON plot of the molecule of compound **2** showing atom labeling scheme and displacement ellipsoids at the 30% probability level.

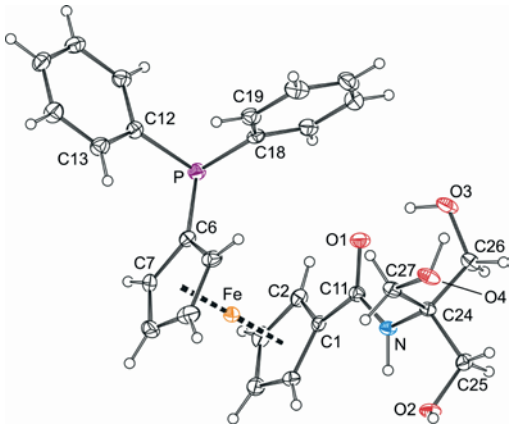

Figure 2. PLATON plot of the molecular structure of compound **3**. Displacement ellipsoids are scaled to 30% probability level.

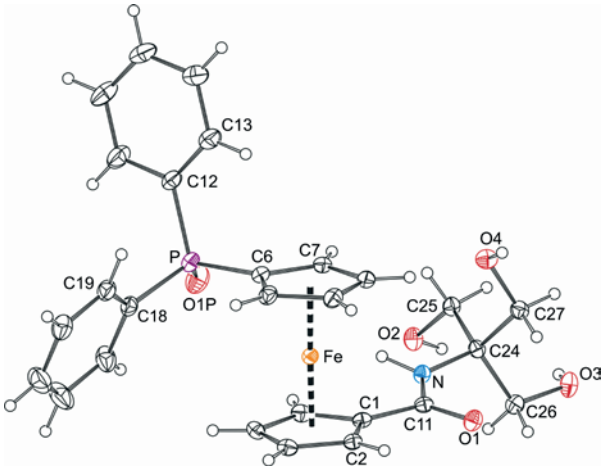

Figure 3. PLATON plot of the molecule of phosphane oxide **3O**. Displacement ellipsoids enclose the 30% probability level.

Table 1. Selected geometric data for **2**, **3** and **3O** (in Å and deg).

Parameter[a]	**2**	**3**	**3O**[b]
Fe-C (range)	2.037(2)-2.053(3)	2.022(3)-2.047(3)	2.032(2)-2.071(2)
Fe-Cg1	1.651(1)	1.641(1)	1.6597(9)
Fe-Cg2	1.643(1)	1.639(1)	1.658(1)
tilt	1.0(1)	1.3(2)	0.9(1)
τ	152.4(2)	79.2(2)	121.4(1)
C1-C11	1.477(3)	1.478(3)	1.482(3)
C11-O1	1.239(2)	1.242(3)	1.236(2)
C11-N	1.347(2)	1.344(3)	1.346(3)
O1-C11-N	122.3(2)	123.8(2)	123.4(2)
φ	17.8(2)	24.7(3)	11.1(2)
C6-P	1.805(3)	1.821(3)	1.775(2)

[a] Definition of the ring planes: Cp1 = C(1-5), Cp2 = C(6-10); Cg1/2 are the centroids of the rings Cp1/2. Tilt = dihedral angle subtended by planes Cp1 and Cp2; τ = torsion angle C1-Cg1-Cg2-C6. φ is the dihedral angle of planes Cp1 and {C11,N,O1}. [b] Further data: P-O1P = 1.456(2) Å.

In their crystals, compounds **2**, **3** and **3O** form complicated supramolecular arrays via hydrogen bonding interactions of the polar amide pendants. In the case of **2**, the individual molecules associate into centrosymmetric pairs by O2-H2O···O1 hydrogen bonds (Figure 4a; for parameters, see Table 2). These dimers, stabilized by intramolecular C8-H8···O3 contacts, are connected to proximal molecules by means of N-H1N···O2 and C2-H2···O3 interactions to form layers oriented parallel to the *bc* plane (Figure 4b). The assembly is further stabilized by O3-H3O···P contacts (Figure 4c) between the hydroxy groups O3-H3O directed above and below the mentioned dimeric units (*N.B.* The O3 atom acts already as an acceptor for two C-H bonds). This rather peculiar interaction is manifested by a distinct electron density peak in an appropriate position, corresponding to lone electron pair at the phosphorus (see Experimental Section). Although considerably weaker than the conventional O···H–O/N hydrogen bonds operating in the structure **2**, the P···H–O interactions have been documented by spectroscopic measurements[18] and can be detected in the crystal structures of other hydroxyphosphanes (including ferrocene-based ones[19]) and adducts formed from phosphanes and alcohols.[20] It is also noteworthy, that the basic dimeric motif in **2** as well as its interactions with adjacent molecules are the *same* as those found in the structure of **1**, from which **2** actually differs by the added CH_2OH arm forming the O-H···P interaction with molecules above and below the dimeric unit.

Table 2. Hydrogen bond parameters for **2**, **3** and **3O**.[a]

D-H···A[b]	D···A distance (Å)	D-H···A angle (°)
	compound **2**	
N-H1N···O2^{i}	3.103(2)	163
O2-H2O···O1P^{ii}	2.745(2)	163
O3-H3O···P^{iii}	3.282(2)	155
C2-H2···O3^{iv}	3.126(3)	132
C8-H8···O3 (I)	3.317(3)	166
	compound **3**	
N-H1N···O2 (I)	2.778(3)	107
N-H1N···O2^{v}	2.952(3)	157
O2-H2O···O4^{vi}	2.675(2)	168
O3-H3O···O1 (I)	2.582(3)	152
O4-H4O···O3^{vii}	2.679(2)	165
	compound **3O**	
N-H1N···O2^{viii}	3.236(2)	170
O2-H2O···O1P^{viii}	2.755(2)	163
O3-H3O···O1P^{viii}	2.695(2)	161
O4-H4O···O1^{ix}	2.780(2)	157
C3–H3···O4^{x}	3.254(2)	153
C5-H5···O2^{viii}	3.288(2)	142
C8-H8···O1^{ix}	3.444(3)	169
C9-H9···O3^{ix}	3.465(3)	157

[a] D = donor, A = acceptor. [b] Symmetry operations: *i*. 1–*x*, *y*–1/2, 3/2–*z*; *ii*. 1–*x*, 2–*y*, 1–*z*; *iii*. *x*, *y*+1, *z*; *iv*. *x*, 3/2–*y*, *z*–1/2; *v*. 1–*x*, –1–*y*, –*z*; *vi*. 2–*x*, –1–*y*, –*z*; *vii*. 2–*x*, –*y*, –*z*, *viii*. 2–*x*, –*y*, 1–*z*; *ix*. 2–*x*, –*y*, 2–*z*; *x*. *x*–1, *y*, *z*. (I) denotes an intramolecular contact.

*** Insert Figure 4 near here ***

The crystal packing of **3** is also dominated by hydrogen bonding interactions of the amide moieties but lacks supportive C-H···O contacts (Figure 5). Each amide unit of **3** forms a closed array with its inversion-related counterpart, where the H1N and O2 atoms act as bifurcated hydrogen bond donors and acceptors, respectively.[21] When combined with additional inter- and intramolecular hydrogen bonds formed by the remaining OH groups, the N/O-H···O interactions give rise to sheets oriented along the *ab* plane. The (phosphanyl)ferrocenyl moieties extending above and below these sheets encase these polar sheets.[22]

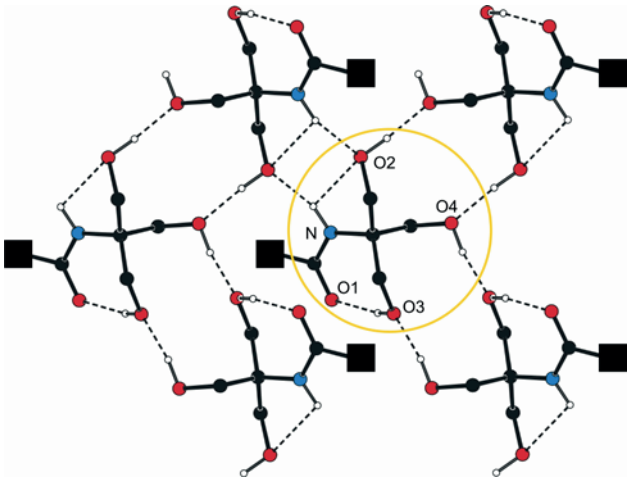

Figure 5. Section of hydrogen-bonded array in the structure of **3**. For clarity, only the OH/NH hydrogens are shown and the bulky phosphanylferrocenyl moieties were replaced with black squares.

The polarized P=O group[23] in **3O** expectedly takes part in hydrogen-bonding (Figure 6). The individual molecules assemble into pairs around inversion centers via N-H···OH and O-H···O=P hydrogen bonds. These dimers are further connected to adjacent dimer units by O-H···O=C interactions, forming double stranded ribbons oriented along the *c* axis. Some C-H···O contacts (Table 2) operate synergistically with these conventional hydrogen bonds.

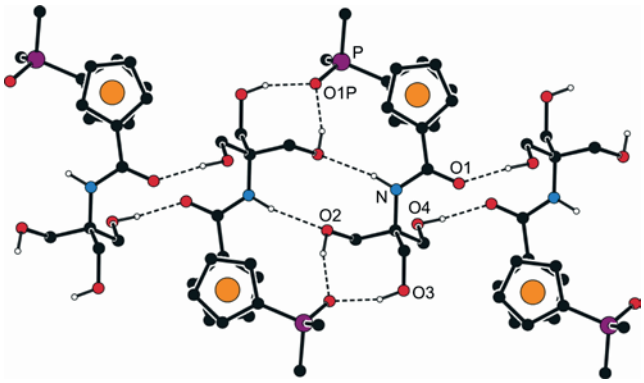

Figure 6. Hydrogen-bonded ribbons in the structure of **3O**. Only OH/NH hydrogens and pivotal carbons from the phenyl rings are shown for clarity.

Synthesis and structural characterization of (η^6-arene)Ru(II) complexes

Ligands **1-3** were employed in the preparation of (η^6-arene)Ru(II) complexes **5-7** (Scheme 3). These complexes resulted readily via bridge-cleavage reactions of the respective chloride dimers [(η^6-arene)$RuCl_2$]$_2$ with stoichiometric amounts of the corresponding phosphanylferrocene ligands and were purified by column chromatography.

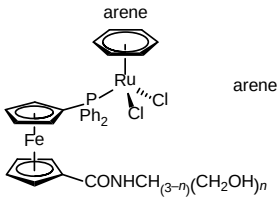

Ligand (n)	1	2	3
benzene	**5a**	**6a**	**7a**
arene = *p*-cymene	**5b**	**6b**	**7b**
C_6Me_6	**5c**	**6c**	**7c**

Scheme 3.

Coordination to the (C_6H_6)Ru and (*p*-cymene)Ru fragments results in a characteristic shift of one ^{1}H NMR signal due to ferrocene CH protons to higher fields (δ_H 3.17-3.72 ppm). In the case of (C_6Me_6)Ru complexes this signal is not observed due to extensive broadening, which reflects a hindered molecular mobility resulting from spatial interactions of the bulky Ru-bound arene and the phosphanylferrocenyl moiety. Similar features have been observed in the spectra of [(η^6-arene)$RuCl_2$(L)] complexes with other phosphanylferrocene carboxamides (L).[8d] The $^{31}P\{^1H\}$ NMR spectra of **5-7** comprise singlet resonances at δ_P 16-20 ppm whereas the ESI MS spectra of **5-7** are dominated by ions resulting by a simultaneous elimination of Cl^- and HCl, $[M - Cl - HCl]^+$.

The molecular structures of solvates **5c**·CH_2Cl_2 and **6c**·Et_2O were determined by single-crystal X-ray diffractions analysis (Figures 7 and 8; Table 3). Both compounds posses the expected three-legged piano stool structures, similar to that determined earlier for [(η^6-*p*-cymene)$RuCl_2$(Hdpf-κ*P*)].[24] The Cl-Ru-Cl and Cl-Ru-P angles do not depart much from the 90° expected for a pseudooctahedral structure in which the arene ligand occupies one trigonal face in the octahedron. On the other hand, the Cg-Ru-Cl and Cg-Ru-P angles involving the centroid of the benzene ring (Cg) differ significantly from each other (Cg-Ru-Cl: 123-126° vs. Cg-Ru-P: 134-135°),[25] reflecting unlike steric demands of the chloride and phosphanylferrocene ligands. Despite this distortion, however, only negligible slanting of the piano-stool structure is seen as indicated by the dihedral angle of the basal plane {Cl1, Cl2, P} and the η^6-arene ring being 4.33(8)° and 5.8(1)° for **5c**·CH_2Cl_2 and **6c**·Et_2O, respectively. The planes of the Ru-bound arene ring and the phosphanyl-substituted cyclopentadienyl ring (Cp2) are mutually rotated by ca. 20°.[26] The ferrocene cyclopentadienyls are tilted by ca. 6° and their substituents adopt an anticlinal eclipsed conformation (cf. the ideal value: τ = 144°). Likewise free ligands, the complexes form hydrogen-bonded supramolecular assemblies in the solid state. Diagrams depicting the crystal packing of **5c**·CH_2Cl_2 and **6c**·Et_2O are presented in Supporting Information (Figures S1 and S2).

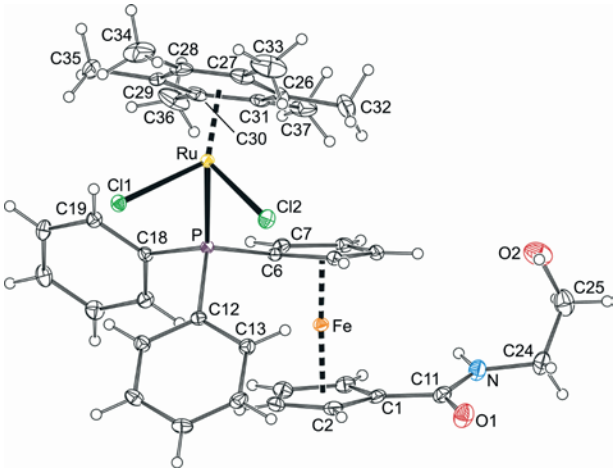

Figure 7. PLATON plot of the complex molecule in the structure of **5c**·CH_2Cl_2. Displacement ellipsoids correspond to the 30% probability level.

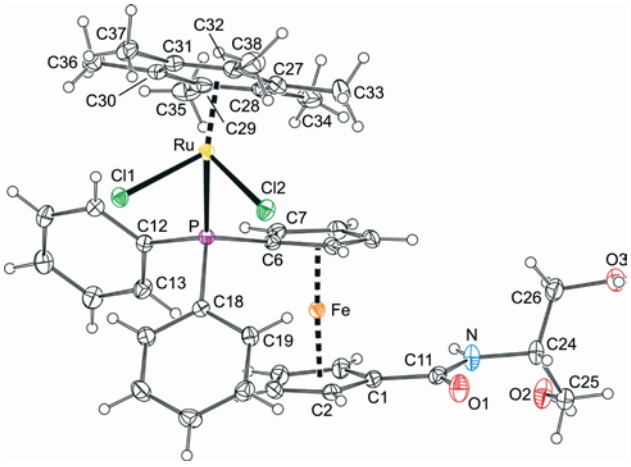

Figure 8. PLATON plot of the complex molecule in the structure of **6c**·Et_2O. Displacement ellipsoids enclose the 30% probability level.

Table 3. Selected geometric data for **5c**·CH_2Cl_2 and **6c**·Et_2O (in Å and deg).

Parameter[a]	**5c**·CH_2Cl_2	**6c**·Et_2O
Ru-Cl1	2.4232(6)	2.4132(6)
Ru-Cl2	2.4228(6)	2.4141(7)
Ru-P	2.3443(5)	2.3569(6)
Ru-C (range)	2.202(2)-2.271(3)	2.211(3)-2.252(3)
Cl1-Ru-Cl2	88.13(2)	88.13(2)
Cl1-Ru-P	85.29(2)	83.59(2)
Cl2-Ru-P	85.99(2)	85.76(2)
Fe-Cg1	1.651(1)	1.650(1)
Fe-Cg2	1.654(1)	1.649(1)
tilt	6.1(1)	5.6(2)

τ	143.0(2)	141.9(2)
C11-O1	1.236(3)	1.239(3)
C11-N	1.344(3)	1.335(3)
O1-C11-N	121.7(2)	121.3(3)
φ	13.7(3)	4.9(3)

[a] Definition of the ring planes: Cp1 = C(1-5), Cp2 = C(6-10); Cg1/2 are the centroids of the rings Cp1/2. Tilt = dihedral angle subtended by planes Cp1 and Cp2; τ = torsion angle C1-Cg1-Cg2-C6. φ denotes the dihedral angle of the planes Cp1 and {C11,N,O1}.

Catalytic tests

Transition metal-catalyzed isomerization of allylic alcohols to saturated carbonyl compounds represents a synthetically useful, atom-economical process that has been growing in importance over the last decade.[27] In the last years, the main effort was focused on the development of efficient catalytic systems promoting this reaction under mild conditions and in short reaction times.[28,29] The progress achieved allowed in turn for the development of various tandem processes (e.g., isomerization/C–C coupling or isomerization/C–F bond formation)[28b] and even an asymmetric variant of this reaction.[30,31] Water as a green solvent with specific properties[32] has been advantageously used as a medium for this reaction, being often employed together with Ru(II) and Ru(IV) catalysts.[33] Recent applications of arene-ruthenium(II) complexes of type [(η^6-arene)$RuCl_2$(L)], where L stands for a hydrophilic ligand,[34] prompted us to test our ruthenium complexes **5**–**7** as defined catalyst precursors for this reaction.

The complexes were firstly assessed in redox isomerization of 1-octen-3-ol as a model substrate (Scheme 4) using 0.5 mol % of the metal catalyst and 2.5 mol.% of KOBu-*t* as a base. Complex **5b** obtained from the most easily accessible Ru precursor and the simplest ligand was chosen for the initial catalytic tests aimed at an optimization of the reaction conditions.

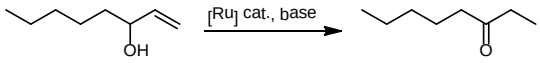

Scheme 4. The model redox isomerization of 1-octen-3-ol to octan-3-one.

Gratifyingly, the model isomerization reaction selectively produced octan-3-one with complete conversion within 1 h in both 1,2-dichloroethane and dioxane at 80 °C. A similar reaction *N*-methylpyrrolidone afforded the ketone with a 33 % conversion, while reactions performed in *N*,*N*-dimethylformamide, *N*,*N*-dimethylacetamide, dimethylsulfoxide, propionitrile, 1-propanol did not proceed in any appreciable extent. The reaction in pure water afforded the desired product with a 55 % conversion after 1 h (at 80 °C) but, surprisingly, no reaction was observed in a 1/1 water-dioxane mixture under similar conditions. The reaction in 1,2-dichloroethane did not proceed in the absence of a base. On the other hand, addition of any common base in catalytic amount (2.5 mol. % of KOBu-*t*, KOAc, KOH, K_2CO_3 or K_3PO_4) ensued in a complete conversion in 1 h.

A possible influence of the structure of the pre-catalysts was investigated next. The results achieved with all Ru–Fe complexes **5–7** in the model reaction (0.5 mol % Ru, 2.5 mol. % KOBu-*t*, 1,2-dichloroethane, 80° C/1 h) are summarized in Table 4. The data clearly indicate that the catalytic performance is determined mainly by the phosphane ligand. Complexes prepared from ligands **1** and **2** afforded practically quantitative conversions. Those resulting from **3** performed considerably worse. The influence of the Ru-bound arene is less pronounced. The best results were achieved with *p*-cymene complexes whereas complexes bearing C_6Me_6 as the most bulky and electron-rich arene ligand afforded the lowest conversions. It should be also noted that all compounds **5**–**7** performed better than the related complex obtained from the parent carboxyphosphane, [(η^6-*p*-cymene)$RuCl_2$(Hdpf-κ*P*)],[24] which gave only 23 % conversion under identical conditions.

Table 4. Catalytic results achieved with (η^6-arene)Ru(II) **5**–**7** in the model isomerization reaction of 1-octen-3-ol to octan-3-one performed in 1,2-dichloroethane.[a]

Ligand/arene	Catalyst/NMR yield[b] (%)		
	C_6H_6	*p*-cymene	C_6Me_6
1	**5a**/100	**5b**/100	**5c**/>98
2	**6a**/100	**6b**/>98	**6c**/37
3	**7a**/29	**7b**/55	**7c**/27

[a] Substrate (1.0 mmol), catalyst (0.5 mol. %), KOBu-*t* (2.5 mol. %), 1,2-dichloroethane (4 mL), 1 h at 80 °C. [b] Determined by ^{1}H NMR. The results are an average of two independent runs.

Since it is known that the course of the redox isomerization is affected by the structure of the substrate,[27,28] the readily accessible and active catalyst **5b** (1 or 2 mol %) was further evaluated in reactions of various substituted allylic alcohols (Scheme 5). The results collected in Table 5 for reactions in 1,2-dichloroethane indicate that secondary allylic alcohols with unsubstituted double bonds are isomerized best (entries 1 and 5). The presence of any substitutents at the double bond (particularly in position adjacent to the OH-substituted carbon) in both primary and secondary allylic alcohols results in relatively lower conversions and can also incite undesired direct oxidation of the substrate to the respective α,β-unsaturated ketone (Scheme 5).

When the same isomerization reactions were performed in water, 1,3-diphenylallyl alcohol (R^1/R^2/R^3 = Ph/H/Ph) was surprisingly fully and cleanly converted to the corresponding saturated ketone in 20 h (**5b**: 2 mol. %). A plausible explanation can be sought in solubility of this compound, which is most hydrophobic in the series and can probably form droplets that accumulate the catalyst (reaction "on-water").[35,32e] Among other substrates tested, only but-3-en-2-ol (R^1/R^2/R^3 = Me/H/H; 17% yield) and 2-methylprop-2-en-1-ol (Ph/H/H, 29% yield; N.B. both are secondary alcohols with unsubstituted double bonds) were converted to the respective saturated ketones in a notable extent. Other substrates substituted at the double bond achieved typically less than 5% conversions (for complete results in a tabular form, see Supporting Information, Table S1.)

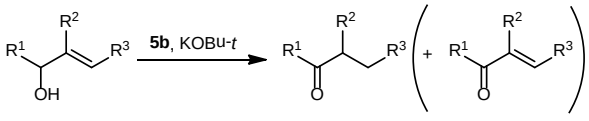

Scheme 5. Redox-isomerization of substituted allylic alcohols.

Table 5. Catalytic results achieved with complex **5b** in redox isomerization of various vinyl alcohols in 1,2-dichloroethane.[a]

Entry	Substrate			NMR yield (%)[b]			
	R^1	R^2	R^3	1 h	3 h	20 h	20 h[c]
1	Me	H	H	11 (2)	13 (3)	17 (6)	78 (3)
2	H	Me	H	0 (0)	3 (0)	4 (0)	7 (0)

3	H	H	Me	8 (0)	14 (0)	18 (7)	25 (0)
4	Me	H	Me	6 (14)	6 (20)	9 (25)	23 (37)
5	Ph	H	H	42 (0)	49 (0)	67 (0)	79 (0)
6	H	H	Ph	0 (0)	4 (5)	10 (6)	30 (6)
7	Ph	H	Ph	0 (0)	19 (0)	39 (0)	40 (0)

[a] Substrate (1.0 mmol), catalyst **5b** (1 mol. % unless specified otherwise) and KOBu-*t* (5 mol. %) in 1,2-dichloroethane (4 mL) at 80 °C. [b] Determined by ^{1}H NMR. The amount of α,β-unsaturatated ketone (oxidation product) is given in parentheses. [c] Reactions in the presence of 2 mol. % of the Ru catalyst.

Conclusion

Compounds **1**–**3** representing a complete series of structurally related phosphanylferrocene carboxamides bearing congeneric polar hydroxyalkyl groups were utilized as P-monodentate ligands in (η^6-arene)Ru(II) complexes of the type [(η^6-arene)RuCl$_2$(L-κ*P*)] (arene = benzene, *p*-cymene and hexamethylbenzene; L = **1**–**3**). Both the ligands and (η^6-arene)Ru(II) complexes thereof form complex supramolecular assemblies in the solid state that are build up by means of hydrogen bonding interactions of their polar hydroxyamide pendants. The complexes were demonstrated to efficiently mediate redox isomerization of allylic alcohols to the respective carbonyl compounds, showing best results for allylic alcohols possessing non-substituted double bonds.

Experimental Section

Materials and methods

All syntheses were performed under an argon atmosphere and with exclusion of the direct daylight. Hdpf,[6a] **1**,[9a] **4**,[9a,16] [(η^6-C$_6$H$_6$)RuCl$_2$]$_2$[36] and [(η^6-C$_6$Me$_6$)RuCl$_2$]$_2$[37] were prepared according to literature procedures. Other chemical were obtained from commercial sources (Alfa-Aesar, Fluka, Sigma-Aldrich) and were used as received. Solvents (Lachner) used for the syntheses and catalytic tests were dried over appropriate drying agents (dichloromethane, 1,2-dichloroethane and chloroform: anhydrous potassium carbonate, 1,4-dioxane: sodium metal, acetonitrile: P_2O_5) and freshly distilled under argon. Solvents used in crystallizations and for chromatography were used without any additional purification.

NMR spectra were recorded with a Varian Unity Inova 400 spectrometer. Chemical shifts (δ in ppm) are given relative to internal SiMe$_4$ (^{1}H and ^{13}C) or external 85% aqueous H$_3$PO$_4$ (^{31}P). In addition to the standard notation of the signal multiplicity, vt and vq are used to distinguish virtual triplets and quartets, respectively, arising from magnetically non-equivalent protons in the AA′BB′ and AA′BB′X spin systems (X = ^{31}P) of the unsymmetrically 1,1′-disubstituted ferrocene moiety (N.B. fc = ferrocene-1,1′-diyl). IR spectra were measured with an FTIR Nicolet Magna 650 spectrometer in the range 400-4000 cm^{-1}. Low-resolution electrospray ionization (ESI) mass spectra were obtained with a Bruker Esquire 3000 instrument using methanolic solutions.

Syntheses

1′-(Diphenylphosphanyl)-1-[*N*-(bis(hydroxymethyl)methyl)carbamoyl]ferrocene (2). Hdpf (1.66 g, 4.0 mmol), serinol (1.46 g, 16.0 mmol), 4-(dimethylamino)pyridine (24 mg, 0.2 mmol) and EEDQ (1.48 g, 6.0 mmol) were dissolved in pyridine (40 mL) and the resulting mixture was stirred at 120 °C (temperature in bath) for 1 h and then at room temperature for 1 day. The volatiles were removed under reduced pressure and the solid residue was purified by column chromatography over silica gel. Elution with dichloromethane-methanol (50:1 v/v) led to a development of three minor bands, which were discarded. The eluent was then changed for dichloromethane-methanol (20:1 v/v) to elute a major orange band due to the product. Following evaporation, the crude product was crystallized from warm ethyl acetate-hexane mixture (60 mL, 1:2 v/v) by slow cooling down to –18 °C. The resulting crystalline material was filtered off, washed with diethyl ether and pentane, and dried under vacuum. Yield of **2**: 0.79 g (40%), orange needles.

^{1}H NMR (400.0 MHz, CDCl$_3$, 25 °C): δ = 3.30 (br s, 2 H, OH), 3.91 (m, 4 H, CH$_2$O), 4.07 (m, 1 H, NHC*H*), 4.10 (vq, *J*′ = 1.8 Hz, 2 H, CH of fc), 4.20 (vt, *J*′ = 2.0 Hz, 2 H, CH of fc), 4.46 (vt, *J*′ = 1.8 Hz, 2 H, CH of fc), 4.62 (vt, *J*′ = 2.0 Hz, 2 H, CH of fc), 6.61 (d, $^3J_{HH}$ = 7.4 Hz, 1 H, NH), 7.31-7.39 (m, 10 H, PPh$_2$) ppm. ^{13}C{^{1}H} NMR (100.6 MHz, CDCl$_3$, 25 °C): δ = 52.53 (NCH), 63.96 (CH$_2$O), 69.70 (CH of fc), 71.61 (CH of fc), 72.76 (d, J_{PC} = 4 Hz, CH of fc), 74.60 (d, J_{PC} = 13 Hz, CH of fc), 76.36 (*C*–CONH of fc), 128.37 (d, $^3J_{PC}$ = 7 Hz, CH$_{meta}$ of PPh$_2$), 128.93 (CH$_{para}$ of PPh$_2$), 133.41 (d, $^2J_{PC}$ = 20 Hz, CH$_{ortho}$ of PPh$_2$), 137.70 (d, $^1J_{PC}$ = 6 Hz, C$_{ipso}$ of PPh$_2$), 170.72 (C=O) ppm. The signal of C–P of fc was not found. ^{31}P{^{1}H} NMR (161.9 MHz, CDCl$_3$, 25 °C): δ = –17.3 (s) ppm. IR (Nujol): ν = 3300 s, 1605 s, 1549 s, 1346 m, 1307 m, 1218 w, 1192 w, 1161 m, 1092 w, 1053 s, 964 w, 846 w, 822 w, 759 w, 743 m, 701 m, 523 m, 490 m, 453 m cm^{-1}. ESI– MS: *m/z* = 486 ([M – H]$^-$). Anal. calcd. (%) for C$_{26}$H$_{26}$O$_3$PFeN (487.30): C 64.08, H 5.38, N 2.88. Found: C 62.95, H 5.30, N 2.67.

1′-(Diphenylphosphanyl)-1-[*N*-(tris(hydroxymethyl)methyl)carbamoyl]ferrocene (3). Method A. Hdpf (1.66 g, 4.0 mmol), tris(hydromethyl)methylamine (1.94 g, 16.0 mmol), 4-(dimethylamino)pyridine (24 mg, 0.20 mmol) and EEDQ (1.48 g, 6.0 mmol) were dissolved in pyridine (40 mL) and the reaction mixture was stirred at 120 °C for 1 h and then at room temperature for overnight. The volatiles were removed under reduced pressure and the solid residue was purified by column chromatography (silica gel, dichloromethane-methanol 50:1 v/v). The first minor band was discarded and the following one was collected and evaporated to afford a crude product, which was crystallized from warm ethyl acetate-hexane (40 mL, 1:1 v/v) by slow cooling down to –18 °C. The obtained crystalline material was isolated by suction, washed successively with diethyl ether and pentane and dried under vacuum. Yield of **3**: 1.16 g (56%), orange microcrystalline solid.

Method B. Reaction flask was charged with active ester **4** (0.58 g, 1 mmol), tris(hydromethyl)methylamine (0.145 g, 1.3 mmol), 4-(dimethylamino)pyridine (6 mg, 0.05 mmol). Dry *N*,*N*-dimethylformamide (15 mL) was added and the resulting solution was stirred for 20 h and then evaporated under vacuum. The solid residue was dissolved in dichloromethane (20 mL), and the solution was washed twice with 5 % aqueous solution of citric acid (10 mL), saturated aqueous solution of NaHCO$_3$ (20 mL) and brine (20 mL) and, finally, dried over MgSO$_4$. The solvent was evaporated under vacuum and the solid residue was purified by column chromatography and crystallized as described above. Yield of **3**: 0.137 g (27%), orange microcrystalline solid.

^{1}H NMR (400.0 MHz, CDCl$_3$, 25 °C): δ = 3.73 (d, $^3J_{HH}$ = 3.9 Hz, 6 H, CH$_2$O), 4.11 (vq, *J*′ = 1.8 Hz, 2 H, CH of fc), 4.23 (vt, *J*′ = 2.0 Hz, 2 H, CH of fc), 4.44 (vt, *J*′ = 1.8 Hz, 2 H, CH of fc), 4.52 (unresolved t, 3 H, OH), 4.59 (vt, *J*′ = 2.0 Hz, 2 H, CH of fc), 6.89 (s, 1 H, NH), 7.31-7.39 (m, 10 H, PPh$_2$) ppm. ^{13}C{^{1}H} NMR (100.6 MHz, CDCl$_3$, 25 °C): δ = 61.58 (NCCH$_2$), 63.36 (CH$_2$O), 69.67 (CH of fc), 71.95 (CH of fc), 72.85 (d, J_{PC} = 4 Hz, CH of fc), 74.60 (d, J_{PC} = 14 Hz, CH of fc), 76.29 (*C*–CONH of fc), 77.54 (d, $^1J_{PC}$ = 5 Hz, C–P of fc), 128.32 (d, $^3J_{PC}$ = 7 Hz, CH$_{meta}$ of PPh$_2$), 128.91 (CH$_{para}$ of PPh$_2$), 133.43 (d, $^2J_{PC}$ = 20 Hz, CH$_{ortho}$ of PPh$_2$), 137.74 (d, $^1J_{PC}$ = 7 Hz, C$_{ipso}$ of PPh$_2$), 171.70 (C=O) ppm. ^{31}P{^{1}H} NMR (161.9 MHz, CDCl$_3$, 25 °C): δ = –17.7 (s) ppm. IR (Nujol): ν = 3262 s, 1626 s, 1532 s, 1351 m, 1305 m, 1287 w, 1192 w, 1160 w, 1124 w, 1084 w, 1055 m, 1027 s, 837 w, 821 w, 771 w, 746 m, 737 m, 696 s, 568 w, 520 w, 498 m, 484 m, 453 w

cm^{-1}. ESI– MS: *m/z* = 516 ([M – H]$^-$). Anal. calcd. (%) for $C_{27}H_{28}O_4PFeN$ (517.32): C 62.68, H 5.46, N 2.71. Found: C 62.62, H 5.58, N 2.60.

1′-(Diphenylphosphanoyl)-1-[*N*-(tris(hydroxymethyl)methyl)carbamoyl]ferrocene (3O). Aqueous hydrogen peroxide (0.21 mL 30%, ca. 2 mmol) was added drop-wise to a solution of phoshine **3** (103.5 mg, 0.2 mmol) in acetone (15 mL) while stirring and cooling in ice. After 30 min, the reaction mixture was quenched with saturated aqueous sodium thiosulfate (10 mL) and the volatiles were evaporated under vacuum. The aqueous residue was diluted with water and extracted with dichloromethane (2 × 15 mL). The organic extracts were washed with brine (1 × 30 mL), dried over magnesium sulfate and evaporated. The product was isolated by column chromatography (silica gel, dichloromethane-methanol, 10:1 v/v), resulting as a yellow solid. Yield: 98 mg (92 %).

^{1}H NMR (400.0 MHz, DMSO-d_6, 25 °C): δ = 3.70 (d, $^3J_{HH}$ = 6.0 Hz, 6 H, CH_2O), 4.13 (vt, *J*′ = 2.0 Hz, 2 H, CH of fc), 4.36 (vt, *J*′ = 1.9 Hz, 2 H, CH of fc), 4.68 (vt, *J*′ = 1.8 Hz, 2 H, CH of fc), 4.81 (vt, *J*′ = 2.0 Hz, 2 H, CH of fc), 4.83 (unresolved t, *J* ≈ 6.0 Hz, 3 H, OH), 7.53-7.72 (m, 11 H, PPh_2 and NH) ppm. ^{13}C{^{1}H} NMR (100.6 MHz, DMSO-d_6, 25 °C): δ = 60.58 (CH_2O), 62.62 (*C*NHCO), 69.99 (CH of fc), 70.57 (CH of fc), 72.61 (d, J_{PC} = 10 Hz, CH of fc), 72.91 (d, $^1J_{PC}$ = 115 Hz, C–P of fc), 74.32 (J_{PC} = 13 Hz, CH of fc), 79.12 (*C*–CONH of fc), 128.57 ($^2J_{PC}$ = 12 Hz, CH_{ortho} of PPh_2), 130.79 ($^3J_{PC}$ = 10 Hz, CH_{meta} of PPh_2), 131.95 ($^4J_{PC}$ = 2 Hz, CH_{para} of PPh_2), 132.76 ($^1J_{PC}$ = 107 Hz, C_{ipso} of PPh_2), 169.08 (C=O) ppm. ^{31}P{^{1}H} NMR (161.9 MHz, DMSO-d_6, 25 °C): δ = 29.9 (s) ppm. HR MS (ESI+) calcd. for $C_{27}H_{28}NO_5P^{56}Fe$ (M^+): 533.1055, found: 533.1057.

General procedure for the preparation of (η^6-arene)Ru(II) complexes. A solution of ligand (0.2 mmol) in dichloromethane (10 mL) was added to solid ruthenium precursor ([(η^6-C_6Me_6)$RuCl_2$]$_2$ or [(η^6-cymene)$RuCl_2$]$_2$) or its suspension in acetonitrile ([(η^6-C_6H_6)$RuCl_2$]$_2$ in 5 mL) (0.1 mmol). The resulting mixture was stirred in the dark for 2 h and then evaporated under under reduced pressure. The crude product was purified by column chromatography over silica gel using dichloromethane-methanol (50:1 or 20:1, v/v) as the eluent. The major reddish band was collected and evaporated to dryness. The solid residue was dissolved in a minimal amount of dichloromethane (1–3 mL) and added drop-wise to diethyl ether (30 mL). The resulting precipitate was cooled to + 4 °C overnight and collected by suction. The obtained material was washed successively with diethyl ether and pentane (10 mL each), and dried under vacuum.

[(η^6-C_6H_6)$RuCl_2$(1-κ*P*)] (5a). Yield: 126 mg (86 %), light orange powder. ^{1}H NMR (400.0 MHz, $CDCl_3$, 25 °C): δ = 3.24 (bs, 2 H, CH of fc), 3.60 (bs, 2 H, CH_2N), 3.70 (bs, 1 H, OH), 3.90 (bs, 2 H, CH_2O), 4.35 (bs, 2 H, CH of fc), 4.64-4.70 (m, 4 H, CH of fc), 5.30 (d, $^2J_{PH}$ = 0.8 Hz, 6 H, C_6H_6), 7.34-7.47 (m, 7 H, PPh_2 and NH), 7.69-7.80 (m, 4 H, PPh_2) ppm. ^{31}P{^{1}H} NMR (161.9 MHz, $CDCl_3$, 25 °C): δ = 16.3 (s) ppm. ESI+ MS: *m/z* = 636 ([M – H – HCl]). Anal. calcd. (%) for $C_{31}H_{30}RuCl_2PFeO_2N{\cdot}1.5H_2O$ (734.4): C 50.70, H 4.53, N 1.91. Found: C 50.74, H 4.52, N 1.94.

[(η^6-cymene)$RuCl_2$(1-κ*P*)] (5b). Yield: 131 mg (86 %), ruby red powder. ^{1}H NMR (400.0 MHz, $CDCl_3$, 25 °C): δ = 0.96 (d, $^3J_{HH}$ = 7.0 Hz, 6 H, CH(CH_3)$_2$), 1.85 (s, 3 H, CH_3), 2.59 (sept, $^3J_{HH}$ = 7.0 Hz, 1 H, C*H*(CH_3)$_2$), 3.19 (m, 2 H, CH of fc), 3.57 (virtual q, *J* = 4.7 Hz, 2 H, CH_2N), 3.84-3.86 (m, 2 H, CH_2O), 4.46-4.47 (m, 2 H, CH of fc), 4.48-4.49 (m, 2 H, CH of fc), 4.52 (vt, *J*′ = 2.0 Hz, 2 H, CH of fc), 5.10-5.14 (m, 4 H, C_6H_4), 7.40-7.47 (m, 6 H, PPh_2), 7.51 (t, $^3J_{HH}$ = 5.1 Hz, 1 H, NH), 7.77-7.83 (m, 4 H, PPh_2) ppm. The resonance due to the OH proton was not seen. ^{31}P{^{1}H} NMR (161.9 MHz, $CDCl_3$, 25 °C): δ = 17.7 (s) ppm. ESI+ MS: *m/z* = 692 ([M – Cl – HCl]$^+$). Anal. calcd. (%) for $C_{35}H_{38}RuCl_2PFeO_2N{\cdot}H_2O$ (768.9): C 54.67, H 5.06, N 1.82. Found: C 54.37, H 5.32, N 1.74.

[(η^6-C_6Me_6)$RuCl_2$(1-κ*P*)] (5c). Yield: 129 mg (81 %), orange powder. ^{1}H NMR (400.0 MHz, $CDCl_3$, 50 °C): δ = 1.67 (s, 18 H, C_6Me_6), 3.58 (virtual q, *J* = 4.9 Hz, 2 H, CH_2N), 3.63 (bs, 1 H, OH), 3.85 (virtual q, *J* = 5.1 Hz, 2 H, CH_2O), 4.43 (bs, 4 H, CH of fc), 4.51 (bs, 2 H, CH of fc), 7.28-7.39 (m, 6 H, PPh_2), 7.42 (bs, 1 H, NH), 7.72-7.90 (m, 4 H, PPh_2) ppm. The resonance due to two protons at the ferrocen-1,1′-diyl backbone was not observed because of an enormous signal broadening. ^{31}P{^{1}H} NMR (161.9 MHz, $CDCl_3$, 50 °C): δ = 19.3 (bs) ppm. ESI+ MS: *m/z* = 720 ([M – Cl – HCl]$^+$). Anal. calcd. (%) for $C_{37}H_{42}O_2RuCl_2PFeN$ (791.5): C 56.14, H 5.35, N 1.77. Found: C 56.02, H 5.37, N 1.67.

[(η^6-C_6H_6)$RuCl_2$(2-κ*P*)] (6a). Yield: 136 mg (87 %), orange powder. ^{1}H NMR (400.0 MHz, $CDCl_3$, 25 °C): δ = 3.62 (bs, 2 H, OH), 3.98 (d, $^3J_{HH}$ = 4.1 Hz, 4 H, CH_2O), 4.19 (m, 1 H, C*H*NH), 4.38 (bs, 2 H, CH of fc), 4.67 (bs, 2 H, CH of fc), 4.71 (vt, *J*′ = 1.8 Hz, 2 H, CH of fc), 5.30 (d, $^2J_{PH}$ = 0.7 Hz, 6 H, C_6H_6), 7.37-7.48 (m, 7 H, PPh_2 and NH), 7.67-7.81 (bs, 4 H, PPh_2) ppm. The resonance due to two protons at the ferrocen-1,1′-diyl backbone was not observed because of an extensive signal broadening. ^{31}P{^{1}H} NMR (161.9 MHz, $CDCl_3$, 25 °C): δ = 16.5 (s) ppm. ESI+ MS: *m/z* = 666 ([M – H – HCl]$^+$). Anal. calcd. (%) for $C_{32}H_{32}O_3RuCl_2PFeN{\cdot}2H_2O{\cdot}0.4Et_2O$ (780.8): C 49.84, H 4.78, N 1.79. Found: C 49.62, H 4.60%, N 1.75.

[(η^6-cymene)$RuCl_2$(2-κ*P*)] (6b). Yield: 143 mg (88 %), light orange powder. ^{1}H NMR (400.0 MHz, $CDCl_3$, 25 °C): δ = 0.94 (d, $^3J_{HH}$ = 7.0 Hz, 6 H, CH(C*H*$_3$)$_2$), 1.87 (s, 3 H, CH_3), 2.65 (sept, $^3J_{HH}$ = 7.0 Hz, 1 H, C*H*(CH_3)$_2$), 3.17 (bs, 2 H, CH of fc), 3.64 (bs, 2 H, OH), 3.92 (d, *J* = 4.0 Hz, 2 H, CH_2O), 4.14 (m, 1 H, C*H*NH), 4.48-4.49 (m, 4 H, CH of fc), 4.59 (vt, *J*′ = 2.0 Hz, 2 H, CH of fc), 5.11 (bs, 4 H, C_6H_4), 7.42-7.50 (m, 6 H, PPh_2), 7.51 (d, $^3J_{HH}$ = 7.1 Hz, 1 H, NH), 7.78-7.83 (m, 4 H, PPh_2) ppm. ^{31}P{^{1}H} NMR (161.9 MHz, $CDCl_3$, 25 °C): δ = 17.7 (s) ppm. ESI+ MS: *m/z* = 722 ([M – H – HCl]$^+$). Anal. calcd. (%) for $C_{36}H_{40}RuCl_2PFeO_3N{\cdot}H_2O$ (811.5): C 53.28, H 5.22, N 1.73. Found: C 53.08, H 5.24, N 1.73.

[(η^6-C_6Me_6)$RuCl_2$(2-κ*P*)] (6c). Yield: 152 mg (93 %), light orange powder. ^{1}H NMR (400.0 MHz, $CDCl_3$, 50 °C): δ = 1.67 (d, $^4J_{PH}$ = 0.7 Hz, 18 H, C_6Me_6), 3.93 (bs, 4 H, CH_2O), 4.06-4.13 (m, 1 H, C*H*NH), 4.39-4.56 (m, 6 H, CH of fc), 7.27-7.42 (m, 7 H, PPh_2 and NH), 7.76-7.90 (m, 4 H, PPh_2). The resonance due to two protons at the ferrocen-1,1′-diyl backbone and the hydroxyl groups were not observed because of extensive signal broadening. ^{31}P{^{1}H} NMR ($CDCl_3$, 50 °C): δ = 19.6 (bs) ppm. ESI+ MS: *m/z* = 750 ([M – Cl – HCl]$^+$). Anal. calcd. (%) for $C_{38}H_{44}O_3RuCl_2PFeN$ (821.5): C 55.55, H 5.40, N 1.71. Found: C 55.32, H 5.26, N 1.63.

[(η^6-C_6H_6)$RuCl_2$(3-κ*P*)] (7a). Yield: 137 mg (83 %), orange microcrystalline solid. ^{1}H NMR (400.0 MHz, DMSO-d_6, 25 °C): δ = 3.64 (d, $^3J_{HH}$ = 5.8 Hz, 6 H, CH_2O), 3.72 (vt, *J*′ = 1.8 Hz, 2 H, CH of fc), 4.48 (br s, 2 H, CH of fc), 4.51-4.55 (m, 4 H, CH of fc), 4.81 (t, $^3J_{HH}$ = 5.7 Hz, 3 H, OH), 5.40 (d, $^2J_{PH}$ = 0.7 Hz, 6 H, C_6H_6), 6.55 (s, 1 H, NH), 7.42-7.52 (m, 6 H, PPh_2), 7.70-7.77 (m, 4 H, PPh_2) ppm. ^{31}P{^{1}H} NMR (161.9 MHz, DMSO-d_6, 25 °C): δ = 20.2 (s) ppm. ESI+ MS: *m/z* = 696 ([M – H – HCl]$^+$). Anal. calcd. (%) for $C_{33}H_{34}O_4RuCl_2PFeN{\cdot}H_2O{\cdot}0.6Et_2O$ (829.9): C 51.23, H 5.10, N 1.69. Found: C 51.02, H 4.84, N 1.70 .

[(η^6-cymene)$RuCl_2$(3-κ*P*)] (7b). Yield: 148 mg (90 %), ruby red microcrystalline solid. ^{1}H NMR (400.0 MHz, DMSO-d_6, 25 °C): δ = 0.83 (d, $^3J_{HH}$ = 7.0 Hz, 6 H, CH(C*H*$_3$)$_2$), 1.71 (s, 3 H, CH_3), 2.31 (sept, $^3J_{HH}$ = 7.0 Hz, 1 H, C*H*(CH_3)$_2$), 3.61 (d, $^3J_{HH}$ = 5.8 Hz, 6 H, CH_2O), 3.65 (vt, *J*′ = 1.8 Hz, 2 H, CH of fc), 4.37-4.39 (m, 4 H, CH of fc), 4.50 (vq, *J*′ = 1.7 Hz, 2 H, CH of fc), 4.81 (t, $^3J_{HH}$ = 5.7 Hz, 3 H, OH), 5.23 (d, *J* = 6.3 Hz, 2 H, C_6H_4), 5.32 (dd, *J* = 6.4, 1.2 Hz, 2 H, C_6H_4), 6.48 (s, 1 H, NH), 7.46-7.53 (m, 6 H, PPh_2), 7.79-7.86 (m, 4 H, PPh_2) ppm. ^{31}P{^{1}H} NMR (161.9 MHz, DMSO-d_6, 25 °C): δ = 20.3 (s) ppm. ESI+ MS: *m/z* = 752 ([M – H – HCl]$^+$). Anal. calcd. (%) for $C_{37}H_{42}RuCl_2PFeO_4N$ (823.5): C 53.96 H 5.14 N 1.70. Found: C 53.75, H 5.21, N 1.58.

[(η^6-C_6Me_6)$RuCl_2$(3-κ*P*)] (7c). Yield: 154 mg (91 %), ruby red powder. ^{1}H NMR (400.0 MHz, $CDCl_3$, 50 °C): δ = 1.67 (s, 18 H, C_6Me_6), 3.83 (d, $^3J_{HH}$ = 4.8 Hz, 6 H, CH_2O), 4.02 (bs, 3 H, OH), 4.39 (d, *J*′ = 1.7 Hz, 2 H, CH of fc), 4.44 (bs, 2 H, CH of fc), 4.53 (bs, 2 H, CH of fc), 7.02 (bs, 1 H, NH), 7.32-7.42 (m, 6 H, PPh_2), 7.77-7.91 (m, 4 H, PPh_2) ppm. The resonance due to two protons at the ferrocen-1,1′-diyl backbone was not

found because of an extensive signal broadening. $^{31}P\{^1H\}$ NMR (161.9 MHz, $CDCl_3$, 50 °C): δ = 20.1 (bs) ppm. ESI+ MS: *m/z* = 780 ([M – H – HCl]$^+$). Anal. calcd. (%) for $C_{39}H_{46}O_4RuCl_2PFeN$ (851.6): C 55.00, H 5.45, N 1.65. Found: C 54.66, H 5.64, N 1.61.

Catalytic tests

A Schlenk tube was charged with the respective allylic alcohol (1.0 mmol) and ruthenium catalyst, base (in appropriate amounts) and 1-methoxy-2-(2-methoxyethoxy)ethane (67 mg, 0.5 mmol) as an internal standard. The tube was flushed with argon and sealed. The solvent (4 mL) was introduced and the resulting mixture was heated at 80 °C.

The conversions were determined by ^1H NMR spectroscopy. The identity of the products was confirmed by a comparison of the NMR spectra with the literature (octan-3-one, *trans*-cinnamaldehyde and propiophenone;[38] 1,3-diphenylpropan-1-one,[39] 2-butanone,[40] 2-pentanone,[41] 3-phenylpropanal,[42] 2-butenal[43] and 3-buten-2-one[44]) or with spectra of authentic samples (butyraldehyde, 2-methylpropanal and 3-penten-2-one).

X-ray crystallography

Single crystals suitable for X-ray diffraction measurements were obtained by liquid-phase diffusion from ethyl acetate-hexane (**2**: orange plate, 0.20 × 0.35 × 0.45 mm^3; **3**: orange plate, 0.03 × 0.10 × 0.25 mm^3; **3O**: orange prism, 0.23 × 0.38 × 0.55 mm^3), dichloromethane-hexane (**5c**·CH_2Cl_2: red plate, 0.20 × 0.40 × 0.50 mm^3) or similarly from chlorofm-methanol/hexane (**5c**·Et_2O: red bar, 0.08 × 0.15 × 0.30 mm^3).

The diffraction data (±*h*±*k*±*l*, θ_{max} = 26-27.5 °, data completeness ≥ 99.3%) were collected with a Nonius KappaCCD diffractometer equipped with a Cryostream Cooler (Oxford Cryosystems) at 150(2) K using graphite monochromated MoKα radiation (λ = 0.71073 Å) and were analyzed with the HKL program package.[45] The structures were solved by the direct methods (SIR97[46]) and refined by full-matrix least squares based on F^2 (SHELXL97[47]) to full convergence. The non-hydrogen atoms were refined with anisotropic displacement parameters. Hydrogen atoms in the OH and NH groups were identified on the difference density maps and refined as riding atoms with U_{iso}(H) assigned to a multiple of 1.2U_{eq}(O/N). Other hydrogen atoms were included in their calculated positions and refined similarly. Relevant crystallographic data and refinement parameters presented in Supporting Information, Table S2. Particular details on structure refinement are as follows.

The solvent present in the structure of **6c**·Et_2O was severely disordered in structural voids and, hence, its contribution to the overall scattering was removed by SQUEEZE[48] routine as incorporated in PLATON program.[49] A total of 110 electrons were found in 566 Å^3 void space per the unit cell (*N.B.* Four molecules of diethyl ether represent 136 electrons). It also is noteworthy that the largest electron density peak at the final difference electron density map (2.4 e Å^{-3}) for compound **2** corresponds very likely to a lone electron pair at the phosphorus atom (N.B. The second largest electron density maximum is only ca. 0.35 e Å^{-3}). This assumption was confirmed by a refinement of this 'peak' as a helium atom (2 electrons), which led to a decrease in the *R*-value to 2.96% and gave reasonable geometry (P···He distance 1.305(5) Å with a clear contact of He to H3O located in a proximal molecules: He···O3 ≈ 2.36 Å, He···H3O–O3 ≈ 173°).

Geometric data and structural drawings were obtained with a recent version of the PLATON program. All numerical values are rounded with respect to their estimated deviations (esd's) given in one decimal. Parameters relating to atoms in constrained positions (hydrogens) are given without esd's.

CCDC-889295 (**2**), -889296 (**3**), -889297 (**3O**), -889298 (**5c**·CH_2Cl_2) and -889299 (**6c**·Et_2O) contain the supplementary crystallographic data for this paper. These data can be obtained free of charge from The Cambridge Crystallographic Data Centre via www.ccdc.cam.ac.uk/data_request/cif.

Supporting Information (see footnote on the first page of this article): Packing diagrams for **5c**·CH_2Cl_2 (Figure S1) and **6c**·Et_2O (Figure S2), histograms showing the distribution of O···O and O–H···O angles in hydrogen bonds P=O···H–O hydrogen bonds (Figures S3 and S4), a summary of catalytic results for the redox isomerisation of allylic alcohols in water (Table S1), and a summary of crystallographic data (Table S2).

Acknowledgments

This work was financially supported by the Grant Agency of Charles University in Prague (project no. 69309) and is also a part of the long-term research plan of Faculty of Science, Charles University in Prague (project no. MSM0021620857).

[1] P. Štěpnička, *Chem. Soc. Rev.* **2012**, *41*, 4273-4305.

[2] *Aqueous-Phase Organometallic Chemistry* (Eds.: B. Cornils, W. A. Herrmann), 2nd ed., Wiley-VCH: Weinheim, **2004**; (b) F. Joó, *Aqueous Organometallic Catalysis*, Kluwer, Dordrecht, **2001**.

[3] (a) *Ferrocenes: Homogeneous Catalysis, Organic Synthesis, Materials Science* (Eds.: A. Togni, T. Hayashi), Wiley-VCH, Weinheim, **1995**; (b) *Ferrocenes: Ligands, Materials and Biomolecules* (Ed. P. Štěpnička), Wiley, Chichester **2008**.

[4] Selected reviews: (a) R. C. J. Atkinson, V. Gibson, N. J. Long, *Chem. Soc. Rev.* **2004**, *33*, 313–328; (b) P. Barbaro, C. Bianchini, G. Giambastiani, S. L. Parisel, *Coord. Chem. Rev.* **2004**, *248*, 2131–2150; (c) R. Goméz Arrayás, J. Adrio, J. C. Carretero, *Angew. Chem. Int. Ed.*, **2006**, *45*, 7674–7715.

[5] (a) X. Feng, B. Pugin, E. Küsters, G. Sedelmeier, H.-U. Blaser, *Adv. Synt. Catal.* **2007**, *349*, 1803–1807; (b) B. Pugin, *Patent WO 2001004131 A1* (2001).

[6] (a) J. Podlaha, P. Štěpnička, J. Ludvík, I. Císařová, *Organometallics* **1996**, *15*, 543–550; (b) P. Štěpnička, *Eur. J. Inorg. Chem.* **2005**, 3787–3808.

[7] J. Schulz, I. Císařová, P. Štěpnička, *Organometallics* **2012**, *31*, 729–738.

[8] (a) J. Tauchman, I. Císařová, P. Štepnička, *Organometallics* **2009**, *28*, 3288–3302; (b) J. Tauchman, I. Císařová, P. Štěpnička, *Eur. J. Org. Chem.* **2010**, 4276–4287; (c) J. Tauchman, I. Císařová, P. Štěpnička, *Dalton Trans.* **2011**, *40*, 11748–11757; (d) J. Tauchman, B. Therrien, G. Süss-Fink, P. Štěpnička, *Organometallics* **2012**, *31*, 3985−3994.

[9] (a) J. Schulz, I. Císařová, P. Štěpnička, *J. Organomet. Chem.* **2009**, *694*, 2519–2530; (b) J. Schulz, A. K. Renfrew, I. Císařová, P. J. Dyson, P. Štěpnička, *Appl. Organomet. Chem.* **2010**, *24*, 392–397.

[10] A prominent but rather solitary example of phosphanyl-carboxamides with 2-hydroxyethyl group is undoubtedly 2-(diphenylphosphanyl)-*N*-(2-hydroxyethyl)benzamide, which was studied as a ligand in Re(V) complexes and due to prospective applications in nuclear medicine: (a) J. D. G. Correia, Â. Domingos, A. Paulo. I. Santos, *J. Chem. Soc., Dalton Trans.* **2000**, 2477–2482; (b) J. D. G. Correia, Â. Domingos, I. Santos, *Eur. J. Inorg. Chem.* **2000**, 1523–1529; (c) J. D. G. Correia, Â. Domingos, I. Santos, H. Spies, *J. Chem. Soc., Dalton Trans.* **2001**, 2245–2250; (d) J. D. G. Correia, Â. Domingos, I. Santos, R. Alberto, K. Ortner, *Inorg. Chem.* **2001**, *40*, 5147–5151; (e) T. Kniess, J. D. G. Correia, Â. Domingos, E. Palma, I. Santos, *Inorg. Chem.* **2003**, *42*, 6130–6135; (f) C. Fernandes, J. D. G. Correia, L. Gano, I. Santos, S. Seifert, R. Syhre, R. Bergmann,H. Spies, *Bioconjugate Chem.* **2005**, *16*, 660–668.

[11] Up to the best of our knowledge, there is no report concerning the preparation of phosphanylamides from $H_2NCH(CH_2OH)_2$ (serinol).

[12] (a) 3-(Diphenylphosphanyl)-*N*-[2-hydroxy-1,1-bis(hydroxymethyl)ethyl]propanamide, a hydrophilic phosphane

prepared by addition of diphenylphosphane to CH_2=CHCONHC($CH_2OH)_3$, was studied as a ligand for Rh comlexes: L. Lavenot, M. H. Bortoletto, A. Roucoux, C. Larpent, H. Patin, *J. Organomet. Chem.* **1996**, *509*, 9–14. (b) Amides of the type RC(O)NHCH_2{CH_2O(CH_2)$_3$NHC(O)CH_2P(O)Y$_2$}$_3$, where Y = R′ or OR′, and some related compounds were evaluated in extractions of metal ions: M. M. Reinoso-García, D. Janczewski, D. N. Reinhoudt, W. Verboom, E. Malinowska, M. Pietrzak, C. Hill, J. Báča, B. Grüner, P. Selucky, C. Grüttner, *New. J. Chem.* **2006**, *30*, 1480–1492.

[13] For related phosphanylferrocene carboxamides, see: (a) W. Zhang, T. Shimanuki, T. Kida, Toshiyuki, Y. Nakatsuji, I. Ikeda, *J. Org. Chem.* **1999**, *64*, 6247–6251; (b) M. Lamač, I. Císařová, P. Štěpnička, *New J. Chem.* **2009**, *33*, 1549–1562.

[14] (a) A. El-Faham, F. Albericio, *Chem. Rev.* **2011**, *111*, 6557–6602 (a review); (b) B. Belleau, G. Malek, *J. Am. Chem. Soc.* **1968**, *90*, 1651–1652.

[15] For an example of application of EEDQ in the synthesis of amides from tris(hydoxymethyl)aminomethane, see: I. Villanueva, B. Hernandez, V. Chang, M. D. Heagy, *Synthesis* **2000**, 1435–1438.

[16] W. Zhang, Y. Yoneda, T. Kida, Y. Nakatsuji, I. Ikeda, *Tetrahedron: Asymmetry* **1998**, *9*, 3371–3380.

[17] (a) H. Jendralla, E. Paulus, *Synlett* **1997**, 471–472; (b) J. Kühnert, M. Dušek, J. Demel, H. Lang, P. Štěpnička, *Dalton Trans.* **2007**, 2802–2811; (c) J. Kühnert, I. Císařová, M. Lamač, P. Štěpnička, *Dalton Trans.* **2008**, 2454–2464; (d) P. Štěpnička, H. Solařová, M. Lamač, I. Císařová, *J. Organomet. Chem.* **2010**, *695*, 2423–2431; (e) P. Štěpnička, H. Solařová, I. Císařová, *J. Organomet. Chem.* **2011**, *696*, 3727–3740.

[18] (a) T. Gramstad, *Acta Chim. Scand.* **1961**, *15*, 1337–1346; (b) J. Mendel, A. Kolbe, *Phosphorus, Sulfur, Rel. Elements* **1977**, *3*, 21–26; (c) E. V. Ryl'tsev, A. K. Shurubura, Y. P. Egorov, V. Y. Semenii, *Teoret. Eksperiment. Khim.* **1980**, *16*, 497–503. (d) For a report concerning ferrocenylphosphanes and the corresponding phosphane oxides, see: L. M. Ephstein, E. S. Shubina, A. I. Krylova, V. S. Tolkunova, V. D. Vil'chevskaya, D. N. Kravtsov, *Iv. Akad. Nauk SSSR, Ser. Khim.* **1987**, 572–575.

[19] (a) P. Štěpnička, I. Císařová, *New J. Chem.* **2002**, *26*, 1389–1396; (b) B. F. M. Kimmich, C. R. Landis, D. R. Powell, *Organometallics* **1996**, **15**, 4141–4146.

[20] A search for intermolecular P···H–O contacts in the Cambridge Crystallographic Database (version 5.33 of November 2011 and updates of November 2011, February 2012 and May 2012) resulted in eleven hits (refcodes: BAXPUM, FEQKOC, GOSLUV, KUYBOW, LAGMIR, MULXIA, NAPYIM, OKAZIJ, TOCHIC, TOCHOI and TOXGAO). The shortest (strongest) contacts were detected for phosphanylphenols possessing acidic OH groups (P···O ca. 3.2–3.5 Å). For references, see: (a) J. Heinicke, R. Kadyrov, M. K. Kindermann, M. Koesling, P. G. Jones, *Chem. Ber.* **1996**, *129*, 1547–1560; (b) R. Kadyrov, J. Heinicke, M. K. Kindermann, D. Heller, C. Fischer, R. Selke, A. K. Fischer, P. G. Jones, *Chem. Ber.* **1997**, *130*, 1663–1670; (c) P. Schober, G. Huttner, A. Jacobi, *J. Organomet. Chem.* **1998**, *571*, 279–288.

[21] The sum of N-H···O and O···H···O angles around H1N is 346°.

[22] π···π Stacking interactions were detected for phenyl ring C(12-17) and its inverted (parallel) image at the distance of the respective ring centroids being 4.140(2) Å.

[23] A search of P=O···O–H contacts in the Cambridge Crystallographic Database (version as above) resulted in 203 hits with R < 10% and free of a disorder. Histograms showing the distribution of the O···O distances and the O–H···O angles (see Supporting Information, Figures S3 and S4) clearly indicate directional nature of these interactions.

[24] P. Štěpnička, J. Demel, J. Čejka, *J. Mol. Catal. A: Chem.* **2004**, *224*, 161–169.

[25] For **5c**·CH_2Cl_2: Cg3-Ru-Cl1 125.83(4)°, Cg3-Ru-Cl2 123.22(4)°, Cg3-Ru-P 134.00(4)°; for **6c**·Et_2O_2: Cg3-Ru-Cl1 126.27(4)°, Cg3-Ru-Cl2 123.27(4)°, Cg3-Ru-P 134.90(4)°; Cg3 denotes the centroid of the η^6-benzene ring.

[26] Dihedral angles subtended by these planes are 20.8(1)° and 19.9(1)° for **5c**·CH_2Cl_2 and **6c**·Et_2O, respectively.

[27] (a) R. C. van der Drift, E. Bouwman, E. Drent, *J. Organomet. Chem.* **2002**, *650*, 1–24; (b) R. Uma, C. Crévisy, R. Grée, *Chem. Rev.* **2003**, *103*, 27–51.

[28] For a recent reviews, see: (a) V. Cadierno, P. Crochet, J. Gimeno, *Synlett* **2008**, 1105–1124; (b) N. Ahlsten, A. Bartoszewicz, B. Martín-Matute, *Dalton Trans.* **2012**, *41*, 1660–1670; (c) P. Lorenzo-Luis, A. Romerosa, M. Serrano-Ruiz, *ACS Catal.* **2012**, *2*, 1079–1086.

[29] (a) C. Slugovc, E. Rüba, R. Schmid, K. Kirchner, *Organometallics* **1999**, *18*, 4230–4233; (b) I. E. Markó, A. Gautier, M. Tsukazaki, A. Llobet, E. Plantalech-Mir, C. J. Urch, S. M. Brown, *Angew. Chem. Int. Ed.* **1999**, *38*, 1960–1962; (c) C. Bianchini, A. Meli, W. Oberhauser, *New. J. Chem.* **2001**, *25*, 11–12; (d) R. C. van der Drift, J. W. Sprengers, E. Bouwman, W. P. Mul, H. Kooijman, A. L. Spek, E. Drent, *Eur. J. Inorg. Chem.* **2002**, 2147–2155; (e) B. Martín-Matute, K. Bogár, M. Edin, F. B. Kaynak, J.-E. Bäckvall, *Chem. Eur. J.* **2005**, *11*, 5832–5842; (f) P. Crochet, M. A. Fernández-Zúmel, J. Gimeno, M. Scheele, *Organometallics* **2006**, *25*, 4846–4849; (g) N. Ahlsten, H. Lundberg, B. Martín-Matute, *Green Chem.* **2010**, *12*, 1628–1633; (h) M. Batuecas, M. A. Esteruelas, C. García-Yebra, E. Oñate, *Organometallics* **2010**, 29, 2166–2175; (i) A. P. da Costa, J. A. Mata, B. Royo, E. Peris, *Organometallics* **2010**, *29*, 1832–1838; (j) V. Bizet, X. Pannecoucke, J.-L. Renaud, D. Cahard, *Angew. Chem. Int. Ed.* **2012**, *51*, 6467–6470.

[30] For a general review on asymmetric isomerization of allylic alcohols, see: L. Mantilli, C. Mazet, *Chem. Lett.* **2011**, *40*, 341–344.

[31] K. Tanaka, G. C. Fu, *J. Org. Chem.* **2001**, *66*, 8177–8186.

[32] Selected reviews: (a) Seth Ribe and Peter Wipf, *Chem. Commun.* **2001**, 299–307; (b) J. B. F. N. Engberts, M. J. Blandamer, *Chem. Commun.* **2001**, 1701–1708; (c) C. J. Li, *Chem. Rev.* **2005**, *105*, 3095–3165; (d) M. C. Pirrung, *Chem. Eur. J.* **2006**, *12*, 1312–1317; (e) R. N. Butler, A. G. Coyne, *Chem. Rev.* **2010**, *110*, 6302–6337; (b) M. O. Simon, C.-J. Li, *Chem. Soc. Rev.* **2012**, *41*, 1415–1427.

[33] (a) V. Cadierno, S. E. García-Garrido, J. Gimeno, *Chem. Commun*, **2004**, 232–233; (b) V. Cadierno, S. E. García-Garrido, J. Gimeno, A. Varela-Álvarez, J. A. Sordo, *J. Am. Chem. Soc.* **2006**, *128*, 1360–1370; (c) T. Campos-Malpartida, M. Fekete, F. Joó, Á. Kathó, A. Romerosa, M. Saoud, W. Wojtków, *J. Organomet. Chem.* **2008**, *693*, 468–474; (d) P. Servin, R. Laurent, L. Gonsalvi, M. Tristany, M. Peruzzini, J.-P. Majoral, A.-M. Caminade, *Dalton Trans.* **2009**, 4432–4434; (e) J. García-Álvarez, J. Gimeno, F. J. Suárez, *Organometallics* **2011**, *30*, 2893–2896; (f) L. Bellarosa, J. Díez, J. Gimeno, A. Lledós, F. J. Suárez, G. Ujaque, C. Vicent, *Chem. Eur. J.* **2012**, *18*, 7749–7765.

[34] (a) V. Cadierno, P. Crochet, S. E. García-Garrido, J. Gimeno, *Dalton Trans.* **2004**, 3635–3641; (b) P. Crochet, J. Díez, M. A. Fernández-Zúmel, J. Gimeno, *Adv. Synth. Catal.* **2006**, *348*, 93–100; (c) A. E. Díaz-Álvarez, P. Crochet, M. Zablocka, C. Duhayon, V. Cadierno, J. Gimeno, J.-P. Majoral, *Adv. Synth. Catal.* **2006**, **348**, 1671–1679; (d) M. Fekete, F. Joó, *Catal. Commun.* **2006**, *7*, 783–786; (g) B. Lastra-Barreira, J. Díez, P. Crochet, *Green Chem.* **2009**, *11*, 1681–1686; (h) A. Azua, S. Sanz, E. Peris, *Organometallics* **2010**, *29*, 3661–3664.

[35] A. Chanda, V. V. Fokin, *Chem. Rev.* **2009**, *109*, 725–74.

[36] R. A. Zelonka, M. C. Baird, *Can. J. Chem.* **1972**, *50*, 3063–3072.

[37] M. A. Bennett, T.–N. Huang, T. W. Matheson, A. K. Smith, *Inorg. Synth.* **1982**, *21*, 74–78.

[38] X. Wang, R. Liu, Y. Jin and X. Liang, *Chem. Eur. J.* **2008**, *14*, 2679–2685.

[39] D. J. Fox, D. S. Pedersen and S. Warren, *Org. Biomol. Chem.* **2006**, *4*, 3102–3107.

[40] S. Pääkkönen, J. Pursiainen and M. Lajunen, *Tetrahedron Lett.* **2010**, *51*, 6695–6699.

[41] M. Puchberger, W. Rupp, U. Bauer and U. Schubert, *New. J. Chem.* **2004**, *28*, 1289–1294.

[42] S. A. Van Arman, *Tetrahedron Lett.* **2009**, *50*, 4693–4695.

[43] M. R. Rohman, M. Rajbangshi, B. M. Laloo, P. R. Sahu and B. Myrboh, *Tetrahedron Lett.* **2010**, *51*, 2862–2864.

[44] R. J. Abraham, M. Mobli, J. Ratti, F. Sancassan and T. A. D. Smith, *J. Phys. Org. Chem.* **2006**, *19*, 384–392.

[45] Z. Otwinowski and W. Minor, *Methods Enzymol.* **1997**, *276*, 307–326.

[46] A. Altomare, M. C. Burla, M. Camalli, G. L. Cascarano, C. Giacovazzo, A. Guagliardi, A. G. G. Moliterni, G. Polidori and R. Spagna, *J. Appl. Crystallogr.* **1999**, *32*, 115–119.

[47] G. M. Sheldrick, *Acta Crystallogr. A* **2008**, *64*, 112–122.

[48] P. van der Sluis and A. L. Spek, *Acta Crystallogr. A* **1990**, *46*, 194–201.

[49] A. L. Spek, *J. Appl. Crystallogr.* **2003**, *36*, 7–13.

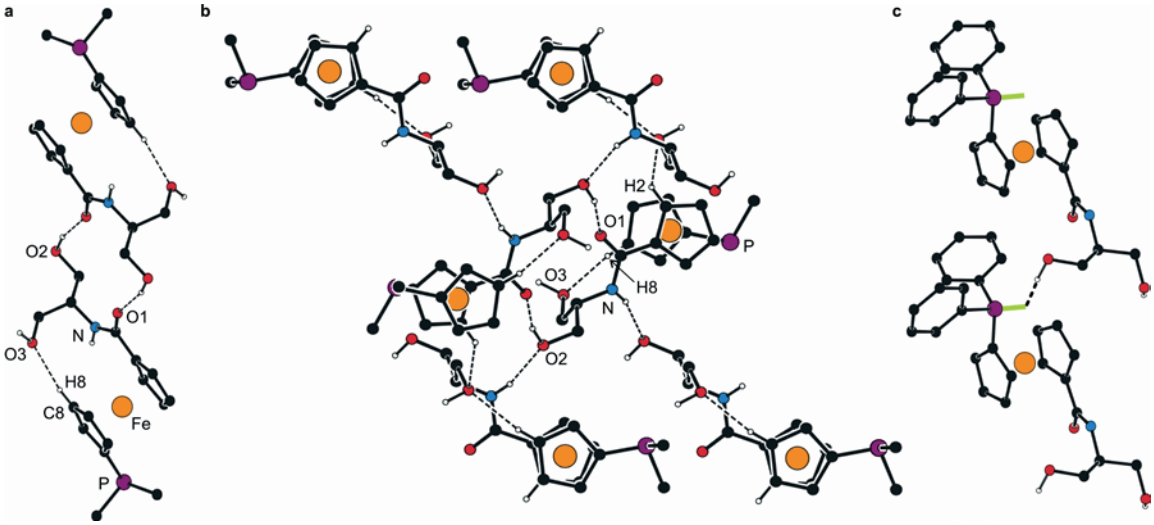

Figure 4. Packing diagrams for compound **2**. (a) View of the hydrogen-bonded dimeric motif in the structure of **2**; (b) a full view showing the same dimeric unit and its interactions with adjacent molecules, (c) O-H···P contacts between molecules related by elemental translation along the *y* axis. For clarity, only OH and NH hydrogens and pivotal carbon atoms from the phenyl rings (in parts **a** and **b**) are shown. The hydrogen bonds are indicated with dashed lines (for parameters, see Table 2). In part **c**, the green lines connect the phosphorus atoms with the refined electron density maxima (see Experimental Section).

Appendix 2

P. Štěpnička, I. Císařová, J. Schulz: "Tri-μ-chlorido-bis[(η^6-hexamethylbenzene)-ruthenium(II)] tetrachloridoferrate(III)." *Acta Cryst.*, 2011, **E67**, m1363.

Acta Crystallographica Section E
Structure Reports Online
ISSN 1600-5368

Tri-μ-chlorido-bis[(η^6-hexamethylbenzene)ruthenium(II)] tetrachloridoferrate(III)

Petr Štěpnička,* Jiří Schulz and Ivana Císařová

Department of Inorganic Chemistry, Faculty of Science, Charles University in Prague, Hlavova 2030, 12840 Prague 2, Czech Republic
Correspondence e-mail: stepnic@natur.cuni.cz

Received 2 September 2011; accepted 5 September 2011

Key indicators: single-crystal X-ray study; T = 150 K; mean σ(C–C) = 0.004 Å; R factor = 0.026; wR factor = 0.061; data-to-parameter ratio = 21.6.

The molecular geometry of the complex cation in the title structure, $[(\mu\text{-Cl})_3\{Ru^{II}(\eta^6\text{-}C_6Me_6)\}_2][Fe^{III}Cl_4]$, compares very well with that reported earlier for the corresponding PF_6^- salt [Pandey *et al.* (1999). *J. Organomet. Chem.* **592**, 278–282]. The $[FeCl_4]^-$ counter ion has a rather regular tetrahedral geometry with Fe—Cl distances and Cl—Fe—Cl angles in the range 2.1891 (7)–2.2018 (8) Å and 107.10 (3)–110.56 (3)°, respectively. There are no significant intermolecular interactions in the crystal except for some weak C—H···Cl contacts, which in turn indicates that the crystal packing is determined predominantly by electrostatic interactions between the ionic constituents.

Related literature

Crystals of the title compound were isolated during attempted recrystallization of $[(\eta^6\text{-}C_6Me_6)RuCl_2\{Ph_2PfcCON(CH_2CH_2OH)_2\}]$ [fc = ferrocene-1,1′-diyl; for the preparation of this ligand, see Schulz *et al.* (2009)] from chloroform–diethyl ether. It is likely a decomposition product as the result of photolytic cleavage of the ferrocene moiety in the halogenated solvent (Brand & Snedden, 1957). For the crystal structure of $[(\mu\text{-Cl})_3\{Ru(\eta^6\text{-}C_6Me_6)\}_2][PF_6]$, see: Pandey *et al.* (1999); Redwine *et al.* (2000). For the first structurally characterized compound of this type, $[(\mu\text{-Cl})_3\{Ru(\eta^6\text{-}C_6Me_6)\}_2][BPh_4]\cdot CH_3OH$, see: Tocher & Walkinshaw (1982). For the structures of simple tetrachloridoferrate(III) salts, see: Wyrzykowski *et al.* (2006); Jin *et al.* (2005).

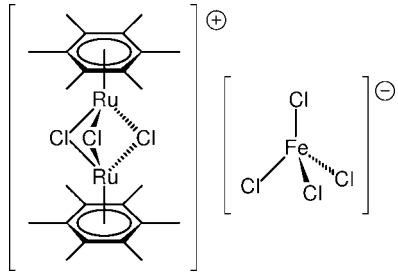

Experimental

Crystal data

$[Ru_2Cl_3(C_{12}H_{18})_2][FeCl_4]$
M_r = 830.67
Triclinic, $P\overline{1}$
a = 8.4490 (2) Å
b = 12.8352 (2) Å
c = 14.6752 (4) Å
α = 106.5767 (12)°
β = 90.4341 (9)°
γ = 99.7915 (12)°
V = 1500.43 (6) Å^3
Z = 2
Mo $K\alpha$ radiation
μ = 2.11 mm^{-1}
T = 150 K
0.30 × 0.20 × 0.08 mm

Data collection

Nonius KappaCCD diffractometer
Absorption correction: Gaussian using the diffractometer software
T_{min} = 0.529, T_{max} = 0.855
27082 measured reflections
6900 independent reflections
6172 reflections with $I > 2\sigma(I)$
R_{int} = 0.036

Refinement

$R[F^2 > 2\sigma(F^2)]$ = 0.026
$wR(F^2)$ = 0.061
S = 1.08
6900 reflections
319 parameters
H-atom parameters constrained
$\Delta\rho_{max}$ = 0.47 e Å^{-3}
$\Delta\rho_{min}$ = −0.68 e Å^{-3}

Table 1
Hydrogen-bond geometry (Å, °).

D—H···A	D—H	H···A	D···A	D—H···A
C9—H9A···Cl3^{i}	0.96	2.80	3.629 (3)	145
C11—H11B···Cl6^{ii}	0.96	2.71	3.588 (3)	153

Symmetry codes: (i) $x+1, y, z$; (ii) $x, y-1, z$.

Data collection: *COLLECT* (Nonius, 2000); cell refinement: *HKL SCALEPACK* (Otwinowski & Minor, 1997); data reduction: *HKL* (Otwinowski & Minor, 1997) *DENZO* and *SCALEPACK*; program(s) used to solve structure: *SIR97* (Altomare *et al.*, 1999); program(s) used to refine structure: *SHELXL97* (Sheldrick, 2008); molecular graphics: *PLATON* (Spek, 2009); software used to prepare material for publication: *SHELXL97* and *PLATON*.

This work was supported financially by the Grant Agency of Charles University in Prague (project No. 69309), and is a part of a long-term research plan supported by the Ministry of Education, Youth and Sports of the Czech Republic (project No. MSM0021620857).

Supplementary data and figures for this paper are available from the IUCr electronic archives (Reference: SU2311).

References

Altomare, A., Burla, M. C., Camalli, M., Cascarano, G. L., Giacovazzo, C., Guagliardi, A., Moliterni, A. G. G., Polidori, G. & Spagna, R. (1999). *J. Appl. Cryst.* **32**, 115–119.

Brand, J. C. D. & Snedden, W. (1957). *Trans. Faraday Soc.* **53**, 894–900.

Jin, Z.-M., Li, Z.-G., Li, L., Li, M.-C. & Hu, M.-L. (2005). *Acta Cryst.* E**61**, m2466–m2468.

Nonius (2000). *COLLECT*. Nonius BV, Delft, The Netherlands.

Otwinowski, Z. & Minor, W. (1997). *Methods in Enzymology*, Vol. 276, *Macromolecular Crystallography*, Part A, edited by C. W. Carter Jr & R. M. Sweet, pp. 307–326. New York: Academic Press.

Pandey, D. S., Sahay, A. N., Sisodia, O. S., Jha, N. K., Sharma, P., Klaus, H. E. & Cabrera, A. (1999). *J. Organomet. Chem.* **592**, 278–282.

Redwine, K. D., Hansen, H. D., Bowley, S., Isbell, J., Sanchnez, M., Vodak, D. & Nelson, J. H. (2000). *Synth. React. Inorg. Met. Org. Chem.* **30**, 379–407.

Schulz, J., Císařová, I. & Štěpnička, P. (2009). *J. Organomet. Chem.* **694**, 2519–2530.

Sheldrick, G. M. (2008). *Acta Cryst.* A**64**, 112–122.

Spek, A. L. (2009). *Acta Cryst.* D**65**, 148–155.

Tocher, D. A. & Walkinshaw, M. D. (1982). *Acta Cryst.* B**38**, 3083–3085.

Wyrzykowski, D., Sikorski, A., Konitz, A. & Warnke, Z. (2006). *Acta Cryst.* E**62**, m3562–m3564.

Appendix 3

J. Schulz, A. K. Renfrew, I. Císařová, P. J. Dyson, P. Štěpnička: "Synthesis and Anticancer Activity of Chalcogenide Derivatives and Platinum(II) and Palladium(II) Complexes Derived from a Polar Ferrocene Phosphanyl-carboxamide." *Appl. Organometal. Chem.*, 2010, **24**, 392.

Full Paper

Applied Organometallic Chemistry

Received: 20 November 2009 Revised: 4 January 2010 Accepted: 4 January 2010 Published online in Wiley Interscience: 17 February 2010

(www.interscience.com) DOI 10.1002/aoc.1626

Synthesis and anticancer activity of chalcogenide derivatives and platinum(II) and palladium(II) complexes derived from a polar ferrocene phosphanyl–carboxamide

Jiří Schulz[a], Anna K. Renfrew[b], Ivana Císařová[a], Paul J. Dyson[b] and Petr Štěpnička[a]*

The polar phosphanyl-carboxamide, 1′-(diphenylphosphanyl)-1-[*N*-(2-hydroxyethyl)carbamoyl]ferrocene (1), reacts readily with hydrogen peroxide and elemental sulfur to give the corresponding phosphane-oxide and phosphane-sulfide, respectively, and with platinum(II) and palladium(II) precursors to afford various bis(phosphane) complexes [$MCl_2(1\text{-}\kappa P)_2$] (M = *trans*-Pd, *trans*-Pt and *cis*-Pt). The anticancer activity of the compounds was evaluated *in vitro* with the complexes showing moderate cytotoxicities towards human ovarian cancer cells. Moreover, the biological activity was found to be strongly influenced by the stereochemistry, with *trans*-[$PtCl_2(1\text{-}\kappa P)_2$] being an order of magnitude more active than the corresponding *cis* isomer.

Supporting information may be found in the online version of this article.

Keywords: ferrocene; phosphanyl-carboxamides; complexes; anticancer properties; X-ray crystallography

Introduction

Cisplatin is one of the most commonly used chemotherapeutic agents in the clinic effective against ovarian and testicular cancer and is also used in the treatment of bladder, cervical, head and neck, oesophageal and small cell lung cancers.[1] While cisplatin is an effective inhibitor of tumor growth, its therapeutic index is limited by a high level of toxicity towards healthy cells, resulting in side effects such as myelosuppression, nausea, hair loss and neurotoxicity. In addition, a high degree of intrinsic and acquired resistance in many tumor types requires cisplatin to be administered at increasingly high doses, causing even more severe side effects.[2] Consequently, recent efforts in metal-based chemotherapeutic agents have focused largely on the development of new drugs, based on both platinum and other transition metals that are able to overcome the limitations of cisplatin. Successful strategies include increasing kinetic stability to limit drug deactivation,[3] improving uptake of the drug into the cell through either lipophillic groups or macromolecular carriers,[4] the conjugation of molecules which inhibit drug resistance[5] and also compounds based on alternative metals which operate by a different mode of action.[6]

During our studies on functionalized polar phosphanylferrocene carboxamides,[7,8] we prepared the hydroxyethyl-substituted derivative **1** (Scheme 1). This compound combines a diphenylphosphanyl moiety that can coordinate to soft metals with a functionalized carboxamide group serving as a solubilizing unit. Amide **1** has a higher solubility in polar solvents compared with the parent 1′-(diphenylphosphanyl)ferrocene-1-carboxylic acid (Hdpf),[9] and proved to be a useful ligand in palladium-catalyzed Suzuki–Miyaura cross-coupling reactions performed in water–organic solvent mixtures (including biphasic ones) and in pure water.[10] Considering the high polarity of the amide pendant and lipophilicity of the ferrocene unit in **1**, we also became interested as to whether this ligand could be used as a tool for delivering metal fragments into cancer cells. In addition, the ferrocene moiety may exert its own cytotoxic effect, with several examples of ferrocene[11] and mixed metal–ferrocene complexes[12] known to inhibit cell proliferation. Herein we report on the preparation of P-chalcogenide derivatives, and palladium(II) and platinum(II) complexes prepared from **1**, along with their structural characterization and antiproliferative activity in the A2780 ovarian cancer cell line.

Results and Discussion

Phosphane-amide **1** was synthesized as previously reported.[10] Its P-chalcogenide derivatives, viz. phosphane-oxide **2** and phosphane-sulfide **3** (Scheme 1), were prepared by oxidation with aqueous hydrogen peroxide or elemental sulfur, respectively. The oxide was isolated by column chromatography and crystallized from ethyl acetate–hexane, whereas the sulfide separated in

* *Correspondence to: Petr Štěpnička, Department of Inorganic Chemistry, Faculty of Science, Charles University, Hlavova 2030, 12840 Prague, Czech Republic. E-mail: stepnic@natur.cuni.cz*

a *Department of Inorganic Chemistry, Faculty of Science, Charles University in Prague, Hlavova 2030, CZ-12840, Prague, Czech Republic*

b *Institute of Chemical Sciences and Engineering, Ecole Polytechnique Fédérale de Lausanne (EPFL), CH-1015, Lausanne, Switzerland*

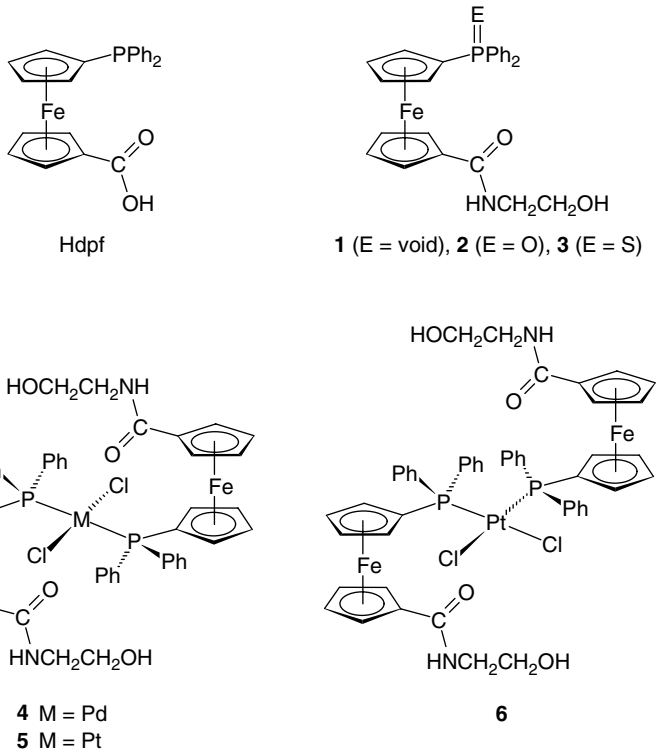

Scheme 1. Structural drawings for compounds presented in this study and their parent acid Hdpf.

pure crystalline form directly from the reaction mixture (i.e. from toluene) upon cooling. Chalcogenides **2** and **3** were characterized by elemental analysis and by spectroscopic methods (multinuclear NMR and electrospray ionization mass spectrometry, ESI-MS).

ESI mass spectra of compounds **2** and **3** are dominated by the pseudomolecular ions, $[M-H]^-$, thus confirming the formulation. The ^{1}H NMR spectra of the P-chalcogenides display characteristic virtual multiplets due to the ferrocene protons, namely two triplets for the amide-substituted ring and two quartets for the phosphorus-substituted ring. The spectra further comprise a pair of multiplets due to the ethane-1,2-diyl linker, signals attributable to the NH (CH_2-coupled triplet) and OH groups, and a multiplet for the phenyl-ring (PPh_2) protons. Likewise, the ^{13}C NMR spectra show resonances due to the phosphanyl-substituted ferrocene unit (four CH and two C_{ipso}) and the PPh_2 moiety, with characteristic J_{PC} coupling constants.[13] The ^{13}C NMR signals of the NCH_2CH_2O moiety as well as the C═O resonance are observed at positions similar to those of the parent phosphane **1**.[10] On the other hand, the modification of the phosphorus substituent (**1** → **2** or **3**) is manifested by changes in the ^{13}C NMR shifts and J_{PC} coupling constants[13] of the $C_5H_4PPh_2$ carbons, and also in ^{31}P NMR spectra, showing single resonances markedly shifted to lower fields relative to **1**. Not surprisingly, the ^{31}P NMR signals are found at positions close to those observed for the respective Hdpf P-chalcogenides.[7b,9a]

In addition to spectroscopic characterization, the solid-state structures of **2** and **3** were established by single-crystal X-ray diffraction analysis. Views of the molecular structures are presented in Figs 1 and 2. Selected bond data are given in Table 1.

The molecular structures of **2** and **3** are unexceptional, particularly in view of the data reported previously for phosphane **1**[10] and P-chalcogenide derivatives prepared from the parent acid Hdpf.[7b,9a] In the crystals, both chalcogenides form intramolecular N–H···E (E = O3 or S) hydrogen bonds which bring the ferrocene substituents to a mutual proximity and result in inclination of the amide NH towards the hydrogen-bond acceptor E (see τ and φ angles in Table 1). Additional hydrogen bonding interactions are responsible for the formation of supramolecular assemblies (Fig. 3). Thus, molecules of **2** associate into centrosymmetric dimers via intermolecular O–H···O hydrogen bonds and, further,

Table 1. Selected distances (Å) and angles (deg) for **2** and **3**

Parameter[a]	**2** (E = O3)	**3** (E = S)
Fe–Cg1	1.6496(7)	1.6484(7)
Fe–Cg2	1.6419(7)	1.6411(7)
<Cp1,Cp2	4.80(9)	1.58(9)
τ[b]	73	83
P═E	1.500(1)	1.9589(6)
C1–C11	1.230(2)	1.478(2)
C11–O1	1.230(2)	1.235(2)
C11–N	1.349(2)	1.339(2)
O1–C11–N	123.5(2)	122.8(2)
φ[c]	24.9(2)	11.7(2)
N–C24	1.453(2)	1.453(2)
C11–N–C24	122.3(1)	122.9(1)
C24–C25	1.512(3)	1.512(2)
C25–O2	1.421(2)	1.409(2)
N–C24–C25–O2	−178.0(1)	67.9(2)

[a] Definition of the ring planes: Cp1 = C(1–5), Cp2 = C(6–10). Cg1 and Cg2 denote the respective ring centroids.
[b] Torsion angle C11–Cg1–Cg2– P.
[c] Dihedral angle of the Cp1 and (C11,O1,N) planes.

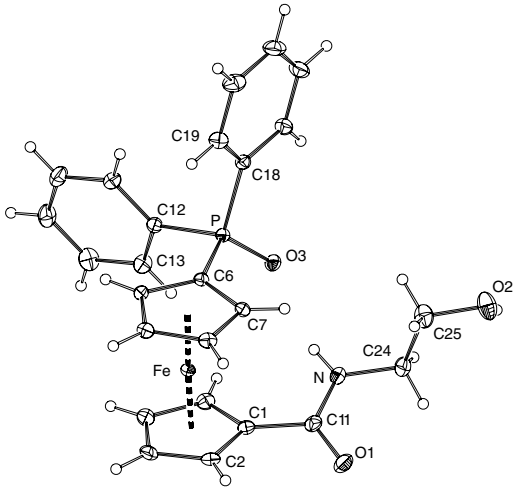

Figure 1. A view of the molecular structure of **2** showing displacement ellipsoids at the 30% probability level.

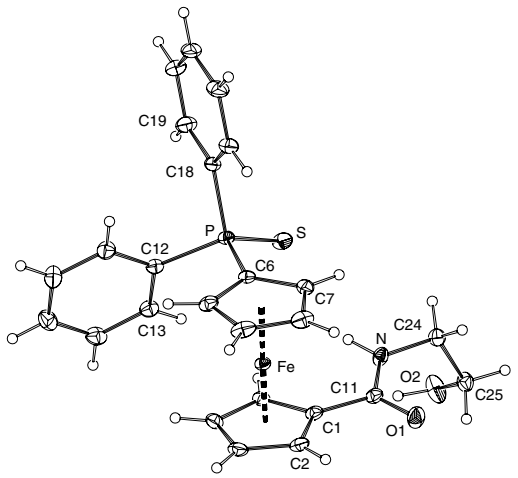

Figure 2. A view of the molecular structure of **3** showing displacement ellipsoids at the 30% probability level.

into three-dimensional arrays via the longer C–H···O contacts. [These intermolecular interactions are as follows: C4–H4···O2^{i}: C4···O2^{i} = 3.302(2) Å, angle at H4 = 136°; C17–H17···O1^{ii}: C17···O1 = 3.197(2) Å, angle at H17 = 137°; C20–H20···O1^{iii}: C20···O1^{iii} = 3.318(2) Å, angle at H20 = 143° (i = 1 + *x*, *y*, *z*; ii = x, −1 + *y*, *z*; iii = 1 − *x*, 1 − *y*, −*z*).] The molecules in the crystal of **3** aggregate by means of O–H···O as well, with the C═O oxygen serving as the acceptor, to form infinite chains. Similarly to **2**, the chains in **3** are cross-linked via the softer C–H···O interactions. [These intermolecular interactions are as follows: C3–H3···O2^{i}: C3···O2^{i} = 3.277(2) Å, angle at H3 = 160°; C21–H21···O2^{ii}: C21–H21···O2^{ii} = 3.461(2) Å, angle at H21 = 161°; C24–H24a···O2^{iii}: C24···O2^{iii} = 3.372(2) Å, angle at H24a = 141° (i = −1 + *x*, 1/2 − *y*, −1/2 + *z*; ii = 1 − *x*, −1/2 + *y*, 1/2 − *z*, iii = *x*, 1/2 − *y*, −1/2 + *z*).]

The palladium(II) bis(phosphane) complex **4** (Scheme 1) was prepared by displacement of the cod ligand in [$PdCl_2$(cod)] (cod = η^2 : η^2-cycloocta-1,5-diene) with two equivalents of **1** as previously reported.[10] In the case of platinum(II), two isomeric square-planar bis(phosphane) complexes **5** and **6** (Scheme 1) were isolated depending on the metal precursor used ([$PtCl_2$(cod)] vs

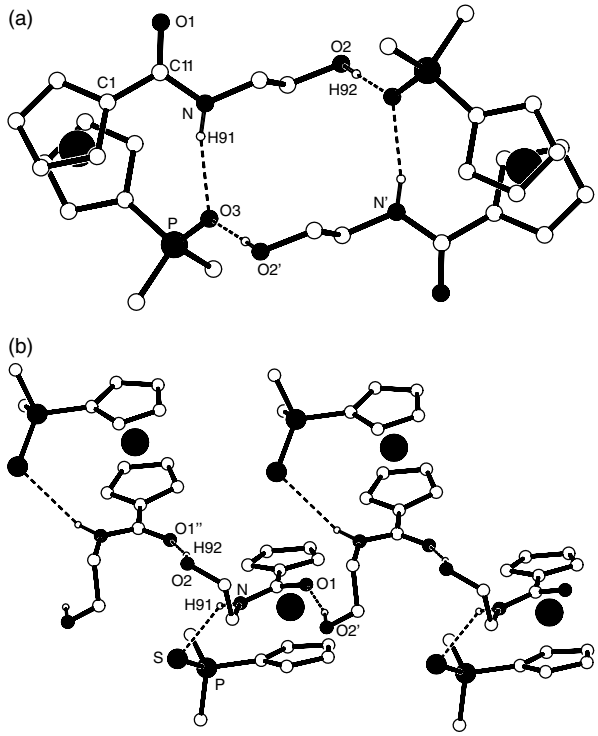

Figure 3. Views of the hydrogen-bonded arrays in the crystals of **2** (a) and **3** (b). For clarity, non-relevant hydrogen and phenyl ring carbon atoms are omitted. H-bond parameters for **2**: N–H91···O3, N···O3 = 2.959(2) Å, angle at H91 = 162°; O2–H92···O3^{i}, O2···O3^{i} = 2.783(2) Å, angle at H92 = 174° (i = 1 − *x*, 1 − *y*, 1 − *z*). H-bond parameters for **3**: N–H91···S, N···S = 3.529(1) Å, angle at H91 = 146°; O2–H92···O1^{ii}, O2···O1^{ii} = 2.762(2) Å, angle at H92 = 166° (ii = *x*, 1/2 − *y*, 1/2 + *z*).

K_2[$PtCl_4$]).[14] The complexes tend to hold solvent molecules in their structures which cannot be removed by simple evacuation. However, the amounts of solvents are easily determined from elemental analysis and NMR spectra.

Complexes **4–6** were characterized by a combination of NMR, ESI-MS and elemental analysis. In the ESI mass spectra, the complexes with a *trans*-geometry, i.e. **4** and **5**, display positively charged fragments resulting by a loss of one or two chloride ligands and Na/H exchange as the highest molecular weight species. In contrast, a pseudomolecular ion $[M + Na]^+$ was seen in the spectrum of compound **6**. The ^{1}H NMR spectra of the complexes showed one set of signals due to the equivalent phosphanylferrocene ligands. The ^{31}P NMR spectra of **4–6** compared very well with those reported for the corresponding Hdpf complexes, [MCl_2(Hdpf-κP)$_2$] (M = Pd, Pt).[15] Also similar to their Hdpf analogs, isomers **5** and **6** were easily distinguished through the characteristic ^1J(^{195}Pt, ^{31}P) coupling constants.[14,16]

Cytotoxicity Studies

The antiproliferative activity of compounds **1–6** was evaluated against the A2780 ovarian cancer cell line, and the results are summarized in Table 2. Initial tests revealed that the free ferrocenes **1–3** do not exert any notable cytotoxicity (IC_{50} > 200 μM) which is, indeed, in accordance with the low cytotoxicity observed for ferrocene and many of its derivatives.[17] In contrast, complexes **4–6** exhibit moderate activity with IC_{50} values ranging from 19 to 155 μM, with the *trans*-bis(phosphane) platinum complex **5** being the most cytotoxic compound in the series. The related palladium

Table 2. IC_{50} values for compounds **1–6** determined in the A2780 ovarian cancer cell line

Compound	IC_{50} (μM)	Compound	IC_{50} (μM)
1	>200	**4**	25 ± 2
2	>200	**5**	19 ± 2
3	>200	**6**	155 ± 5

complex **4** was found to be 2-fold less cytotoxic than the platinum analog **5**, in agreement with previous studies comparing palladium and platinum compounds.[18] The fast reaction kinetics of dichlorido-palladium complexes with respect to platinum analogs are proposed to result in a higher degree of side reactions prior to reaching the desired cellular targets, and consequently, lower drug efficacy. A considerable difference in cytotoxicity was also observed between the *trans*- and *cis*-platinum isomers **5** and **6**, with the *trans* isomer being 10-fold more active. Interestingly, the opposite effect was noted for cisplatin, where the *trans* isomer showed little cytotoxicity with respect to its *cis* analog, attributed to greater reactivity of the *trans* complex resulting in turn in a higher degree of drug deactivation.[19] Although *trans*-platinum complexes were initially thought to be poor drug candidates, in recent years, several *trans*-platinum complexes have been found to effectively inhibit cell proliferation,[20] with some compounds currently being in Phase II clinical trials.[21] Experiments have shown that *trans*-platinum complexes bind to DNA in a manner different to cisplatin and other *cis*-platinum based complexes.[22] As cisplatin resistance is strongly associated with DNA repair mechanisms, compounds that interact differently with DNA may overcome these mechanisms and consequently certain *trans*-complexes show high cytotoxicty in cisplatin resistant tumors.[23]

Conclusions

1′-(Diphenylphosphanyl)-1-[*N*-(2-hydroxyethyl)carbamoyl]-ferrocene (**1**) is easily oxidized at the phosphorus atom or can be converted to bis(phosphane) platinum(II) and palladium(II) complexes using standard protocols. *In vitro*, compound **1** and its P-oxidized derivatives **2** and **3** do not show any considerable cytotoxicity against A2780 ovarian cancer cells; however the bis(phosphane) complexes **4–6** are moderately cytotoxic. The cytotoxicity is strongly influenced by the stereochemistry, with the *trans*-platinum complex **5** being an order of magnitude more active than the *cis* isomer **6**. At this stage it is not known which ligands are released when the complex binds to a biomolecular target. However, should the phosphane be released, then rapid oxidation of the P(III) center can be expected. Also, despite the relatively lower cytotoxicity of the complexes tested (cf. IC_{50} = 1.6 μM for cisplatin under identical conditions), the present study provides an example of the influence of structural effects on cytotoxicity. Hence, further studies will be carried out to determine the influence of stereochemistry on kinetic stability and binding to potential cellular targets.

Experimental

Materials and Methods

Reactions were performed under argon atmosphere with exclusion of direct sunlight. Dichloromethane and toluene were dried with an appropriate drying agent (K_2CO_3 and potassium metal, respectively) and distilled under argon. Amide **1**[10] and [MCl_2(cod)] (M = Pd, Pt; cod = $\eta^2:\eta^2$-cycloocta-1,5-diene)[24] were prepared using the literature procedures. Other chemicals and solvents (Fluka; solvents from Lach-Ner) were used without further purification.

NMR spectra were recorded with a Varian Unity Inova spectrometer (^{1}H, 399.95; ^{13}C, 100.58; ^{31}P, 161.90 MHz) at 25 °C. Chemical shifts (δ) are given relative to internal $SiMe_4$ (^{13}C and ^{1}H) or to external 85% aqueous H_3PO_4 (^{31}P). Electrospray (ESI) mass spectra were measured on a Bruker Esquire 3000 spectrometer. The samples were dissolved in dichloromethane or dimethylsulfoxide and the solutions were diluted with a large excess of methanol prior to analysis.

Preparation 1′-(diphenylphosphanoyl)-1-[*N*-(2-hydroxyethyl) carbamoyl]ferrocene (2)

Phosphane **1** (91.5 mg, 0.2 mmol) was dissolved in acetone (10 ml), the solution was cooled in an ice bath and treated with 30% aqueous hydrogen peroxide (0.25 ml, 0.2 mmol). The reaction mixture was stirred for 30 min at 0 °C, and unreacted hydrogen peroxide was destroyed by addition of 10% aqueous sodium thiosulfate solution (5 ml) and stirring for another 15 min. The acetone was evaporated under vacuum and the residue was extracted with CH_2Cl_2 (3 × 10 ml). Combined organic extracts were washed with brine (10 ml), dried with magnesium sulfate and evaporated. The residue was purified by flash chromatography (silica gel, MeOH-AcOEt 1 : 9 v/v) and the product further purified by crystallization from ethyl acetate–hexane. Yield: 38.5 mg (41%), orange crystalline solid.

^{1}H NMR ($CDCl_3$): δ = 3.57 (m, 2 H, NCH_2), 3.81 (m, 2 H, OCH_2), 4.11 (vt, 2 H), 4.16 (vq, 2 H), 4.62 (vq, 2 H), 5.01 (vt, 2 H), 5.18 (dt, $^3J_{HH}$ = 6.8 Hz, J = 2.0 Hz, 1 H, OH), 7.46–7.72 (m, 10 H, Ph), 8.67 (t, $^3J_{HH} \approx$ 4.5 Hz, 1 H, NH) ppm. ^{13}C{^{1}H} NMR ($CDCl_3$): δ = 43.50 (NCH_2), 62.16 (OCH_2), 70.51, 70.63, 72.77 (d, J_{PC} = 11 Hz) (CH of fc); 72.91 (d, $^1J_{PC}$ = 97 Hz, *C*–P of fc), 74.98 (d, J_{PC} = 13 Hz, CH of fc), 79.06 (*C*–CO of fc), 128.61 (d, J_{PC} = 12 Hz), 131.31 (d, J_{PC} = 10 Hz) (CH of Ph); 132.15 (d, $^1J_{PC}$ = 109 Hz, *C*–P of Ph), 132.23 (d, J_{PC} = 3 Hz, CH of Ph), 169.80 (C═O) ppm. ^{31}P{^{1}H} NMR ($CDCl_3$): δ = 33.3 (s) ppm. ESI–MS (methanol): m/z = 472 ([M − H]$^-$). Anal. calcd for $C_{25}H_{24}FeNO_3P$ (473.3): C 63.44, H 5.11, N 2.96%. Found: C 63.39, H 5.23, N 2.80%.

Preparation of 1′-(Diphenylthiophosphanoyl)-1-[*N*-(2-hydroxyethyl)carbamoyl]ferrocene (3)

Phosphane **1** (91.5 mg; 0.2 mmol) and elemental sulfur (7.1 mg; 0.22 mmol) were dissolved in toluene (10 ml), and the mixture was heated to 60 °C for 1 h. The resulting solution was filtered (PTFE syringe filter, 0.45 μm pore size) and cooled to −18 °C. The crystalline solid was isolated by filtration, washed with diethyl ether and pentane, and dried under vacuum. Yield: 65.5 mg (67%), orange crystalline solid.

^{1}H NMR ($CDCl_3$): δ = 3.36 (t, $^3J_{HH}$ = 5.6 Hz, 1H, OH), 3.57 (vq, 2H, NCH_2), 3.85 (vq, 2H, OCH_2), 3.99 (vt, 2H), 4.25 (vq, 2H), 4.64 (vq, 2H), 4.96 (vt, 2H) (fc); 7.43–7.75 (m, 10 H, Ph), 7.79 (t, $^3J_{HH}$ = 5.3 Hz, 1 H, NH) ppm. ^{13}C{^{1}H} NMR ($CDCl_3$): δ = 43.14 (NCH_2), 63.16 (OCH_2), 71.19 (2C), 73.20 (d, J_{PC} = 10 Hz), 75.04 (d, J_{PC} = 13 Hz) (CH of fc); 76.18 (d, $^1J_{PC}$ = 97 Hz, *C*–P of fc), 78.02 (*C*–CO of fc), 128.44 (d, J_{PC} = 12 Hz), 131.62 (d, J_{PC} = 11 Hz), 131.73 (d, J_{PC} = 3 Hz) (CH of Ph); 133.24 (d, J_{PC} = 88 Hz, *C*–P of Ph), 171.13 (C═O) ppm. ^{31}P{^{1}H} NMR ($CDCl_3$): δ = 43.0 (s) ppm. ESI–MS (methanol):

m/z = 488 ([M − H]$^-$). Anal. calcd for $C_{25}H_{24}FeNO_2PS$ (489.3): C 61.36, H 4.94, N 2.86%. Found: C 61.06, H 5.02, N 2.74%.

Preparation of *trans*-[$PdCl_2$(1-κP)$_2$] (4)

Compound **4** was prepared according to a published procedure.[10] [$PdCl_2$(cod)] (28.5 mg, 0.1 mmol) and **1** (91.5 mg, 0.2 mmol) were dissolved in dichloromethane (5 ml). The resulting deep red reaction mixture was stirred for 30 min, filtered (PTFE syringe filter, 0.45 µm pore size) and evaporated under vacuum. The crude product was crystallized from hot ethanol (10 ml). The separated solid was isolated by filtration, washed with diethyl ether and pentane, and dried in argon stream. Yield: 103 mg (87%), deep red crystalline solid.

^{1}H NMR ($CDCl_3$): δ = 3.11 (t, $^3J_{HH}$ = 5.0 Hz, 1 H, OH), 3.37 (vq, 2 H, NCH_2), 3.69 (vq, 2 H, OCH_2), 4.52 (vt, 2 H), 4.57 (vt, 4 H), 4.92 (vt, 2 H), 6.55 (t, $^3J_{HH}$ = 5.8 Hz, 1 H, NH), 7.39–7.65 (m, 10 H, Ph) ppm. ^{31}P{^{1}H} NMR ($CDCl_3$): δ = 16.2 (s) ppm. The NMR data are consistent with the literature.[10] ESI$^+$ MS (methanol): m/z = 1099 ([M + 2Na − 2H − Cl]$^+$). Anal. calcd for $C_{50}H_{48}Fe_2N_2O_4P_2Cl_2Pd$ × 2EtOH × 0.1$CHCl_3$ (1183.98): C 54.33, H 5.07, N 2.34%. Found: C 53.91, H 5.21, N 2.20%.

Preparation of *trans*-[$PtCl_2$(1κ-*P*)$_2$] (5)

Ligand **1** (91.5 mg, 0.2 mmol) was dissolved in EtOH (5 ml) and the solution was treated with a solution of $K_2[PtCl_4]$ (41.5 mg, 0.1 mmol) in H_2O (0.2 ml). The resulting mixture was stirred for 2 h, filtered (PTFE syringe filter, 0.45 µm pore size) and precipitated with diethyl ether (20 ml). The yellow precipitate was isolated by filtration, washed with diethyl ether, pentane, and dried under vacuum. Yield of **5**: 85 mg (72%), yellow powder.

^{1}H NMR ($CDCl_3$): δ = 3.59 (m, 2 H), 3.85 (m, 2 H), 4.14 (vt, 2 H), 4.39 (bs, 2 H), 4.52 (bs, 2 H), 4.84 (vt, 2 H), 7.07 (t, 1 H), 7.15–7.52 (m, 10 H) ppm. ^{31}P{^{1}H} NMR ($CDCl_3$): δ = 10.4 (s with ^{195}Pt satellites, $^1J_{PtP}$ = 3820 Hz) ppm. ESI$^+$ MS: m/z = 1109 ([M − 2Cl]$^+$). Anal. calcd for $C_{50}H_{48}Fe_2N_2O_4P_2Cl_2Pt$ × EtOH × 0.5$CHCl_3$ (1286.3): C 49.02, H 4.27, N 2.18%. Found: C 48.55, H 4.32, N 2.07%.

Preparation of *cis*-[$PtCl_2$(1-κP)$_2$] (6)

[$PtCl_2$(cod)] (37.5 mg, 0.1 mmol) and **1** (91.5 mg, 0.2 mmol) were dissolved in dichloromethane (5 ml) and stirred for 30 min. The resulting orange solution was filtered (PTFE syringe filter, 0.45 µm pore size), and the filtrate was treated with hexane (20 ml). The yellow precipitate was collected by filtration, washed with pentane and dried under vacuum. Yield of **6**: 96 mg (81%), yellow powder.

^{1}H NMR ($CDCl_3$): δ = 3.37 (vq, 2 H, NCH_2), 3.68 (t, $^3J_{HH}$ = 5.2 Hz, 2 H, OCH_2), 4.51 (vt, 2 H), 4.57 (vt, 2 H), 4.59 (bs, 2 H), 4.92 (vt, 2 H) (fc); 6.52 (t, $^3J_{HH}$ = 5.5 Hz, 1 H, NH), 7.37–7.67 (m, 10 H, Ph) ppm. ^{31}P{^{1}H} NMR ($CDCl_3$): δ = 11.2 (s with ^{195}Pt satellites, $^1J_{PP}$ = 2610 Hz) ppm. ESI$^+$ MS (methanol): m/z = 1202 ([M + Na]$^+$). Anal. calcd for $C_{50}H_{48}Fe_2N_2O_4P_2Cl_2Pt$ × 0.5EtOH × 0.3$CHCl_3$ (1239.7): C 49.70, H 4.20, N 2.26%. Found: C 49.50, H 4.71, N 2.05% (sample crystallized from ethanol–chloroform).

X-ray Crystallography

Single crystals of **2** and **3** suitable for X-ray diffraction analysis were grown by crystallization from ethyl acetate–hexane (**2**: orange-brown prism, 0.18 × 0.33 × 0.50 mm^3; **3**: orange-brown prism, 0.15 × 0.30 × 0.50 mm^3). Full-set diffraction data ($\pm h \pm k \pm l$; 2θ < 55°) were collected with a Nonius KappaCCD image plate diffractometer equipped with a Cryostream Cooler (Oxford Cryosystems) using graphite monochromatized MoKα radiation (λ = 0.71073 Å) and were analyzed with the HKL program package.[25]

The structures were solved by direct methods (SIR97[26]) and refined by full-matrix least-squares procedure based on F^2 (SHELXL97[27]). All non-hydrogen atoms were refined with anisotropic displacement parameters. The NH and OH hydrogens (H91 and H92, respectively) were identified on difference density maps and refined as riding atoms. Other hydrogens were included in calculated positions and refined as riding atoms with U_{iso}(H) assigned to a multiple of U_{eq}(C) of their bonding carbon atom. The final difference electron density maps did not show any peaks of chemical significance.

Relevant crystallographic data and structure refinement parameters are given in Table 3. Geometric parameters and structural drawings were obtained with a recent version of PLATON program.[28] All numerical values are rounded with respect to their estimated standard deviations given with one decimal.

Table 3. Crystallographic data and data collection and structure refinement parameters for **2** and **3**[a]

Compound	**2**	**3**
Formula	$C_{25}H_{24}FeNO_3P$	$C_{25}H_{24}FeNO_2PS$
M (g mol^{-1})	473.27	489.33
Crystal system	triclinic	monoclinic
Space group	$P-1$ (no. 2)	$P2_1/c$ (no. 14)
a (Å)	10.2181(2)	9.5781(1)
b (Å)	10.6864(2)	26.6658(3)
c (Å)	10.8632(3)	8.9900(1)
α (deg)	72.049(1)	
β (deg)	83.887(1)	100.7649(6)
γ (deg)	72.416(1)	
V (Å^3)	1075.62(4)	2255.71(4)
Z	2	4
D_{calc} (g ml^{-1})	1.461	1.441
μ (MoKα) (mm^{-1})	0.803	0.855
Diffractions total	25 263	43 071
Unique/observed[b] diffractions	4936/4473	5190/4554
R_{int} (%)[c]	1.43	1.41
R (observed data) (%)[b,d]	2.66	2.78
R, wR (all data) (%)[d]	3.08, 6.59	3.43, 7.01
$\Delta\rho$ (e Å^{-3})	0.31, −0.35	0.32, −0.32

[a] Common details: T = 150(2) K.
[b] Diffractions with $I_o > 2\sigma(I_o)$.
[c] $R_{int} = \Sigma|F_o^2 - F_o^2(\text{mean})|/\Sigma F_o^2$, where F_o^2(mean) is the average intensity of symmetry-equivalent diffractions.
[d] $R = \Sigma||F_o| - |F_c||/\Sigma|F_o|$, w$R = [\Sigma\{w(F_o^2 - F_c^2)^2\}/\Sigma\, w(F_o^2)^2]^{1/2}$.

Cytotoxicity Studies

The human A2780 ovarian cancer cell line was obtained from the European Collection of Cell Cultures (Salisbury, UK). Cells were grown routinely in RPMI medium containing glucose, 5% fetal calf serum and antibiotics at 37 °C and 5% CO_2. Cytotoxicity was determined using the MTT assay (MTT = 3-(4,5-dimethyl-2-thiazolyl)-2,5-diphenyl-2H-tetrazolium bromide).[29] Cells were seeded in 96-well plates as monolayers with 100 µl of cell solution (approximately 20 000 cells per well) and pre-incubated for 24 h in medium supplemented with 10% fetal calf serum.

Compounds for testing were pre-dissolved in dimethylsulfoxide (DMSO) then added to the culture medium (to give a final DMSO concentration of 0.5%) and serially diluted to the appropriate concentration; 100 µl of drug solution was added to each well and the plates were incubated for another 72 h. Subsequently, MTT (5 mg ml^{-1} solution) was added to the cells and the plates were incubated for a further 2 h. The culture medium was aspirated, and the purple formazan crystals formed by the mitochondrial dehydrogenase activity of vital cells were dissolved in DMSO. The optical density, directly proportional to the number of surviving cells, was quantified at 540 nm using a multi-well plate reader and the fraction of surviving cells was calculated from the absorbance of untreated control cells. Evaluation is based on means from two independent experiments, each comprising three microcultures per concentration level.

Supporting Information

CCDC–755389 (**2**) and –755 390 (**3**) contain the supplementary crystallographic data for this paper. These data can be obtained free of charge from The Cambridge Crystallographic Data Centre via www.ccdc.cam.ac.uk/data_request/cif. Supporting information can be found in the online version of this article.

Acknowledgment

This work was financially supported by the Grant Agency of Charles University (project no. 39 309) and is a part of the long-term research projects of the Faculty of Science, Charles University supported by the Ministry of Education of the Czech Republic (project nos LC06070 and MSM0021620857).

References

[1] G. Giaccone, *Drugs* **2000**, *59*, 9.
[2] M. A. Fuertes, C. Alonso, J. M. Perez, *Chem. Rev.* **2003**, *103*, 645.
[3] a) L. R. Kelland, G. Abel, M. J. Mckeage, M. Jones, P. M. Goddard, M. Valenti, B. A. Murrer, K. R. Harrap, *Cancer Res.* **1993**, *53*, 2581; b) M. A. Jakupec, M. Galanski, B. K. Keppler, *Rev. Physiol. Biochem. Pharmacol.* **2003**, *146*, 1.
[4] a) W. H. Ang, S. Pilet, R. Scopelliti, F. Bussy, L. Juillerat-Jeanneret, P. J. Dyson, *J. Med. Chem.* **2005**, *48*, 8060; b) T. Boulikas, *Oncol. Rep.* **2004**, *12*, 3; c) S. Dhar, F. X. Gu, R. Langer, O. C. Farokhzad, S. J. Lippard, *Proc. Natl Acad. Sci. USA* **2008**, *105*, 17356.
[5] W. H. Ang, I. Khalaila, C. S. Allardyce, L. Juillerat-Jeanneret, P. J. Dyson, *J. Am. Chem. Soc.* **2005**, *127*, 1382.
[6] Selected examples: a) S. Urig, K. Fritz-Wolf, R. Reau, C. Herold-Mende, K. Toth, E. Davioud-Charvet, K. Becker, *Angew. Chem. Int. Ed.* **2006**, *45*, 1881; b) T.W. Failes, C. Cullinane, C. I. Diakos, N. Yamamoto, J. G. Lyons, T.W. Hambley, *Chem. Eur. J.* **2007**, *13*, 2974; c) H. Weber, J. Claffey, M. Hogan, C. Pampillon, M. Tacke, *Toxicol. in Vitro* **2008**, *22*, 531; d) E. Alessio, G. Mestroni, A. Bergamo, G. Sava, *Curr. Top. Med. Chem.* **2004**, *4*, 1525; e) C. G. Hartinger, S. Hann, G. Koellensperger, M. Sulyok, M. Groessl, A. R. Timerbaev, A. V. Rudnev, G. Stingeder, B. K. Keppler, *Int. J. Clin. Pharmacol. Ther.* **2005**, *43*, 583; f) C. Scolaro, A. Bergamo, L. Brescacin, R. Delfino, M. Cocchietto, G. Laurenczy, T. J. Geldbach, G. Sava, P. J. Dyson, *J. Med. Chem.* **2005**, *48*, 4161.
[7] a) L. Meca, D. Dvořák, J. Ludvík, I. Císařová, P. Štěpnička, *Organometallics* **2004**, *23*, 2541; b) P. Štěpnička, J. Schulz, I. Císařová, K. Fejfarová, *Collect. Czech. Chem. Commun.* **2007**, *72*, 453; c) M. Lamač, I. Císařová, P. Štěpnička, *Eur. J. Inorg. Chem.* **2007**, 2274; d) J. Kühnert, M. Dušek, J. Demel, H. Lang, P. Štěpnička, *Dalton Trans.* **2007**, 2802; e) M. Lamač, J. Tauchman, I. Císařová, P. Štěpnička, *Organometallics* **2007**, *26*, 5042; f) J. Kühnert, M. Lamač, J. Demel, A. Nicolai, H. Lang, P. Štěpnička, *J. Mol. Catal. A: Chem.* **2008**, *285*, 41; g) J. Kühnert, I. Císařová, M. Lamač, P. Štěpnička, *Dalton Trans.* **2008**, 2454; h) J. Tauchman, I. Císařová, P. Štěpnička, *Organometallics* **2009**, *28*, 3288; i) J. Schulz, I. Císařová, P. Štěpnička, *J. Organomet. Chem.* **2009**, *694*, 2519; j) M. Lamač, I. Císařová, P. Štěpnička, *New J. Chem.* **2009**, *33*, 1549; k) P. Štěpnička, M. Krupa, M. Lamač, I. Císařová *J. Organomet. Chem.* **2009**, *694*, 2987.
[8] For related references concerning phosphanyl*ferrocene* carboxamides, see: a) W. Zhang, T. Shimanuki, T. Kida, Y. Nakatsuji, I. Ikeda, *J. Org. Chem.* **1999**, *64*, 6247; b) J. M. Longmire, B. Wang, X. J. Zhang, *J. Am. Chem. Soc.* **2002**, *124*, 13400; c) S.-L. You, X.-L. Hou, L.-X. Dai, *J. Organomet. Chem.* **2001**, *637–639*, 762; d) J. M. Longmire, B. Wang, X. Zhang, *Tetrahedron Lett.* **2000**, *41*, 5435; e) S.-L. You, X.-L. Hou, L.-X. Dai, B.-X. Cao, J. Sun, *Chem. Commun.* **2000**, 1933; f) M. Tsukazaki, M. Tinkl, A. Roglans, B.J. Chapell, N. J. Taylor, V. Snieckus, *J. Am. Chem. Soc.* **1996**, *118*, 685; g) H. Jendralla, E. Paulus, *Synlett* **1997**, 471.
[9] a) J. Podlaha, P. Štěpnička, J. Ludvík, I. Císařová, *Organometallics* **1996**, *15*, 543; b) P. Štěpnička, *Eur. J. Inorg. Chem.* **2005**, 3787.
[10] J. Schulz, I. Císařová, P. Štěpnička, *J. Organomet. Chem.* **2009**, *694*, 2519.
[11] a) C. J. Swarts, T. G. Vosloo, S. J. Cronje, W. C. Du Plessis, C. E. J. Van Rensburg, C. E. Kreft, J. E. Van Lier, *Anticancer Res.* **2008**, *28*, 2781; b) W. C. M. Duivenvoorden, Y. Liu, G. Schatte, H.-B. Kraatz, *Inorg. Chim. Acta* **2005**, *358*, 3183; c) G. Jaouen, S. Top, A. Vessières, in *Bioorganometallics* (Ed. G. Jaouen), Wiley-VCH: Weinhein, **2005**, p. 65.
[12] M. Auzias, B. Therrien, G. Süss-Fink, P. Štěpnička, W. H. Ang, P. J. Dyson, *Inorg. Chem.* **2008**, *47*, 578; b) B. Weber, A. Serafin, J. Michie, C. Van Rensburg, J. C. Swarts, L. Bohm, *Anticancer Res.* **2004**, *24*, 763; c) J. Rajput, J. R. Moss, A. T. Hutton, D. T. Hendricks, C. E. Arendse, C. Imrie, *J. Organomet. Chem.* **2004**, *689*, 1553.
[13] H.-O. Kalinowski, S. Berger, S. Braun, *^{13}C-NMR-Spektroskopie*, Thieme: Stuttgart, **1984**, chapter 4.
[14] F. R. Hartley, *The Chemistry of Platinum and Palladium*, Applied Science: London, **1973**.
[15] P. Štěpnička, J. Podlaha, R. Gyepes, M. Polášek, *J. Organomet. Chem.* **1998**, *552*, 293.
[16] P. S. Pregosin, R. W. Kunz, in *^{31}P and ^{13}C NMR of Transition Metal Phosphane Complexes*, *NMR Basic Principles and Progress*, Vol. 16 (Eds.: P. Diehl, E. Fluck, R. Kosfeld), Springer: Berlin, **1979**, Chapter E, p. 65 and references therein.
[17] N. Metzler-Nolte, M. Salmain, in *Ferrocenes: Ligands, Materials and Biomolecules* (Ed.: P. Štěpnička), Wiley: Chichester, **2008**, chapter 13, pp. 499–639.
[18] a) G. R. Gale, J. A. Howle, A. B. Smith, *Proc. Soc. Exp. Biol. Med.* **1970**, *135*, 690; b) M. J. Cleare, J. D. Hoeschele, *Platinum Met. Rev.* **1973**, *17*, 2.
[19] V. Brabec, M. Leng, *Proc. Natl Acad. Sci. USA* **1993**, *90*, 5345.
[20] a) K. R. Harrap, *Cancer Res.* **1995**, *55*, 2761; b) G. Natile, M. Coluccia, *Coord. Chem. Rev.* **2001**, *216*, 383; c) J. M. Perez, M. A. Fuertes, C. Alonso, C. Navarro-Ranninger, *Crit. Rev. Oncol./Hematol.* **2000**, *35*, 109.
[21] P. M. Calvert, M. S. Highley, A. N. Hughes, E. R. Plummer, A. S. T. Azzabi, M. W. Verrill, M. G. Camboni, B. A. Verdie, M. Zuchetti, A. M. Robinson, J. Carmichael, A. H. Calvert, *Clin. Cancer Res.* **1999**, *5*, 3796.
[22] M. Van Beusichem, N. Farrell, *Inorg. Chem.* **1992**, *31*, 634; b) N. Farrell, L. R. Kelland, J. D. Roberts, M. Van Beusichem, *Cancer Res.* **1992**, *52*, 5065; c) J. Jawbry, I. Freikman, Y. Najajreh, J. M. Perez, D. Gibson, *J. Inorg. Biochem.* **2005**, *99*, 1983.
[23] M. Ohmichi, J. Hayakawa, K. Tasaka, H. Kurachi, Y. Murata, *Trends Pharmacol. Sci.* **2005**, *26*, 113.
[24] D. Drew, J. R. Doyle, *Inorg. Synth.* **1972**, *13*, 47.
[25] Z. Otwinowski, W. Minor, *HKL Denzo* and *Scalepack* Program Package, Nonius BV, Delft. For a reference, see: Z. Otwinowski, W. Minor, *Meth. Enzymol.* **1997**, *276*, 307.
[26] A. Altomare, M. C. Burla, M. Camalli, G. L. Cascarano, C. Giacovazzo, A. Guagliardi, A. G. G. Moliterni, G. Polidori, R. Spagna, *J. Appl. Crystallogr.* **1999**, *32*, 115.
[27] G.M. Sheldrick, *SHELXL97*. Program for Crystal Structure Refinement from Diffraction Data, University of Göttingen, Göttingen, **1997**.
[28] A. L. Spek, Platon – a multipurpose crystallographic tool, Utrecht University, Utrecht, 2003 and updates. Available from: http://www.cryst.chem.uu.nl/platon/.
[29] T. Mosmann, *J. Immunol. Meth.* **1983**, *65*, 55.

Appendix 4

J. Schulz, R. Gyepés, I. Císařová, P. Štěpnička: "Synthesis, Structural Characterisation and Bonding in an Anionic Hexavanadate Bearing Redox-Active Ferrocenyl Groups at the Periphery." *New. J. Chem.*, 2010, **34**, 2749.

Synthesis, structural characterisation and bonding in an anionic hexavanadate bearing redox-active ferrocenyl groups at the periphery†

Jiří Schulz,[a] Róbert Gyepes,[ab] Ivana Císařová[a] and Petr Štěpnička*[a]

Received (in Victoria, Australia) 2nd June 2010, Accepted 18th July 2010
DOI: 10.1039/c0nj00421a

Amide $FcCONHC(CH_2OH)_3$ (**1**; Fc = ferrocenyl), prepared from fluorocarbonylferrocene and tris(hydroxymethyl)methylamine, reacts with $(Bu_4N)_3[H_3V_{10}O_{28}]$ in *N*,*N*-dimethylacetamide to afford a salt containing a bis(triolato) capped hexavanadate anion bearing two ferrocenyl groups at its periphery, $(Bu_4N)_2[\{FcC(O)NHC(CH_2O)_3\}_2V_6O_{13}]$ (**2**). Compounds **1** and **2** were characterised by elemental analysis, spectroscopic methods (IR, NMR, and MS) and by cyclic voltammetry; the crystal structures of $\mathbf{1}\cdot 1/2CH_3CO_2Et$ and $(Bu_4N)_2[\{FcC(O)NHC(CH_2O)_3\}_2V_6O_{13}]\cdot 2Me_2NCHO$ were determined by X-ray diffraction analysis. Single-point DFT calculations performed for the isolated hexavanadate anion revealed the presence of 3-centre 4-electron (3c4e) O–V–O bonds on the hexavanadate cage, which are responsible for the high energy of the occupied frontier orbitals. The upper eleven occupied molecular orbitals including the HOMO are all delocalized over the hexavanadate cage and, therefore, any electrochemical oxidation can be expected to occur preferentially at the hexavanadate anion without affecting the pendant ferrocene moieties.

Introduction

Early transition metal polyoxoanions, commonly called polyoxometalates,[1] have been studied originally as structurally attractive and synthetically challenging compounds. More recently, the interest in these compounds renewed, being stimulated by attempts to find new cluster types and large cages mimicking the properties of metal oxides. Further motivation comes from the applications of polyoxometalates and their derivatives in a broad range of fields ranging from material science and catalysis to biology and biomedicine.[2]

Hexavanadate clusters are no exception and a number of compounds having the parent hexavanadate core modified *via* incorporation of late transition metal organometallic units[3] or a (formal) replacement of the bridging oxygen atoms with alkoxo groups[4] have been reported. Compounds in which triolate units replace the bridging oxygen atoms at the open tetrahedral cavities of the parent $\{V_6O_{19}\}$ core are particularly attractive due to their synthetic accessibility.[5] For instance, the bis-capped anions $[V_6O_{13}\{(OCH_2)_3CR\}]^{2-}$ can be prepared *via* condensation of $[H_3V_{10}O_{28}]^{3-}$ with triols $(HOCH_2)_3C–R$[5a] with a range of functional groups at the periphery (variation of R).[5c,6] The practical potential of such materials was already demonstrated by the preparation of coordination networks showing catalytic activity in oxidation reactions.[6]

Aiming at the preparation of hitherto unknown ferrocenyl-modified polyvanadates, we utilised the mentioned synthetic approach using *N*-{[tris(hydroxymethyl)methyl]carbamoyl}-ferrocene as a source of the ferrocenyl (Fc) unit. Herein, we describe the synthesis of a novel hexavanadate bearing two amidoferrocene pendants and its structural characterisation *via* a combination of spectroscopic methods, X-ray diffraction analysis, cyclic voltammetry and DFT calculations.

Results and discussion

Syntheses and structural characterisation

The starting triol derivative, $FcCONHC(CH_2OH)_3$ (**1**), was prepared (Scheme 1) by reacting fluorocarbonylferrocene with tris(hydroxymethyl)methylamine in the presence of 4-(dimethylamino)pyridine and triethylamine using dry *N*,*N*-dimethylformamide (DMF) as a solvent. Isolation by column chromatography followed by crystallisation from ethyl acetate–hexane afforded an unstable solvate $\mathbf{1}\cdot 1/2CH_3CO_2Et$ (**1a**). Upon drying under vacuum, this adduct partly liberated the solvent of crystallisation being converted to a non-stoichiometric though somewhat more stable solvate analysed as $\mathbf{1}\cdot 1/3CH_3CO_2Et$ (**1b**), which was used in the subsequent reactions.

Compound **1b** was characterised by elemental analysis and by spectroscopic methods. In its IR spectrum, it displays diagnostic amide bands[7] at 1619 and 1535 cm^{-1}, and a carbonyl stretching band of the solvating ethyl acetate at 1740 cm^{-1}. The NMR spectra of **1b** show signals attributable to the ferrocenyl moiety and the amide pendant. The amide C=O signal is seen at δ_C 170.10, similarly to an analogous 2-hydroxyethyl substituted amide, $FcCONHCH_2CH_2OH$.[8]

[a] *Department of Inorganic Chemistry, Faculty of Science, Charles University in Prague, Hlavova 2030, 12840 Prague, Czech Republic. E-mail: stepnic@natur.cuni.cz; Fax: +420 221 951 253*
[b] *J. Heyrovský Institute of Physical Chemistry, Academy of Sciences of the Czech Republic, v.v.i., Dolejškova 3, 18223 Prague 8, Czech Republic*

† Electronic supplementary information (ESI) available: A 'full view' of the crystal structure of **2a**, a superposition of the two crystallographically independent anions in the structure of **2a**, and the crystallographic data for **1a** and **2a**. CCDC reference numbers 779152 and 779153. For crystallographic data in CIF or other electronic format see DOI: 10.1039/c0nj00421a

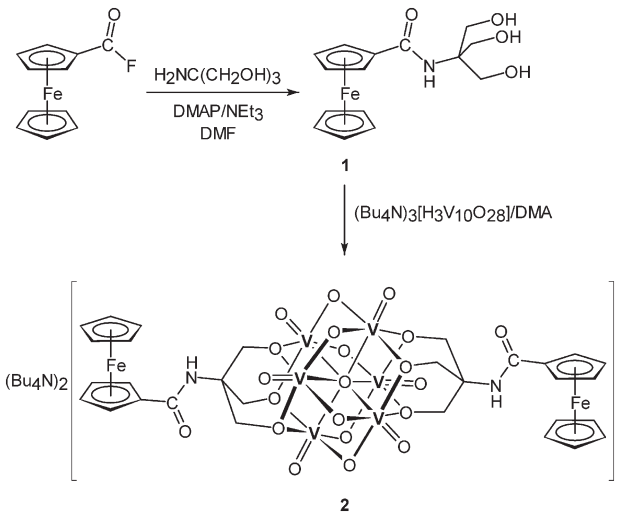

Scheme 1 The synthesis of **1** and **2** (DMAP = 4-(dimethylamino)-pyridine, DMA = *N*,*N*-dimethylacetamide, DMF = *N*,*N*-dimethyl formamide).

The molecular structure of **1a** as determined by X-ray crystallography (Fig. 1) is rather unexceptional. The ferrocene unit possessed a regular geometry, showing negligible tilting of its cyclopentadienyl rings (dihedral angle being only 1.2(1)°) and variation in the individual Fe–C(ring) distances (2.032(1)–2.055(2) Å). The distances of the iron atom to the cyclopentadienyl ring centroids are 1.6465(8) and 1.6505(9) Å for the substituted and unsubstituted rings, respectively. The geometry of the amide group does not differ much from that of the mentioned 2-hydroxyethyl amide,[8] or the non-functional amides FcCONHR, where R = *i*-Pr,[9] *n*-Bu, C_6H_{11}, Ph,[10] and CH_2Ph.[11]

In the crystal, the molecules of the amide associate *via* conventional O–H···O hydrogen bonds (Fig. 2). The molecular array can be described such that the molecules related by the crystallographic two-fold axes assemble into pairs by O4–H4O···O3 contacts, whilst the dimers formed aggregate

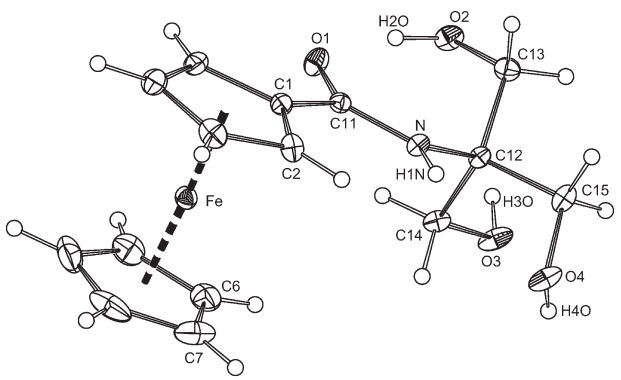

Fig. 1 PLATON[12] plot of the amide molecule in the structure of **1a** showing the atom labelling and displacement ellipsoids at the 30% probability level. Selected distances and angles (in Å and °): C1–C11 1.477(2), C11–O1 1.244(2), C11–N 1.343(2), N–C12 1.474(2), C12–C13 1.544(2), C12–C14 1.534(2), C12–C15 1.530(2), C13–O2 1.416(2), C14–O3 1.423(2), C15–O4 1.426(2); O1–C11–N 122.8(1), C11–N–C12 124.4(1), N–C12–C(13/14/15) 106.6(1)–112.8(1), C12–C(13/14/15)–O(2/3/4) 110.8(1)–115.2(1).

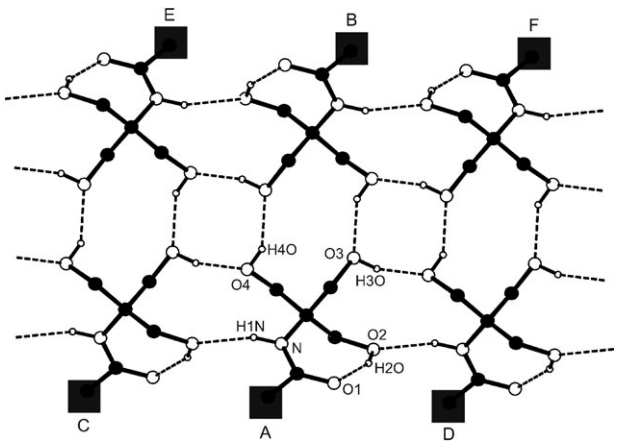

Fig. 2 A section of the hydrogen bonded array in the structure of **1a** as viewed along the crystallographic *b* axis. For clarity, the ferrocenyl units have been replaced with filled black squares. Hydrogen bond parameters are as follows: N–H1N···O2^{C}, N···O2^{C} = 3.076(2) Å, angle at H1N = 148°; O2–H2O···O1, O2···O1 = 2.649(2) Å, angle at H2O = 152°; O3–H3O···O4^{D}, O3···O4^{D} = 2.663(2) Å, angle at H3O = 164°; O4–H4O···O3^{B}, O4···O3^{B} = 2.671(2) Å, angle at H4O = 147°. Symmetry operations: *A* = (*x*, *y*, *z*), *B* = (−*x*, *y*, 1/2 − *z*), *C* = (*x*, 1 − *y*, −1/2 + *z*), *D* = (*x*, 1 − *y*, 1/2 + *z*), *E* = (−*x*, 1 − *y*, −*z*), *F* = (−*x*, 1 − *y*, 1 − *z*).

further into infinite ribbons oriented parallel to the *ac* plane by means of the O3–H3O···O4 and N–H1N···O2 lateral hydrogen bonds. Besides, the mutual orientation of the polar groups allows for the formation of structure-stabilising intramolecular O2–H2O···O1 contacts.[13] Molecules of the solvent occupy structural voids defined by the relatively bulkier amide molecules and do not interact apparently with the mentioned molecular assembly.

When reacted with $(Bu_4N)_3[H_3V_{10}O_{28}]$ in dry *N*,*N*-dimethylacetamide (DMA) at elevated temperatures, amide **1** behaved similarly to other tris(hydroxymethyl)methyl derivatives, affording the respective cationic hexavanadate, $(Bu_4N)_2[FcC(O)NHC(CH_2O)_3V_6O_{13}(OCH_2)_3CNHC(O)Fc]$ (**2**; Scheme 1). Compound **2** could be conveniently isolated by column chromatography (silica gel/MeCN). However, a better defined, air-stable red crystalline solvate **2**·2Me_2NCHO (**2a**) resulted *via* a subsequent crystallisation from a MeCN–DMF–diethyl ether mixture (15% isolated yield of analytically pure product after chromatography and two crystallisations).

The formulation of **2a** is consistent with elemental analysis data and also with electrospray mass spectra indicating the presence of the ionic constituents through the signals due to Bu_4N^+ (*m*/*z* 242), $[\{FcCONHC(CH_2O)_3\}_2V_6O_{13}]^{2-}$ (*m*/*z* 587), and $[\{FcCONHC(CH_2O)_3\}_2V_6O_{13} + Na]^-$ (*m*/*z* 1197). The IR spectra of **2a** suggest the presence of the vanadate unit and carbonyl groups. A very strong $\nu_{V=O}$ band is seen at 952 cm^{-1}. Amide bands attributable to the amidoferrocene pendants appear at 1655/1652 and 1536/1533 cm^{-1}. Notably, the former band, largely $\nu_{C=O}$ (amide I), is shifted to higher energies as compared to **1b**, reflecting the differences in hydrogen bonding patterns. On the other hand, the other (amide II, δ_{NH}) band remains virtually unaffected. An additional $\nu_{C=O}$ band due to solvating DMF occurs at 1674 cm^{-1}.

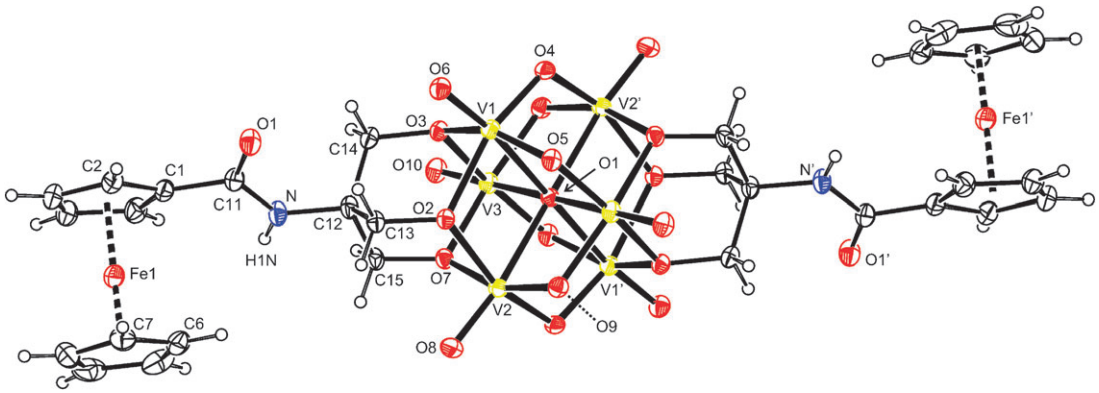

Fig. 3 PLATON[12] plot of anion 1 in the structure of **2a** showing displacement ellipsoids with 30% probability. The primed atoms are generated by the crystallographic inversion. The structure and atom labelling scheme of anion 2 in the structure of **2a** are essentially identical. Atomic labels in anion 2 are obtained by adding 20 to the respective label in anion 1.

The ^{51}V NMR spectrum of **2a** recorded in CD_3CN exhibits a single broad resonance at δ_V −498. The ^{1}H and ^{13}C NMR spectra confirm the presence of the amidoferrocene pendant, the counterions and the solvating DMF. Whereas the resonances of the FcC(O) moiety remain virtually intact upon 'complexation' (*cf.* δ_C(C═O) 170.90), those due to the $C(CH_2O)_3$ are affected significantly. The signals of the CH_2O groups are shifted to lower fields in both the ^{1}H and ^{13}C NMR spectra ($\Delta\delta_H \approx 1.7$ ppm, $\Delta\delta_C \approx 23$ ppm), and the C-13 resonance of the $C(CH_2O)_3$ carbon moves by *ca.* 8 ppm upfield (*N.B.* the spectra of **1b** and **2a** were recorded in different solvents).

The solid-state structure of **2a** was determined by single-crystal X-ray diffraction analysis (Fig. 3 and Table 1). It

Table 1 Selected distances and angles for the hexavanadate anions in the structure of **2a** (in Å and °)[a]

Anion 1		Anion 2	
V1–O1 (c)	2.2491(5)	V21–O21 (c)	2.2362(5)
V1–O2 (a)	2.057(2)	V21–O22 (a)	2.046(2)
V1–O3 (a)	1.983(2)	V21–O23 (a)	1.991(2)
V1–O4 (b)	1.771(2)	V21–O24 (b)	1.779(2)
V1–O5 (b)	1.886(2)	V21–O25 (b)	1.876(2)
V1–O6 (t)	1.603(2)	V21–O26 (t)	1.605(2)
V2–O1 (c)	2.2276(5)	V22–O21 (c)	2.2320(4)
V2–O2 (a)	1.982(2)	V22–O22 (a)	1.992(2)
V2–O7 (a)	2.064(2)	V22–O27 (a)	2.063(2)
V2–O4′ (b)	1.887(2)	V22–O24′ (b)	1.864(2)
V2–O9 (b)	1.761(2)	V22–O29 (b)	1.773(2)
V2–O8 (t)	1.605(2)	V22–O28 (t)	1.611(2)
V3–O1 (c)	2.2439(5)	V23–O21 (c)	2.2594(5)
V3–O3 (a)	2.062(2)	V23–O23 (a)	2.052(2)
V3–O7 (a)	1.975(2)	V23–O27 (a)	1.989(2)
V3–O9′ (b)	1.886(2)	V23–O29′ (b)	1.882(2)
V3–O5′ (b)	1.761(2)	V23–O25′ (b)	1.777(2)
V3–O10 (t)	1.605(2)	V23–O30 (t)	1.603(2)
V–O(a)–V	109.23(8)–110.05(8)		109.02(8)–110.13(8)
O(c)–V–O(t)	171.88(8)–171.89(8)		172.66(7)–172.76(7)
Fe1–Cg1	1.650(2)	Fe21–Cg21	1.650(2)
Fe1–Cg2	1.654(2)	Fe21–Cg22	1.651(2)
∠Cp1,Cp2	2.0(2)	∠Cp21,Cp22	1.8(2)
C11–O11	1.227(4)	C31–O31	1.232(4)
C11–N1	1.349(4)	C31–N21	1.352(4)
O11–C11–N1	123.9(3)	O31–C31–N21	123.8(3)
N1–C12	1.470(4)	N21–C32	1.476(4)
C12–C13	1.541(4)	C32–C33	1.532(4)
C13–O2	1.431(3)	C33–O22	1.424(3)
C12–C14	1.537(4)	C32–C34	1.535(4)
C14–O3	1.428(3)	C34–O23	1.434(3)
C12–C15	1.534(4)	C32–C35	1.541(4)
C15–O7	1.421(3)	C35–O27	1.429(3)
V–O(a)–C	117.4(2)–120.2(2)		117.9(2)–120.0(2)

[a] For atom labelling scheme, see Fig. 1. The prime-labelled atoms are generated by inversion operations. Definitions: a = alcoholate oxygen atom (O2, O3, and O7), b = bridging oxido ligands (O4, O5, O9), c = central oxygen atom (O1), t = terminal oxido ligands (O6, O8, O10). Cp1 and Cp2 are the substituted and unsubstituted cyclopentadienyl rings, respectively. Cg1 and Cg2 stand for their respective centroids.

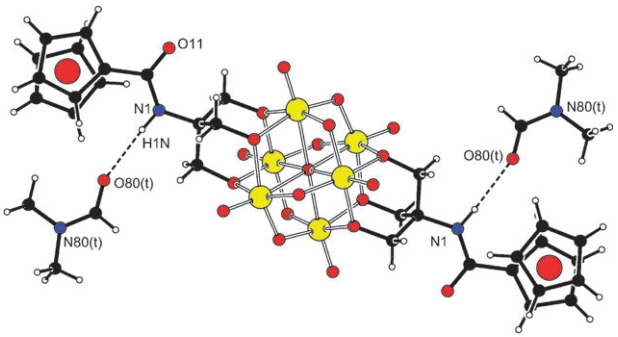

Fig. 4 Hydrogen bonds formed between cation 1 and the solvating DMF in the structure of **2a**. The hydrogen bonding pattern generated by cation 2 is similar. Hydrogen bond parameters: cation 1, N1–H1N···O80, N1···O80 = 3.114(4) Å, angle at H1N = 175°; cation 2, N21–H21N···O90, N21···O90 = 3.042(4) Å, angle at H21N = 167°; t = molecules generated by lattice translations.

consists of discrete Bu_4N^+ ions and hexavanadate anions, which bind two DMF molecules *via* FcCO*N*–*H*···*O*C(H)NMe$_2$ hydrogen bonds (Fig. 4). Notably, there are two structurally independent albeit practically identical[14] hexavanadate ions in the crystal structure, each residing on the crystallographic inversion centres (for an overlap and a 'full view', see ESI†). As a result, the asymmetric unit contains two Bu_4N^+ cations, two halves of the hexavanadate anions and two molecules of solvating DMF.

The triolate units in the anion of **2a** are mutually *trans* as dictated by the imposed symmetry and the overall geometry compares well with that reported for the structurally related anions $[\{RC(CH_2O)_3\}_2V_6O_{13}]^{2-}$, where R = NO_2,[5a] CH_3,[5c,d] NHC(O)CH=CH_2,[5c] or CH_2OH.[5g] Likewise these reference compounds, the V–O distances in **2a** follow the trend: V–O(terminal) < V–O(oxo bridge) < V–O(alkoxide bridge) < V–O1 (central oxygen), which in turn leads to an alternation of the V–O distances within the three V_4O_4 rings encircling the central oxygen atom O1.

The geometry of the V_6O (O = O1) core is quite regular, only with the V2–O1 distance being slightly longer than those involving vanadium atoms V2 and V3. The in-cage V–O1–V angles amount either to *ca.* 95° or *ca.* 85°, accordingly as the respective vanadium atoms belong to an alkoxide- or oxide-bridged edge of the V_6 octahedron. Another deformation is detected at the outer surface of the hexavanadate core because the terminal oxygen atoms, O(6,8,10), are all displaced from the respective O1–V axes and moved away from the closest triol-capped face. Nevertheless, this deformation is relatively minor (*cf.* the O1–V–O(t) angles being *ca.* 171.9° [172.7°])[15] and very likely reflects steric interactions of the terminal V=O groups with the CH_2O arms.

Despite these distortions and unlike V–O distances, the oxygen atoms forming the 'central layer', *viz.* O1, O(7/7′), O(8,8′), O(9,9′) and O(10,10′), are coplanar within *ca.* 0.06 Å [0.04 Å], whilst the V2 and V3 atoms deviate from this central plane by 0.044(1) Å and 0.132(1) Å [0.058(1) and 0.124(1) Å], respectively. The oxygen atoms constituting 'equatorial' O_4 planes, which are roughly perpendicular to the O=V–O1 axes (*i.e.*, O(2–5) for V1, O(2,7,9,4′) for V2, and O(3,7,5′,9′) for V3), are coplanar within less than 0.01 Å. However, their 'central' vanadium atoms, V(1–3), are displaced from these planes away from the central oxygen O1. The distances from the respective mean O_4-planes are 0.356(1) Å [0.348(1) Å] for V1, 0.337(1) Å [0.341(1) Å] for V2, and 0.350(1) Å [0.363(1) Å] for V3. The O(2–5) plane is almost coplanar with the central plane (the dihedral angle being 0.49(6)° [0.48(6)°]), whereas the remaining two O_4-planes are oriented perpendicularly (the dihedral angles are 89.71(6)° [89.86(6)°] for O(2,7,9,4′), and 89.65(6)° [89.59(6)°] for O(3,7,5′,9′)).

The arms of the triolato unit constitute three OVOCCC metallorings, which assume similar chair conformations and bear the pivotal N–C(O) bond in equatorial positions. Structural parameters of the ferrocenyl pendant differ only marginally from those of **1a**. The ferrocene cyclopentadienyls in **2a** are negligibly tilted and bind symmetrically to the iron atom. Notably, the amide planes {CON} are rotated with respect to their bonding cyclopentadienyl ring by 25.9(4)° [23.6(4)°], with the oxygen atom being moved away from the ferrocene core. On the other hand, changes in the arrangement of the amide moiety as well as the variation in the C–CH_2O and CCH_2–O bond lengths are rather insignificant. All other parameters (including those of the Bu_4N^+ cations and the solvating DMF)[16] are unexceptional.

Electrochemistry

Compounds **1b** and **2a** were studied by cyclic voltammetry at Pt-disc electrode using *ca.* 5×10^{-4} M acetonitrile solutions containing 0.1 M Bu_4NPF_6 as the supporting electrolyte. The amide expectedly showed a single, one-electron reversible wave attributable to ferrocene/ferrocenium couple. This wave was observed at more positive potentials than for ferrocene itself ($E^{\circ\prime}$ = 0.20 V), which is, indeed, in accordance with the electron-withdrawing nature of the carbamoyl unit (*cf.* σ_P = 0.36 for $CONH_2$).[17]

Compound **2a** also displayed a single oxidative wave in the potential window provided by the solvent (Fig. 5). However, this wave was found to be electrochemically irreversible (anodic peak potential, E_{pa} = +0.12 V at the scan rate of 100 mV s^{-1}; no reduction counter-peak was seen up to 10 V s^{-1}).

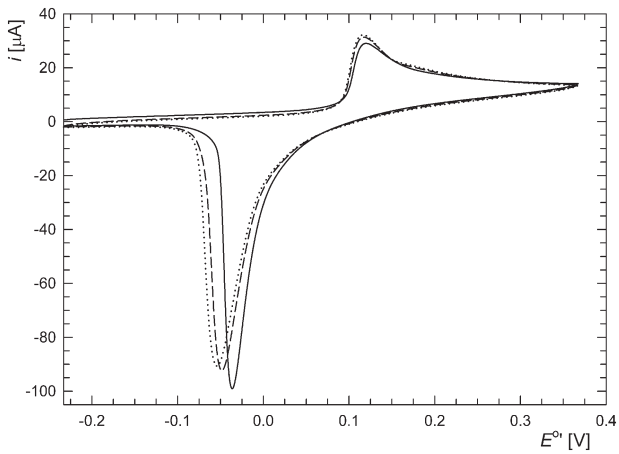

Fig. 5 Cyclic voltammogram of **2a** as recorded on a Pt-disc electrode in MeCN (c = 0.5 mM in 0.1 M Bu_4NPF_6). The first scan (full line) and the following scans are distinguished by the line type (second scan in dashed line, third in dotted line).

Moreover, a stripping-like peak (probably desorption) developed upon back scanning which shifted to slightly less positive potentials during the following scans (Fig. 5). This indicates some structural changes to be associated with the primary electron-transfer process that makes the redox change electrochemically (and also chemically) irreversible.

Notably, no reduction peak was seen for **2a** down to −2.4 V *vs*. the ferrocene/ferrocenium reference. This contrasts with the behaviour of $[\{RC(CH_2O)_3\}_2V_6O_{13}]^{2-}$, where R = CH_3, CH_2CH_3, CH_2Ph, NO_2, and NMe_2, that all display one-electron reversible *reductions* in the potential range of *ca*. −0.65 to −1.2 V (*vs*. ferrocene/ferrocenium) depending on R.[5a,d] An explanation of the overall redox response of **2a** can be sought in the electron-donating character of the ferrocenyl group, which makes the hexavanadate unit (relatively) electron rich and thus renders any reduction more difficult while facilitating oxidation processes.

DFT calculations

The solid state structure of the anion in **2** has been subjected to single-point DFT studies in order to obtain some insight into the bonding relations within the hexavanadate unit.

The peculiar structure of the hexavanadate cage owes its existence to a rather complicated bonding scheme, which is impossible to describe properly by the 'classical' Lewis terms (*i.e*., *via* σ- and π-bonds between atoms and nonbonding electron lone pairs). Although the natural charges of the individual vanadium atoms were found to be practically the same (1.54 for V1/1′ and V3/3′; 1.53 for V2/2′), those of the hexavanadate oxygen atoms exhibited a large variation depending on the number of the bonding partners (Table 2). In addition, the Mayer bond orders[18] were dependent on the chemical nature of the individual oxygen atoms (Table 3), while the fractional values obtained for the V–O bonds suggested that only a resonance description of the bonding could be adequate.

The nearly regular octahedron around the central oxygen atom O1 cannot be the result of any dominant O–V covalent interactions, since an octahedral arrangement is achievable by the formation of a sp^3d^2 hybrid, which is however beyond the possibilities of the second-row oxygen atom. The primary role of the O1 atom is thus to act as an 'anchor' for the surrounding vanadium cations by means of its marked negative charge, alleviating the repulsion between the metallic centres and providing some necessary electrostatic stabilization for the hexavanadate cage.

Owing to their octahedral environment, the O1 2s and 2p orbitals remain unmixed and despite being virtually nonbonding, they still provide some covalent bonding contributions to the surrounding metallic centres. However, due to the large interatomic O1–V separations, these covalent contributions are rather weak; thus the Natural Bond Orbital[19] (NBO) default search reported four lone pairs on O1 with the covalent overlaps treated as perturbations (delocalizations). The largest delocalization energies were found for the six V–O bonds between the six cage vanadiums and their terminal oxido groups. The most significant delocalization energies were observed for the 2s orbitals of O1 (Table 4).

Attempts to describe the bonding of the bridging alcoholate and oxido oxygen atoms by means of 'classical' two-centre bonds have all failed and the formalism of the 3-center 4-electron (3c4e) 'hyperbonds' had to be adopted instead. The concept of 3c4e bonding, introduced originally by Pimentel,[20] considers interactions of this type as a bonding between a triad of atoms (denoted henceforth as A1, A2, and A3), whose hybrids form three molecular orbitals (MO) of which the lowest two are populated by four electrons. Since a 3c4e interaction is usually of an $n_{A1} \rightarrow \sigma^*_{A2-A3}$ delocalization, the second populated orbital is quite high in energy. Using Coulson's description,[21] one can regard a 3c4e bond as a resonance between two limiting Lewis structures A1–A2:A3 and A1:A2–A3, denoted usually as A1┠A2┨A3.

Actually, the bridging oxygen atoms in the hexavanadate anion of **2** are all bonded by the 3c4e bonds (Table 5) with the vanadium atoms acting as centres for these three-centre interactions. Although the ratios between the two Lewis forms of the resonance triads are based on estimation and should be regarded as correct qualitatively,[22] the fractional bonding of the individual oxygen atoms is very well apparent.

The incorporation of σ* interactions in the second (and populated) orbitals of all the 3c4e hyperbonds leads to their energy becoming high. The oxygen nonbonding lone pairs remain also virtually nonbonding and as a consequence

Table 2 Natural charges (q_{nat}) of the hexavanadate oxygen atoms

Atom(s)	q_{nat}	Atoms	q_{nat}
O1	−1.11	O9/9′	−0.68
O2/2′, O3/3′, O7/7′	−0.74	O6/6′	−0.53
O4/4′, O5/5′	−0.69	O8/8′, O10/10′	−0.56

Table 3 Mayer bond orders (BO) for the VO_6 octahedron around V2

Bond	Mayer BO	Bond	Mayer BO
V2–O1(c)	0.634	V2–O8(t)	0.235
V2–O2(a)	0.776	V2–O9(b)	1.673
V2–O7(a)	0.686	V2–O4′(b)	1.153

Table 4 Delocalization energies (in kcal mol^{-1}) of the O1 2s orbital based on second-order perturbative estimates

Acceptor	E_{deloc} LP(2s)	Acceptor	E_{deloc} LP(2s)
V1–O6	21.97	V3–O10	23.30
V′–O6′	22.17	V3′–O10′	24.01
V2–O8, V2′–O8′	26.17	—	—

Table 5 The 3c4e hyperbonds in the hexavanadate anion[a]

Hyperbond A1┠A2┨A3	%A1–A2/%A2–A3	Occupancy
O3┠V1┨O4	37.4/62.6	3.9220
O3┠V1┨O5	47.1/52.9	3.9259
O4┠V1┨O2	60.4/39.6	3.9833
O5┠V1┨O3	59.3/40.7	3.9351
O2┠V2┨O9	39.6/60.4	3.9047
O9┠V2┨O7	61.1/38.9	3.9389

[a] Only contributions involving the oxygen atoms in the asymmetric part are listed.

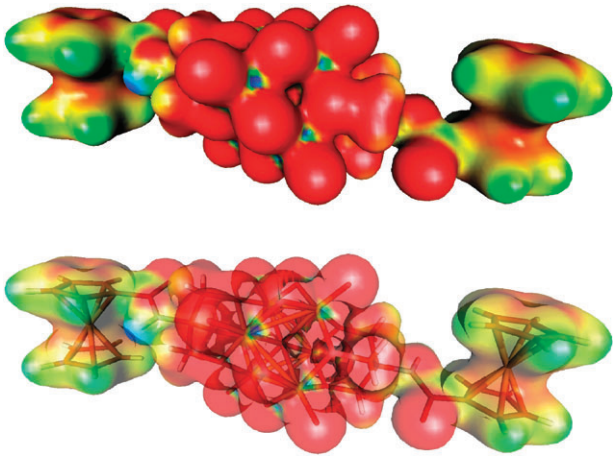

Fig. 6 Electrostatic potential mapped onto the 2% probability isosurface of **2a** (top) and orientation of the molecule in the isodensity contour (bottom). Blue regions are electrophilic, green electroneutral, and the red nucleophilic.

of both these phenomena, the highest occupied canonical orbitals delocalize over the hexavanadate cage. Due to the presence of the highly electronegative oxygen atoms, the overall electrostatic potential is also markedly negative (Fig. 6).

Since the upper 11 occupied molecular orbitals (including the HOMO) are delocalized over the hexavanadate cage, any oxidation processes will affect the anionic part of the molecule without the involvement of redox changes on the ferrocene units. The HOMO orbital particularly is a combination of the nonbonding lone pairs on the six bridging oxido atoms, each contributing with comparable fractions. The next occupied orbitals, still close in energy to the HOMO, incorporate already the bonds to the vanadium atoms. The irreversible oxidative wave observed during cyclic voltammetry (oxidation) thus probably reflects structural reorganisation at the hexavanadate cage, possibly due to changes occurring in the O⊣V⊣O triads.

Conclusions

This contribution demonstrates that the synthetic methodology developed for the synthesis of triolato-capped hexavanadates can be advantageously used for the preparation of well-defined compounds bearing the ferrocenyl groups as redox-active organometallic pendants. Electrochemical data and, mainly, theoretical computations indicate the ferrocenyl groups to behave largely as auxiliary modifiers without any pronounced electronic interaction with the anionic hexavanadate core. DFT calculations also reveal the presence of 3-centre 4-electron (3c4e) O–V–O bonds and delocalised bonding within the polyoxometalate cage where the central oxygen atom acts as an electrostatic pivot.

Experimental

Materials and methods

Syntheses were performed under argon atmosphere in the dark. Fluorocarbonylferrocene[23] and $(Bu_4N)_3[H_3V_{10}O_{28}]$[24] were synthesised according to literature procedures. Dry acetonitrile, DMF and DMA were purchased from Fluka and Aldrich. Other chemicals and solvents were used as received (Fluka, Aldrich; solvents from Lach-Ner).

NMR spectra were measured with a Varian UNITY Inova 400 spectrometer (^{1}H, 399.95; ^{13}C, 100.58; ^{51}V, 105.18 MHz) at 298 K. Chemical shifts (δ/ppm) are given relative to internal $SiMe_4$ (^{1}H and ^{13}C) or to external neat $VOCl_3$ (^{51}V). In addition to the standard notation of the signal multiplicity, vt is used to denote virtual triplets arising from magnetically non-equivalent AA′BB′ spin systems formed by the protons at the substituted cyclopentadienyl rings (C_5H_4). IR spectra were recorded with an FTIR Nicolet 7600 (Thermo Fisher Scientific) instrument in the range 400–4000 cm^{-1}. Electrospray ionisation mass spectra (ESI MS) were recorded with a Esquire 3000 (Bruker) spectrometer in methanol.

Electrochemical measurements were carried out with a computer-controlled multipurpose potentiostat μAUTOLAB III (Eco Chemie) at room temperature using a standard three-electrode cell with platinum disc electrode (AUTOLAB RDE, 3 mm diameter) as the working electrode, platinum sheet auxiliary electrode, and saturated calomel reference electrode (SCE), which was separated from the analysed solution by a salt-bridge (0.1 M Bu_4NPF_6 in MeCN). The analysed compounds were dissolved in MeCN (Aldrich, absolute) to give a solution containing *ca.* 5×10^{-4} M of the analyte and 0.1 M Bu_4NPF_6 (Fluka, puriss for electrochemistry) as the supporting electrolyte. The solutions were deaerated with argon prior to the measurement and then kept under an argon blanket. The redox potentials are given relative to the ferrocene/ferrocenium reference.

Syntheses

{*N*-[Tris(hydroxymethyl)methyl]carbamoyl}ferrocene (1). (Fluorocarbonyl)ferrocene (1.160 g, 5.0 mmol), tris(hydroxymethyl)methylamine (0.787 g, 6.5 mmol) and 4-(dimethylamino)-pyridine (0.122 g, 1.0 mmol) were dissolved in a mixture of dry DMF (20 mL) and triethylamine (1 mL), and the resulting mixture was stirred at 60 °C for 16 h. Then, the volatiles were removed under reduced pressure, and the solid residue was purified by column chromatography (silica, CH_2Cl_2–methanol, 10 : 1 v/v). Two bands were collected. The second band containing the desired product was evaporated and the residue was crystallised from hot ethyl acetate (20 mL) by slow cooling down to −18 °C. Yield of **1**·1/3AcOEt: 0.358 g (20%), orange brown crystalline solid.

^{1}H NMR (DMSO): δ 1.18 (t, $^3J_{HH}$ = 7.1 Hz, 1 H, $CH_3CO_2CH_2CH_3$), 1.99 (s, 1 H, CH_3CO_2Et), 3.64 (d, $^2J_{HH}$ = 5.7 Hz, 6 H, CH_2OH; the signal collapses into a singlet upon addition of D_2O), 4.03 (q, $^3J_{HH}$ = 7.1 Hz, 2/3 H, $CH_3CO_2CH_2CH_3$), 4.21 (s, 5 H, C_5H_5), 4.36 and 4.76 (2× virtual t, $J \approx 2.0$ Hz, 2 H, C_5H_4); 4.88 (t, $^3J_{HH}$ = 5.9 Hz, 3 H, CH_2OH; the signal disappears after the addition of D_2O), 6.63 (s, 1 H, CONH). ^{13}C{^{1}H} NMR ($CDCl_3$): δ 13.98 ($CH_3CO_2CH_2CH_3$), 20.65 (CH_3CO_2Et), 59.64 ($CH_3CO_2CH_2CH_3$), 60.58 (CH_2OH), 62.06 (CNH), 68.19 (CH of C_5H_4), 69.49 (C_5H_5), 70.03 (CH of C_5H_4), 76.56 (C_{ipso} of C_5H_4), 170.10 (C═O; only one C═O resonance

was observed). IR (neat): ν/cm^{-1} 3260 br s, 3108 m, 2959 m, 2938 m, 2896 w, 2872 w, 1740 s, 1619 vs, 1535 s, 1459 w, 1449 w, 1412 w, 1375 m, 1344 m, 1307 m, 1286 w, 1240 m, 1190 m, 1122 m, 1106 w, 1074 w, 1054 s, 1036 m, 1020 s, 930 w, 906 w, 872 w, 847 w, 831 m, 773 m, 730 br m, 620 w, 584 w, 560 w, 529 m, 499 m, 484 m, 467 w cm^{-1}. Anal. Calc. for $C_{15}H_{19}FeNO_4 \cdot 1/3CH_3CO_2Et$ (359.6): C 54.11, H 6.00, N 3.90%. Found: C 53.74, H 5.97, N 3.75%.

Compound 2. A solution of amide **1b** (0.321 g, 0.9 mmol) and $(Bu_4N)_3[H_3V_{10}O_{28}]$ (0.502 g, 0.3 mmol) in dry DMA (10 mL) was heated at 90 °C for 60 h, whereupon the colour turned from orange to brown. The reaction mixture was cooled to room temperature and then slowly added to diethyl ether (100 mL). The separated brown precipitate was filtered off and purified by column chromatography (silica gel, MeCN). The first brown and green coloured bands were discarded, and the following red band was collected and evaporated under vacuum. The solid residue, which was shown to be essentially pure *unsolvated* **2** by NMR spectra, was dissolved in dry DMF (2 mL). The solution was carefully layered with MeCN (1 mL) and diethyl ether (20 mL), and the mixture was allowed to crystallise over several days to afford crystalline **2a**, which was isolated by suction. The isolated product was recrystallised once again to afford analytically pure **2a** as a dark red crystalline solid. Yield: 81 mg (15%).

^{1}H NMR (CD_3CN): δ 0.98 (br t, 12 H, $NCH_2(CH_2)_2CH_3$), 1.38 and 1.63 (2× br s, 8 H, $NCH_2(CH_2)_2CH_3$); 2.78 and 2.90 (2× s, 3 H, Me_2NCHO); 3.14 (br s, 8 H, $NCH_2(CH_2)_2CH_3$), 4.16 (s, 5 H, C_5H_5), 4.32 and 4.71 (2× virtual t, J = 1.9 Hz, 2 H, C_5H_4); 5.37 (s, 6 H, $NHC(CH_2O)_3$), 5.77 (s, 1 H, $NHC(CH_2O)_3$), 7.95 (br s, 1 H, Me_2NCHO). $^{13}C\{^1H\}$ NMR (CD_3CN): δ 13.94 ($NCH_2(CH_2)_2CH_3$), 20.45 and 24.47 ($NCH_2(CH_2)_2CH_3$); 31.34 and 36.62 (Me_2NCHO); 54.26 (*C*NH), 59.44 (t(1 : 1 : 1), $^1J(^{14}N,^{13}C) \approx 3$ Hz, $NCH_2(CH_2)_2CH_3$), 69.52 (*C*H of C_5H_4), 70.80 (C_5H_5), 71.35 (*C*H of C_5H_4), 77.61 (C_{ipso} of C_5H_4), 83.88 (CH_2O), 170.90 (Fc*C*O); the C=O signal due to Me_2NCHO was not observed. ^{51}V NMR (CD_3CN): δ −498 (br s, $\Delta\nu_{\frac{1}{2}} \approx 530$ Hz). ESI± MS (CH_3OH): m/z 242 (Bu_4N^+); 587 ($[\{FcCONHC(CH_2O)_3\}_2V_6O_{13}]^{2-}$) and 1197 ($[\{FcCONHC(CH_2O)_3\}_2V_6O_{13} + Na]^-$). IR (neat): ν/cm^{-1} 3337 m, 3308 m, 3101 w, 3084 w, 2962 m, 2938 m, 2873 m, 2856 m, 1674 s, 1655/1652 s, 1536/1533 s, 1471 m, 1410 w, 1386 m, 1312 m, 1275 m, 1195 w, 1170 w, 1106 s, 1060 m, 1047 m, 1020 w, 952 vs, 817/810 s, 722 s, 584 s, 497 w, 481 w, 422 m. Anal. Calc. for $(C_{16}H_{36}N)_2[C_{30}H_{32}Fe_2N_2O_{21}V_6] \cdot 2C_3H_7NO$ (1805.0): C 45.24, H 6.59, N 4.66%. Found: C 44.92, H 6.51, N 4.55%.

X-Ray crystallography

Single crystals suitable for X-ray diffraction measurements were grown from warm ethyl acetate (**1**·1/2CH_3CO_2Et: brown plate, 0.20 × 0.32 × 0.40 mm^3) or selected directly from the reaction batch (**2a**: red-brown fragment, 0.20 × 0.25 × 0.28 mm^3). The selected specimens were mounted onto glass fibres with poly(perfluoroalkylether) oil.

Full-set diffraction data ($2\theta \leq 54.9$ for **1**, and 52.8° for **2a**; $\pm h \pm k \pm l$, data completeness 99.9%) were collected with a Nonius KappaCCD diffractometer equipped with a Cryostream Cooler (Oxford Cryosystems) using graphite-monochromatised MoKα radiation (λ = 0.71073 Å). The data were analysed with the HKL program package;[25] absorption was neglected.

Table 6 Selected crystallographic data and structure refinement parameters for **1a** and **2a**[a]

Compound	**1a**	**2a**
Formula	$C_{17}H_{23}FeNO_5$[e]	$C_{68}H_{118}Fe_2N_6O_{23}V_6$[f]
M	377.21	1805.02
Crystal system	Monoclinic	Triclinic
Space group	$C2/c$ (no. 15)	$P\bar{1}$ (no. 2)
a/Å	29.2486(4)	12.6480(2)
b/Å	10.1996(1)	15.8602(2)
c/Å	11.8137(1)	20.3923(3)
α/°	—	84.8847(8)
β/°	103.1641(9)	79.9909(7)
γ/°	—	78.0411(8)
V/Å^3	3431.70(8)	3935.0(1)
Z	8	2
D_c/g mL^{-1}	1.460	1.523
μ(MoKα)/mm^{-1}	0.905	1.113
Diffractions collected	45736	105274
Independent/observed[b] diffrns	3930/3622	16120/12513
R_{int}[c] (%)	2.9	5.8
R[d] observed diffractions (%)	3.02	4.25
R, wR[d] all data (%)	3.30, 7.91	6.20, 11.3
$\Delta\rho$/e Å^{-3}	0.58, −0.52	0.82, −0.55
CCDC reference number	779152	779153

[a] Common details: T = 150(2) K. [b] Diffractions with $I > 2\sigma(I)$. [c] $R_{int} = \sum|F_o^2 - F_o^2(\text{mean})|/\sum F_o^2$, where F_o^2(mean) is the average intensity of symmetry-equivalent diffractions. [d] $R_1 = \sum||F_o| - |F_c||/\sum|F_o|$, w$R = [\sum\{w(F_o^2 - F_c^2)^2\}/\Sigma w(F_o^2)^2]^{\frac{1}{2}}$. [e] $C_{15}H_{19}FeNO_4 \cdot 1/2C_4H_8O_2$. [f] $(C_{16}H_{36}N)_2[C_{30}H_{32}Fe_2N_2O_{21}V_6] \cdot 2C_3H_7NO$.

The phase problems were solved by direct methods (SIR97)[26] and the structures were refined by full-matrix least-squares on F^2 (SHELXL-97).[27] The non-hydrogen atoms were refined with anisotropic displacement parameters except for disordered ethyl acetate in the structure of amide **1**. The NH and OH hydrogens were located on difference electron density maps and refined as riding atoms with U_{iso}(H) assigned to a multiple of U_{eq} of their bonding atom. All other hydrogen atoms were included in their theoretical positions and refined as riding atoms.

Geometric calculations were performed with a recent version of the PLATON program.[12] All numerical values are rounded with respect to their estimated standard deviations (esd's) given with one decimal; parameters involving fixed hydrogen atoms are given without esd's. Relevant crystallographic data and structure refinement parameters are presented in Table 6.

Theoretical calculations

DFT computations have been conducted at the *fermi* cluster of the Computer Centre at the J. Heyrovský Institute of Physical Chemistry, Academy of Sciences of the Czech Republic, using Gaussian 03, Revision E.01.[28] The calculations were carried out as single point on the solid state geometry with the cationic parts excluded. The B3P86 functional was employed and the 6-31+G(d) basis set was used for all atoms. Natural Bond Orbital Analyses were done with the NBO 5.G[29] program;

visualization of the canonical molecular orbitals and the overall electrostatic potential was accomplished by Molden.[30]

Acknowledgements

This work was financially supported by the Grant Agency of Charles University in Prague (project no. 69309) and is a part of long-term research projects of Faculty of Science, Charles University in Prague, supported by the Ministry of Education, Youth and Sports of the Czech Republic (projects nos. MSM0021620857 and LC06070).

Notes and references

1 (*a*) M. T. Pope, *Heteropoly and Isopoly Oxometalates*, Springer, Berlin, 1983; (*b*) M. T. Pope, *Isopolyanions and Heteropolyanions*, in *Comprehensive Coordination Chemistry II*, ed. J. A. McCleverty and T. B. Mayer, Elsevier, Amsterdam, **2004**, vol. 4, ch. 4.10, p. 635; (*c*) C. M. Hill, *Polyoxo Anions: Reactivity*, in *Comprehensive Coordination Chemistry II*, ed. J. A. McCleverty and T. B. Mayer, Elsevier, Amsterdam, 2004, vol. 4, ch. 4.11, p. 679; (*d*) J. Zubieta, *Solid State Methods, Hydrothermal*, in *Comprehensive Coordination Chemistry II*, ed. J. A. McCleverty and T. J. Meyer, Elsevier, Amsterdam, 2004, vol. 1, ch. 1.39, p. 697.
2 (*a*) See the special issue of *Chem. Rev*. published in 1998: C. L. Hill, *Chem. Rev*., 1998, **98**, 1; (*b*) D.-L. Long, E. Burkholder and L. Cronin, *Chem. Soc. Rev*., 2007, **36**, 105.
3 (*a*) Y. Hayashi, Y. Ozawa and K. Isobe, *Chem. Lett*., 1989, 425; (*b*) Y. Hayashi, Y. Ozawa and K. Isobe, *Inorg. Chem*., 1991, **30**, 1025; (*c*) H. K. Chae, W. G. Klemperer and V. W. Day, *Inorg. Chem*., 1989, **28**, 1423; (*d*) G. Süss-Fink, L. Plasseraud, V. Ferrand, S. Stanislas, A. Neels, H. Stoeckli-Evans, M. Henry, G. Laurenczy and R. Roulet, *Polyhedron*, 1998, **17**, 2817.
4 For representative examples, see: (*a*) D. Hou, G.-S. Kim, K. S. Hagen and C. L. Hill, *Inorg. Chim. Acta*, 1993, **211**, 127; (*b*) J. Spandl, C. Daniel, I. Brudga and H. Hartl, *Angew. Chem., Int. Ed*., 2003, **42**, 1163; (*c*) C. Daniel and H. Hartl, *J. Am. Chem. Soc*., 2005, **127**, 13978; (*d*) M. A. Augustyniak-Jablokow, C. Daniel, H. Hartl, J. Spandl and Y. V. Yablokov, *Inorg. Chem*., 2008, **47**, 322.
5 (*a*) Q. Chen and J. Zubieta, *Inorg. Chem*., 1990, **29**, 1456; (*b*) M. I. Khan, Q. Chen, J. Zubieta and D. P. Goshorn, *Inorg. Chem*., 1992, **31**, 1556; (*c*) Q. Chen and J. Zubieta, *Inorg. Chim. Acta*, 1992, **198–200**, 95; (*d*) Q. Chen, D. P. Goshorn, C. P. Scholes, X. Tan and J. Zubieta, *J. Am. Chem. Soc*., 1992, **114**, 4667; (*e*) Q. Chen and J. Zubieta, *Chem. Commun*., 1993, 1180; (*f*) M. I. Khan, Q. Chen, H. Hope, S. Parkin, C. J. O'Connor and J. Zubieta, *Inorg. Chem*., 1993, **32**, 2929; (*g*) A. Müller, J. Meyer, H. Bögge, A. Stammler and A. Botar, *Z. Anorg. Allg. Chem*., 1995, **621**, 1818.
6 (*a*) J. W. Han, K. I. Hardcastle and C. L. Hill, *Eur. J. Inorg. Chem*., 2006, 2598; (*b*) C. L. Hill, T. M. Anderson, J. W. Han, D. A. Hillesheim, Y. V. Geletii, N. M. Okun, R. Cao, B. Botar, D. G. Musaev and K. Morokuma, *J. Mol. Catal. A: Chem*., 2006, **251**, 234; (*c*) J. W. Han and C. L. Hill, *J. Am. Chem. Soc*., 2007, **129**, 15094.
7 R. M. Silverstein, F. X. Webster and D. J. Kiemle, *Spectrometric Identification of Organic Compounds*, Wiley, New York, 7th edn, 2005, ch. 2, p. 99.
8 P. Štěpnička and I. Císařová, *CrystEngComm*, 2005, **7**, 37.
9 L. Lin, A. Berces and H.-B. Kraatz, *J. Organomet. Chem*., 1998, **556**, 11.
10 M. Oberhoff, L. Duda, J. Karl, E. Mohr, G. Erker, R. Fröhlich and M. Grehl, *Organometallics*, 1996, **15**, 4005.
11 M. B. Hursthouse, S. J. Coles and J. H. R. Tucker, private communication to the Cambridge Crystallographic Data Centre (refcode: BATLEO).
12 (*a*) A. L. Spek, *J. Appl. Crystallogr*., 2003, **36**, 7; (*b*) The program is available *via* the Internet at http://xray5.chem.uu.nl/spek/platon/.
13 Another potential intramoleculear N–H1N···O4 contact has a rather unfavourable geometry: N–H1N···O4, N···O4 = 2.789(2) Å, angle at H1N = 107°.
14 Molecular structures of the crystallographically independent anions differ by the orientation of the C(O)NH unit (*i.e*., O and NH interchange their positions) to the vanadate core (see ESI†, Fig. S2).
15 Values in the square brackets refer to cation 2.
16 For both structurally independent cations, the N–C distances and C–N–C angles fall into the ranges of 1.503(2)–1.528(2) Å and 105.2(2)–111.7(2)°, respectively. For the DMF molecules, the C═O and C–N distances are 1.191(6)/1.188(6) and 1.330(6)/1.316(6) Å, respectively (molecule 1/molecule 2). The respective N–C–O angles are 125.7(5)/126.5(5)°.
17 C. Hansch, A. Leo and R. W. Taft, *Chem. Rev*., 1991, **91**, 165.
18 (*a*) I. Mayer, *Chem. Phys. Lett*., 1983, **97**, 270; (*b*) I. Mayer, *Int. J. Quantum Chem*., 1984, **26**, 151.
19 J. P. Foster and F. Weinhold, *J. Am. Chem. Soc*., 1980, **102**, 7211.
20 G. C. Pimentel, *J. Chem. Phys*., 1951, **19**, 446.
21 C. A. Coulson, *J. Chem. Soc*., 1964, 1442.
22 F. Weinhold and C. R. Landis, *Valency and Bonding: A Natural Bond Orbital Donor-Acceptor Perspective*, Cambridge University Press, Cambridge, UK, 2005.
23 T. H. Galow, J. Rodrigo, K. Cleary, G. Cooke and V. M. Rotello, *J. Org. Chem*., 1999, **64**, 3745.
24 V. W. Day, W. G. Klemper and D. J. Maltbie, *J. Am. Chem. Soc*., 1987, **109**, 2991.
25 Z. Otwinowski and W. Minor, *Methods Enzymol*., 1997, **276**, 307.
26 A. Altomare, M. C. Burla, M. Camalli, G. L. Cascarano, C. Giacovazzo, A. Guagliardi, A. G. G. Moliterni, G. Polidori and R. Spagna, *J. Appl. Crystallogr*., 1999, **32**, 115.
27 (*a*) G. M. Sheldrick, *Acta Crystallogr., Sect. A: Found. Crystallogr*., 2008, **64**, 112; (*b*) The program is available *via* the Internet at http://shelx.uni-ac.gwdg.de/SHELX/.
28 M. J. Frisch, G. W. Trucks, H. B. Schlegel, G. E. Scuseria, M. A. Robb, J. R. Cheeseman, J. A. Montgomery, Jr., T. Vreven, K. N. Kudin, J. C. Burant, J. M. Millam, S. S. Iyengar, J. Tomasi, V. Barone, B. Mennucci, M. Cossi, G. Scalmani, N. Rega, G. A. Petersson, H. Nakatsuji, M. Hada, M. Ehara, K. Toyota, R. Fukuda, J. Hasegawa, M. Ishida, T. Nakajima, Y. Honda, O. Kitao, H. Nakai, M. Klene, X. Li, J. E. Knox, H. P. Hratchian, J. B. Cross, V. Bakken, C. Adamo, J. Jaramillo, R. Gomperts, R. E. Stratmann, O. Yazyev, A. J. Austin, R. Cammi, C. Pomelli, J. W. Ochterski, P. Y. Ayala, K. Morokuma, G. A. Voth, P. Salvador, J. J. Dannenberg, V. G. Zakrzewski, S. Dapprich, A. D. Daniels, M. C. Strain, Ö. Farkas, D. K. Malick, A. D. Rabuck, K. Raghavachari, J. B. Foresman, J. V. Ortiz, Q. Cui, A. G. Baboul, S. Clifford, J. Cioslowski, B. B. Stefanov, G. Liu, A. Liashenko, P. Piskorz, I. Komaromi, R. L. Martin, D. J. Fox, T. Keith, M. A. Al-Laham, C. Y. Peng, A. Nanayakkara, M. Challacombe, P. M. W. Gill, B. Johnson, W. Chen, M. W. Wong, C. Gonzalez and J. A. Pople, *Gaussian 03, Revision E.01*, Gaussian, Inc., Wallingford CT, USA, 2004.
29 E. D. Glendening, J. Badenhoop, A. E. Reed, J. E. Carpenter, J. A. Bohmann, C. M. Morales and F. Weinhold, *Theoretical Chemistry Institute*, University of Wisconsin, Madison, USA, 2001.
30 G. Schaftenaar and J. H. Noordik, *J. Comput.-Aided Mol. Des*., 2000, **14**, 123.

Appendix 5

J. Schulz, I. Císařová, P. Štěpnička: "Phosphinoferrocene Amidosulfonates: Synthesis, Palladium Complexes, and Catalytic Use in Pd-Catalyzed Cyanation of Aryl Bromides in an Aqueous Reaction Medium." *Organometallics*, 2012, **31**, 729.

ORGANOMETALLICS

Article

pubs.acs.org/Organometallics

Phosphinoferrocene Amidosulfonates: Synthesis, Palladium Complexes, and Catalytic Use in Pd-Catalyzed Cyanation of Aryl Bromides in an Aqueous Reaction Medium

Jiří Schulz, Ivana Císařová, and Petr Štěpnička*

Department of Inorganic Chemistry, Faculty of Science, Charles University in Prague, Hlavova 2030, 128 40 Prague 2, Czech Republic

Supporting Information

ABSTRACT: The reaction of pentafluorophenyl 1′-(diphenylphosphino)ferrocene-1-carboxylate (**4**) with ω-aminosulfonic acids $H_2N(CH_2)_nSO_3H$ (n = 1−3) in the presence of 4-(dimethylamino)pyridine and triethylamine affords the respective phosphinoferrocene amidosulfonates as crystalline triethylammonium salts, viz., $(Et_3NH)[Ph_2PfcCONH(CH_2)_nSO_3]$ (**1**, n = 1; **2**, n = 2; **3**, n = 3; fc = ferrocene-1,1′-diyl), in good yields. These ligands react smoothly with $[PdCl_2(cod)]$ (cod = η^2:η^2-cycloocta-1,5-diene) to give the anionic square-planar bis-phosphine complexes *trans*-$(Et_3NH)_2[PdCl_2(Ph_2PfcCONH(CH_2)_nSO_3$-$\kappa P)_2]$ (**5**, n = 1; **6**, n = 2; and **7**, n = 3). The chloride-bridged dimer $[L^{NC}PdCl]_2$, where L^{NC} is 2-[(dimethylamino-κN)methyl]phenyl-κC^1 auxiliary ligand, is cleaved with **1** to give $(Et_3NH)[L^{NC}Pd(Ph_2PfcCONHCH_2SO_3$-$\kappa P)]$ (**8**), in which the amidosulfonate coordinates as a simple phosphine. A similar reaction of $[L^{NC}Pd(OAc)]_2$ and **1** proceeds under a partial elimination of $(Et_3NH)OAc$ to afford a mixture of zwitterionic bis-chelate $[L^{NC}Pd(Ph_2PfcCONHCH_2SO_3$-$\kappa^2O,P)]$ (**9**) and another Pd(II) complex tentatively formulated as $[L^{NC}Pd(OAc)(Ph_2PfcCONHCH_2SO_3$-$\kappa P)]$ (**9a**), from which the former complex separates as an analytically pure crystalline solid. All compounds have been characterized by spectroscopic methods and elemental analysis. The crystal structures of **1**, **3**, **5**·2.5CH_2Cl_2, and **9**·2$CHCl_3$ were determined by single-crystal X-ray diffraction analysis. In addition, complexes **5**−**7** were tested as defined precatalysts for Pd-catalyzed cyanation of aryl bromides with $K_4[Fe(CN)_6]\cdot 3H_2O$ in aqueous dioxane. Complex **5** proved the most active and generally applicable, affording the nitrile products in good to excellent yields.

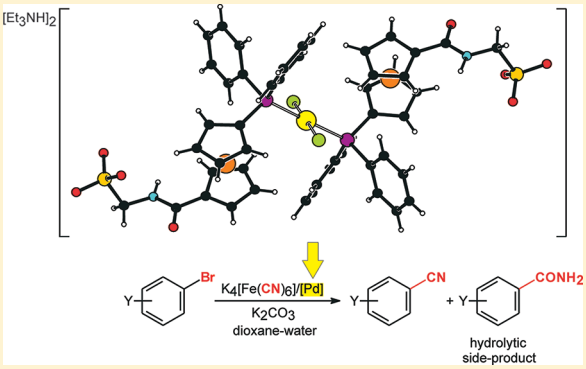

INTRODUCTION

Shortly after the synthesis of the first sulfonated phosphines,[1] it was recognized that the introduction of the highly polar and hydrophilic sulfonate group markedly improves solubility of these donors in water. Since then, there have been reported a number of phosphines sulfonated at their organic backbone. Among these, however, only sulfonated triphenylphosphine derivatives became the real privileged ligands that allowed for transferring numerous important transition metal-catalyzed reactions from organic solvents to water as an environmentally benign reaction medium without compromising their efficacy.[2]

Stimulated very likely by the applications of water-soluble phosphinosulfonate ligands, Whitesides and co-workers designed a series of donors combining extended carboxamido-ω-sulfonate polar tags with a diphosphine ligating unit (Chart 1, A).[3] This concept was later utilized by Sinou et al. in the preparation of water-soluble amidophosphine ligands based on chiral 2-[(diphenylphosphino)methyl]-4-(diphenylphosphino)pyrrolidine.[4] In the mid 1990s, Morteaux, Ziolkowski, et al.[5] and Patin et al.[6] reported the synthesis of another phosphine amidosulfonate ligand (Chart 1, B) by addition of diphenylphosphine or $LiPPh_2$ across the terminal double bond in the readily available

Chart 1

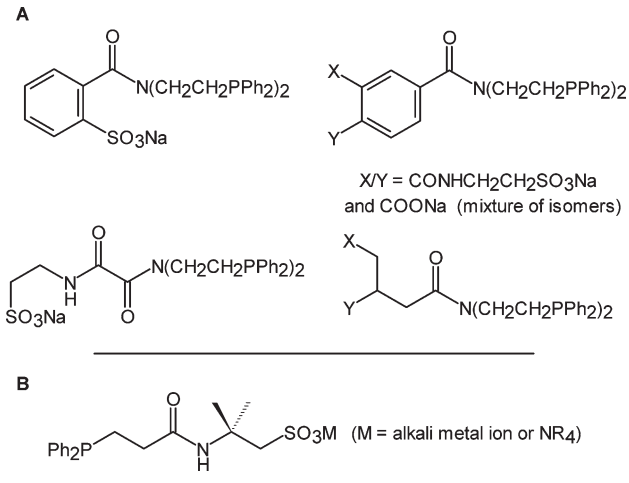

Received: November 18, 2011
Published: December 29, 2011

2-acrylamido-2-methyl-1-propanesulfonic acid. The former group further studied this hydrophilic phosphine as a ligand for Rh(I)-catalyzed hydrogenation and hydroformylation reactions in various solvents including water and biphasic mixtures,[5,7] and also for Pd-catalyzed carbonylation of organic halides to the respective acids or esters in water/toluene or water/alcohol mixed solvents.[8]

While exploring the coordination properties and synthetic applications of simple[9] and functional (typically donor-substituted)[10] *phosphinoferrocene carboxamides*, we recently turned also to compounds bearing highly polar amide substituents. So far, we have synthesized phosphinoferrocene amides bearing pendant 2-hydroxyethyl and α-amino acid substituents. The former compounds proved useful ligands for Pd-catalyzed Suzuki–Miyaura cross-coupling in biphasic reaction media,[11] whereas the latter were successfully utilized as ligands for Suzuki–Miyaura cross-coupling in aqueous reaction media (achiral ligands based on glycine)[12] or for enantioselective Cu-catalyzed conjugate addition of diethyl zinc to chalcones[13] and Pd-catalyzed asymmetric allylic alkylation (ligands prepared from chiral amino acids).[14] In a search of other lead structures, we became inspired by the polar phosphine-amides mentioned above and decided to prepare a series of new homologous amides from 1′-(diphenylphosphino)-1-ferrocenecarboxylic acid (Hdpf)[15] and ω-aminosulfonic acids $H_2N(CH_2)_nSO_3H$. This contribution reports the synthesis and structural characterization of three such polar phosphinoferrocene ligands and palladium(II) complexes thereof. Also reported are results of testing of defined Pd(II) diphosphine complexes prepared from these polar donors as catalysts for metal-catalyzed cyanation of aryl bromides in water/dioxane mixtures.

RESULTS AND DISCUSSION

Synthesis and Characterization of the Ligands. Amidosulfonate ligands **1**–**3** were obtained upon reacting the appropriate ω-aminosulfonic acid with Hdpf pentafluorophenyl ester **4**[11] in dry DMF in the presence of triethylamine and a catalytic amount of 4-(dimethylamino)pyridine at room temperature (Scheme 1). Subsequent isolation by column chromatography and recrystallization from hot ethyl acetate afforded the products as air-stable, crystalline triethylammonium salts in good yields. The compounds were characterized by elemental analysis and by spectroscopic methods. In addition, the crystal structures of **1** and **3** have been determined by single-crystal diffraction analysis.

Scheme 1. Preparation of Amidosulfonate Ligands 1–3[a]

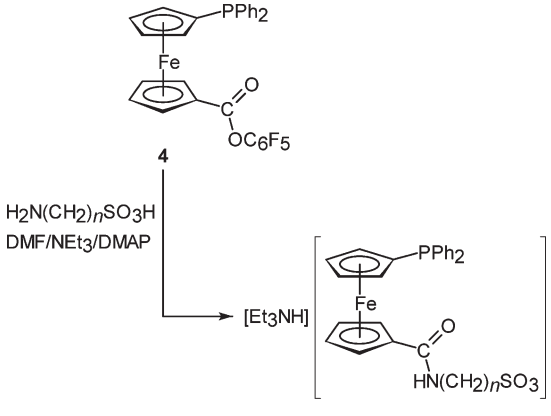

1 (n =1), **2** (n =2), **3** (n =3)

[a]DMAP = 4-(dimethylamino)pyridine, DMF = *N*,*N*-dimethylformamide.

Electrospray ionization (ESI) mass spectra of **1**–**3** corroborate the formulation by showing highly abundant signals due to $[Ph_2PfcCONH(CH_2)_nSO_3]^-$ (n = 1–3, fc = ferrocene-1,1′-diyl) and $[Et_3NH]^+$. In NMR spectra, the compounds display characteristic signals of the PPh_2-substituted ferrocene-1,1′-diyl moiety, the $(CH_2)_n$ linking groups, and the triethylammonium counterions. Additional ^{1}H NMR signals due to Et_3NH and the amide protons are observed as broad singlets and CH_2-coupled triplets, respectively, whose positions may change with the temperature and sample concentration. The IR spectra of **1**–**3** show strong amide bands at ca. 1645 (amide I) and 1550 cm^{-1} (amide II); bands due to the terminal sulfonate groups are seen at ca. 1150–1170 ($\nu_{as}(SO_3)$) and 1025–1040 ($\nu_s(SO_3)$).

The crystal structures of **1** and **3** are presented in Figure 1. Selected distances and angles are given in Table 1. The molecular structures are rather unexceptional, especially when compared to the crystal structures determined earlier for the related amides $Ph_2PfcCONHR$, where R = H,[9d] $NHCH_2Py$ (Py = pyrid-2-yl),[10a] CH_2CH_2OH,[11] and CH_2CO_2t-Bu.[12] The ferrocene

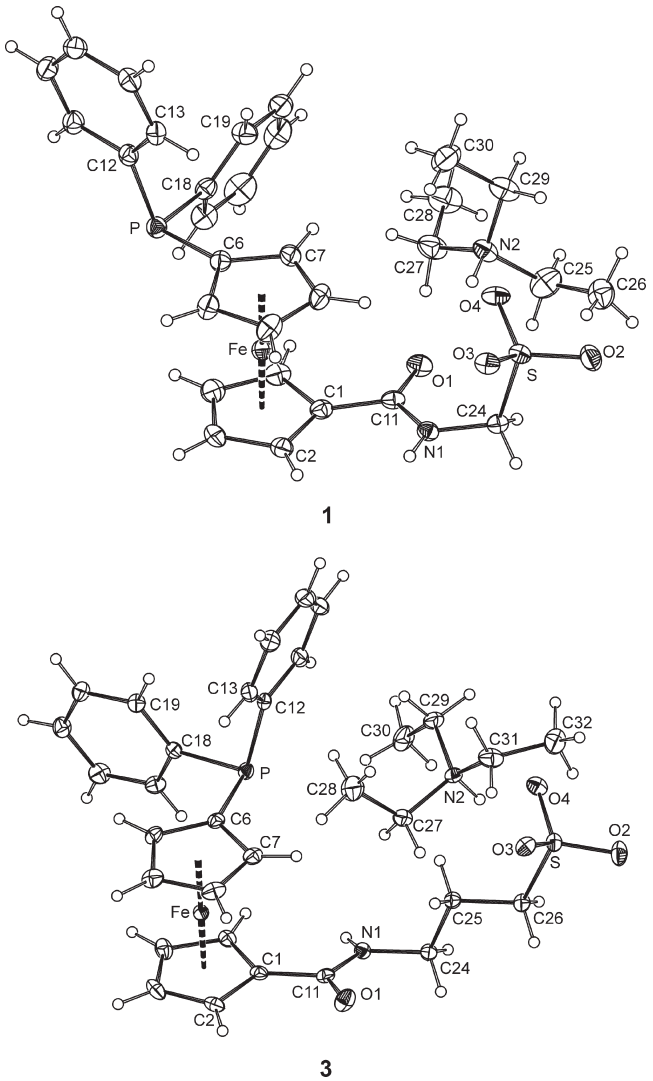

Figure 1. Views of the molecular structures of compound **1** (top) and **3** (bottom). Displacement ellipsoids enclose the 30% probability level.

dx.doi.org/10.1021/om2011529 | *Organometallics* 2012, 31, 729–738

Table 1. Selected Distances and Angles for 1 and 3[a]

parameter	1	3
Fe−Cg^P	1.642(1)	1.6397(8)
Fe−Cg^C	1.647(1)	1.6440(8)
∠Cp^C,Cp^P	1.1(2)	3.2(1)
τ^b	131	78
C11═O1	1.235(3)	1.229(2)
C11−N1	1.352(3)	1.344(2)
N1−C11═O1	122.3(2)	122.6(2)
N1−C24	1.434(3)	1.456(2)
Cp^C vs {CON}^{c}	5.0(3)	9.9(2)
CH_2−S	1.799(3)	1.773(2)
S−O	1.449(2)−1.459(2)	1.446(1)−1.470(1)

[a]Definitions: Cp^P and Cp^C are the PPh_2- and amide-substituted cyclopentadienyl rings. Cg^P and Cg^C are the respective centroids. [b]Torsion angle C1−Cg1−Cg2−C6. [c]Dihedral angle of the Cp^C and amide plane {C11,N1,O1}.

units in **1** and **3** are regular with almost identical Fe−ring centroid distances and tilt angles below 5°. In the case of compound **1**, the substituents at the ferrocene unit assume an intermediate conformation close to anticlinal eclipsed (see τ in Table 1). The amide group is rotated by only ca. 5° from the plane of its parent cyclopentadienyl ring (Cp^C), while the attached sulfonatomethyl group is oriented above the Cp^C plane so that the vector of the C24−S bond intersects this ring plane at an angle of 73.5(2)°. The amide pendant in **3** still points toward the PPh_2-substituted cyclopentadienyl ring, but the ferrocene unit adopts a more compact conformation (synclinal eclipsed). The amide plane in **3** is rotated from the Cp^C plane by ca. 10° though without any torsion at the amide pendant (cf. the distance of C24 from the amide plane being only 0.018(2) Å).

Anions in the crystals of **1** and **3** assemble into dimers via N−H···O hydrogen bonds toward one of the sulfonate oxygens (Figure 2; N1···O3 = 2.830(3) Å for **1** and N1···O4 = 2.908(2) Å for **3**). The triethylammonium counterions "decorate" these dimers at the outside, being connected via Et_3N−H···O_3S hydrogen bonds (N2···O4 = 3.044(3) Å for **1** and N2···O3 = 2.704(2) Å for **3**). In the case of **1**, featuring a shorter linking group (methylene), the latter interaction operates synergistically with a relatively shorter (stronger) N−H···O═C contact (N2···O1 = 2.767(3) Å).

Preparation of Pd(II) Complexes. Ligands **1**−**3** react cleanly with [$PdCl_2$(cod)] (cod = η^5:η^5-cycloocta-1,5-diene) to afford the expected square-planar diphosphine complexes **5**−**7** in high yields (Scheme 2). In ^{1}H NMR spectra, these complexes display signals due to the phosphinoferrocene ligands and the ammonium counterions. The $^{31}P\{^1H\}$ NMR spectra of all three complexes comprise one singlet resonance at δ_P 16.9, which is practically identical to that of the related Hdpf complex *trans*-[$PdCl_2$(Hdpf-κP)$_2$][16] and, in turn, suggests the *trans* geometry for all compounds. Indeed, this was confirmed by structure determination for compound **5** as a representative. A view of the complex anion in the crystal structure of solvate **5**·2.5CH_2Cl_2 is presented in Figure 3; a "full" view is available as Supporting Information, Figure S1.

The molecular structure of the complex anion in **5**, particularly the coordination geometry, compares very well with that of *trans*-[$PdCl_2$(Hdpf-κP)$_2$]·2CH_3CO_2H[16] and all other structurally characterized complexes of the type *trans*-[$PdCl_2$(Ph_2PfcY-κP)$_2$], where Y is a *non*chiral[17] functional group.[18,19] Unlike these complexes, however, compound **5** crystallizes without any imposed

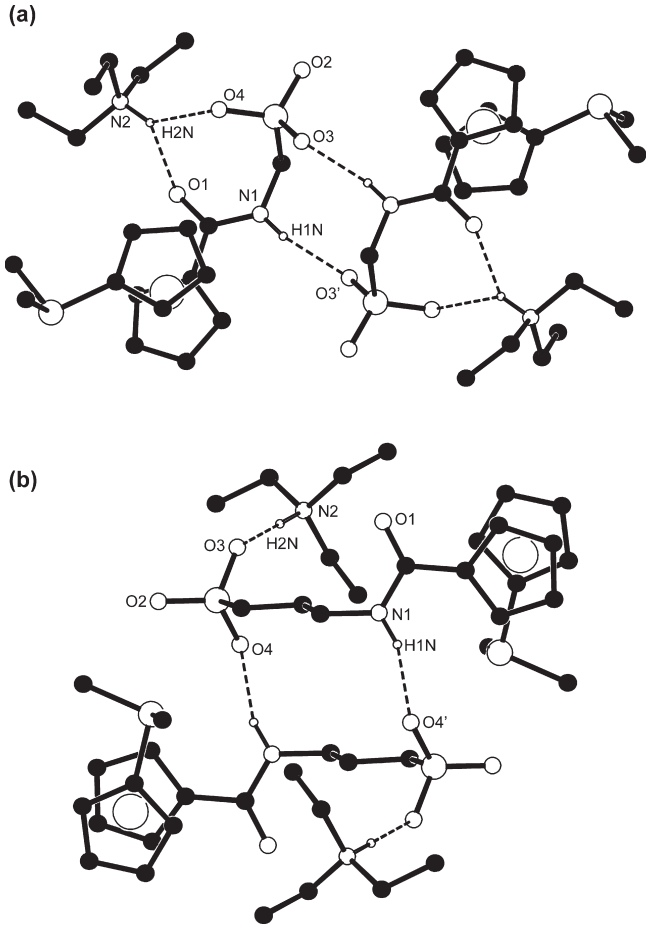

Figure 2. Views of the hydrogen-bonded assemblies in the crystal structures of **1** (a) and **3** (b). Only NH hydrogens and pivotal carbon atoms from the phenyl rings are shown for clarity.

Scheme 2. Preparation of Pd(II) Complexes 5−7[a]

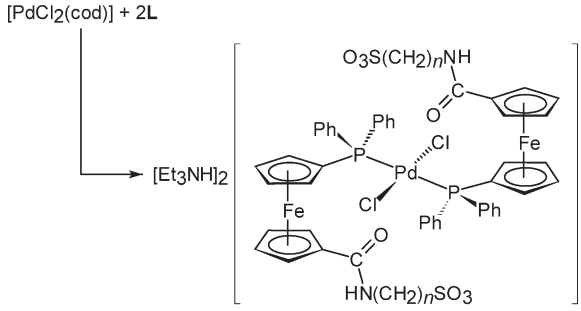

5 (*n* = 1), **6** (*n* = 2), **7** (*n* = 3)

[a]cod = cycloocta-1,5-diene.

symmetry, which can be tentatively attributed to crystal packing effects (most likely to an inefficient packing of the bulky counterions). Nonetheless, the complex anion tends to mimic a higher symmetry with very similar geometry for the two structurally independent $PdCl(Ph_2PfcCONHCH_2SO_3)$ subunits.

The palladium Pd and its four ligating atoms in **5** are coplanar within ca. 0.03 Å, which is in line with the sum of the interligand angles being 360.0°. The ferrocene units exert tilt angles below ca. 4° and a marginal variation in the Fe−C(Cp) distances (ca. 0.04 Å). Compared to the structure of the free ligand, the ferrocene substituents in **5** are more distant, as

dx.doi.org/10.1021/om2011529 | *Organometallics* 2012, 31, 729−738

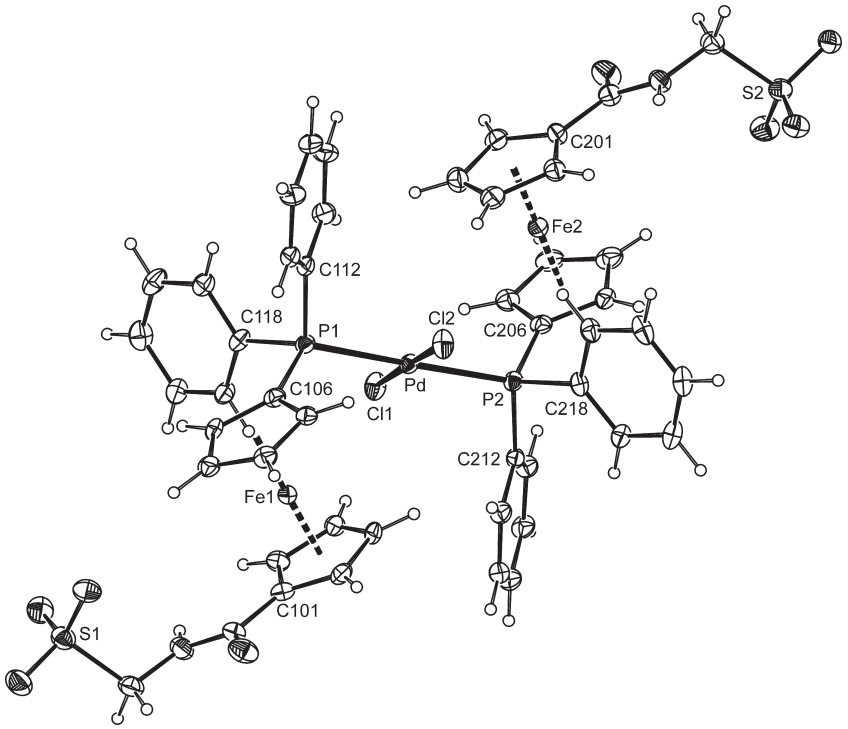

Figure 3. View of the complex anion in the crystal structure of **5**·2.5CH_2Cl_2. Displacement ellipsoids correspond to the 30% probability level.

indicated by the τ angles of 155° and 148° for ferrocene units comprising atoms Fe1 and Fe2, respectively. The amide planes are rotated by 4.4(5)° (moiety 1) and 12.4(5)° (moiety 2) with respect to the planes of their bonding Cp rings.

In the solid state, the molecules of complex **5** aggregate analogously to the free ligand (see Supporting Information, Figure S2). The only notable exception is that the pairs formed through N−H···O_3S hydrogen bonds bind the counterions only via Et_3N−H···O═C interactions (i.e., without supportive Et_3N−H···O_3S contacts such as in **1**) since the cations are shifted with respect to the amidosulfonate chains. Furthermore, because of the presence of two polar chains extending in roughly opposite positions, the anions associate into infinite chains in a brick wall-like fashion.

In another series of experiments, we studied the reactivity of ligand **1** as a representative toward C,N-chelated Pd precursors. Thus, compound **1** reacted with the dimer $[L^{NC}PdCl]_2$ (L^{NC} = 2-[(dimethylamino-κN)methyl]phenyl-κC^1) to afford (Et_3NH)-$[L^{NC}PdCl(Ph_2PfcCONHCH_2SO_3$-$\kappa P)]$ (**8** in Scheme 3) as the sole product. An analogous reaction with the acetate-bridged dimer $[L^{NC}Pd(OAc)]_2$ proved more complicated, producing a mixture of two new Pd complexes and triethylammonium acetate (Scheme 3). The major Pd-containing product (ca. 60%) was found to crystallize preferentially from the reaction mixture (either spontaneously or by addition of a less polar solvent) and was structurally characterized as O,P-chelated zwitterion **9** (see below). This bis-chelate complex apparently results by metathesis-like displacement of the Pd-bound acetate with **1** with concomitant elimination of $(Et_3NH)OAc$. Although the replacement of the acetate ligand is probably assisted by the charge of the terminal sulfonate group, it is the amide oxygen that becomes coordinated to palladium, most likely due to a favorable size of the chelate ring thus formed. A similar motif was found in the structures of $[L^{NC}Pd(Ph_2PfcCONHR$-$\kappa^2O,P)]^+$ salts prepared

Scheme 3. Preparation of Palladium(II) Complexes with L^{NC} Auxiliary Ligand[a]

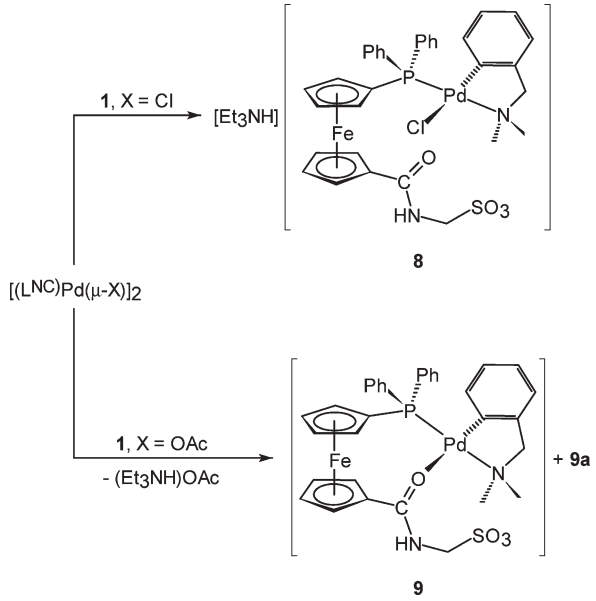

[a] L^{NC} = 2-[(dimethylamino-κN)methyl]phenyl-κC^1.

from simple (R = Ph)[9b] and functional (R = CH_2CO_2Me)[12] phosphinoferrocene carboxamide ligands.

In view of the literature precedents[20] and our reaction tests (see Experimental Section), the minor component in the reaction mixture was tentatively formulated as the bridge-cleavage product $(Et_3NH)[L^{NC}Pd(OAc)(Ph_2PfcCONHCH_2SO_3$-$\kappa P)]$ (**9a**), representing a plausible reaction intermediate occurring en route from $[L^{NC}Pd(OAc)]_2$ to **9**. Unfortunately, neither *in situ* NMR nor IR spectra of the reaction mixture provided an unambiguous proof for this formulation owing to the presence of broad resonances

dx.doi.org/10.1021/om2011529 | *Organometallics* 2012, 31, 729−738

indicating a dynamic system and extensive band overlaps, respectively. Supporting evidence was finally inferred from ESI-MS spectra of the reaction mixture containing **9** and **9a** that clearly showed ions due to $[(L^{NC})Pd(Ph_2PfcCONHCH_2SO_3) + H]^+$ (m/z 747), $[(L^{NC})Pd(Ph_2PfcCONHCH_2SO_3) + Na]^+$ (m/z 769), and $[(L^{NC})Pd(Ph_2PfcCONHCH_2SO_3)(HNEt_3)]^+$ (m/z 848) in positive ion mode and ions attributable to $Ph_2PfcCONHCH_2SO_3^-$ (m/z 506) and $[(L^{NC})Pd(Ph_2Pfc-CONHCH_2SO_3)(X) - H]^+$, where X = Cl ($m/z$ 781) and OAc (m/z 805), in the negative ion mode. The latter species in particular authenticates the formulation of **9a** as an (L^{NC})Pd–acetato complex. Other support came from the model reaction of $[(L^{NC})Pd(OAc)]_2$ with $FcPPh_2$ (Fc = ferrocenyl; Pd:$FcPPh_2$ = 1:1), which cleanly afforded $[(L^{NC})Pd(FcPPh_2)(OAc)]$, showing ions $[(L^{NC})Pd(FcPPh_2)(OAc) + Na]^+$ and $[(L^{NC})Pd(FcPPh_2) + H]^+$ in its ESI$^+$-MS spectrum.

The structure of the solvate **9**·2$CHCl_3$ was determined by X-ray diffraction analysis (Figure 4). It confirms the *trans*-P–N

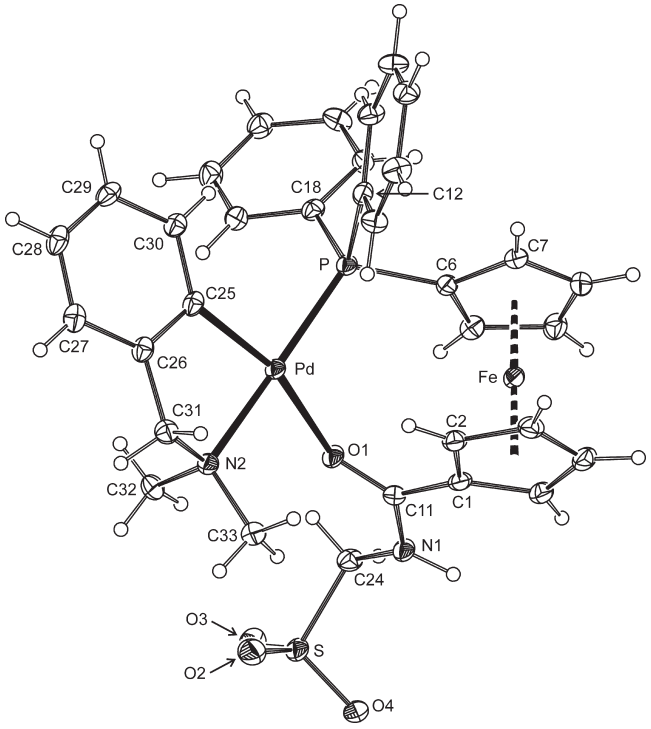

Figure 4. View of the complex molecule in the structure of **9**·2$CHCl_3$. Displacement ellipsoids are drawn at the 30% probability level.

geometry suggested already by the $^4J_{PH}$ coupling constants.[21] The overall coordination geometry is similar to that found in the mentioned cations $[L^{NC}Pd(Ph_2PfcCONHR\text{-}\kappa^2O,P)]^+$ (R = CH_2CO_2Me[12] or Ph[9b]). The coordination plane in **9** is angularly twisted, with the dihedral angle of the in-ring planes {Pd,P,O1} and {Pd,N2,C25} being 13.7(3)°. The donor moieties at the ferrocene unit are brought into proximity by rotation of the Cp rings (τ = 58.4(4)°) and the amide plane, which deviates from coplanarity with its parent Cp^C ring by as much as 26.0(6)°. Otherwise, the geometry of the ferrocene unit remains quite regular.[22] The C11═O1 and C11–N1 bonds are both shorter by 0.01 Å than those in noncoordinated **1**.

Likewise **1** and **5**·2.5CH_2Cl_2, the individual molecules of **9**, assemble into centrosymmetric dimers in the crystal (see Supporting Information, Figure S3). In addition, one of the two independent solvating chloroform molecules is connected to two sulfonate oxygens via bifurcate C–H···O contacts (C···O = 3.107(9) and 3.063(8) Å).

Catalytic Tests. Palladium-catalyzed cyanation of aryl halides[23] offers an alternative access to synthetically highly valued benzonitriles. The attractiveness of this reaction, which is complementary to conventional synthetic methods, markedly increased over the past decade, during which time several efficient catalytic systems were discovered, and simultaneously, the hazardous conventional cyanide sources (e.g., alkali metal cyanides, metal cyanides, or Me_3SiCN)[23] were replaced with the practically nontoxic potassium hexacyanoferrate(II).[24] Typically, the cyanations with $K_4[Fe(CN)_6]$ are now performed with ligand-supported[25] or deposited Pd metal[26] catalysts in various polar solvents, their aqueous mixtures, or even in pure water. Having prepared new phosphine ligands with highly polar amidosulfonate tags, we decided to test their defined Pd(II) complexes **5**–**7** as catalysts for this reaction in an aqueous reaction medium (Scheme 4 and Table 2).

Scheme 4. Pd-Catalyzed Cyanation of Aryl Bromides[a]

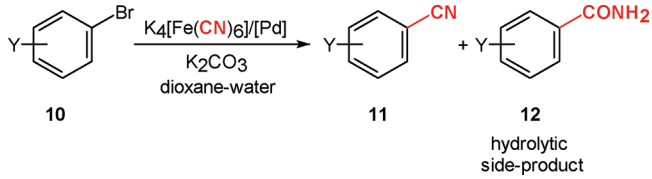

[a]Substrates: Y = 4-OMe (**a**), 4-Me (**b**), 3-Me (**c**), 2-Me (**d**), 4-CMe_3 (**e**), 4-CF_3 (**f**), 4-C(O)Me (**g**), 4- Ph (**h**), 4-Cl (**i**), 4-NO_2 (**j**), 4-NMe_2 (**k**), 4-CO_2H (**l**), and 4-CH_2CO_2H (**m**). Conditions: 2 mol % of Pd catalyst, 1.0 equiv K_2CO_3, 0.5 equiv $K_4[Fe(CN)_6]\cdot 3H_2O$, dioxane/water, 100 °C/18 h. For catalytic results, see Table 2.

Indeed, the initial screening tests were promising, as the cyanation of 4-bromoanisole as a deactivated substrate performed in the presence of 1 mol % of complex **5**, 0.5 equiv of $K_4[Fe(CN)_6]\cdot 3H_2O$ (corresponds to 3 equiv of CN^-), and 1 equiv of K_2CO_3 as a base in dioxane/water (1:1) afforded the desired nitrile **11a** with a 58% conversion. Rather surprisingly, the homologous compounds **6** and **7** performed considerably worse under strictly analogous conditions (see entries 1–3 in Table 2). Upon increasing the amount of catalyst **5** to 2 mol %, nitrile **11a** was formed with full conversion. On the other hand, lowering the amount of K_2CO_3 to 0.5 equiv resulted in a lower conversion and, in the absence of any base, the reaction stopped entirely (entries 5 and 6 in Table 2).

Additional tests revealed that the reaction outcome depends strongly on the composition of the reaction medium, namely, on the dioxane/water ratio (Figure 5). Whereas the reaction did not proceed in pure dioxane, after the addition of 20 vol % of water to dioxane, **11a** was formed with 77% conversion. Complete conversions were achieved in mixed solvents containing 40, 50, and 60 vol % of water. Any further addition of water incited an unwanted hydrolysis of the initially formed nitrile to amide **12a**. The ratio of **12a**:**11a** increased with the water content, being 17:83 in 20 vol % dioxane and 40:60 in pure water.

A survey of various halide substrates revealed that the cyanation reaction promoted by complex **5** proceeds cleanly and completely with *para*-substituted bromobenzenes bearing simple alkyl, aryl, and acetyl groups and that, in the series of tolyl bromides, it is not affected by the substitution patterns. Substrates with dissociable carboxyl substituents reacted equally

dx.doi.org/10.1021/om2011529 | *Organometallics* 2012, 31, 729–738

Table 2. Summary of Catalytic Results in the Pd-Catalyzed Cyanation of Aryl Bromides[a]

			nitrile **11**	amide **12**
enry	substrate **10**	catalyst	^{1}H NMR yield (isolated yield) (%)	^{1}H NMR yield (%)
1	**10a** (4-MeO)	**5**[b]	58	n.d.
2	**10a** (4-MeO)	**6**[b]	20	n.d.
3	**10a** (4-MeO)	**7**[b]	27	n.d.
4	**10a** (4-MeO)	**5**	100 (95)	n.d.
5	**10a** (4-MeO)	**5**[c]	0	n.d.
6	**10a** (4-MeO)	**5**[d]	56	n.d.
7	**10b** (4-Me)	**5**	100 (90)	n.d.
8	**10c** (3-Me)	**5**	100 (76)	n.d.
9	**10d** (2-Me)	**5**	100 (86)	n.d.
10	**10e** (4-CMe_3)	**5**	100 (82)	n.d.
11	**10f** (4-CF_3)	**5**	62	38
12	**10g** (4-C(O)Me)	**5**	100 (93)	n.d.
13	**10h** (4-Ph)	**5**	100 (91)	n.d.
14	**10i** (4-Cl)	**5**	56	44
15	**10j** (4-NO_2)	**5**	<5	n.d.
16	**10k** (4-NMe_2)	**5**	17	n.d.
17	**10l** (4-CO_2H)	**5**[e]	100 (87)	n.d.
18	**10m** (4-CH_2CO_2H)	**5**[e]	100 (89)	n.d.

[a]Conditions: aryl bromide **10** (1.0 mmol), K_2CO_3 (1.0 mmol), and $K_4[Fe(CN)_6]\cdot 3H_2O$ (0.5 mmol) were reacted in the presence of 2 mol % Pd catalyst in dioxane/water (1:1 mixture, 4 mL) at 100 °C for 18 h. n.d. = product was not detected in the reaction mixture. [b]Reaction with 1 mol % of Pd complex. [c]Reaction without added K_2CO_3. [d]Reaction in the presence of 0.50 mmol of K_2CO_3. [e]Reaction in the presence of 2.0 mmol of K_2CO_3 (2 equiv with respect to the substrate). The product was isolated after acidification of the reaction mixture.

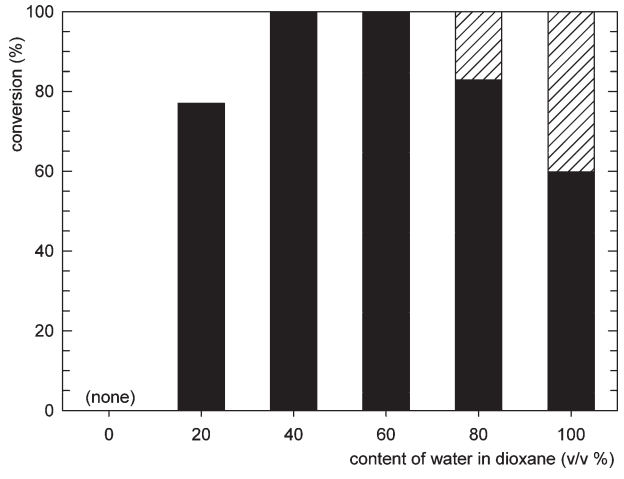

Figure 5. Influence of the amount of water in the water/dioxane reaction medium on the conversion of 4-bromoanisole (**10a**) to 4-cyanoanisole (**11a**, solid bars) and to 4-methoxybenzamide (**12a**, hatched bars). Conditions: **10a** (1.0 mmol), $K_4[Fe(CN)_6]\cdot 3H_2O$ (0.5 mmol), K_2CO_3 (1.0 mmol), and 2 mol % of **5** in dioxane/water (4 mL), 100 °C/18 h.

well (entries 17 and 18), while a poor conversion was achieved for 4-(dimethylamino)bromobenzene (entry 16). This, however, can be accounted for by a catalyst scavenging effect exerted by the donor group in this substrate, which is present in a large excess. It is also noteworthy that reactions involving substrates bearing electron-withdrawing substituents (4-CF_3 and 4-Cl; −*I*-effect) proceeded still with complete consumptions of the starting bromide but were accompanied by hydrolysis of the initially formed nitrile to the corresponding amide (in dioxane/water, 1:1). Apparently, these substituents reduce electron density at the nitrile group and make it thus more prone toward attack of OH^-, which opens the hydrolytic sequence. Finally, the cyanation of 4-nitrobromobenzene[27] proceeded in only a negligible extent (entry 15), while heterocyclic bromides (2- and 3-bromopyridine and 4-bromopyridine hydrochloride) did not react at all.

CONCLUSIONS

Amidosulfonate ligands reported in this paper represent a new entry among the still rather uncommon nonchiral phosphinoferrocene ligands equipped with highly polar functional groups.[28] The particular combination of the donor groups makes them typical hybrid ligands[29] with adaptable coordination properties. Compared to phosphines sulfonated directly at the backbone,[30] they are easier to prepare and, hence, also more structurally versatile (tunable). The presence of a relatively larger hydrophobic group than in sulfonated triphenylphosphines could make compounds **1**−**3** suitable for use in transition metal-catalyzed reactions at water−organic solvent interfaces.[31] This possibility is currently being checked in our laboratory.

EXPERIMENTAL SECTION

Materials and Methods. All syntheses were carried out under an argon atmosphere and with exclusion of direct daylight. Ester **4**,[11] $[PdCl_2(cod)]$,[32] $[(L^{NC})Pd(\mu\text{-}Cl)]_2$,[33] $[(L^{NC})Pd(\mu\text{-}OAc)]_2$,[34] and (diphenylphosphino)ferrocene[35] were synthesized according to literature procedures. Dichloromethane and chloroform were dried over anhydrous potassium carbonate and distilled. (1,4-)Dioxane and triethylamine were freshly distilled from sodium metal. Anhydrous DMF was purchased from Sigma-Aldrich. Other chemicals and solvents used for crystallizations and in chromatography were used as received without any additional purification.

NMR spectra were measured with a Varian UNITY Inova 400 spectrometer at 298 K. Chemical shifts (δ/ppm) are given relative to internal $SiMe_4$ (^{1}H and ^{13}C) or to external 85% H_3PO_4 (^{31}P). In addition to the standard notation of signal multiplicity, vt and vq are used to denote virtual multiplets due to protons of constituting the AA′BB′ and AA′BB′X spin systems in the amide- and PPh_2-substituted cyclopentadienyl rings, respectively (fc = ferrocene-1,1′-diyl). IR spectra were recorded with an FT IR Nicolet Magna 760 instrument. Low-resolution electrospray ionization (ESI) mass spectra were obtained with an LCQ Deca XP (Thermo Finnigan) or an Esquire 3000 (Bruker) spectrometer. High-resolution ESI-MS spectra were recorded with an LTQ Orbitrap XL spectrometer (Thermo Fisher Scientific).

Preparation of Amide 1. Ester **4** (2.0 mmol, 1.160 g), aminomethanesulfonic acid (2.5 mmol, 0.278 g), and 4-(*N*,*N*-dimethylamino)pyridine (0.06 mmol, 7.3 mg) were dissolved in a mixture of anhydrous *N*,*N*-dimethylformamide (10 mL) and triethylamine (1 mL). The resulting mixture was stirred at room temperature for 6 h and then evaporated under reduced pressure. The residue was extracted with dichloromethane (20 mL) in an ultrasonic bath. The extract was filtered and evaporated to afford a crude product, which was purified by column chromatography over silica gel using CH_2Cl_2/MeOH/Et_3N (100:5:2) as the eluent. The first orange band was collected and evaporated. The product was further recrystallized from hot ethyl acetate (ca. 100 mL) to give crystalline **1**, which was isolated by suction and dried under reduced pressure. Yield: 0.998 g (82%,), orange crystalline solid.

^{1}H NMR ($CDCl_3$): δ 1.32 (t, $^3J_{HH}$ = 7.3 Hz, 9 H, CH_3 of Et_3NH^+), 3.11 (dq; $^3J_{HH}$ = 7.2 and 3.4 Hz, 6 H, CH_2 of Et_3NH^+), 4.19 (vq, J = 1.8 Hz, 2 H, fc), 4.20 (vt, J = 2.0 Hz, 2 H, fc), 4.47 (d, $^3J_{HH}$ = 6.5 Hz, 2 H, CH_2S), 4.56 (vt, J_{HH} = 1.8 Hz, 2 H, fc), 4.61 (vt, J = 1.8 Hz, 2 H, fc), 6.50 (t, J_{HH} = 6.1 Hz, 1 H, NH), 7.28−7.38 (m, 10 H, PPh_2), 9.97 (br s, 1 H, Et_3NH^+). ^{13}C{^{1}H} NMR ($CDCl_3$): δ 8.64 (CH_3 of Et_3NH^+), 46.19 (CH_2 of Et_3NH^+), 55.65 (CH_2S), 69.16, 72.06, 73.35

dx.doi.org/10.1021/om2011529 | *Organometallics* 2012, 31, 729−738

(d, J_{PC} = 4 Hz) and 74.33 (d, J_{PC} = 4 Hz) (4× CH of fc); 75.82 (*C*-CONH of fc), 128.23 (d, $^3J_{PC}$ = 7 Hz, CH_{meta} of Ph), 128.66 (CH_{para} of PPh_2), 133.45 (d, $^2J_{PC}$ = 20 Hz, CH_{ortho} of PPh_2), 138.64 (d, $^1J_{PC}$ = 9 Hz, C_{ipso} of PPh_2), 169.78 (C═O). The signal due to *C*-P of fc was not found. $^{31}P\{^1H\}$ NMR ($CDCl_3$): δ −17.0 (s). IR (Nujol, cm^{-1}): ν 3269 (s), 1642 (vs), 1550 (vs), 1399 (w), 1345 (vw), 1317 (m), 1308 (m), 1291 (vw), 1242 (w), 1227 (s), 1213 (s), 1197 (vw), 1170 (vs), 1092 (w), 1070 (w), 1037 (vs), 996 (w), 977 (vw), 959 (w), 924 (vw), 894 (w), 842 (vw), 834 (m), 815 (w), 791 (w), 752 (m), 746 (m), 698 (s), 620 (m), 592 (w), 541 (w), 530 (w), 520 (w), 503 (m), 480 (w), 455 (w), 446 (w), 431 (w). ESI^+-MS: *m*/*z* 102 (Et_3NH^+). ESI^--MS: *m*/*z* 506 ($Ph_2PfcCONHCH_2SO_3^-$). Anal. Calcd for $C_{30}H_{37}O_4PFeN_2S$ (608.5): C 59.21, H 6.13, N 4.60. Found: C 58.99, H 6.10, N 4.53.

Preparation of Amide 2. Ester **4** (2.0 mmol, 1.160 g), 2-aminoethane-1-sulfonic acid (taurine; 2.5 mmol, 0.313 g), and 4-(*N*,*N*-dimethylamino)pyridine (0.06 mmol, 7.3 mg) were dissolved in a mixture of *N*,*N*-dimethylformamide (10 mL) and triethylamine (1 mL). After the reaction mixture was stirred at room temperature for 30 min, 0.1 mL of distilled water was introduced via a syringe, and the stirring was continued for another 20 h. Then the mixture was evaporated under reduced pressure, and the solid residue was taken up with dichloromethane (20 mL). The extract was dried over $MgSO_4$ and evaporated, affording a crude product, which was purified by column chromatography on silica with CH_2Cl_2/MeOH/Et_3N (100:5:2) as the eluent. The first minor band was discarded, and the second, orange band was collected and evaporated. The residue was dissolved in boiling ethyl acetate (ca. 60 mL) and slowly cooled to −4 °C to afford a crystalline solid, which was collected by suction and dried *in vacuo*. Yield of **2**: 1.108 g (89%), orange polycrystalline solid.

^1H NMR ($CDCl_3$): δ 1.35 (t, $^3J_{HH}$ = 7.3 Hz, 9 H, CH_3 of Et_3NH^+), 3.03 (m, 2 H, CH_2S), 3.13 (dq, $^3J_{HH}$ = 7.4 and 4.8 Hz, 6 H, CH_2 of Et_3NH^+), 3.80 (m, 2 H, CH_2N), 4.14−4.17 (m, 4 H, fc), 4.44 (vt, J' = 1.8 Hz, 2 H, fc), 4.61 (vt, J' = 1.9 Hz, 2 H, fc), 7.25−7.38 (m, 11 H, PPh_2 + NH), 10.02 (br s, 1 H, Et_3NH^+). $^{13}C\{^1H\}$ NMR (DMSO): δ 15.06 (CH_3 of Et_3NH^+), 35.60 (CH_2S), 45.64 (CH_2 of Et_3NH^+), 50.56 (CH_2N), 68.69, 71.06, 72.86 (d, J_{PC} = 4 Hz) and 73.47 (d, J_{PC} = 15 Hz) (4× CH of fc); 76.59 (d, $^1J_{PC}$ = 9 Hz, *C*-P of fc), 77.42 (*C*-CONH of fc), 128.21 (d, $^3J_{PC}$ = 7 Hz, CH_{meta} of PPh_2), 128.53 (CH_{para} of PPh_2), 132.91 (d, $^2J_{PC}$ = 19 Hz, CH_{ortho} of PPh_2), 138.31 (d, $^1J_{PC}$ = 10 Hz, C_{ipso} of PPh_2), 167.86 (C═O). $^{31}P\{^1H\}$ NMR (DMSO): δ −18.1 (s). IR (Nujol, cm^{-1}): ν 3337 (s), 2678 (m), 1649 (vs), 1548 (vs), 1299 (m), 1257 (w), 1229 (m), 1220 (m), 1186 (m), 1162 (s), 1092 (vw), 1067 (vw), 1025 (vs), 839 (m), 807 (w), 749 (m), 701 (m), 669 (w), 617 (w), 570 (vw), 539 (vw), 523 (vw), 504 (m), 468 (w), 456 (w), 444 (w). ESI^+-MS: *m*/*z* 102 (Et_3NH^+). ESI^--MS: *m*/*z* 520 ($Ph_2PfcCONHCH_2CH_2SO_3^-$). Anal. Calcd for $C_{31}H_{39}O_4PFeN_2S\cdot 0.5AcOEt\cdot 0.1CH_2Cl_2$ (675.1): C 58.89, H 6.45, N 4.15. Found: C 58.53, H 6.42, N 4.24. The amount of residual solvents was verified by ^1H NMR spectrum.

Preparation of Amide 3. The synthesis of **3** was carried out exactly as described for **2** starting from ester **4** (2.0 mmol, 1.160 g), 3-aminopropane-1-sulfonic acid (2.5 mmol, 0.348 g), and 4-(*N*,*N*-dimethylamino)pyridine (0.06 mmol, 7.3 mg) in *N*,*N*-dimethylformamide (10 mL) and triethylamine (1 mL). The reaction mixture was stirred for 30 min before distilled water (0.1 mL) was introduced via syringe, and stirring was continued at room temperature for 20 h. Isolation as described above afforded **3** as an orange crystalline solid. Yield: 1.006 g (79%).

^1H NMR ($CDCl_3$): δ 1.34 (t, $^3J_{HH}$ = 7.4 Hz, 9 H, CH_3 of Et_3NH^+), 2.09 (quintet, J = 6.6 Hz, 2 H, CH_2CH_2S), 2.98 (t, $^3J_{HH}$ = 6.8 Hz, 2 H, CH_2S), 3.11 (dq, $^3J_{HH}$ = 7.4 and 4.8 Hz, 6 H, CH_2 of Et_3NH^+), 3.51 (q, J = 6.2, 2 H, CH_2N), 4.13 (vq, J' = 1.8 Hz, 2H, fc), 4.16 (vt, J' = 2.0 Hz, 2 H, fc), 4.42 (vt, J' = 1.8 Hz, 2 H, fc), 4.64 (vt, J' = 1.9 Hz, 2 H, fc), 6.86 (t, $^3J_{HH}$ = 5.5 Hz, 1 H, N*H*), 7.30−7.39 (m, 10 H, PPh_2), 10.38 (br s, 1 H, Et_3NH^+). $^{13}C\{^1H\}$ NMR (DMSO): δ 9.04 (CH_3 of Et_3NH^+), 25.42 (CH_2CH_2S), 38.34 (CH_2S), 45.63 (CH_2 of Et_3NH^+), 49.47 (CH_2N), 68.78, 71.06, 72.91 (d, J_{PC} = 5 Hz) and 73.35 (d, J_{PC} = 15 Hz) (4× CH of fc); 76.30 (d, $^1J_{PC}$ = 8 Hz, C−P of fc), 77.42 (C−CONH of fc), 128.20 (d, $^3J_{PC}$ = 7 Hz, CH_{meta} of PPh_2), 128.52 (CH_{para} of PPh_2), 132.91 (d, $^2J_{PC}$ = 20 Hz, CH_{ortho} of PPh_2), 138.35 (d, $^1J_{PC}$ = 11 Hz, C_{ipso} of PPh_2), 167.91 (C═O). $^{31}P\{^1H\}$ NMR (DMSO): δ −18.1 (s). IR (Nujol, cm^{-1}): ν 3314 (s), 2692 (s), 1648 (vs), 1545 (vs), 1398 (w), 1343 (vw), 1314 (m), 1296 (m), 1272 (w), 1238 (m), 1222 (w), 1214 (m), 1181 (s), 1150 (vs), 1092 (vw), 1035 (vs), 835 (m), 823 (w), 747 (s), 697 (s), 596 (m), 561 (m), 525 (m), 506 (m), 503 (m), 491 (m), 448 (w), 416 (w). ESI^+-MS: *m*/*z* 102 (Et_3NH^+). ESI^--MS: *m*/*z* 534 ($Ph_2PfcCONHCH_2CH_2CH_2SO_3^-$). Anal. Calcd for $C_{32}H_{41}O_4PFeN_2S$ (636.5): C 60.38, H 6.49, N 4.40. Found: C 60.23, H 6.58, N 4.33.

Preparation of $[HNEt_3]_2[PdCl_2(Ph_2PfcCONHCH_2SO_3$-$\kappa P)_2]$ (5). Ligand **1** (0.20 mmol, 122 mg) was dissolved in dichloromethane (5 mL), and the solution was mixed with a solution of $[PdCl_2(cod)]$ (0.10 mmol, 28.5 mg) in the same solvent (5 mL). After the resulting red reaction mixture was stirred for 1 h, the formed precipitate was collected by suction, washed with diethyl ether and pentane, and dried *in vacuo*. Yield: 123 mg (88%), orange powder.

^1H NMR ($CDCl_3$): δ 1.17 (t, $^3J_{HH}$ = 7.2 Hz, 9 H, CH_3 of Et_3NH^+), 3.08 (q, $^3J_{HH}$ = 7.2 Hz, 6 H, CH_2 of Et_3NH^+), 4.04 (d, J = 6.4 Hz, 2 H, CH_2N), 4.51 (br s, 2 H, fc), 4.68 (vt, J' = 1.7 Hz, 2 H, fc), 4.79 (br s, 2 H, fc), 5.08 (vt, J' = 1.8 Hz, 2 H, fc), 7.44−7.59 (m, 10 H, PPh_2), 8.17 (t, $^3J_{HH}$ ≈ 7 Hz, 1 H, NH). $^{31}P\{^1H\}$ NMR (DMSO): δ 16.9 (s). IR (Nujol, cm^{-1}): ν 3306 (s), 2694 (m), 1663 (m), 1652 (m), 1623 (w), 1544 (s), 1399 (w), 1341 (vw), 1311 (m), 1280 (w), 1251 (m), 1238 (vw), 1203 (m), 1183 (m), 1165 (s), 1100 (w), 1071 (w), 1037 (vs), 999 (vw), 964 (vw), 896 (vw), 838 (m), 756 (m), 698 (s), 625 (w), 609 (m), 570 (vw), 541 (w), 526 (w), 517 (m), 504 (m), 474 (m), 461 (w), 435 (w). Anal. Calcd for $C_{60}H_{74}Cl_2Fe_2N_4O_8P_2PdS_2\cdot 0.2CH_2Cl_2$ (1411.3): C 51.23, H 5.31, N 3.97. Found: C 51.24, H 5.25, N 3.83. The presence of residual solvent was confirmed by ^1H NMR spectrum.

Preparation of $[HNEt_3]_2[PdCl_2(Ph_2PfcCONHCH_2CH_2SO_3$-$\kappa P)_2]$ (6). Ligand **2** (0.20 mmol, 124.5 mg) was dissolved in dry dichloromethane (5 mL), and the solution was added to a solution of $[PdCl_2(cod)]$ (0.10 mmol, 28.5 mg) in the same solvent (5 mL). The resulting red solution was stirred for 24 h, concentrated to ca. 5 mL under reduced pressure, and precipitated with diethyl ether/pentane (20 mL, 1:1). The brown-red precipitate was filtered off, washed with diethyl ether and pentane, and dried *in vacuo*. Yield: 139 mg (98%), brown-red powder.

^1H NMR (DMSO-d_6): δ 1.18 (t, $^3J_{HH}$ = 7.3 Hz, 9 H, CH_3 of Et_3NH^+), 2.63 (t, $^3J_{HH}$ = 7.2 Hz, 2 H, CH_2S), 3.09 (m, 6 H, CH_2 of Et_3NH^+), 3.41−3.50 (m, CH_2N; overlapping with H_2O signal), 4.48−4.55 (m, 4 H, fc), 4.65 (vt, J' = 1.8 Hz, 2 H, fc), 4.88 (vt, J' = 1.8 Hz, 2 H, fc), 7.43−7.59 (m, 10 H, PPh_2), 7.96 (t, $^3J_{HH}$ = 5.5 Hz, 1 H, NH), 8.99 (br s, 1 H, Et_3NH^+). $^{31}P\{^1H\}$ NMR (DMSO-d_6): δ 16.9 (s). IR (Nujol, cm^{-1}): ν 3329 (vs), 2715 (s), 1636 (s), 1542 (s), 1303 (m), 1246 (w), 1193 (s), 1165 (s), 1099 (m), 1060 (w), 1036 (vs), 999 (vw), 839 (m), 796 (w), 747 (m), 725 (w), 708 (w), 695 (m), 623 (m), 516 (m), 505 (m), 482 (w). Anal. Calcd for $C_{62}H_{78}Cl_2Fe_2N_4O_8P_2PdS_2\cdot 0.8CH_2Cl_2$ (1481.8): C 50.61, H 5.38, N 3.76. Found: C 50.82, H 5.40, N 3.78. The presence of residual solvent was confirmed by ^1H NMR spectrum.

Preparation of $[HNEt_3]_2[PdCl_2(Ph_2PfcCONHCH_2CH_2CH_2SO_3$-$\kappa P)_2]$ (7). Ligand **3** (0.20 mmol, 127.3 mg) and $[PdCl_2(cod)]$ (0.10 mmol, 28.5 mg) were reacted in dichloromethane (total 10 mL) as described above. The reaction mixture deposited a precipitate, which was filtered off, washed with diethyl ether and pentane, and dried *in vacuo*. Yield: 132 mg (91%), orange powder.

^1H NMR (DMSO-d_6): δ 1.17 (t, $^3J_{HH}$ = 7.3 Hz, 9 H, CH_3 of Et_3NH^+), 1.80 (p, $^3J_{HH}$ = 7.7 Hz, 2 H, CH_2CH_2S), 2.47−2.53 (m, CH_2S overlapping with the DMSO resonance), 3.09 (q, $^3J_{HH}$ = 7.3 Hz, 6 H, CH_3 of Et_3NH^+), 3.23 (q, J ≈ 6.3 Hz, 2 H, CH_2N), 4.46−4.52 (m, 4 H, fc), 4.66 (vt, J' = 1.9 Hz, 2 H, fc), 4.97 (vt, J' = 1.9 Hz, 2 H, fc), 7.43−7.59 (m, 10 H, PPh_2), 8.10 (t, $^3J_{HH}$ = 5.6 Hz, 1 H, NH), 8.95 (bs, 1 H, Et_3NH^+). $^{31}P\{^1H\}$ NMR (DMSO-d_6): δ 16.9 (s). IR (Nujol, cm^{-1}): ν 3322 (s), 2689 (s), 1655 (m), 1646 (m), 1549 (s), 1344 (vw), 1295 (m), 1268 (w), 1236 (m), 1227 (m), 1206 (w), 1196 (w), 1166 (s), 1099 (m), 1070 (w), 1032 (vs), 999 (vw), 835 (m), 789 (w), 742 (m), 730 (m), 708 (w), 696 (w), 691 (m), 627 (w), 598 (m), 563 (vw), 542 (w), 526 (w), 517 (m), 506 (m), 495 (w), 477 (m), 443 (w). Anal. Calcd for $C_{64}H_{82}Cl_2Fe_2N_4O_8P_2PdS_2\cdot 0.3CH_2Cl_2$ (1475.9):

dx.doi.org/10.1021/om2011529 | *Organometallics* 2012, 31, 729−738

C 52.32, H 5.64, N 3.80. Found: C 52.03, H 5.49, N 3.68. The presence of residual solvent was confirmed by ^{1}H NMR spectrum.

Preparation of [HNEt$_3$][(L^{NC})PdCl(Ph$_2$PfcCONHCH$_2$SO$_3$-κ*P*)] (8). A solution of ligand **1** (0.10 mmol, 61 mg) in dry dichloromethane (5 mL) was added to solid [(L^{NC})PdCl]$_2$ (0.050 mmol, 27.5 mg). The resulting solution was stirred for 1 h and then concentrated to ca. 1 mL on a rotary evaporator. The concentrated solution was added dropwise into boiling ethyl acetate (10 mL), and the mixture was slowly cooled to room temperature. The separated crystalline material was isolated by suction and dried *in vacuo*. Yield: 73 mg (83%), ruby red crystals.

^{1}H NMR ($CDCl_3$): δ 1.32 (t, $^3J_{HH}$ = 7.4 Hz, 9 H, CH_3 of Et_3NH^+), 2.85 (d, $^4J_{PH}$ = 2.7 Hz, 6 H, CH_3N), 2.99 (q, $^3J_{HH}$ = 7.4 Hz, 6 H, CH_3CH_2), 4.12 (d, $^4J_{PH}$ = 2.2 Hz, 2 H, CH_2NMe_2), 4.46–4.51 (m, 4 H, $C_{10}H_8$ + CH_2S), 4.63 (bs, 2 H, fc), 4.84 (br s, 2 H, fc), 4.90 (br s, 2 H, fc), 6.24 (td, J = 6.4, 1.1 Hz, 1 H, C_6H_4), 6.38 (td, J = 7.5, 1.3 Hz, 1 H, C_6H_4), 6.83 (td, J = 7.4, 1.1 Hz, 1 H, C_6H_4), 6.90 (unresolved t, 1 H, NH), 6.38 (dd, J = 7.4, 1.5 Hz, 1 H, C_6H_4), 7.30–7.44 (m, 6 H, PPh_2), 7.50–7.60 (m, 4 H, PPh_2). ^{13}C{^{1}H} NMR ($CDCl_3$): δ 8.70 (CH_3 of Et_3NH^+), 46.19 (CH_2 of Et_3NH^+), 50.16 (d, $^3J_{PC}$ = 2 Hz, NCH_3), 53.43, 55.72 (CH_2S and CH_2NMe_2); 69.69, 73.62, 74.20 (CH of fc); 74.34 (d, J_{PC} = 7 Hz, CH of fc), 74.98 (C_{ipso} of fc), 122.49 (CH of C_6H_4), 123.77 (CH of C_6H_4), 124.92 (d, J_{PC} = 5 Hz, CH of C_6H_4), 127.99 (d, J_{PC} = 11 Hz, CH of PPh_2), 130.82 (CH of PPh_2), 131.41 (d, $^1J_{PC}$ = 49 Hz, C_{ipso} of PPh_2), 134.34 (d, J_{PC} = 12 Hz, CH of PPh_2), 138.39 (d, J_{PC} = 11 Hz, CH of C_6H_4), 148.10 (d, J_{PC} = 2 Hz, *C*-Pd of C_6H_4), 152.17 (*C*-CH_2 of C_6H_4), 169.58 (C═O). ^{31}P{^{1}H} NMR ($CDCl_3$): δ 32.8 (s). IR (Nujol, cm^{-1}): ν 3293 (s), 2695 (s), 1738 (m), 1650 (m), 1633 (m), 1580 (w), 1535 (s), 1305 (m), 1288 (m), 1246 (m), 1214 (m), 1174 (vs), 1098 (m), 1068 (w), 1041 (s), 996 (vw), 969 (vw), 845 (m), 814 (vw), 751 (m), 744 (m), 696 (m), 622 (m), 543 (w), 522 (m), 509 (m), 487 (vw), 471 (w), 437 (m). ESI$^-$-MS: m/z 783 ([(L^{NC})PdCl(Ph_2PfcCONHCH$_2$SO$_3$)]$^-$). Anal. Calcd for $C_{39}H_{39}N_3PdClPFeO_4S{\cdot}0.3CH_2Cl_2{\cdot}0.3AcOEt$ (936.5): C 51.94, H 5.60, N 4.49. Found: C 51.35, H 5.60, N 4.31. The amount of clathrated solvents was corroborated by ^{1}H NMR spectroscopy.

Preparation of [(L^{NC})Pd(Ph$_2$PfcCONHCH$_2$SO$_3$-κ^2*P,O*)] (9). Ligand **1** (0.10 mmol, 61 mg) was dissolved in chloroform (3 mL), and the solution was added to a solution of [(L^{NC})Pd(OAc)]$_2$ (0.050 mol, 28 mg) in the same solvent (2 mL). The resulting mixture was stirred for 24 h and concentrated to ca. 1 mL. The solution was filtered through a pad of Celite, and the filtrate containing **9** and **9a** was carefully layered with diethyl ether. Subsequent crystallization by liquid-phase diffusion over several days gave a crystalline material, which was filtered off, washed with diethyl ether, and carefully dried to afford analytically pure **9**. Yield: 43 mg (58%), orange crystals.

^{1}H NMR ($CDCl_3$): δ 2.84 (d, $^4J_{PH}$ = 2.5 Hz, 6 H, CH_3N), 3.98 (vq, J' = 2.0 Hz, 2 H, fc), 4.09 (br s, 2 H, fc), 4.44 (d, $^3J_{HH}$ = 6.5 Hz, 2 H, CH_2S), 4.50 (vt, J' = 2.0 Hz, 2 H, fc), 4.56 (br s, 2 H, fc), 5.69 (s, 2 H, CH_2NMe_2), 6.26 (t, J = 6.7 Hz, 1 H, C_6H_4), 6.36 (dt, J = 7.6, 1.2 Hz, 1 H, C_6H_4), 6.83 (dt, J = 7.2, 0.6 Hz, 1 H, C_6H_4), 6.96 (dd, J = 7.5, 1.5 Hz, 1 H, C_6H_4), 7.34–7.47 (m, 6 H, PPh_2), 7.67–7.76 (m, 4 H, PPh_2), 9.09 (t, $^3J_{HH}$ = 6.5 Hz, 1 H, NH). ^{13}C{^{1}H} NMR ($CDCl_3$): δ 49.88 (d, $^3J_{PC}$ = 2 Hz, NCH_3), 56.34 (CH_2S), 72.10 (d, $^3J_{PC}$ = 4 Hz, CH_2NMe_2), 72.19 (d, $^1J_{PC}$ = 57 Hz, *C*-P of fc), 72.87, 73.35 (unresolved d) and 73.40 (CH of fc); 74.98 (*C*-CONH of fc), 76.37 (d, J_{PC} = 10 Hz, CH of fc), 122.76 (CH of C_6H_4), 124.58 (CH of C_6H_4), 125.40 (d, J_{PC} = 5 Hz, CH of C_6H_4), 128.64 (d, $^3J_{PC}$ = 11 Hz, CH_{meta} of PPh_2), 129.96 (d, $^1J_{PC}$ = 49 Hz, C_{ipso} of PPh_2), 131.34 (d, $^4J_{PC}$ = 2 Hz, CH_{para} of PPh_2), 128.20 (d, $^2J_{PC}$ = 13 Hz, CH_{ortho} of PPh_2), 138.65 (d, J_{PC} = 13 Hz, CH of C_6H_4), 143.23 (d, J_{PC} = 4 Hz, C_{ipso} of C_6H_4), 148.21 (d, J_{PC} = 2 Hz, C_{ipso} of C_6H_4), 173.07 (C═O). ^{31}P{^{1}H} NMR ($CDCl_3$): δ 30.4 (s). IR (Nujol, cm^{-1}): ν 3238 (s), 1588 (m), 1578 (vs), 1556 (vs), 1402 (m), 1338 (w), 1323 (m), 1294 (vw), 1250 (m), 1214 (s), 1195 (vw), 1180 (vs), 1157 (vw), 1095 (m), 1072 (vw), 1037 (vs), 1002 (w), 978 (vw), 964 (vw), 898 (w), 870 (w), 845 (w), 830 (vw), 752 (m), 746 (m), 706 (w), 697 (m), 630 (m), 596 (m), 540 (w), 518 (m), 491 (m), 479 (m), 456 (vw), 445 (m), 440 (w). ESI$^+$-MS: m/z 769 ([(L^{NC})Pd(Ph_2PfcCONHCH$_2$SO$_3$) + Na]$^+$), 747 ([(L^{NC})Pd(Ph_2PfcCONHCH$_2$SO$_3$) + H]$^+$). Anal. Calcd for $C_{33}H_{33}O_4PFeN_2S$ (746.9): C 53.06, H 4.45, N 3.75. Found: C 52.69, H 4.57, N 3.57.

***In Situ* NMR Study.** A solution of ligand **1** (0.02 mmol, 12.2 mg in 0.8 mL of deuterated solvent) was added to solid [(L^{NC})Pd(OAc)]$_2$ (0.01 mmol, 6.0 mg). The resulting mixture was stirred for 24 h in the dark and analyzed by ^{1}H and ^{31}P{^{1}H} NMR spectrometry. The reactions in dmso-d_6 (δ_P 28.9 major, 30.6 minor), CD_3CN (δ_P 29.4 major, 32.7 minor), or $CDCl_3$ (δ_P ca. 29.6 major, 30.1 minor; broad signals) produced mixtures of two Pd complexes in ca. 60:40 molar ratio. When the reaction was conducted in CD_3OD, pure **9** separated directly from the reaction mixture as a microcrystalline solid.

Reaction of [(L^{NC})Pd(OAc)]$_2$ with (Diphenylphosphino)-ferrocene. A solution of $FcPPh_2$ (74 mg, 0.20 mmol) in THF (5 mL) was added to solid [(L^{NC})Pd(OAc)]$_2$ (60 mg, 0.10 mmol). The reaction mixture was stirred for 1 h and evaporated, and the solid residue was dried *in vacuo*. Yield: 134 mg (quant.), yellow compound.

^{1}H NMR ($CDCl_3$): δ 1.38 (s, 3 H, CH_3CO_2), 2.75 (d, $^4J_{PH}$ = 2.7 Hz, 6 H, NMe_2), 4.00 (virtual q, J' = 2.0 Hz, 2 H, fc), 4.05 (d, $^4J_{PH}$ = 2.3 Hz, 2 H, NCH_2), 4.32 (m, 2 H, fc), 4.40 (s, 5 H, fc), 6.49 (dd, J = 5.5, 1.3 Hz, 1 H, C_6H_4), 6.55 (td, J = 7.7, 1.6 Hz, 1 H, C_6H_4), 6.92 (td, J = 7.3, 1.2 Hz, 1 H, C_6H_4), 7.05 (dd, J = 7.4, 1.5 Hz, 1 H, C_6H_4), 7.36–7.47 (m, 6 H, PPh_2), 7.69 (m, 4 H, PPh_2). ^{13}C{^{1}H} NMR ($CDCl_3$): δ 24.05 (CH_3CO_2), 49.91 (d, $^3J_{PC}$ = 2 Hz, N*Me*$_2$), 70.21 (s, CH of fc), 71.15 (d, J_{PC} = 7 Hz, CH of fc), 72.51 (d, $^3J_{PC}$ = 3 Hz, NCH_2), 72.72 (d, J_{PC} = 57 Hz, *C*-P of fc), 74.51 (d, J_{PC} = 10 Hz, CH of fc), 122.76, 123.88, 124.62 (d, J_{PC} = 5 Hz) (3× CH of C_6H_4); 127.84 (d, J_{PC} = 10 Hz, CH of PPh_2), 130.24 (d, $^4J_{PC}$ = 2 Hz, CH_{para} of PPh_2), 131.34 (d, $^1J_{PC}$ = 49 Hz, C_{ipso} of PPh_2), 134.39 (d, J_{PC} = 12 Hz, CH of PPh_2), 138.02 (d, J_{PC} = 10 Hz, CH of C_6H_4), 146.25 (d, J_{PC} = 5 Hz, *C*-Pd of C_6H_4), 148.63 (d, J_{PC} = 2 Hz, *C*-CH_2 of C_6H_4), 176.92 (CH_3CO_2). ^{31}P{^{1}H} NMR ($CDCl_3$): δ 29.6 (s). ESI$^+$-MS: m/z 692 ([M + Na]$^+$), 611 ([(L^{NC})Pd(FcPPh$_2$) + H]$^+$).

Pd-Catalyzed Cyanation of Aryl Bromides. A General Procedure. A reaction vessel was charged with aryl bromide (1.0 mmol), potassium carbonate (138 mg, 1.0 mmol), potassium hexacyanoferrate(II) trihydrate (212 mg, 0.5 mmol), and a palladium source (2 mol % with respect to the aryl bromide). The flask was equipped with a magnetic stirring bar, flushed with argon, and sealed. The solvent (1,4-dioxane/water, 1:1; 4 mL) was added via syringe, and the sealed flask was transferred into an oil bath maintained at 100 °C. After stirring for 18 h, the reaction mixture was cooled and quenched with water (2 mL), ethyl acetate (5 mL), and mesitylene (120 mg, 1.0 mmol) as an internal standard. After the organic layer was analyzed by NMR spectroscopy, it was separated and washed with brine (10 mL). The aqueous layer was extracted with ethyl acetate (3× 5 mL). The organic extracts were combined, dried over magnesium sulfate, and evaporated under reduced pressure. The crude product was purified by flash column chromatography over silica using an ethyl acetate/hexanes mixture to give pure nitriles after evaporation. Carboxylic acids **11k** and **11l** were isolated similarly after acidification of the reaction mixture with 3 M HCl.

Characterization Data. 4-Cyanoanisole (11a): ^{1}H NMR ($CDCl_3$): δ 3.86 (s, 3 H, CH_3O), 6.96 (dm, $^3J_{HH}$ = 6.8 Hz, 2 H, C_6H_4), 7.59 (dm, $^3J_{HH}$ = 7.0 Hz, 2 H, C_6H_4) (ref 36). **4-Cyanotoluene (11b):** ^{1}H NMR ($CDCl_3$): δ 2.42 (s, 3 H, CH_3), 7.27 (dm, $^3J_{HH}$ = 7.9 Hz, 2 H, C_6H_4), 7.54 (dm, $^3J_{HH}$ = 8.1 Hz, 2 H, C_6H_4) (ref 36). **3-Cyanotoluene (11c):** ^{1}H NMR ($CDCl_3$): δ 2.34 (s, 3 H, CH_3), 7.32–7.49 (m, 4 H, C_6H_4) (ref 37). **2-Cyanotoluene (11d):** ^{1}H NMR ($CDCl_3$): δ 2.55 (s, 3 H, CH_3), 7.27 (tm, $^3J_{HH}$ = 8.2 Hz, 1 H, H^5 of C_6H_4), 7.32 (dm, $^2J_{HH}$ = 7.3 Hz, 1 H, H^6 of C_6H_4), 7.48 (td, $^3J_{HH}$ = 7.6 Hz, $^4J_{HH}$ = 1.4 Hz, 1 H, H^4 of C_6H_4), 7.60 (dd, $^3J_{HH}$ = 8.2 Hz, $^4J_{HH}$ = 1.4 Hz, 1 H, H^3 of C_6H_4) (ref 36). **4-*tert*-Butylbenzonitrile (11e):** ^{1}H NMR ($CDCl_3$): δ 1.33 (s, 9 H, CH_3), 7.48 (dm, $^3J_{HH}$ = 8.8 Hz, 2 H, C_6H_4), 7.59 (dm, $^3J_{HH}$ = 8.8 Hz, 2 H, C_6H_4) (ref 38). **4-(Trifluoromethyl)benzonitrile (11f):** ^{1}H NMR (DMSO-d_6): δ 7.84 (d, $^3J_{HH}$ = 7.7 Hz, 2 H, C_6H_4), 8.06 (d, $^3J_{HH}$ = 7.9 Hz, 2 H, C_6H_4). Spectra recorded in $CDCl_3$ corresponded with the literature data (ref 36). **4-Cyanoacetophenone (11g):** ^{1}H NMR ($CDCl_3$): δ 2.65 (s, 3 H, CH_3), 7.78 (dm, $^3J_{HH}$ = 8.0 Hz, 2 H, C_6H_4), 8.05 (dm, $^3J_{HH}$ = 8.1 Hz, 2 H, C_6H_4) (ref 39). **4-Cyanobiphenyl (11h):** ^{1}H NMR ($CDCl_3$): δ 7.42–7.51 (m, 3 H, $C_{12}H_9$), 7.57–7.61 (m, 2 H, $C_{12}H_9$), 7.66–7.74 (m, 4 H, $C_{12}H_9$) (ref 38). **4-Chlorobenzonitrile (11i):** ^{1}H NMR ($CDCl_3$): δ 7.47 (dm, $^3J_{HH}$ = 8.8 Hz, 2 H, C_6H_4),

dx.doi.org/10.1021/om2011529 | *Organometallics* 2012, 31, 729–738

7.61 (d, $^3J_{HH}$ = 8.8 Hz, 2 H, C_6H_4) (ref 36). **4-(Dimethylamino)-benzonitrile (11k):** ^{1}H NMR ($CDCl_3$): δ 3.04 (s, 6 H, NMe_2), 6.64 (d, $^3J_{HH}$ = 9.2 Hz, 2 H, C_6H_4), 7.47 (d, $^3J_{HH}$ = 9.0 Hz, 2 H, C_6H_4) (ref 36). **4-Cyanobenzoic acid (11l):** ^{1}H NMR (DMSO-d_6): δ 7.99 (dm, $^3J_{HH}$ = 8.0 Hz, 2 H, C_6H_4), 8.09 (dm, $^3J_{HH}$ = 8.1 Hz, 2 H, C_6H_4), 13.56 (br s, 1 H, CO_2H) (ref 37). **(4-Cyanophenyl)acetic acid (11m):** ^{1}H NMR (DMSO-d_6): δ 3.72 (s, 2 H, CH_2), 7.48 (dm, $^3J_{HH}$ = 8.0 Hz, 2 H, C_6H_4), 7.78 (dm, $^3J_{HH}$ = 8.4 Hz, 2 H, C_6H_4) (ref 40). 4-Nitrobenzonitrile (**11j**)[41] and the amides (**12a**, **12f**, and **12i**)[42] were identified upon comparing ^{1}H NMR spectra of the reaction mixture with the literature data.

X-ray Crystallography. Single crystals suitable for X-ray diffraction analysis were grown from hot ethyl acetate (**1**: yellow plate, 0.08 × 0.20 × 0.38 mm^3; **3**: orange prism, 0.25 × 0.44 × 0.47 mm^3) or by liquid-phase diffusion from diethyl ether/dichloromethane (**5**·2.5CH_2Cl_2: brown plate, 0.05 × 0.25 × 0.30 mm^3) and from diethyl ether/chloroform (**9**·2$CHCl_3$: orange plate, 0.08 × 0.13 × 0.33 mm^3).

Full-set diffraction data ($\pm h \pm k \pm l$; θ_{max} = 26.0−27.6°, data completeness ≥97%) were collected with a KappaCCD or Apex2 diffractometer equipped with a Cryostream Cooler (Oxford Cryosystems) at 150(2) K using graphite-monochromated Mo Kα radiation (λ = 0.71073 Å). The structures were solved by the direct methods (SIR-97[43] or SHELXS-87[44]) and refined by full-matrix least-squares on F^2 (SHELXL-97[44]). Unless noted otherwise, the non-hydrogen atoms were refined with anisotropic displacement parameters. The NH hydrogens were identified on difference density maps and refined either freely (**1**) or as riding atoms with U_{iso} = 1.2 U_{eq}(N) (all other structures). All CH hydrogen atoms were included in calculated positions and refined as riding atoms. Selected crystallographic data and structure refinement parameters are available as Supporting Information, Table S1. Particular details on structure refinement are as follows.

One of the Et_3NH^+ cations in the structure of **5**·2.5CH_2Cl_2 is disordered and was refined with isotropic displacement parameters for the carbon atoms. In addition, the solvent of crystallization in the same structure was found to be severely disordered, and its contribution to the scattering was numerically removed using the SQUEEZE[45] routine as incorporated in the PLATON program.[46]

Geometric data and structural drawings were obtained with a recent version of the PLATON program. The numerical values are rounded with respect to their estimated deviations (esd's) given in one decimal. Parameters relating to atoms in constrained positions are given without esd's.

■ ASSOCIATED CONTENT

Ⓢ Supporting Information

Additional structural drawings, summary of crystallographic data (Table S1), and CIF files for all structurally characterized compounds are available free of charge via the Internet at http://pubs.acs.org.

■ AUTHOR INFORMATION

Corresponding Author

*E-mail: stepnic@natur.cuni.cz.

■ ACKNOWLEDGMENTS

This work was financially supported by the Grant Agency of Charles University in Prague (project no. 69309) and is part of a long-term research project by the Ministry of Education, Youths and Sports of the Czech Republic (project no. MSM0021620857). Prof. Jana Roithová is thanked for her assistance during ESI-MS measurements.

■ REFERENCES

(1) Monosulfonated triphenylphosphine, 3-$Ph_2PC_6H_4SO_3H$, was the first reported compound of this kind: Ahrland, S.; Chatt, J.; Davies, N. R.; Williams, A. A. *J. Chem. Soc.* **1958**, 276.

(2) (a) *Aqueous-Phase Organometallic Chemistry*, 2nd ed.; Cornils, B.; Herrmann, W. A., Eds.; Wiley-VCH: Weinheim, 2004. (b) Joó, F. *Aqueous Organometallic Catalysis*; Kluwer: Dordrecht, 2001. Selected reviews: (c) Butler, R. N.; Coyne, A. G. *Chem. Rev.* **2010**, *110*, 6302. (d) Shaughnessy, K. H. *Chem. Rev.* **2009**, *109*, 643. (e) Pinault, N.; Bruce, D. W. *Coord. Chem. Rev.* **2003**, *241*, 1. (f) Genet, J. P.; Savignac, M. *J. Organomet. Chem.* **1999**, *576*, 305. (g) Herrmann, W. A.; Kohlpaintner, C. W. *Angew. Chem., Int. Ed. Engl.* **1993**, *32*, 1524. (h) Kalck, P.; Monteil, F. *Adv. Organomet. Chem.* **1992**, *34*, 219. (i) Nomura, K. *J. Mol. Catal. A: Chem.* **1998**, *130*, 1. (j) Joó, F.; Kathó, Á. *J. Mol. Catal. A: Chem.* **1997**, *116*, 3.

(3) (a) Nuzzo, R. G.; Feitler, D.; Whitesides, G. M. *J. Am. Chem. Soc.* **1979**, *101*, 3683. (b) Nuzzo, R.; Haynie, S. L.; Wilson, M. E.; Whitesides, G. M. *J. Org. Chem.* **1981**, *46*, 2861.

(4) Benhamza, R.; Amrani, Y.; Sinou, D. *J. Organomet. Chem.* **1985**, *288*, C37.

(5) Fremy, G.; Castanet, Y.; Grzybek, R.; Monflier, E.; Morteux, A.; Trzeciak, A. M.; Ziolkowski, J. J. *J. Organomet. Chem.* **1995**, *505*, 11.

(6) (a) Lavenot, L.; Bortoletto, M. H.; Roucoux, A.; Larpent, C.; Patin, H. *J. Organomet. Chem.* **1996**, *509*, 9.

(7) (a) Grzybek, R. *React. Kinet. Catal. Lett.* **1996**, *58*, 315. (b) Mieczyńska, E.; Trzeciak, A. M.; Grzybek, R.; Ziólkowski, J. J. *J. Mol. Catal. A: Chem.* **1998**, *132*, 203. (c) Mieczyńska, E.; Trzeciak, A. M.; Ziólkowski, J. J. *J. Mol. Catal. A: Chem.* **1999**, *148*, 59.

(8) (a) Trzeciak, A. M.; Ziólkowski, J. J. *J. Mol. Catal. A: Chem.* **2000**, *154*, 93. (b) Trzeciak, A. M.; Wojtków, W.; Ciunik, Z.; Ziólkowski, J. J. *Catal. Lett.* **2001**, *77*, 245.

(9) (a) Lamač, M.; Tauchman, J.; Císařová, I.; Štěpnička, P. *Organometallics* **2007**, *26*, 5042. (b) Štěpnička, P.; Solařová, H.; Lamač, M.; Císařová, I. *J. Organomet. Chem.* **2010**, *695*, 2423. (c) Štěpnička, P.; Solařová, H.; Císařová, I. *J. Organomet. Chem.* **2011**, *696*, 3727. (d) Meca, L.; Dvořák, D.; Ludvík, J.; Císařová, I.; Štěpnička, P. *Organometallics* **2004**, *23*, 2541. (e) Drahoňovský, D.; Císařová, I.; Štěpnička, P.; Dvořáková, H.; Maloň, P.; Dvořák, D. *Collect. Czech. Chem. Commun.* **2001**, *66*, 588.

(10) (a) Kühnert, J.; Dušek, M.; Demel, J.; Lang, H.; Štěpnička, P. *Dalton Trans.* **2007**, 2802. (b) Kühnert, J.; Císařová, I.; Lamač, M.; Štěpnička, P. *Dalton Trans.* **2008**, 2454. (c) Štěpnička, P.; Krupa, M.; Lamač, M.; Císařová, I. *J. Organomet. Chem.* **2009**, *694*, 2987. (d) Kühnert, J.; Lamač, M.; Demel, J.; Nicolai, A.; Lang, H.; Štěpnička, P. *J. Mol. Catal. A: Chem.* **2008**, *285*, 41. (e) Lamač, M.; Tauchman, J.; Dietrich, S.; Císařová, I.; Lang, H.; Štěpnička, P. *Appl. Organomet. Chem.* **2010**, *24*, 326. (f) Štěpnička, P.; Schulz, J.; Císařová, I.; Fejfarová, K. *Collect. Czech. Chem. Commun.* **2007**, *72*, 453.

(11) Schulz, J.; Císařová, I.; Štěpnička, P. *J. Organomet. Chem.* **2009**, *694*, 2519.

(12) Tauchman, J.; Císařová, I.; Štěpnička, P. *Organometallics* **2009**, *28*, 3288.

(13) Tauchman, J.; Císařová, I.; Štěpnička, P. *Eur. J. Org. Chem.* **2010**, 4276.

(14) Tauchman, J.; Císařová, I.; Štěpnička, P. *Dalton Trans.* **2011**, *40*, 11748.

(15) (a) Podlaha, J.; Štěpnička, P.; Císařová, I.; Ludvík, J. *Organometallics* **1996**, *15*, 543. (b) Štěpnička, P. *Eur. J. Inorg. Chem.* **2005**, 3787.

(16) Štěpnička, P.; Podlaha, J.; Gyepes, R.; Polášek, M. *J. Organomet. Chem.* **1998**, *552*, 293.

(17) Even thoughthe overall molecular geometry can be *very* similarto that found in centrosymmetric structures, the presence of chiralityelements inevitably renders the whole molecule chiral and thus structurallyindependent. For an example, see the structure of *trans*-[$PdCl_2(Ph_2PfcY$-$\kappa P)_2$], where Y is a C-chiral 4,5-dihydroxazol-2-yl group: Drahoňovský, D.; Císařová, I.; Štěpnička, P.; Dvořáková, H.; Maloň, P.; Dvořák, D. *Collect. Czech. Chem. Commun.* **2001**, *66*, 588.

(18) Eighteen different structures of this type (though sometimes as solvatomorphs) were found in the Cambridge Structural Database, version 5.32 of November 2010, with updates of November 2010, and February, May, and August 2011.

(19) Y = $P(O)Ph_2$: (a) Coyle, R. J.; Slovokhotov, Y. L.; Antipin, M. Y.; Grushin, V. V. *Polyhedron* **1998**, *17*, 3059. (b) Hursthouse, M. B.; Hibbs, D. E.; Butler, I. R. *Private communication to CCDC*, 2003 (refcode: BATGAF); Y = $SiPh_2$(*n*-Pr): (c) Hursthouse, M. B.; Coles, S. J.; Butler, I. R. *Private communication to CCDC*, 2003 (refcode: EKAQUC); Y = SMe: (d) Gibson, V. C.; Long, N. J.; White, A. J. P.; Williams, C. K.; Williams, D. J.; Fontani, M.; Zanello, P. *J. Chem. Soc., Dalton Trans.* **2002**, 3280. Y = CH═CH_2: (e) Štěpnička, P.; Císařová, I. *Collect. Czech. Chem. Commun.* **2006**, *71*, 215. Y = PO_3Et_2: (f) Štěpnička, P.; Císařová, I.; Gyepes, R. *Eur. J. Inorg. Chem.* **2006**, 926. Y = CO_2H: (g) Ref 16. Y = CONHPh: (h) Ref 9b. Y = $CONHCH_2CH_2OH$ or $CON(CH_2CH_2OH)_2$: (i) Ref 11. Y = $CONHCH_2CH_2Py$: (j) Kühnert, J.; Dušek, M.; Demel, J.; Lang, H.; Štěpnička, P. *Dalton Trans.* **2007**, 2802. Y = $CONHCH_2CONH_2$: (k) Ref 12. Y = Py or CH_2Py (Py = pyrid-2-yl): (l) Štěpnička, P.; Schulz, J.; Klemann, T.; Siemeling, U.; Císařová, I. *Organometallics* **2010**, *29*, 3187.

(20) Dimer $[(L^{NC})Pd(OAc)]_2$ was shown react with stoichiometric amounts of phosphines to afford mononuclear complexes of the type $[(L^{NC})Pd(OAc)(PR_3)]$: Ciba Specialty Chemicals (Van Der Schaaf, P. A.; Kolly, R.; Tinkl, M.) Patent WO 200301372, 2003.

(21) $(L^{NC})Pd$ complexes with simple phosphinocarboxylic ligands: (a) Braunstein, P.; Matt, D.; Dusausoy, Y.; Fischer, J.; Mitschler, A.; Ricard, L. *J. Am. Chem. Soc.* **1981**, *103*, 5115. (b) Braunstein, P.; Matt, D.; Nobel, D.; Bouaoud, S.-E.; Grandjean, D. *J. Organomet. Chem.* **1986**, *301*, 401. Representative examples for phosphinoferrocene donors: (c) Štěpnička, P.; Císařová, I. *Organometallics* **2003**, *22*, 1728. (d) Štěpnička, P.; Lamač, M.; Císařová, I. *Polyhedron* **2004**, *23*, 921. (e) Lamač, M.; Císařová, I.; Štěpnička, P. *Collect. Czech. Chem. Commun.* **2007**, *72*, 985, and refs 9b, 10c, 12, 19f.

(22) The Fe−Cp ring centroid distances are identical within the precision of the measurement (1.650(3) Å for Cp^C and 1.649(3) Å for Cp^P). However, the individual Fe−C bond lengths slightly but distinctly increase in the order *ipso* < α < β for each of the four C-CH-CH moieties within the Cp rings. The tilt angle remains relatively small (4.1(3)°).

(23) Sundermeier, M.; Zapf, A.; Beller, M. *Eur. J. Inorg. Chem.* **2003**, 3513.

(24) (a) Schareina, T.; Zapf, A.; Beller, M. *Chem. Commun.* **2004**, 1388. (b) Schareina, T.; Zapf, A.; Beller, M. *J. Organomet. Chem.* **2004**, *689*, 4576.

(25) (a) Grossman, O.; Gelman, D. *Org. Lett.* **2006**, *8*, 1189. (b) Schareina, T.; Jackstell, R.; Schulz, T.; Zapf, A.; Cotté, A.; Gotta, M.; Beller, M. *Adv. Synth. Catal.* **2009**, *351*, 643. (c) Zhang, J.; Chen, X.; Hu, T.; Zhang, Y.; Xu, K.; Yu, Y.; Huang, J. *Catal. Lett.* **2010**, *139*, 56. (d) Yeung, P. Y.; So, C. M.; Lau, C. P.; Kwong, F. Y. *Org. Lett.* **2011**, *13*, 648.

(26) (a) Pd/C in the presence of NBu_3 and Na_2CO_3: Zhu, Y.-Z.; Cai, C. *Eur. J. Org. Chem.* **2007**, 2401. (b) For use of Pd/C inaqueous poly(ethylene glycol) under microwave irradiation, see: Chen, G.; Wen, J.; Zheng, Z.; Zhu, X.; Cai, Y.; Cai, J.; Wan, Y. *Eur. J. Org. Chem.* **2008**, 3524.

(27) The NO_2 group is the strongest electron-withdrawing moiety (−*I* and −*M*) in the series tested.

(28) (a) *Ferrocenes: Ligands, Materials and Biomolecules*; Štěpnička, P., Ed.; Wiley: Chichester, 2008. For a recent example, see: (b) Atkinson, R. C. J.; Gibson, V. C.; Long, N. J.; White, A. J. P. *Dalton Trans.* **2010**, *39*, 7540.

(29) (a) Braunstein, P.; Naud, F. *Angew. Chem., Int. Ed.* **2001**, *40*, 680. (b) Slone, C. S.; Weinberger, D. A.; Mirkin, C. A. *Prog. Inorg. Chem.* **1999**, *48*, 233. (c) Bader, A.; Lindner, E. *Coord. Chem. Rev.* **1991**, *108*, 27.

(30) While our work was in progress, synthesis of the first phosphinoferrocene sulfonic acid, $[Fe(\eta^5\text{-}C_5H_3\text{-}1\text{-}SO_3H\text{-}2\text{-}PPh_2)(\eta^5\text{-}C_5H_5)]$, was reported by Erker and co-workers: Chen, C.; Anselment, T. M. J.; Fröhlich, R.; Rieger, B.; Kehr, G.; Erker, G. *Organometallics* **2011**, *30*, 5248.

(31) The solubility of compound **1** in water at 25 °C exceeds 1.24 g (2.0 mmol) per 5 mL. Attempts to determine partition coefficients of **1** in water/dichloroethane, water/ethyl acetate, and water/toluene mixtures were unsuccessful due to formation of stable emulsions.

(32) Drew, D.; Doyle, J. R. *Inorg. Synth.* **1972**, *13*, 47.

(33) Cope, A. C.; Friedrich, E. C. *J. Am. Chem. Soc.* **1968**, *90*, 909.

(34) Cockburn, B. N.; Howe, D. V.; Keating, T.; Johnson, B. F. G.; Lewis, J. *J. Chem. Soc., Dalton Trans.* **1973**, 404.

(35) (a) Sollott, G. P.; Mertwoy, H. E.; Portnoy, S.; Snead, J. L. *J. Org. Chem.* **1963**, *28*, 1090. (b) Kotz, J. C.; Nivert, C. L. *J. Organomet. Chem.* **1973**, *52*, 387.

(36) Anbarasan, P.; Neumann, H.; Beller, M. *Chem.—Eur. J.* **2010**, *16*, 4725.

(37) Littke, A.; Soumeillant, M.; Kaltenbach, R. F. III; Cherney, R. J.; Tarby, C. M.; Kiau, S. *Org. Lett.* **2007**, *9*, 1711.

(38) Grossman, O.; Gelman, D. *Org. Lett.* **2006**, *8*, 1189.

(39) Murphy, J. A.; Commeureuc, A. G. J.; Snaddon, T. N.; McGuire, T. M.; Khan, T. A.; Hisler, K.; Dewis, M. L.; Carling, R. *Org. Lett.* **2005**, *7*, 1427.

(40) Ohkoshi, M.; Michinishi, J.; Hara, S.; Senboku, H. *Tetrahedron* **2010**, *66*, 7732.

(41) Sasson, R.; Rozen, S. *Org. Lett.* **2005**, *7*, 2177.

(42) (a) Ramón, R. S.; Bosson, J.; Díez-González, S.; Marion, N.; Nolan, S. P. *J. Org. Chem.* **2010**, *75*, 1197. (b) Owston, N. A.; Parker, A. J.; Williams, J. M. J. *Org. Lett.* **2007**, *9*, 73.

(43) Altomare, A.; Burla, M. C.; Camalli, M.; Cascarano, G. L.; Giacovazzo, C.; Guagliardi, A.; Moliterni, A. G. G.; Polidori, G.; Spagna, R. *J. Appl. Crystallogr.* **1999**, *32*, 115.

(44) Sheldrick, G. M. *Acta Crystallogr., Sect. A* **2008**, *64*, 112.

(45) van der Sluis, P.; Spek, A. L. *Acta Crystallogr., Sect. A* **1990**, *46*, 194.

(46) Spek, A. L. *Acta Crystallogr., Sect. D* **2009**, *65*, 148.